Control of Deterministic and Stochastic Hamiltonian Systems

Application to Optimal Gait Generation for Walking Robots

Dissertation

SATOH Satoshi

Nagoya University
January 2010

Abstract

In the recent active research and development of walking robots, a lot of techniques to realize dynamic walking have been proposed. In this thesis, we will develop a novel optimal gait generation framework based on physical property and learning control with stochastic control theory. This aim is tackled from two approaches. One is control of deterministic Hamiltonian systems and the other is that of stochastic Hamiltonian ones.

We consider walking robots as Hamiltonian systems, rather than as just nonlinear systems, and take advantage of their physical properties. Iterative learning control based on variational symmetry of Hamiltonian systems was proposed and it allows one to solve a class of optimal control problems by iteration of laboratory experiments. Thanks to the symmetric property, it does not require the precise knowledge of the plant model and it can deal with infinite dimensional optimal control problems. Although this method works well for some control problems, it can not be directly applied to the optimal gait generation problem for several reasons. One reason is that this method can not deal with discontinuous state transitions caused by collisions between a foot of the walking robot and the ground. In the former part of this thesis, we will propose some techniques which extend this method in order to deal with such transitions, and will eventually construct an optimal gait generation framework based on variational symmetry of Hamiltonian systems. The proposed framework is summarized as follows. Firstly, we equip virtual constraints by shaping the potential energy of the Hamiltonian system (walking robot) in order to prevent the robot from falling. Secondly, we execute two kinds of learning procedures: one procedure updates the control inputs and the other one tunes the potential gains to mitigate the strength of the virtual constraints. Consequently, this framework is expected to generate an optimal periodic gait trajectory without constraints, which minimizes the L_2 norm of the control input. Furthermore, it does not require the models of the plant system nor the discontinuous state transitions. The feature of the proposed method is that the robot improves his walk keeping on walking due to the constraints, that is, this method does not require to repeat experiments under the same initial condition, which is necessary for conventional iterative learning control frameworks.

Many conventional results of iterative learning control have not sufficiently considered uncertainties during experiments, such as environmental disturbance, measurement noise and so on. Since walking robots dynamically interact with their environment and there must exist measurement noise in experiments with real robots, it is very important to take such disturbances into account. In the latter part of the thesis, we consider the plant system with the above uncertainties as a stochastic system and we focus on stochastic control theory to take disturbances during experiments into account. We will introduce stochastic (port-)Hamiltonian systems which are extension of deterministic Hamiltonian ones, and will clarify some of their properties such as passivity and symmetry. We will provide conditions under which stochastic Hamiltonian systems become stochastic passive and they possess a symmetric property corresponding to variational symmetry of deterministic Hamiltonian systems which plays an important role in the conventional iterative learning control method. By utilizing these properties, we will propose the following useful frameworks for control of stochastic Hamiltonian systems. One is a stabilization method based on stochastic passivity and stochastic generalized canonical transformations. Stochastic generalized canonical transformations are pairs of coordinate and feedback transformations under which the stochastic Hamiltonian structure is preserved. Although stabilization of general nonlinear stochastic systems is very difficult, the proposed framework can achieve stochastic stabilization easily and intuitively. The other is an observer based stochastic trajectory tracking control method. It provides conditions for the controller and observer gains under which tracking and estimation errors remain bounded in probability and the margin of errors is assignable. The stochastic bounded stability has been proven by utilizing supermartingale property.

Since such learning framework based on a stochastic physical system's properties has not been proposed so far, this thesis provides a new perspective to the optimal gait generation problem from the stochastic control view point.

Acknowledgement

It would be difficult for me to finish this thesis without the help and support of many people. I cannot help feeling fortunate in having been given an opportunity to study with them.

First and foremost, I would like to express my deepest respect and gratitude to Associate Professor Kenji Fujimoto for the supervision and his constant support. He has shown great tolerance and patience throughout this work. Valuable discussions with him gave me a lot of things and guided me into several interesting research fields. Without his significant advice and encouragement, this thesis would not be completed.

I would also like to acknowledge to Professor Yoshikazu Hayakawa for his good advice and comment. They are great help to complete this work. His critical reading of the manuscript provides me with many valuable suggestions.

I would like to thank Dr. Sang-Ho Hyon of JST-ICORP/ ATR. He has collaborated on the researches in this thesis and gave me a significant advice and encouragement.

I am grateful to Professor Tatsuya Suzuki of Nagoya University and Associate Professor Fumihiko Asano of Japan Advanced Institute of Science and Technology for being committee members of this dissertation and for their technical advice and careful reading of the manuscript.

I would like to thank Dr. Akira Nakashima for his valuable advice and encouragement.

I would like to appreciate Dr. Harry Berghuis in Medtronic, Inc. for sending me a copy of his PhD thesis and for providing many valuable comments.

I would like to thank my colleagues who have collaborated on my researches, Mr. Keitaro Kuba of The University of Tokyo, Ms. Rosa Veenbaas of University of Groningen and Mr. Masahito Ikeda of Nagoya University for beneficial discussions. I would also like to thank Dr. Shuichi Fukunaga of Tokyo Metropolitan College of Industrial Technology, Dr. Yuki Minami of Maizuru National College of Technology, Dr. Yuki Nishimura of Yamaguchi University, Mr. Yuji Harata and Mr. Masayasu Suzuki of Nagoya University and Dr. Tudor Ionescu of University of Groningen for their support and exciting discussions.

For providing a simultaneous environment for my work, I would like to thank all the staff and students of Mechatronics Control Laboratory of Nagoya University.

Finally, I would like to thank those closest to me, whose support helped make it to the end of this thesis. Thanks to my parents Kazuhiro and Kyoko Satoh and entire family and thanks to Mikiko for all the support and warm encouragements.

Notation

$\mathbb{R}$	field of real numbers
L_2^n	space of n-dimensional square integrable functions
$L_2^n[t^0, t^1]$	L_2^n on a finite time interval $[t^0, t^1]$
Ω	sample space
$\mathcal{F}$	sigma algebra of the observable random events
$\{\mathcal{F}_t\}_{t\geq 0}$	filtration
$\mathcal{P}$	probability measure on a sample space
$(\Omega, \mathcal{F}, \mathcal{P})$	probability space
$E[\cdot]$	expectation with respect to the measure $\mathcal{P}$
$E[\cdot\|\mathcal{F}]$	conditional expectation with respect to $\mathcal{F}$
$\\|\cdot\\|_X$	norm on some Banach space X
$\langle\cdot,\cdot\rangle_X$	inner product on some Hilbert space X
$o(\cdot)$	Landau notation (see Eq. (2.2))
L_f	Lie derivative with respect to the vector field f
$[f, g]$	Lie bracket of the vector fields f and g
$\mathrm{ad}_f^k g,$	$[f, \mathrm{ad}_f^{k-1} g]$ setting $\mathrm{ad}_f^0 g = g$
I, I_n	identity matrix and $n \times n$ identity matrix, respectively
O, O_{mn}	zero matrix and $m \times n$ zero matrix, respectively
A^i, A_j	i-th row and j-th column of the matrix A, respectively
$[A]_{i^1 i^2 \cdots i^m}$	$(i^1, i^2, \cdots, i^m)$-th element of the m-order tensor $A \in \mathbb{R}^{\overbrace{n \times \cdots \times n}^{m}}$
$A^\top$	transpose of the matrix A or the second order tensor A
A^{-1}	inverse of the matrix A
$A^{-\top}$	$(A^\top)^{-1} = (A^{-1})^\top$
$A^\dagger$	pseudo inverse of the matrix A
$\lambda(A)$	eigenvalue of the matrix A
$\lambda_{\max}(A)$	maximum eigenvalue of the matrix A
$\\|A\\|$	norm of the matrix A defined by $\sqrt{\lambda_{\max}(A^\top A)}$

$\mathrm{tr}\{A\}$	trace of the matrix A
$\mathrm{diag}\{a^1, \cdots, a^n\}$	diagonal matrix with diagonal elements a^1 to a^n
id	identity mapping
$\mathbf{1}(t)$	identity operator defined by $\mathbf{1}(t) = \mathrm{id}\ \ (t^0 \leq t \leq t^1)$
δ	Fréchet derivative (see Definition 2.1)
$\partial_{(\cdot)}$	partial Fréchet derivative with respect to $(\cdot)$
$\mathcal{D}_{(\cdot)} = \frac{\partial}{\partial(\cdot)}$	differential operator with respect to $(\cdot)$
$\dot{(\cdot)} = \mathcal{D}_t(\cdot)$	total time derivative
$\mathcal{L}(\cdot)$	infinitesimal generator (see Eq. (4.45))
$\pi_{(\cdot)}$	projection mapping onto $(\cdot)$
$\mathcal{R}(\cdot)$	time-reversal operator on $[t^0, t^1]$ (see Eq. (2.9))
$\mathfrak{h}(\cdot)$	0-order hold operator on $[t^0, t^1]$ (see Eq. (3.1))
$(\cdot)_{-/+}$	just before/after a discontinuous transition
$\nu_1(t)$	filter function defined by Eq. (2.40) (see also Fig. 2.4)
$\nu_2(t)$	filter function defined by Eq. (3.14) (see also Fig. 3.3)

In this thesis, we sometimes treat a matrix as a second order tensor and the Einstein summation convention is utilized (particularly, this rule will be often utilized in Chapter 5). Consider a matrix $M(q) \in \mathbb{R}^{n\times n}$ of a vector $q \in \mathbb{R}^n$, which will often appear in this thesis as the inertia matrix of the configuration coordinate. For example, for $\alpha, \beta \in \mathbb{R}^n$, $M(q)(\alpha, \beta) := [M(q)]_{ij}\alpha^i\beta^j \equiv \alpha^\top M(q)\beta$. Here we use the Einstein summation convention. Tensor notation is a convenient way to describe derivatives. For example, $\mathcal{D}_q M(q)(\alpha, \beta)(\cdot)$ and $\mathcal{D}_q^2 M(q)(\alpha, \beta)(\cdot)(\cdot)$ are first and second order tensors and they are defined as

$$\begin{aligned}
[\mathcal{D}_q M(q)(\alpha, \beta)(\cdot)]_k &= \frac{\partial [M(q)]_{ij}}{\partial q^k}\alpha^i\beta^j, \\
[\mathcal{D}_q^2 M(q)(\alpha, \beta)(\cdot)(\cdot)]_{kl} &= [\mathcal{D}_q([\mathcal{D}_q M(q)(\alpha, \beta)(\cdot)]_k)]_l \\
&= \frac{\partial^2 [M(q)]_{ij}}{\partial q^l \partial q^k}\alpha^i\beta^j.
\end{aligned}$$

For a second order tensor $A(\cdot, \cdot)$, we define the transposition $A^\top(\cdot, \cdot)$ as $[A^\top]_{ij} = [A]_{ji}$, that is, $A^\top(\alpha, \beta) = [A^\top]_{ij}\alpha^i\beta^j = [A]_{ji}\alpha^i\beta^j$.

Contents

Chapter 1

Introduction

Recently, control of walking robots has become an active research area. As the technology for walking robots evolves, an optimization problem of gaits with respect to the energy consumption becomes increasingly important. However, some factors make it very difficult to design a priori the optimal walking trajectory. One factor is that the avoidance of falling down has to be considered unlike motion planning of robot manipulators. Another factor is that the model of walking motion is complicated. Since a collision between a foot and the ground causes a discontinuous change in velocity, the behavior of the walking robot is generally described by a nonlinear hybrid system.

Most of walking pattern generation and control methods have been based on the zero moment point (ZMP) criterion, e.g., [91, 84, 35, 43]. The ZMP is defined as the point on the ground where the resultant ground-reaction force acts. The main idea of the ZMP based framework is as follows. Firstly, a desired trajectory of the center of mass is designed so that the ZMP remains inside the convex hull of the foot support region. Then with this trajectory, a desired trajectory of each joint is calculated by the inverse kinematics. Finally, a controller is designed to achieve trajectory tracking control. This method can generate stable walking pattern of the walking robot with multi degrees of freedom, where stable walking means that the robot does not fall, and its implementation is relatively easy. However, the desired trajectory of the center of mass is designed heuristically in many cases and energy efficiency has not been considered sufficiently. Passive dynamic walker studied by McGeer [53] also attracts attention. This robot has a certain simple structure and it walks down on a gentle slope with no actuation of any kind, i.e., powered only by gravity. The dynamics of the robot intrinsically possesses a stable limit cycle, even though the region of attraction is small and the gait is very sensitive to changes in its environment and physical parameters of the robot. Behavior analysis of passive walkers were studied by, e.g., [60, 66]. Walking control methods based on passive dynamic walking have been proposed by many researchers, e.g. [30, 82, 3, 2], as is antithetical to the ZMP based control with respect to the energy consumption. The generated gaits are energy efficient. However, these methods are only applicable to certain specially structured robots so far. Besides those methods, walking control methods using virtual constraints based on the output zeroing control are proposed in [32, 39]. Since appropriately chosen holonomic constraints reduce the order of the system, these methods are applicable to complicated robots such as the robot with multi degrees of freedom, under actuation and so on. However, there is no systematic way to choose constraints which generate a target motion, and such constraints consume a lot of control energy.

Gait generation frameworks based on random search are also studied, e.g., [86, 36]. The method can generate unknown walking pattern without information of the plant system. However, since it randomly explores the whole search space, it can not work with high dimensional problems: so called curse of dimensionality is well known.

On the other hand, we consider that physical property and learning control are useful tools to tackle this challenging problem. The ultimate goal of this thesis is to propose a novel optimal gait generation framework based on these tools with stochastic control theory. This thesis consists of two parts: control of deterministic Hamiltonian systems and that of stochastic Hamiltonian systems. In the former part, we will propose an extension of iterative learning control (ILC) of Hamiltonian systems mentioned later to deal with optimal gait generation problem. In the latter part, we will introduce a stochastic Hamiltonian system and clarify some useful properties of the system. We will show that these properties are generalizations of those of deterministic Hamiltonian systems and they are fundamental bases to achieve our aim.

Physical systems are practically important and they have good properties for the control design such as passivity, symmetry and so on. Hamiltonian systems have been introduced to represent physical systems and they explicitly possess such characteristics. We consider walking robots as Hamiltonian systems, rather than as just nonlinear systems, and take advantage of their physical properties. Iterative learning control based on variational symmetry of Hamiltonian systems was proposed and it allows one to solve a class of optimal control problems by iteration of laboratory experiments. Thanks to the symmetric property, it does not require the precise knowledge of the plant model and it can deal with infinite dimensional optimal control problems, more concretely, optimal control problems on L_2 signal space will be considered. Although this method works well for some control problems, it can not be directly applied to the optimal gait generation problem for several reasons mentioned in the next section. In the former part of this thesis, we will propose some techniques which extend this method in order to deal with the walking motion, and will eventually construct an optimal gait generation framework based on variational symmetry of Hamiltonian systems.

So far many conventional results of iterative learning control assume an ideal experimental environment, that is, any environmental disturbance and measurement noise during experiments are not considered. Since walking robots dynamically interact with their environment and there must exist measurement noise in experiments with real robots, it is very important to take such disturbances into account. However, standard disturbance attenuation methods, e.g. robust and adaptive control methods, are not available, because we do not know the plant model. In this thesis, we consider the plant system with the above uncertainties as a stochastic system and we focus on stochastic control theory to take disturbances during experiments into account. The dynamics of a stochastic system is described by a stochastic differential equation and its solution is a random process, so this system inherently has uncertainty. In the latter part of the thesis, we will introduce stochastic Hamiltonian systems which are extension of deterministic Hamiltonian systems. Furthermore, we will clarify some of their properties such as passivity and symmetry. They play important roles in the proposed novel learning control method based on stochastic physical properties.

In the following sections we shall outline the proposed methods in this thesis, that is, an optimal gait generation framework based on variational symmetry of Hamiltonian systems and some fundamental results of stochastic Hamiltonian systems. A brief overview of the organization of this thesis will follow them.

1.1 Control of deterministic Hamiltonian systems

As explained above, the first part of the thesis focuses on control of deterministic Hamiltonian systems, particularly iterative learning control based on variational symmetry of those systems.

As one of the representations of physical systems, Hamiltonian systems have been introduced [52, 88]. They can represent not only the conventional Hamilton's canonical equations [13] but also passive electro-mechanical systems, mechanical systems with nonholonomic constraints [90] and so on. Iterative learning control method based on variational symmetry of Hamiltonian systems was proposed by Fujimoto et al. [27]. The original result of iterative learning control proposed by Arimoto et al. [1] is an algorithm to generate a feedforward input achieving a trajectory tracking control on a finite time interval by repeating laboratory experiments. Since this algorithm does not require the precise model of the plant system, it is robust against modeling errors and many researchers worked on this topic, e.g. [12, 94]. While the conventional iterative learning control algorithm was only applicable to trajectory tracking control problems, the method in [27] can deal with a class of optimal control problems by taking advantage of variational symmetry of Hamiltonian systems. Here let us illustrate the iterative learning control scheme in [27].

Suppose a mechanical system with the input u and the output y on a finite time interval. In the case of robot manipulators, for example, y represents a set of the joint angles of the links, and u represents a set of the control torques acting on the joints. Firstly we set a cost function $\Gamma(u, y)$, which is a functional with respect to u and y to achieve a control objective. Secondly, we execute the first laboratory experiment with an initial condition and an appropriate initial control input $u_{(1)}$ and then we obtain the output data $y_{(1)}$. By an iteration law with the first experimental data $u_{(1)}$ and $y_{(1)}$, we calculate an updated control input $u_{(2)}$. We execute the second experiment with $u_{(2)}$ under the same initial condition and repeat these procedures. Eventually, optimal feedforward input u_d and output trajectory y_d which (locally) minimize the cost function $\Gamma(u, y)$ are generated. This method employs the adjoint system of the plant system in its iteration law. Although calculating the input-output data of the adjoint system generally requires the precise knowledge of the plant system, variational symmetry, which is related to a self-adjoint property of Hamiltonian systems, allows one to calculate the data by only input-output data of the plant system. The details of the adjoint systems of Hamiltonian systems and derivation of the iteration law will be referred in Section 2.1.

There are mainly two difficulties to apply the conventional iterative learning control method in [27] to the optimal gait generation problem. The first one is that this method can not deal with a functional of the time derivative of the output $\dot{y}$ as a cost function. The signal $\dot{y}$ represents the generalized velocity of mechanical systems. Since the behavior of the generalized velocity severely affects the walking motion, it is important to check $\dot{y}$ for the optimal gait generation problem. The other difficulty is that the conventional learning method can not take discontinuous state transitions into account. As already mentioned, such discontinuous changes involved in general walking motions also have to be considered. Chapter 2 will solve these problems. Firstly, we will propose an extension by employing a pseudo adjoint operator of the time derivative operator. This extended method enables us to optimize a new cost function defined in Section 2.3 which consists of the constraint term with respect to necessary conditions for periodic trajectories, and the minimization term of the L_2 norm of the control input. The necessary conditions considered here are that the configuration coordinate and the generalized velocity of the robot just before the collision are equivalent to those just after the collision. Since this cost function is a functional of $\dot{y}$, the conventional learning method in [27] can not deal with it. Secondly, we call a function which maps from the velocity just before the collision to that just after the collision, the transition mapping. We will consider this mapping to be a general nonlinear function and the Jacobian of the mapping will be estimated by the least-squares with stored experimental data. Then we will combine the two proposed method. The extended learning control method with the pseudo adjoint of the time derivative operator is utilized to learn the continuous part of a walking trajectory and the estimation algorithm is utilized to learn the discontinuous state transition part. The proposed framework is expected to generate an optimal periodic gait trajectory which minimizes the L_2 norm of the control input. Furthermore, this method does not require the information of the robot parameters nor the model of the transition mapping.

Since the proposed method in Chapter 2 is classified as iterative learning control framework, it requires a lot of laboratory experiments under the same initial condition as well as many conventional results, e.g. [1, 12, 27]. However, this experimental condition with respect to the initial condition is sometimes strict, because it is difficult to realize the desired initial velocity of the mechanical systems including walking robots. To solve the problem, Chapter 3 will propose a repetitive control type optimal gait generation framework based on learning optimal control of Hamiltonian systems and virtual constraints. In this thesis, we refer to the combination of iterative learning control (ILC) [27] and iterative feedback tuning (IFT) [19] based on variational symmetry of Hamiltonian systems as learning optimal control of Hamiltonian ones. While iterative learning control [1, 12, 27] is to find an optimal feedforward input minimizing a given cost function, iterative feedback tuning [9, 37, 19] is to find optimal parameters of a given feedback controller. Figure 1.1 illustrates the difference between them.

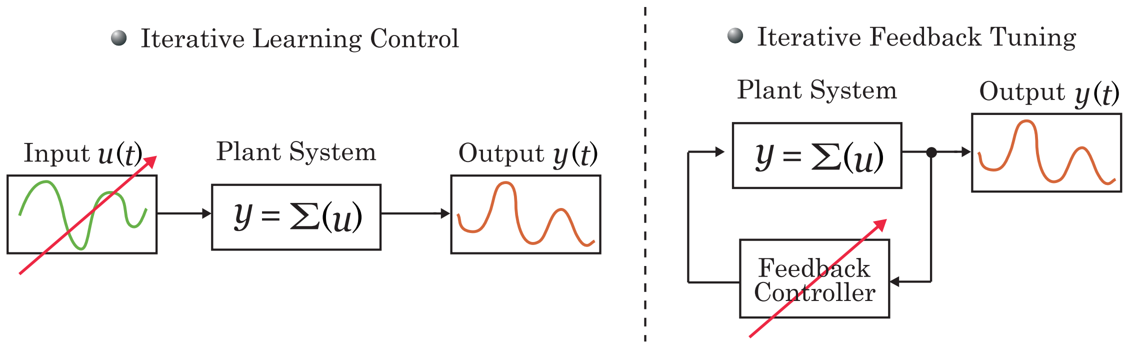

Figure 1.1: Illustrations of ILC and IFT

A conventional repetitive control method [33, 29, 22] is also a kind of a learning method for a trajectory tracking control problem with time periodic reference trajectories. Only the difference between repetitive control and iterative learning control is the type of the reference trajectories: time periodic one (with the infinite length) and one on a finite time interval, respectively. However, repetitive control for optimal control problems, as in the iterative leaning control case, was not investigated so far. Since an iteration procedure of the proposed method in Chapter 3 is automatically executed and eventually an optimal periodic walking trajectory is expected to be generated, it is classified as repetitive control framework rather than iterative learning control one. Figures 1.2 and 1.3 illustrate the difference between the proposed methods in Chapters 2 and 3. The repetitive control type optimal gait generation method is summarized as follows.

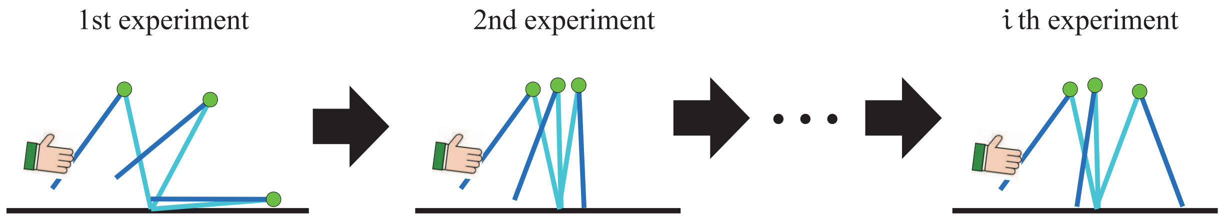

Figure 1.2: Illustration of the proposed method in Chapter2 (Iterative learning control type)

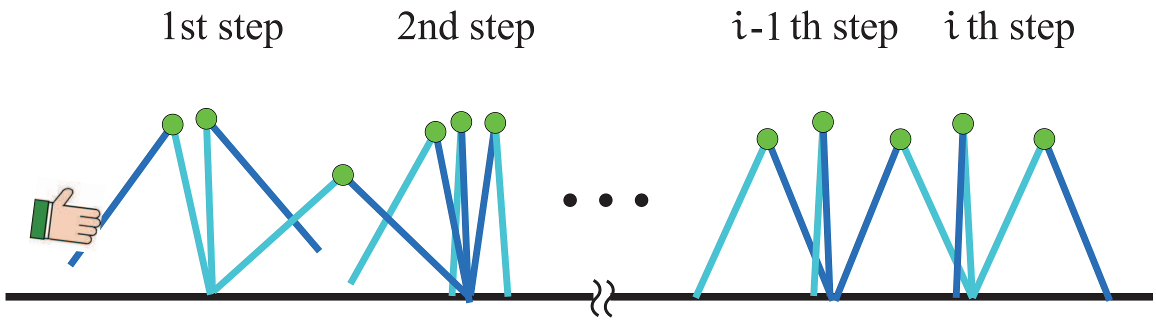

Figure 1.3: Illustration of the proposed method in Chapter3 (Repetitive control type)

Firstly, we add a constraint by adding a virtual potential energy to prevent the robot from falling. Secondly, we execute the learning procedure proposed in Chapter 2. The proposed technique restricts the motion of the robot to a symmetric trajectory by the virtual constraint. Due to this additional constraint, we does not need to repeat experiments under the same initial condition. Thirdly, by regarding the potential gain for the constraint as a tuning parameter, we execute iterative feedback tuning to mitigate the strength of the virtual constraint automatically according to the progress of learning control. Consequently, it is expected to generate an optimal gait without constraint eventually. In this method ILC and IFT of Hamiltonian systems are utilized simultaneously. However, since both methods influence each other, they regularly can not be used simultaneously. In order to take interference of both methods into account, we will introduce an extended system which again has variational symmetry. By considering the extended system instead of the plant system, we will be able to apply ILC and IFT simultaneously.

1.2 Control of stochastic Hamiltonian systems

There exist various disturbances such as measurement noise, modeling error and so on in controlling real plants. Since they sometimes cause performance degradation or destabilization of the plant system, it is important to consider them. Stochastic control theory is one of the efficient ways which can take such disturbances into account. Theories and techniques for the deterministic dynamical systems described by ordinary differential equations are applied to stochastic ones described by stochastic differential equations [40]. In the literatures [54, 55, 28], the notions of conserved quantities and symmetry are formulated for the stochastic systems described by stochastic differential equations written in the senses of Itô and Stratonovich. Lyapunov function approaches to the stochastic stability of stochastic systems are introduced in [10, 48]. In these frameworks, nonnegative supermartingales are used as stochastic Lyapunov functions, and asymptotic convergence of sample trajectories, or flows of the stochastic differential equations is proven by the martingale convergence theorem (see also [34, 50, 51]). The notion of the stochastic passivity for the stochastic systems is introduced in [16]. One can utilize the well-known results of the stabilization method by the output feedback for the passive systems [92, 93, 11] to achieve the asymptotic stability for the stochastic nonlinear systems in probability.

The aim of Chapter 4 is to introduce Stochastic (Port-)Hamiltonian Systems (SPHSs) which are extension of (port-)Hamiltonian systems, and clarify some of their properties. Here a port-Hamiltonian system [52, 90, 88] is an input-affine Hamiltonian system. Although deterministic Hamiltonian systems intrinsically have some properties such as invariance under a class of transformations and passivity, stochastic Hamiltonian ones do not always possess similar properties. Firstly, we concentrate on the time-invariant case and will show a necessary and sufficient condition to preserve the stochastic Hamiltonian structure of the original system under time-invariant coordinate transformations. Secondly, we will derive a condition to maintain stochastic passivity of the system. Thirdly, we will introduce stochastic generalized canonical transformations which are extension of generalized canonical transformations proposed in [25]. Stochastic generalized canonical transformations are pairs of coordinate and feedback transformations under which the stochastic Hamiltonian structure is preserved. Finally, we will propose a stabilization method based on stochastic passivity and stochastic generalized canonical transformations. The stabilization framework is summarized as follows: we transform a stochastic Hamiltonian system (Fig. 1.4) to another stochastic passive one (Fig. 1.5) by a generalized canonical transformation and then stabilize the transformed system by the output feedback based on stochastic passivity (Fig. 1.6). Although stabilization of general nonlinear stochastic systems is very difficult,

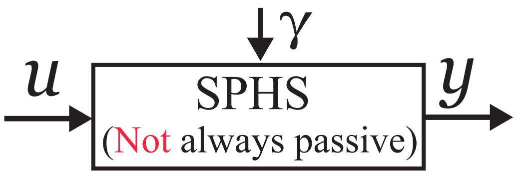

Figure 1.4: Plant system

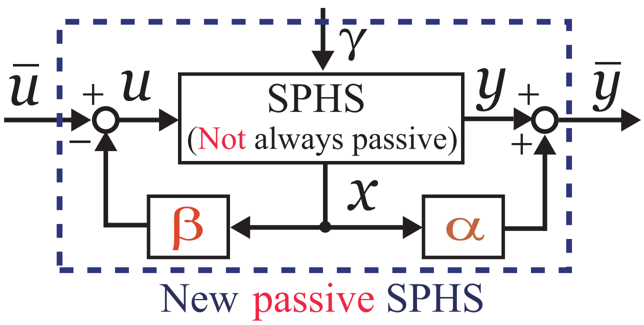

Figure 1.5: Transformed system by a generalized canonical transformation

the proposed framework can achieve stochastic stabilization easily and intuitively. We will also extend the results on the time-invariant stochastic Hamiltonian systems to the time-varying case.

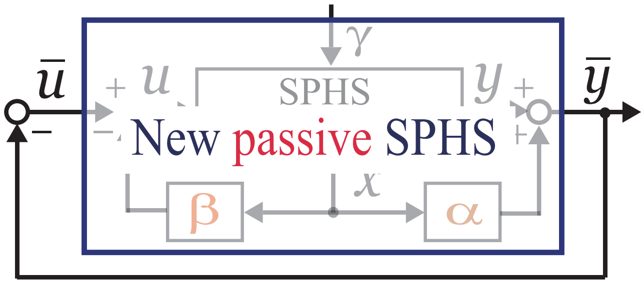

Figure 1.6: Closed loop system via the output feedback

Then Chapter 5 will consider an observer based stochastic trajectory tracking control problem. A motivation is that the proposed controllers in Chapter 4 are state feedback ones, so full state information is necessary to implement them. However, in practice, there are a lot of mechanical systems whose position measurements are only available because of the lack of velocity sensors. On output feedback control of deterministic mechanical systems, various methods are proposed, e.g. [85, 83, 58]. Observer based control is also studied by many researchers in, e.g., [56, 5], where the velocity signal is reconstructed by an observer and is utilized for a state feedback controller instead of the true signal. On the other hand, in the stochastic control research area, there are few methods to deal with such a problem. A stochastic output feedback stabilization controller based on the backstepping technique is proposed in [14]. However, a stochastic trajectory tracking framework by only using position measurements is not considered so far. Here we assume that only position measurements are available. Velocity information is reconstructed by the position information. We will consider general mechanical systems in the presence of noise as stochastic systems and will derive conditions for stabilizing and tracking controllers based on [81, 61, 5] to achieve each control objective. The controller and observer proposed in [81, 5] utilize the sliding mode control theory. By taking advantage of those results, the proposed method will provide conditions for controller and observer gains under which the norm of the set of tracking and estimation errors remains arbitrarily small in probability. Figure 1.7 shows a conceptual illustration of the proposed framework.

Off course, stochastic stabilization and trajectory tracking control frameworks proposed in Chapters 4 and 5 play important roles in the proposed novel learning control method based on stochastic physical properties. Before the conventional iterative learning control method for deterministic systems is applied, feedback controllers are typically employed to the control system in order to render the system asymptotically stable. Moreover, since the learning control method generates an optimal feedforward control input, the generated periodic optimal trajectory should be orbitally stabilized by a kind of trajectory tracking control scheme. So the proposed techniques in Chapters 4 and 5 are necessary.

Eventually, Chapter 6 will introduce the variational and its adjoint systems of stochastic Hamiltonian systems and will reveal some of their properties, particularly a property corresponding to variational symmetry of deterministic Hamiltonian systems, which is fundamental to optimal learning control of Hamiltonian systems mentioned in Chapters 2 and 3. Firstly we will define the variational systems of general nonlinear stochastic systems. Then their adjoint systems will be defined based on systems utilized in the stochastic maximum principle in stochastic optimal control, e.g. [95]. Here let us note that the stochastic adjoint system is a nontrivial

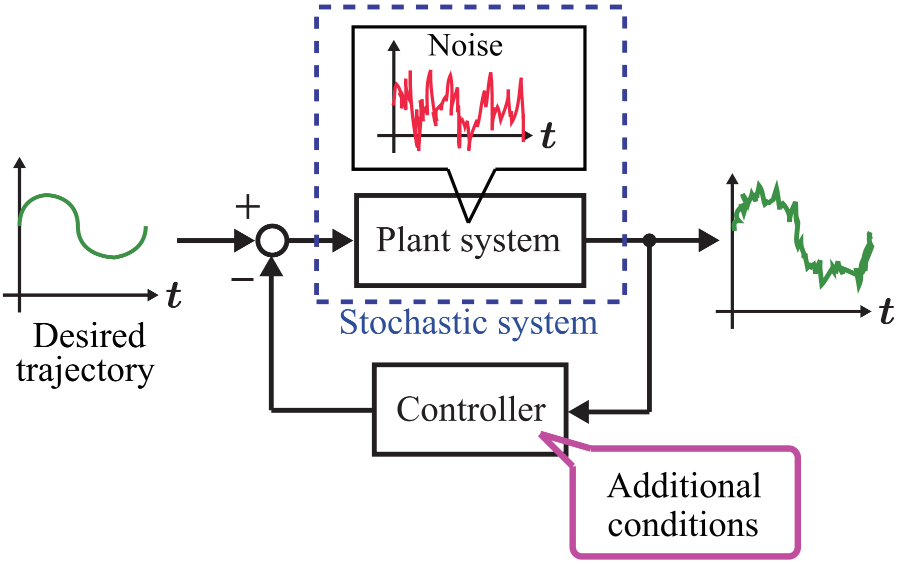

Figure 1.7: Illustration of the proposed framework

extension of the deterministic one [13]. An input-output relation between the variational and its adjoint systems will be shown. Secondly, stochastic Hamiltonian systems will be focused on. We will show that the variational system of a stochastic Hamiltonian system is described by another linear one. Then we will derive a condition under which the adjoint system coincides with the time-reversal version of the variational one. It will be proven that this property is an extension of variational symmetry of deterministic Hamiltonian systems.

1.3 Goals and contributions of this thesis

In this thesis, the ultimate goal is to develop a novel optimal gait generation framework based on physical property and learning control with stochastic control theory. This aim is tackled from two approaches. The first approach is control of deterministic Hamiltonian systems and the other is that of stochastic Hamiltonian ones. Since Hamiltonian systems can represent many important practical systems, we can provide a unified framework for walking robots with various degrees of freedom, numbers of legs and leg structures. In addition, since our framework is based on iterative learning control of Hamiltonian systems [27], we can solve a class of infinite dimensional optimal control problems without using the precise knowledge of the plant model.

In the former part, firstly, Chapter 2 proposes an extension method of the conventional learning method of Hamiltonian systems [27], because the conventional method can not be applied to the optimal gait generation problem. Then we propose an iterative learning control type optimal gait generation framework of Hamiltonian systems considering discontinuous state transitions. Although the discontinuous transition phenomena by collisions are often modeled as transition mappings with the conservation law of the angular momentum, the angular momentum is not preserved exactly for real robots. The proposed framework is expected to generate an optimal periodic gait trajectory which minimizes the L_2 norm of the control input and it does not require the precise information of the robot model nor the transition mapping. Secondly, Chapter 3 proposes a repetitive control type optimal gait generation framework by utilizing virtual constraints. While standard iterative learning control frameworks require initializations and executions of laboratory experiments, in the proposed framework, a learning procedure is automatically executed and then an optimal periodic walking trajectory is expected to be generated eventually. A repetitive control approach such as the proposed method for optimal control problems was not investigated so far.

In the latter part, firstly, Chapter 4 introduces stochastic (port-)Hamiltonian systems. It has not been considered so far a non-autonomous stochastic Hamiltonian system whose dynamics is described by a stochastic differential equation written in the sense of Itô. Some properties of the system such as stochastic passivity and invariance under a class of transformations are clarified. A stabilization method is proposed based on stochastic passivity and stochastic generalized canonical transformations. Although stabilization of general nonlinear stochastic systems is very difficult, the proposed framework can achieve stochastic stabilization easily and intuitively. Secondly, Chapter 5 considers an observer based stochastic trajectory tracking control framework. Conditions for controller and observer gains are proposed under which the norm of the set of tracking and estimation errors remains arbitrarily small in probability. A stochastic trajectory tracking framework by only using position measurements is not considered so far. Finally, Chapter 6 defines the variational and its adjoint systems of stochastic Hamiltonian systems. Furthermore, we provide a condition under which the stochastic Hamiltonian system has a symmetric property corresponding to variational symmetry of deterministic Hamiltonian systems which plays an important role in the novel learning control method based on stochastic physical properties.

By regarding the plant system with disturbances as a stochastic system and taking advantage of the above results, we can take uncertainties during the learning such as environmental disturbance and measurement noise into account. These disturbances have not been dealt with in many conventional results of iterative learning control. Such learning framework based on a stochastic physical system's properties has not been proposed. We believe that the results obtained herein contain significant contributions to various optimal motion planning problems of mechanical systems and provide a new application of stochastic control.

1.4 Organization of the thesis

Chapter 2 proposes an iterative learning control type optimal gait generation framework of Hamiltonian systems considering discontinuous state transitions. The main result follows a brief reference to variational symmetry of Hamiltonian systems and the conventional iterative learning control method based on this property [27]. We propose a cost function by which an optimal periodic trajectory minimizing the L_2 norm of the control input is expected to be generated. Then an iteration law with respect to the cost function is derived by combining the iterative learning control method and the estimation of the discontinuous transition mapping by the least-squares. Numerical simulations of the compass gait biped demonstrate the validity of the proposed framework.

Chapter 3 proposes a repetitive control type optimal gait generation framework by utilizing virtual constraints and learning optimal control of Hamiltonian systems. In this novel framework, a learning procedure is automatically executed and eventually an optimal periodic walking trajectory is expected to be generated. Here the combination of iterative learning control (ILC) [27] and iterative feedback tuning (IFT) [19] based on variational symmetry of Hamiltonian systems are referred to as learning optimal control of Hamiltonian systems. A brief explanation of iterative feedback tuning is provided. We equip virtual constraints to prevent the walking robot from falling. Then we introduce an extended system which has again variational symmetry in order to utilize ILC and IFT simultaneously. The algorithm of the main result is exhibited. Numerical simulations of the compass gait biped with a torso demonstrate the validity of the proposed method.

Chapter 4 introduces stochastic (port-)Hamiltonian systems and clarifies some of their properties. Firstly, we concentrate on the time-invariant case. We show a necessary and sufficient condition to preserve the stochastic Hamiltonian structure of the original system under time-invariant coordinate transformations. A condition to maintain stochastic passivity of the system is also derived. Then we introduce stochastic generalized canonical transformations which are pairs of coordinate and feedback transformations under which the stochastic Hamiltonian structure is preserved. A stabilization method is proposed based on stochastic passivity and stochastic generalized canonical transformations. Secondly, we extend the above results to the time-varying stochastic Hamiltonian systems. Numerical simulations of the rolling coin in the presence of noise exhibit the effectiveness of the proposed method.

Chapter 5 considers an observer based stochastic trajectory tracking control framework. Here we assume that only position measurements are available. Velocity information is reconstructed by the position information. We consider general mechanical systems as stochastic ones and derive conditions for stabilizing and tracking controllers based on [81, 61, 5] to achieve each control objective in the presence of noise. Conditions for controller and observer gains are proposed under which the norm of the set of tracking and estimation errors remains arbitrarily small in probability. Numerical simulation of a 2-link robot manipulator in the presence of noise demonstrates the effectiveness of the proposed method.

Chapter 6 addresses the variational and its adjoint systems of stochastic Hamiltonian systems and reveals some of their properties, particularly an extension of variational symmetry of deterministic Hamiltonian systems. Firstly, we investigate the variational and its adjoint systems of general nonlinear stochastic systems in a manner analogous to the deterministic ones. Secondly, we focus on stochastic Hamiltonian systems. It is proven that the variational system of the stochastic Hamiltonian system is described by another linear one. Then, we derive a condition under which the adjoint system coincides with the time-reversal version of the variational one. This property corresponds to variational symmetry of deterministic Hamiltonian systems which plays an important role in learning optimal control mentioned in Chapters 2 and 3.

In Chapter 7, we present a brief summary of the thesis. This is followed by concluding remarks and discussions for future research.

Pathways through the thesis

For those only interested in applications to optimal gait generation for walking robots from the viewpoint of deterministic control, the following sequence is recommended: Chapters 1, 2, 3 and 7. For extension of the above techniques to stochastic control framework, Chapters 4 and 6 should be included in the pathway. For those only interested in control of stochastic systems, the following sequence is recommended: Chapters 1, 4, 5, (6) and 7.

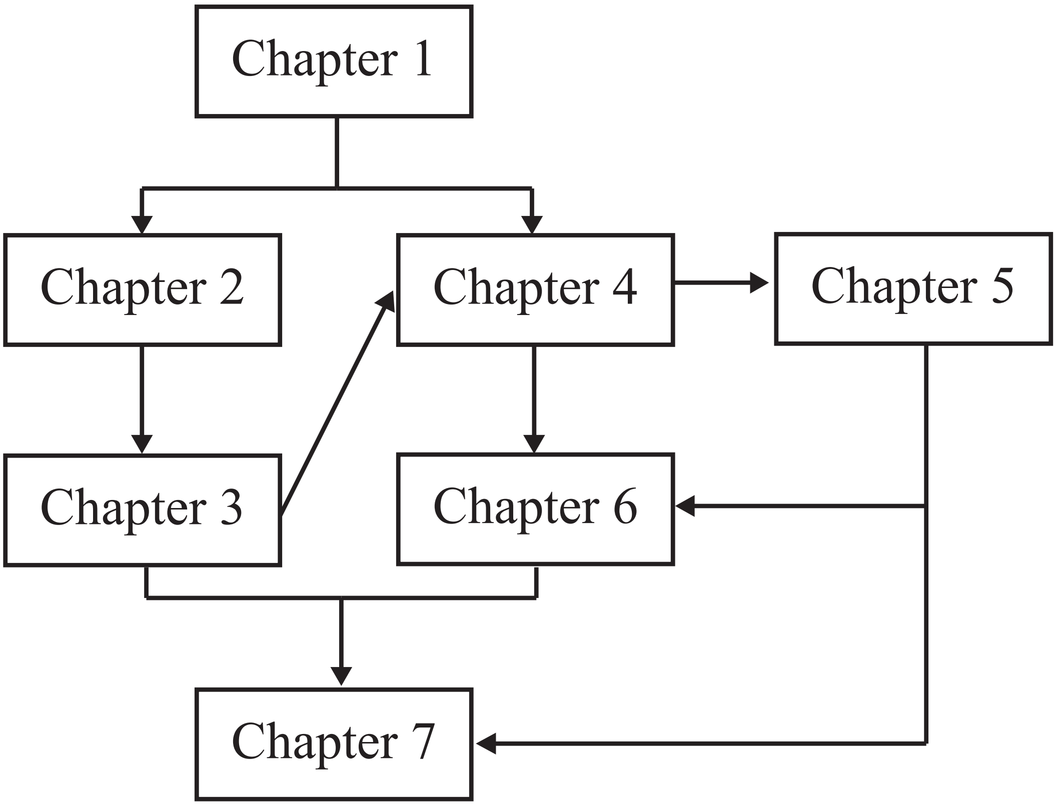

Figure 1.8: Logical dependence of the chapters

Chapter 2

Iterative learning control framework considering discontinuous state transitions

In this chapter, we propose a framework to generate an optimal gait trajectory via iterative learning control (ILC) method based on a symmetric property of Hamiltonian systems considering discontinuous state transitions.

In Section 2.1, Hamiltonian systems and their symmetric property called **variational symmetry** are referred to and then an iterative learning control method of Hamiltonian systems based on the property [27, 17, 18] is explained.

In section 2.2, the compass gait biped is mentioned as a plant system, which is a full-actuated planar compass-like biped robot, and is often considered as a classical benchmark problem, e.g. [53, 31].

In section 2.3, the main result of this chapter is proposed. Firstly, a cost function is defined, by which one can generate an (at least locally) optimal periodic trajectory minimizing the L_2 norm of the control input. Then, an iteration law with respect to the cost function is derived. We equip an extension of the conventional iterative learning control method by employing a pseudo adjoint operator of the time derivative operator in order to deal with the new cost function defined in this section. Generally in walking motions, there are discontinuous state transitions caused by collisions between a foot of a walking robot and the ground. However, the conventional iterative leaning control framework does not deal with such discontinuous transitions [27, 17, 18]. Furthermore, although the transition phenomena are often modeled as transition mappings with the conservation law of the angular momentum, the angular momentum is not preserved exactly for real robots. In the proposed framework, the transition mapping is considered to be a general nonlinear function and the Jacobian of the mapping is estimated by the least-squares with stored experimental data. Then we combine the extended learning control method with the pseudo adjoint operator to learn the continuous part of a walking trajectory, and the estimation method with the least-squares to learn the discontinuous state transition part. The proposed framework does not require the information of the robot parameters nor the transition mapping.

Finally, in section 2.4, this technique is applied to the compass gait biped in order to generate an optimal gait trajectory on the level ground. Numerical simulations demonstrate the validity of the proposed framework.

2.1 Iterative learning control (ILC) based on variational symmetry of Hamiltonian systems

This section refers to iterative learning control based on variational symmetry of Hamiltonian systems [27, 17, 18], which is an important basis for our framework. Firstly, a Hamiltonian system is considered as a plant system in this chapter. Secondly, a symmetric property of this system called variational symmetry [27] is mentioned. This property relates the variational system of the Hamiltonian system and its adjoint system. Finally, an iteration algorithm utilizing this property for ILC is derived.

2.1.1 Hamiltonian systems and variational symmetry

We consider a Hamiltonian system with dissipation [13, 52, 88]. This system is one of the representations of the physical systems and it includes not only the conventional Hamiltonian systems [13] but also passive electro-mechanical systems, mechanical systems with nonholonomic constraints [90] and so on. It is described as

$$(x_{t^1}, y) = \Sigma(x_{t^0}, u) \ : \ \begin{cases} \dot{x} &= (J(x,t) - R(x,t)) \dfrac{\partial H(x,u,t)}{\partial x}^\top, \quad x(t^0) = x_{t^0} \\ y &= -\dfrac{\partial H(x,u,t)}{\partial u}^\top \\ x_{t^1} &= x(t^1) \end{cases} . \tag{2.1}$$

Here $x(t) \in \mathbb{R}^n$ and $u(t), y(t) \in \mathbb{R}^m$ describe the state, the input and the output, respectively. The structure matrix $J(x,t) \in \mathbb{R}^{n\times n}$ and the dissipation matrix $R(x,t) \in \mathbb{R}^{n\times n}$ are skew-symmetric and symmetric positive semi-definite, respectively. In this thesis, we consider behaviors of the system (2.1) on a finite time interval $[t^0, t^1]$ and often describe the system as $\Sigma : X \times U \to X \times Y : (x_{t^0}, u) \mapsto (x_{t^1}, y)$ with Hilbert spaces X, U and Y. Typically, $X = \mathbb{R}^n$ and $U, Y = L_2^m[t^0, t^1]$. In considering the input-output mapping under a fixed initial state x_{t^0}, the system is described as $\Sigma^{x_{t^0}} : U \to Y : u \mapsto y$. Here let us recall the Fréchet derivative of nonlinear operators.

Definition 2.1 Consider an operator $f : \tilde{X} \to Y$ with Banach spaces X and Y, and an open subset $\tilde{X} \subset X$. f is said to be *Fréchet differentiable* at $x \in \tilde{X}$ if there exists an operator $\delta f : \tilde{X} \times X \to Y$ such that $\delta f(x)(\xi)$ is linear in ξ and the following holds: For $^\forall \xi \in X$ such that $x + \xi \in \tilde{X}$,

$$f(x+\xi) = f(x) + \delta f(x)(\xi) + o(\|\xi\|_X),$$

where

$$\lim_{\|\xi\|_X \to 0} \frac{o(\|\xi\|_X)}{\|\xi\|_X} = 0. \tag{2.2}$$

Under these circumstances, $\delta f(x)(\cdot)$ is called the *Fréchet derivative* of f at x.

The variational system $\delta\Sigma$ is the Fréchet derivative of the system Σ. Let us refer to the following lemma.

Lemma 2.1 *[27] Consider the Hamiltonian system Σ in* (2.1)*. Suppose that J and R are constant. Then the variational system of Σ is described by another linear Hamiltonian system*

$$(x_{v,t^1}, y_v) = (\delta\Sigma(x_{t^0}, u))(x_{v,t^0}, u_v):$$
$$\begin{cases} \dot{x} &= (J-R)\dfrac{\partial H(x,u,t)}{\partial x}^\top, \qquad x(t^0) = x_{t^0} \\ \dot{x}_v &= (J-R)\dfrac{\partial H_v(x,u,x_v,u_v,t)}{\partial x_v}^\top, \quad x_v(t^0) = x_{v,t^0} \\ y_v &= -\dfrac{\partial H_v(x,u,x_v,u_v,t)}{\partial u_v}^\top \\ x_{v,t^1} &= x_v(t^1) \end{cases}, \tag{2.3}$$

where the controlled Hamiltonian $H_v(x,u,x_v,u_v,t)$ is given by

$$H_v(x,u,x_v,u_v,t) = \frac{1}{2}\begin{pmatrix} x_v \\ u_v \end{pmatrix}^\top \frac{\partial^2 H(x,u,t)}{\partial(x,u)^2}\begin{pmatrix} x_v \\ u_v \end{pmatrix}.$$

The adjoint operator plays an important role in solving optimal control problems, e.g.[64]. The adjoint system of the variational system is defined by

$$(x_{a,t^0}, y_a) = (\delta\Sigma(x_{t^0}, u))^*(x_{a,t^1}, u_a): \tag{2.4}$$
$$\begin{cases} \dot{x} &= (J-R)\dfrac{\partial H(x,u,t)}{\partial x}^\top, \quad x(t^0) = x_{t^0} \\ \begin{pmatrix} \dot{x}_a \\ y_a \end{pmatrix} &= \begin{pmatrix} -I_n & O_{nn} \\ O_{nn} & I_n \end{pmatrix}\left(\begin{pmatrix} J-R & O_{nn} \\ O_{nn} & -I_n \end{pmatrix}\dfrac{\partial^2 H(x,u,t)}{\partial(x,u)^2}\right)^\top\begin{pmatrix} x_a \\ u_a \end{pmatrix}, \\ & x_a(t^1) = x_{a,t^1} \\ x_{a,t^0} &= x_a(t^0) \end{cases}$$

where I_n and O_{nn} denote the $n \times n$ identity matrix and the $n \times n$ zero matrix, respectively [13, 27].

For the system (2.1), the following lemma holds. This property is called **variational symmetry** of Hamiltonian systems.

Lemma 2.2 *[27] Consider the Hamiltonian system* (2.1)*. Suppose that J and R are constant and $J-R$ is nonsingular and that there exists a nonsingular matrix $T \in \mathbb{R}^{n\times n}$ satisfying*

$$J = -TJT^{-1}, \qquad R = TRT^{-1} \tag{2.5}$$

$$\frac{\partial^2 H(x,u,t)}{\partial(x,u)^2} = \begin{pmatrix} T & O_{nn} \\ O_{nn} & I_n \end{pmatrix}\frac{\partial^2 H(x,u,t)}{\partial(x,u)^2}\begin{pmatrix} T^{-1} & O_{nn} \\ O_{nn} & I_n \end{pmatrix}. \tag{2.6}$$

Then a state-space realization of the adjoint of the variational system coincides with a time-reversal version of that of the variational system (2.3)*, that is,*

$$(x_{a,t^0}, y_a) = (\delta\Sigma(x_{t^0}, u))^*(x_{a,t^1}, u_a) :$$
$$\begin{cases} \dot{x} &= (J-R)\dfrac{\partial H(x,u,t)}{\partial x}^\top, \quad x(t^0) = x_{t^0} \\ \dot{\bar{x}}_v &= -(J-R)\dfrac{\partial H_v(x,u,\bar{x}_v,u_a,t)}{\partial \bar{x}_v}^\top, \\ & \quad \bar{x}_v(t^1) = -(J-R)T\; x_{a,t^1} \\ y_a &= -\dfrac{\partial H_v(x,u,\bar{x}_v,u_a,t)}{\partial u_a}^\top \\ x_{a,t^0} &= -T^{-1}(J-R)^{-1}\bar{x}_v(t^0) \end{cases} . \tag{2.7}$$

Regarding variational symmetry, the following theorem is useful.

Theorem 2.3 *[18, 19] Consider the Hamiltonian system* (2.1) *and suppose that conditions of lemma 2.2 are satisfied. Suppose moreover that, for two inputs $v, w \in U$, the corresponding state trajectories $\phi(t), \psi(t) \in X, t \in [t^0, t^1]$ satisfy*

$$\mathcal{R}\left(\left.\frac{\partial^2 H(x,u,t)}{\partial (x,u)^2}\right|_{\substack{x=\phi \\ u=v}}\right) = \left.\frac{\partial^2 H(x,u,t)}{\partial (x,u)^2}\right|_{\substack{x=\psi \\ u=w}}, \tag{2.8}$$

where $\mathcal{R}$ represents the time reversal operator on $[t^0, t^1]$ defined by

$$\mathcal{R}(u)(t) = u(t^1 - t + t^0), \quad \forall t \in [t^0, t^1]. \tag{2.9}$$

Then the following relationships hold

$$\mathcal{S}(\delta\Sigma(\phi(t^0), v))^* = (\delta\Sigma(\psi(t^0), w))\mathcal{S}, \tag{2.10}$$

$$(\delta\Sigma^{\phi(t^0)}(v))^* = \mathcal{R}(\delta\Sigma^{\psi(t^0)}(w))\mathcal{R}. \tag{2.11}$$

Here the operator $\mathcal{S} : X \times U \to X \times U$ is defined by

$$\mathcal{S}(x_{t^0}, u) := (-(J-R)Tx_{t^0}, \mathcal{R}(u)).$$

Remark 2.2 State trajectories under which the configuration coordinate q and the phase coordinate $\dot{q}$ satisfy

$$q(t) = q(t^1 - t + t^0)\,, \quad \dot{q}(t) = -\dot{q}(t^1 - t + t^0), \quad \forall t \in [t^0, t^1] \tag{2.12}$$

represent time-symmetric motions with respect to the middle point of time $t = (t^0 + t^1)/2$. We call trajectories satisfying Eq.(2.12) symmetric trajectories. Suppose a state trajectory ϕ corresponding an input v is symmetric trajectory. Then the condition (2.8) in Theorem2.3 is satisfied with $\psi = \phi$ and $w = v$, and therefore the following simpler relationships than Eqs. (2.10) and (2.11) hold

$$\mathcal{S}(\delta\Sigma(\phi(t^0), v))^* = (\delta\Sigma(\phi(t^0), v))\mathcal{S}, \tag{2.13}$$

$$(\delta\Sigma^{\phi(t^0)}(v))^* = \mathcal{R}(\delta\Sigma^{\phi(t^0)}(v))\mathcal{R}. \tag{2.14}$$

2.1.2 Optimal control via iterative learning control

This section explains how to solve a class of optimal control problems via iterative learning control utilizing variational symmetry of Hamiltonian systems referred to in the previous subsection.

Let us consider the system $\Sigma : X \times U \to X \times Y$ in (2.1) and a cost function $\hat{\Gamma}(x_{t^0}, u, x_{t^1}, y) : X^2 \times U \times Y \to \mathbb{R}$. The objective is to find an optimal input (locally) minimizing the cost function $\hat{\Gamma}$. By utilizing the relation $(x_{t^1}, y) = \Sigma(x_{t^0}, u)$, the cost function can be written by $\Gamma(x_{t^0}, u) : X \times U \to \mathbb{R} := \hat{\Gamma}((x_{t^0}, u), \Sigma(x_{t^0}, u))$. Here we can calculate the Fréchet derivative of the cost function as

$$\begin{aligned}
&\delta\hat{\Gamma}(x_{t^0}, u, x_{t^1}, y)(\delta x_{t^0}, \delta u, \delta x_{t^1}, \delta y)\\
&\quad = \delta\hat{\Gamma}((x_{t^0}, u),\Sigma(x_{t^0}, u))\left((\delta x_{t^0}, \delta u), \delta\Sigma(x_{t^0}, u)(\delta x_{t^0}, \delta u)\right)\\
&\quad = \langle \nabla\hat{\Gamma}((x_{t^0}, u), \Sigma(x_{t^0}, u)), \begin{pmatrix} \mathrm{id} \\ \delta\Sigma(x_{t^0}, u)\end{pmatrix}(\delta x_{t^0}, \delta u)\rangle_{X^2\times U\times Y}\\
&\quad = \langle (\mathrm{id}, (\delta\Sigma(x_{t^0}, u))^*)\, \nabla\hat{\Gamma}(x_{t^0}, u, x_{t^1}, y), (\delta x_{t^0}, \delta u)\rangle_{X\times U}\\
&\quad = \langle \underbrace{\nabla_{x_{t^0}}\hat{\Gamma} + \pi_X \circ (\delta\Sigma(x_{t^0}, u))^*(\nabla_{x_{t^1}}\hat{\Gamma}, \nabla_y\hat{\Gamma})}_{=:\ \nabla_{x_{t^0}}\Gamma(x_{t^0}, u)}, \delta x_{t^0}\rangle_X\\
&\qquad + \langle \underbrace{\nabla_u\hat{\Gamma} + \pi_U \circ (\delta\Sigma(x_{t^0}, u))^*(\nabla_{x_{t^1}}\hat{\Gamma}, \nabla_y\hat{\Gamma})}_{=:\ \nabla_u\Gamma(x_{t^0}, u)}, \delta u\rangle_U,
\end{aligned} \tag{2.15}$$

where id and $\pi_{(\cdot)}$ represent the identity mapping and the projection mapping onto $(\cdot)$, respectively. Well-known Riesz's representation theorem and the linearity of the Fréchet derivative guarantee that there exists a function $\nabla\hat{\Gamma}(x_{t^0}, u, x_{t^1}, y) \equiv (\nabla_{x_{t^0}}\hat{\Gamma}^\top, \nabla_u\hat{\Gamma}^\top, \nabla_{x_{t^1}}\hat{\Gamma}^\top, \nabla_y\hat{\Gamma}^\top)^\top$ as above. Since $\nabla_{x_{t^0}}\Gamma(x_{t^0}, u)$ and $\nabla_u\Gamma(x_{t^0}, u)$ in Eq.(2.15) represent gradients of the cost function with respect to the input u and the initial state x_{t^0}, respectively, one can reduce the cost function down at least to a local minimum by the following iteration law with a positive definite matrix $K_{(i)}$

$$u_{(i+1)} = u_{(i)} - K_{(i)}\nabla_u\Gamma(x_{t^0(i)}, u_{(i)}). \tag{2.16}$$

Here i denotes the i-th iteration in a laboratory experiment. However, calculation of the gradient $\nabla_u\Gamma(x_{t^0}, u)$ generally requires the precise knowledge of the plant system Σ, because it contains the output signal of $(\delta\Sigma(x_{t^0}, u))^*$ corresponding to the input signal $(\nabla_{x_{t^1}}\hat{\Gamma}, \nabla_y\hat{\Gamma})$. If the assumption in Theorem2.3 holds, the following approximation is obtained with a sufficiently small constant $\epsilon > 0$

$$\begin{aligned}
&\mathcal{S}(\delta\Sigma(x_{t^0}, u))^*(\nabla_{x_{t^1}}\hat{\Gamma}, \nabla_y\hat{\Gamma})\\
&\quad = \delta\Sigma(\psi(t^0), w)(-(J-R)T\nabla_{x_{t^1}}\hat{\Gamma}, \mathcal{R}(\nabla_y\hat{\Gamma}))\\
&\quad \approx \frac{\Sigma(\psi(t^0) - \epsilon(J-R)T\nabla_{x_{t^1}}\hat{\Gamma}, w + \epsilon\mathcal{R}(\nabla_y\hat{\Gamma})) - \Sigma(\psi(t^0), w)}{\epsilon}.
\end{aligned} \tag{2.17}$$

The approximation (2.17) enables one to execute the iteration procedure with Eq. (2.16) by only using the input-output data of the plant system Σ.

2.2 Description of the plant

Let us consider a full-actuated planar compass-like biped robot called the compass gait biped [31] depicted in Fig. 2.1. In this robot, the legs are rigid bars without knee, and they are connected by

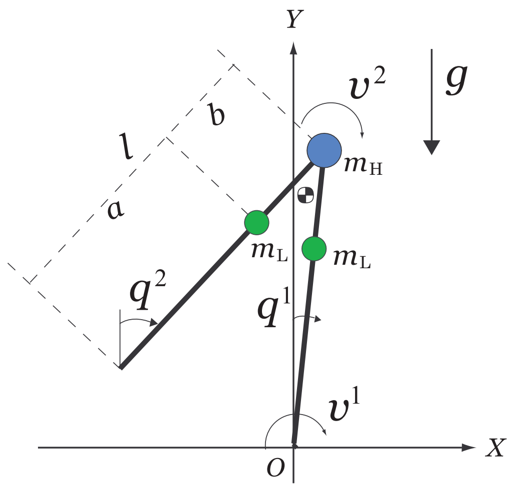

Figure 2.1: Model of the compass gait biped

a frictionless hinge at the hip. 1-period of walking describes the period between the take-off of one foot from the ground and its subsequent landing. The robot can walk down on a gentle slope without any control inputs under appropriate initial conditions [53]. Table 2.1 shows physical parameters and variables. In this thesis, we define the input u as

Table 2.1: Parameters and variables

Notation	Meaning	Unit
m_H	hip mass	kg
m_L	leg mass	kg
a	length from m_L to the ground	m
b	length from the hip to m_L	m
$l = a + b$	total leg length	m
g	gravity acceleration	$\mathrm{m/s^2}$
q^1	stance leg angle w.r.t vertical	rad
q^2	swing leg angle w.r.t vertical	rad
v^1	ankle torque	Nm
v^2	hip torque	Nm

$$u = \begin{pmatrix} u^1 \\ u^2 \end{pmatrix} := \begin{pmatrix} v^1 + v^2 \\ -v^2 \end{pmatrix} \tag{2.18}$$

in order to simplify the input-output relation in the Hamiltonian form mentioned later. Furthermore, We assume some assumptions on this robot. Some important ones are shown and the rest of them conforms [31].

Table 2.2: Some notations

Notation	Meaning
$q := (q^1, q^2)^\top$	angles of legs
$\dot{q} := (\dot{q}^1, \dot{q}^2)^\top$	angular velocities of legs
$p := (p^1, p^2)^\top$	generalized momentum
$x := (q^\top, p^\top)^\top$	state
$Q := (q^\top, \dot{q}^\top)^\top$	angles and their velocities
$(q_{t^0}, p_{t^0}) := (q(t^0), p(t^0))$	initial state
$(q_{t^1}, p_{t^1}) := (q(t^1), p(t^1))$	terminal state
$(\cdot)_{-/+}$	just before/after a discontinuous transition Note that $x_- \equiv x_{t^1}$.

Assumption 2.3 There exists a foot link whose thickness and mass can be ignored, and the ankle torque v^1 can be occurred relative to it.

Assumption 2.4 The foot of the stance leg is attached to the ground during the single support phase.

Assumption 2.5 The foot of the swing leg does not bounce back nor slip on the ground at the collision (inelastic impulsive impact is assumed).

Assumption 2.6 Transfer of support between the stance and the swing legs is instantaneous.

Assumption 2.7 The foot-scuffing during the single support phase can be ignored.

We use number of notations with respect to the state. Table 2.2 summarizes them.

A typical mechanical system can be described by a Hamiltonian system in (2.1) with the state $x = (q^\top, p^\top)^\top \in \mathbb{R}^{2m}$ as

$$\begin{cases} \begin{pmatrix} \dot{q} \\ \dot{p} \end{pmatrix} = \left(\begin{pmatrix} O_{mm} & I_m \\ -I_m & O_{mm} \end{pmatrix} - \begin{pmatrix} O_{mm} & O_{mm} \\ O_{mm} & R_D \end{pmatrix} \right) \begin{pmatrix} \dfrac{\partial H(q,p,u)}{\partial q}^\top \\ \dfrac{\partial H(q,p,u)}{\partial p}^\top \end{pmatrix} \\ y = -\dfrac{\partial H(q,p,u)}{\partial u}^\top = q \end{cases} \tag{2.19}$$

with the Hamiltonian

$$H(q,p,u) = \frac{1}{2} p^\top M(q)^{-1} p + V(q) - u^\top q. \tag{2.20}$$

Here a positive definite matrix $M(q) \in \mathbb{R}^{m \times m}$ denotes the inertia matrix. The generalized momentum $p \in \mathbb{R}^m$ is given by $p := M(q)\dot{q}$. A positive semi-definite matrix $R_D \in \mathbb{R}^{m \times m}$ denotes the friction coefficients, and a scalar function $V(q) \in \mathbb{R}$ denotes the potential energy of the system. The dynamics of the compass gait biped depicted in Fig.2.1 is described as a typical mechanical system in (2.19) with $m = 2$, the friction coefficients $R_D = O_{22}$ and the following inertia matrix and the potential energy

$$\begin{aligned} M(\alpha(q)) &= \begin{pmatrix} m_H l^2 + m_L a^2 + m_L l^2 & -m_L bl\cos(\alpha(q)) \\ -m_L bl\cos(\alpha(q)) & m_L b^2 \end{pmatrix} \\ \alpha(q) &:= q^1 - q^2 \\ V(q) &= \{(m_H l + m_L a + m_L l)\cos q^1 - m_L b \cos q^2\} g. \end{aligned} \tag{2.21}$$

The output y corresponding to the input u defined in Eq.(2.18) is given by $y = q$. At the end of a walking period, a collision between a leg and the ground causes a discontinuous change in angular velocities. Assumptions 2.5 and 2.6 imply that there exists no double support phase. Since the support and swing legs change each other instantly, we have

$$q_+ = \begin{pmatrix} 0 & 1 \\ 1 & 0 \end{pmatrix} q_- =: Cq_-, \tag{2.22}$$

where q_- and q_+ denote the leg angles just before and just after the collision, respectively. Following the law of conservation of the angular momentum, we can obtain a transition equation [31] as

$$\Pi_+(\alpha(q_-))\dot{q}_+ = \Pi_-(\alpha(q_-))\dot{q}_-, \tag{2.23}$$

where

$$\Pi_-(\alpha(q_-)) = \begin{pmatrix} (m_H l^2 + 2m_L al)\cos(\alpha(q_-)) - m_L ab & -m_L ab \\ -m_L ab & 0 \end{pmatrix},$$

$$\Pi_+(\alpha(q_-)) = \begin{pmatrix} m_L l(l - b\cos(\alpha(q_-))) + m_L a^2 + m_H l^2 & m_L b(b - l\cos(\alpha(q_-))) \\ -m_L bl\cos(\alpha(q_-)) & m_L b^2 \end{pmatrix}.$$

Here we rewrite the transition equation in (2.23) as

$$\dot{q}_+ = \bar{\Pi}(\alpha(q_-))\dot{q}_-, \tag{2.24}$$

where $\bar{\Pi}(\alpha(q_-)) := \Pi_+(\alpha(q_-))^{-1}\,\Pi_-(\alpha(q_-))$. We call $\bar{\Pi}(\alpha(q_-))$ the transition mapping.

Before the iterative learning control method mentioned in Section2.1 is applied, feedback controllers are typically employed to the control system in order to render the system asymptotically stable. However, the feedback system is not generally Hamiltonian system (2.1) any more with arbitrary feedback controller. A feedback controller design for a Hamiltonian system is proposed, e.g. [59, 25]. In [25], a generalized canonical transformation, which is a pair of feedback and coordinate transformations preserving the Hamiltonian structure in (2.1), is proposed. It is known that in the case of a typical mechanical system in (2.19), a simple PD feedback preserves the structure of the Hamiltonian system [25, 27]. Let us consider a PD controller

$$u = -K_P q - K_D \dot{q} + \bar{u}, \tag{2.25}$$

where $\bar{u}$ is a new input for iterative learning control and $K_P, K_D \in \mathbb{R}^{m\times m}$ are symmetric positive definite matrices. Figure 2.2 illustrates the closed loop system, where q^r and $\dot{q}^r$ represent

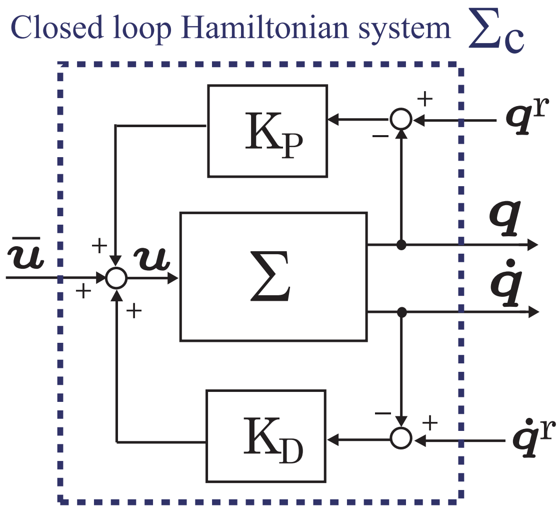

Figure 2.2: Feedback system

reference signals for PD feedback, respectively. The PD controller in (2.25) corresponds to the case where $q^r \equiv \dot{q}^r \equiv 0$. It converts the system Σ in (2.19) into another Hamiltonian system Σ_c in (2.19) with a new Hamiltonian H_c, a new structure matrix J_c and a new dissipation matrix R_c as

$$H_c(q,p,\bar{u}) \;=\; \frac{1}{2}p^\top M(q)^{-1}p + V(q) + \frac{1}{2}q^\top K_P q - \bar{u}^\top q,$$

$$J_c \;=\; \begin{pmatrix} O_{mm} & I_m \\ -I_m & O_{mm} \end{pmatrix}, \quad R_c = \begin{pmatrix} O_{mm} & O_{mm} \\ O_{mm} & R_D + K_D \end{pmatrix}. \tag{2.26}$$

Remark 2.8 [27] Consider the feedback system (2.26). If the inertia matrix $M(q)$ of the system does not depend on the configuration coordinate q, then the conditions (2.5) and (2.6) in Lemma 2.2 are satisfied with the following nonsingular matrix

$$T = \begin{pmatrix} I_m & O_{mm} \\ O_{mm} & -I_m \end{pmatrix}. \tag{2.27}$$

Otherwise, however, if PD gains K_P and K_D in (2.25) are chosen large enough, the conditions (2.5) and (2.6) are satisfied approximately with the same matrix T as Eq. (2.27).

In what follows, we consider the feedback system (2.26) with sufficiently large gains K_P and K_D so that the conditions in Lemma 2.2 are satisfied approximately, and derive the iteration law for the input $\bar{u}$ in Eq. (2.25).

2.3 Optimal gait generation via ILC considering discontinuous state transitions

In this section, we propose a framework to generate an optimal gait trajectory via iterative learning control method mentioned in Section 2.1. Firstly in subsection 2.3.1, a cost function is defined, by which one can generate optimal periodic trajectories minimizing the L_2 norm of the control input. Such periodic trajectories satisfy one of the necessary conditions for periodic gaits. Then, the iteration law with respect to the cost function is derived. However, the iteration procedure requires the precise knowledge of the inertia matrix and the Jacobian of the transition mapping $\bar{\Pi}(\alpha(q_-))$ defined by Eq. (2.24). Furthermore, let us note that the transition equation in (2.24) does not hold exactly for real robots, because the angular momentum is not preserved.

Regarding this, secondly, a modified learning algorithm is proposed in subsection 2.3.2. In this method, the transition mapping is considered to be a nonlinear function with respect to q_- and $\dot{q}_-$. We estimate the Jacobian of the transition mapping via the least-squares by utilizing stored experimental data of the state transitions and we combine this estimation part and the learning part via iterative learning control. The proposed framework does not require the information of the robot parameters nor the transition mapping.

2.3.1 Derivation of the iteration law

It is known that a spring-driven one-legged hopping robot depicted in Fig.2.3 can run on the ground with zero control input under appropriate initial conditions [87]. A sufficient condition for running is shown in [38] and the authors have proposed a learning algorithm for the robot with a special cost function by which trajectories satisfying the sufficient condition can be generated in [74, 75, 77]. However, it is very difficult to find a sufficient condition that a general walking

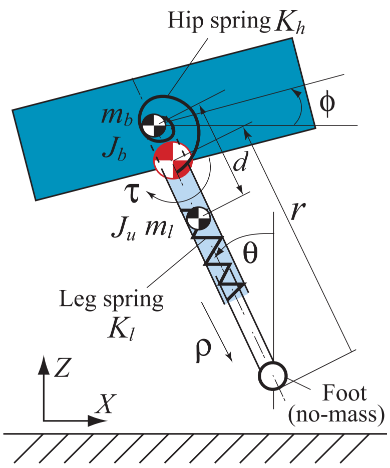

Figure 2.3: One-legged hopping robot

robot can walk. Even for the compass gait biped, it is unknown. Regarding this, we propose a cost function by which an optimal periodic trajectories minimizing the L_2 norm of the control input can be generated. Such periodic trajectories satisfy one of the necessary conditions for periodic gaits.

Let us propose a cost function as

$$\begin{aligned}\hat{\Gamma}_Q(Q_{t^0},\bar{u},Q_{t^1}) &:= \frac{1}{2}(Q_{t^0}-\Phi(Q_{t^1}))^\top\Lambda_x(Q_{t^0}-\Phi(Q_{t^1}))+\frac{1}{2}\int_{t^0}^{t^1}\bar{u}(\tau)^\top\Lambda_{\bar{u}}\,\bar{u}(\tau)\,\mathrm{d}\tau\\ &= \frac{1}{2}(\Psi_0(x_{t^0})-\Psi_1(x_{t^1}))^\top\Lambda_x(\Psi_0(x_{t^0})-\Psi_1(x_{t^1}))+\frac{1}{2}\int_{t^0}^{t^1}\bar{u}(\tau)^\top\Lambda_{\bar{u}}\,\bar{u}(\tau)\,\mathrm{d}\tau\\ &=: \hat{\Gamma}_x(x_{t^0},\bar{u},x_{t^1}),\end{aligned}\tag{2.28}$$

where appropriate positive definite matrices $\Lambda_x\in\mathbb{R}^{4\times4}$ and $\Lambda_{\bar{u}}\in\mathbb{R}^{2\times2}$ represent weight matrices for the state restriction and the input minimization, respectively. According to Table 2.2, Q represents $Q=(q^\top,\dot{q}^\top)^\top$. Here $\Phi(Q_{t^1})$ is defined to be the angles and their velocities just after the transition with exchanging legs as

$$\Phi(Q_{t^1}) := \begin{pmatrix} q_+ \\ \dot{q}_+ \end{pmatrix} = \begin{pmatrix} C & O_{22} \\ O_{22} & \bar{\Pi}(\alpha(q_-)) \end{pmatrix} Q_{t^1}.\tag{2.29}$$

Regarding the relation between x and Q, we have

$$x = \begin{pmatrix} q \\ p \end{pmatrix} = \begin{pmatrix} q \\ M(q)\dot{q} \end{pmatrix} = \begin{pmatrix} I_2 & O_{22} \\ O_{22} & M(q) \end{pmatrix} Q.\tag{2.30}$$

Equations (2.29) and (2.30) imply that $\Psi_0(x_{t^0})$ and $\Psi_1(x_{t^1})$ are also defined as

$$\begin{aligned}\Psi_0(x_{t^0}) &:= \begin{pmatrix} I_2 & O_{22} \\ O_{22} & M(q_{t^0})^{-1} \end{pmatrix} x_{t^0}\\ \Psi_1(x_{t^1}) &:= \begin{pmatrix} C & O_{22} \\ O_{22} & \bar{\Pi}(\alpha(q_-))M(q_-)^{-1} \end{pmatrix} x_{t^1}.\end{aligned}\tag{2.31}$$

Let us derive the iteration law with respect to the cost function (2.28) in the same manner as referred to in Subsection 2.1.2. The Fréchet derivative of the cost function $\hat{\Gamma}_x(x_{t^0},\bar{u},x_{t^1})$ can be calculated as follows:

$$\begin{aligned}&\delta\hat{\Gamma}_x(x_{t^0},\bar{u},x_{t^1})(\delta x_{t^0},\delta\bar{u},\delta x_{t^1},\delta y)\\ &= \langle(\Lambda_x(\Psi_0(x_{t^0})-\Psi_1(x_{t^1})),\Lambda_{\bar{u}}\bar{u}),(\delta\Psi_0(x_{t^0})(\delta x_{t^0}),\delta\bar{u})\rangle_{X\times U}\\ &\quad+\langle(\Lambda_x(\Psi_0(x_{t^0})-\Psi_1(x_{t^1})),0),(-\delta\Psi_1(x_{t^1})(\delta x_{t^1}),\delta y)\rangle_{X\times Y}\\ &= \langle(\delta\Psi_0(x_{t^0})^*\Lambda_x(\Psi_0(x_{t^0})-\Psi_1(x_{t^1})),\Lambda_{\bar{u}}\bar{u})\\ &\quad+\delta\Sigma(x_{t^0},\bar{u})^*\,(-\delta\Psi_1(x_{t^1})^*\Lambda_x(\Psi_0(x_{t^0})-\Psi_1(x_{t^1})),0),(\delta x_{t^0},\delta\bar{u})\rangle_{X\times U}\\ &=: \langle(\nabla_{x_{t^0}}\hat{\Gamma},\nabla_{\bar{u}}\hat{\Gamma})+\delta\Sigma(x_{t^0},\bar{u})^*(\nabla_{x_{t^1}}\hat{\Gamma},0),(\delta x_{t^0},\delta\bar{u})\rangle_{X\times U},\end{aligned}\tag{2.32}$$

where

$$\begin{aligned}\nabla_{x_{t^0}}\hat{\Gamma} &:= \delta\Psi_0(x_{t^0})^*\Lambda_x(\Psi_0(x_{t^0})-\Psi_1(x_{t^1})),\\ \nabla_{\bar{u}}\hat{\Gamma} &:= \Lambda_{\bar{u}}\bar{u},\\ \nabla_{x_{t^1}}\hat{\Gamma} &:= -\delta\Psi_1(x_{t^1})^*\Lambda_x(\Psi_0(x_{t^0})-\Psi_1(x_{t^1})).\end{aligned}$$

Operators $\delta\Psi_0(x_{t^0})^*$ and $\delta\Psi_1(x_{t^1})^*$ in (2.32) can be calculated from their definitions in (2.31) as

$$\delta\Psi_0(x_{t^0})^* = \begin{pmatrix} I_2 & O_{22} \\ \mathcal{D}_\alpha M(\alpha)^{-1} p_{t^0} \mathcal{D}_{q_{t^0}} \alpha(q_{t^0}) & M(\alpha(q_{t^0}))^{-1} \end{pmatrix}^\top$$

$$\delta\Psi_1(x_{t^1})^* = \begin{pmatrix} C & O_{22} \\ \mathcal{D}_\alpha(\bar{\Pi}(\alpha) M(\alpha)^{-1}) p_{t^1} \mathcal{D}_{q_-} \alpha(q_-) & \bar{\Pi}(\alpha(q_-)) M(\alpha(q_-))^{-1} \end{pmatrix}^\top . \tag{2.33}$$

Here $\mathcal{D}_{(\cdot)}$ denotes the derivative with respect to $(\cdot)$. In order to calculate the output $\delta\Sigma(x_{t^0}, \bar{u})^*(\nabla_{x_{t^1}} \hat{\Gamma}, 0)$ in (2.32), we utilize Theorem 2.3. The literature [18] (see also [19]) gives a way to produce the trajectory ψ satisfying the condition (2.8) for a given trajectory ϕ. The reference signals q^r and $\dot{q}^r$ for PD feedback (2.25) in Fig.2.2 should be selected as

$$(q^r, \dot{q}^r) = (\mathcal{R}(q|_{x=\phi}), -\mathcal{R}(\dot{q}|_{x=\phi})). \tag{2.34}$$

Then the input w is given by $w = K_P q^r + K_D \dot{q}^r$. Consider ψ to be the trajectory which is generated by the trajectory tracking control by PD feedback along the reference signals (2.34). Then ψ is approximately time-reversal version of ϕ and from Eqs. (2.10) and (2.17), we have

$$\begin{aligned} \delta\Sigma(x_{t^0}, \bar{u})^*(\nabla_{x_{t^1}} \hat{\Gamma}, 0) &= \mathcal{S}^{-1} \delta\Sigma(\psi(t^0), w)(-(J_c - R_c) T \nabla_{x_{t^1}} \hat{\Gamma}, 0) \\ &\approx \mathcal{S}^{-1} \frac{1}{\epsilon} \Big(\Sigma(\psi(t^0) - \epsilon(J_c - R_c) T \nabla_{x_{t^1}} \hat{\Gamma}, w) - \Sigma(\psi(t^0), w) \Big) . \end{aligned} \tag{2.35}$$

Consequently, from Eqs. (2.32) and (2.35), the iterative learning control algorithm for the optimal gait is given by

$$\begin{aligned} &\begin{cases} x_{t^0(3i+1)} = (q_{t^1(3i)}^\top, -p_{t^1(3i)}^\top)^\top \\ \bar{u}_{(3i+1)} = K_P \mathcal{R}(q_{(3i)}) - K_D \mathcal{R}(\dot{q}_{(3i)}) \end{cases} \\ &\begin{cases} x_{t^0(3i+2)} = x_{t^0(3i+1)} + \epsilon_{(i)} (J_c - R_c) T \delta\Psi_1(x_{t^1(3i)})^* \Lambda_x (\Psi_0(x_{t^0(3i)}) - \Psi_1(x_{t^1(3i)})) \\ \bar{u}_{(3i+2)} = \bar{u}_{(3i+1)} \end{cases} \\ &\begin{cases} x_{t^0(3i+3)} = x_{t^0(3i)} \\ \bar{u}_{(3i+3)} = \bar{u}_{(3i)} - K_{(i)} \big(\Lambda_{\bar{u}} \bar{u}_{(3i)} + \dfrac{1}{\epsilon_{(i)}} \mathcal{R}(y_{(3i+2)} - y_{(3i+1)}) \big) \end{cases} \end{aligned} \tag{2.36}$$

provided that the initial input $\bar{u}_{(0)} \equiv 0$ (or an appropriate initial input) and that the initial condition $x_{t^0(0)}$ is appropriately chosen. Here $\epsilon_{(\cdot)}$ denotes a sufficiently small positive constant and an appropriate positive definite matrix $K_{(\cdot)}$ represents a gain. The triple iteration laws imply that this learning procedure needs three experiments to execute a single update in (2.16). In the (3i+1)-th iteration, the trajectory ϕ corresponds to $x_{(3i)}$ and we produce its time-reversal trajectory ψ by utilizing the reference signals (2.34). In the (3i+2)-th iteration, we calculate the output $\Sigma(\psi(t^0) - \epsilon(J_c - R_c) T \nabla_{x_{t^1}} \hat{\Gamma}, w)$ in Eq. (2.35) (note that in this case ψ corresponds to $x_{(3i+1)}$). Then the input and output signals of $\delta\Sigma(x_{t^0}, \bar{u})^*(\nabla_{x_{t^1}} \hat{\Gamma}, 0)$ can be calculated from Eq. (2.35). With this information, the gradient of the cost function with respect to the input $\nabla_{\bar{u}} \hat{\Gamma}_x$ (see Eq. (2.15)) is obtained. Finally, the input for the (3i+3)-th iteration is given by Eq. (2.16) with these signals.

Remark 2.9 Since the conventional iterative learning control frameworks, e.g. [1, 27], assume that all the initial conditions are the same in each laboratory experiment, the iteration algorithm in (2.36) updates only the input $\bar{u}$ for a given initial condition x_{t^0}. However, the choice of initial condition is sometimes important, for example, in the cases of passive running of the one-legged hopping robot depicted in Fig. 2.3 and passive walking of the compass gait biped and so on. The authors have proposed a learning algorithm by employing an update law for the initial condition as well as that for the input and have demonstrated its effectiveness in [75, 76]. One can generate an optimal initial condition as well as an optimal input by utilizing the following updating law for the initial condition in place of that in (2.36)

$$x_{t^0(3i+3)} = x_{t^0(3i)} - K_{(i)}^{x_{t^0}} \Big(\delta\Psi_0(x_{t^0(3i)})^* \Lambda_x (\Psi_0(x_{t^0(3i)}) - \Psi_1(x_{t^1(3i)})) \\ - \frac{1}{\epsilon_{(i)}} T^{-1} (J_c - R_c)^{-1} (x_{t^1(3k+2)} - x_{t^1(3k+1)}) \Big), \tag{2.37}$$

where an appropriate positive definite matrix $K_{(\cdot)}^{x_{t^0}}$ represents a gain for the initial state updating. The updating law (2.37) follows from the steepest descent method as Eq.(2.16) with the gradient of the cost function with respect to the initial state $\nabla_{x_{t^0}} \hat{\Gamma}_x$, calculated by utilizing variational symmetry.

Remark 2.10 If the learning procedure is executed around a symmetric trajectory and a trajectory in each experiment approximately satisfies the condition (2.12), then one can use the following iterative learning control algorithm which is simpler than that in (2.36)

$$\begin{cases} x_{t^0(2i+1)} = x_{t^0(2i)} + \epsilon_{(i)} (J_c - R_c) T \delta\Psi_1(x_{t^1(2i)})^* \Lambda_x (\Psi_0(x_{t^0(2i)}) - \Psi_1(x_{t^1(2i)})) \\ \bar{u}_{(2i+1)} = \bar{u}_{(2i)} \end{cases}$$
$$\begin{cases} x_{t^0(2i+2)} = x_{t^0(2i)} \\ \bar{u}_{(2i+1)} = \bar{u}_{(2i)} - K_{(i)} \Big(\Lambda_{\bar{u}} \bar{u}_{(2i)} + \dfrac{1}{\epsilon_{(i)}} \mathcal{R}(y_{(2i+1)} - y_{(2i)}) \Big) \end{cases} . \tag{2.38}$$

Since the learning algorithm given by (2.36) (or (2.38)) requires $\delta\Psi_1(x_{t^1})^*$, and the state x includes the momentum $p = M(q)\dot{q}$, the proposed procedure requires the precise knowledge of the transition mapping and the inertia matrix. Regarding real robots, however, the numerical model of the state transition equation does not hold exactly and it is sometimes difficult to get the accurate inertia information of robots. So in the next subsection, we derive a modified learning algorithm which does not require such information.

2.3.2 Modified algorithm by combining ILC and the least-squares

In this subsection, we reconsider the iteration law (2.36) (or (2.38)) in order not to use the models of the state transition mapping nor the inertia matrix. Firstly, we derive a cost function with respect to the output $y = q$ and its time derivative $\dot{y} = \dot{q}$ instead of the state $x = (q^\top, p^\top)^\top$, which is expected to have a similar effect as that in (2.28). Secondly, we estimate the Jacobian of the transition mapping via the least-squares by utilizing stored experimental data of the state transitions and we combine this estimation part and the learning part via iterative learning control.

Let us approximate the cost function (2.28) by the following one so that we deal with the functional of the output $y = q$ and its time derivative instead of the state

$$\begin{aligned}\hat{\Gamma}_y(y, \dot{y}, \bar{u}) := & \frac{1}{2}\int_{t^0}^{t^1} (y(\tau) - C\mathcal{R}(y)(\tau))^\top \nu_1(\tau)\Lambda_y(y(\tau) - C\mathcal{R}(y)(\tau))\,\mathrm{d}\tau \\ & +\frac{1}{2}\int_{t^0}^{t^1}(\dot{y}(\tau)-\mathcal{R}(f_\Pi(y,\dot{y}))(\tau))^\top\nu_1(\tau)\Lambda_{\dot{y}}(\dot{y}(\tau)-\mathcal{R}(f_\Pi(y,\dot{y}))(\tau)) \\ & +\frac{1}{2}\int_{t^0}^{t^1} \bar{u}(\tau)^\top \Lambda_{\bar{u}}\bar{u}(\tau)\,\mathrm{d}\tau, \end{aligned} \tag{2.39}$$

where appropriate positive definite matrices $\Lambda_y, \Lambda_{\dot{y}}, \Lambda_{\bar{u}} \in \mathbb{R}^{2\times 2}$ represent weight matrices for the configuration and phase coordinates restrictions and the input minimization, respectively. $\nu_1(t) \in \mathbb{R}$ represents a filter function with respect to the time t defined as

$$\nu_1(t) := \begin{cases} \frac{1}{2}\left(1 - \cos\left(\frac{t^0 + \Delta t - t}{\Delta t}\pi\right)\right) & (t^0 \le t \le t^0 + \Delta t) \\ 0 & (t^0 + \Delta t < t \le t^1) \end{cases}, \tag{2.40}$$

where a design parameter Δt is an appropriate positive number. Figure 2.4 illustrates $\nu_1(t)$. Due

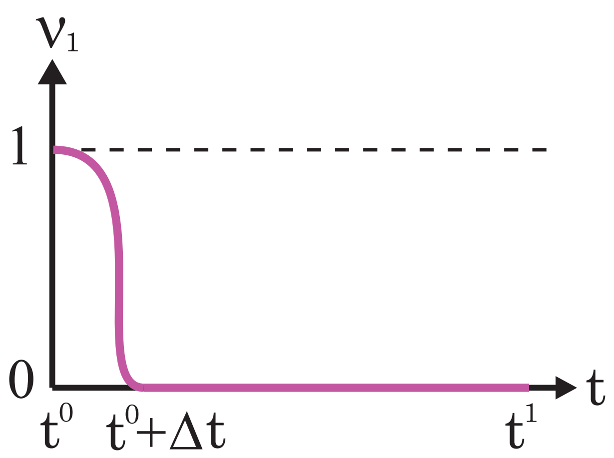

Figure 2.4: Illustration of the filter function $\nu_1(t)$

to the time-reversal operator $\mathcal{R}$ and the filter function $\nu_1(t)$, we can only evaluate the difference between Q_{t^0} and Q_+ approximately by choosing the design parameter Δt in (2.40) sufficiently small. In what follows, the transition mapping is considered to be a general nonlinear function with respect to q_- and $\dot{q}_-$ and it is denoted as

$$\dot{q}_+ = f_\Pi(q_-, \dot{q}_-). \tag{2.41}$$

Equation (2.24) gives a special case of f_Π.

In the conventional iterative learning control method [27, 17, 18] mentioned in Section 2.1, it is not possible to choose a functional of the time derivative of the output $\dot{y}$ as cost function. The authors have proposed an extension by employing a pseudo adjoint of the time derivative operator to take the time derivative of the output into account in [74].

Lemma 2.4 *[74] Consider differentiable signals ξ and $\eta \in L_2^n[t^0, t^1]$. Suppose that the signal ξ satisfies the condition*

$$\xi(t^0) = \xi(t^1) = 0. \tag{2.42}$$

Then the following equation holds.

$$\langle \eta, \mathcal{D}_t(\xi) \rangle_{L_2[t^0,t^1]} = \langle -\mathcal{D}_t(\eta), \xi \rangle_{L_2[t^0,t^1]} \tag{2.43}$$

Proof The inner product of η and $\mathcal{D}_t(\xi)$ is calculated as

$$\begin{aligned} \langle \eta, \mathcal{D}_t(\xi) \rangle_{L_2[t^0,t^1]} &= \int_{t^0}^{t^1} \eta(t)^\top \frac{\mathrm{d}\xi(t)}{\mathrm{d}t} \,\mathrm{d}t \\ &= \Big[\eta(t)^\top \xi(t)\Big]_{t^0}^{t^1} - \int_{t^0}^{t^1} \frac{\mathrm{d}\eta(t)}{\mathrm{d}t}^\top \xi(t) \,\mathrm{d}t. \end{aligned}$$

Since ξ satisfies the condition (2.42), $\Big[\eta(t)^\top \xi(t)\Big]_{t^0}^{t^1} = 0$ holds. Then we can calculate that

$$\begin{aligned} \langle \eta, \mathcal{D}_t(\xi) \rangle_{L_2[t^0,t^1]} &= -\int_{t^0}^{t^1} \frac{\mathrm{d}\eta(t)}{\mathrm{d}t}^\top \xi(t) \,\mathrm{d}t \\ &= \langle -\mathcal{D}_t(\eta), \xi \rangle_{L_2[t^0,t^1]}. \end{aligned}$$

■

This lemma implies that the adjoint operator of the time derivative operator is given by $\mathcal{D}_t^* = -\mathcal{D}_t$ for a certain class of input signals. We call Eq. (2.43) pseudo adjoint relation of the time derivative operator.

Assumption 2.11 In order to utilize Eq. (2.43), we assume that the following conditions hold for each i-th laboratory experiment

$$\|y_{(i)}(t^0) - y_{(i-1)}(t^0)\| \ll 1 \tag{2.44}$$
$$\|y_{(i)}(t^1) - y_{(i-1)}(t^1)\| \ll 1. \tag{2.45}$$

In the conventional iterative learning control frameworks, it is assumed that all the initial conditions are the same, which is almost equivalent to the condition (2.44). In our method, an additional condition (2.45) is assumed. In order to let Eq. (2.45) approximately hold by the penalty function method, we can add an extra cost function (2.46) to Eq. (2.39) with an appropriately large positive gain K_{pnl} and a sufficiently small positive constant ϵ

$$\int_{t^1-\epsilon}^{t^1} K_{pnl} \|y(\tau) - C q_{t^0} \mathbf{1}(\tau)\|^2 \,\mathrm{d}\tau, \tag{2.46}$$

where $\mathbf{1}(t)$ represents an identity operator $\mathbf{1}(t) = \mathrm{id} \ \ (t^0 \le t \le t^1)$. The cost function (2.46) weights the difference between the output and its desired value around $t = t^1$ and penalizes the left hand side of the inequality (2.45). Here let us provide the following lemma for the adjoint of the time-reversal operator, which is utilized in calculation of the Fréchet derivative of the cost function (2.39).

Lemma 2.5 *Consider the time-reversal operator $\mathcal{R}(\cdot)$ defined in Eq.* (2.9)*, then the following equation holds*

$$(\mathcal{R}(\cdot))^* = \mathcal{R}(\cdot) \tag{2.47}$$

Proof Consider signals ξ and $\eta \in L_2^n[t^0, t^1]$. Let us calculate the inner product of ξ and $\mathcal{R}(\eta)$ as

$$\begin{aligned}\langle \xi, \mathcal{R}(\eta)\rangle_{L_2[t^0,t^1]} &= \int_{t^0}^{t^1} \xi(t)^\top \eta(t^1 - t + t^0)\,\mathrm{d}t \\ &= \int_{t^0}^{t^1} \xi(t^1 - s + t^0)^\top \eta(s)\,\mathrm{d}s \\ &= \langle \mathcal{R}(\xi), \eta\rangle_{L_2[t^0,t^1]},\end{aligned}$$

where $s = t^0 + t^1 - t$. This implies Eq. (2.47). ■

By utilizing Eqs. (2.43) and (2.47), the Fréchet derivative of the cost function (2.39) can be calculated as

$$\begin{aligned}&\delta\hat{\Gamma}_y\,(y, \dot{y}, \bar{u})(\delta y, \delta\dot{y}, \delta\bar{u}) \\ &\quad= \langle \nu_1\Lambda_y(y - C\mathcal{R}(y)), \delta y - C\mathcal{R}(\delta y)\rangle + \langle \nu_1\Lambda_{\dot{y}}(\dot{y} - \mathcal{R}(f_\Pi(y,\dot{y}))), \\ &\qquad \delta\dot{y} - \mathcal{R}(\partial_y f_\Pi(y,\dot{y})(\delta y) + \partial_{\dot{y}} f_\Pi(y,\dot{y})(\delta\dot{y}))\rangle + \langle \Lambda_{\bar{u}}\bar{u}, \delta\bar{u}\rangle \\ &\quad= \langle (\mathrm{id} - \mathcal{R}C)\nu_1\Lambda_y(\mathrm{id} - C\mathcal{R})(y), \delta y\rangle + \langle \nu_1\Lambda_{\dot{y}}(\dot{y} - \mathcal{R}(f_\Pi(y,\dot{y}))), \delta\dot{y}\rangle \\ &\qquad -\langle \partial_y f_\Pi(y,\dot{y})^*\mathcal{R}\nu_1\Lambda_{\dot{y}}(\dot{y} - \mathcal{R}(f_\Pi(y,\dot{y}))), \delta y\rangle \\ &\qquad -\langle \partial_{\dot{y}} f_\Pi(y,\dot{y})^*\mathcal{R}\nu_1\Lambda_{\dot{y}}(\dot{y} - \mathcal{R}(f_\Pi(y,\dot{y}))), \delta\dot{y}\rangle + \langle \Lambda_{\bar{u}}\bar{u}, \delta\bar{u}\rangle \\ &\quad= \langle (\mathrm{id} - \mathcal{R}C)\nu_1\Lambda_y(\mathrm{id} - C\mathcal{R})(y) - \partial_y f_\Pi(y,\dot{y})^*\mathcal{R}\nu_1\Lambda_{\dot{y}}(\dot{y} - \mathcal{R}(f_\Pi(y,\dot{y}))), \delta y\rangle \\ &\qquad +\langle \nu_1\Lambda_{\dot{y}}(\dot{y} - \mathcal{R}(f_\Pi(y,\dot{y}))) - \partial_{\dot{y}} f_\Pi(y,\dot{y})^*\mathcal{R}\nu_1\Lambda_{\dot{y}}(\dot{y} - \mathcal{R}(f_\Pi(y,\dot{y}))), \mathcal{D}_t(\delta y)\rangle + \langle \Lambda_{\bar{u}}\bar{u}, \delta\bar{u}\rangle \\ &\quad= \langle (\mathrm{id} - \mathcal{R}C)\nu_1\Lambda_y(\mathrm{id} - C\mathcal{R})(y) - \partial_y f_\Pi(y,\dot{y})^*\mathcal{R}\nu_1\Lambda_{\dot{y}}(\dot{y} - \mathcal{R}(f_\Pi(y,\dot{y})))\rangle \\ &\qquad -\mathcal{D}_t\big((\mathrm{id} - \partial_{\dot{y}} f_\Pi(y,\dot{y})^*\mathcal{R})\nu_1\Lambda_{\dot{y}}(\dot{y} - \mathcal{R}(f_\Pi(y,\dot{y})))\big), \delta y\rangle + \langle \Lambda_{\bar{u}}\bar{u}, \delta\bar{u}\rangle \\ &\quad=: \langle \nabla_y\hat{\Gamma}_y, \delta y\rangle + \langle \nabla_{\bar{u}}\hat{\Gamma}_y, \delta\bar{u}\rangle \\ &\quad= \langle \nabla_{\bar{u}}\hat{\Gamma}_y + \delta\Sigma^{x_{t^0}}(\bar{u})^*(\nabla_y\hat{\Gamma}_y), \delta\bar{u}\rangle.\end{aligned} \tag{2.48}$$

Here $\partial_y f_\Pi(y,\dot{y})$ and $\partial_{\dot{y}} f_\Pi(y,\dot{y})$ represent the partial Fréchet derivatives of $f_\Pi(y,\dot{y})$ with respect to y and $\dot{y}$, respectively. The third equality follows from the linearity of the differential operator

$\mathcal{D}_t$, that is,

$$\begin{aligned}\delta\dot{y} &= \delta\mathcal{D}_t(y)\\ &= \mathcal{D}_t(y+\delta y) - \mathcal{D}_t(y) + o(\|\delta y\|)\\ &= \mathcal{D}_t(\delta y) + o(\|\delta y\|).\end{aligned}$$

The pseudo adjoint relation of the time derivative operator (2.43) yields the fourth equality.

Now the concrete calculation method of $\nabla_y \hat{\Gamma}_y$ is explained. Firstly, calculation of $f_\Pi(y,\dot{y})$ is considered. Since every $f_\Pi(y,\dot{y})$ in Eq. (2.48) is multiplied by the time-reversal operator $\mathcal{R}$ and the filter function $\nu_1(t)$ in Eq. (2.40), only $f_\Pi(y,\dot{y})$ at the collision, that is $t = t^1$, is necessary. $f_\Pi(y_-,\dot{y}_-)$ represents the angular velocity just after the collision and is available from the experiment. Secondly, $\partial_y f_\Pi(y,\dot{y})^*$ and $\partial_{\dot{y}} f_\Pi(y,\dot{y})^*$ are considered. For the same reason as the case of $f_\Pi(y,\dot{y})$ and the relation that

$$\frac{\partial f_\Pi}{\partial(y,\dot{y})} = (\partial_y f_\Pi, \partial_{\dot{y}} f_\Pi), \tag{2.49}$$

only the Jacobian of $f_\Pi(y,\dot{y})$ with respect to $(y,\dot{y})$ at $t = t^1$ is required. Since the following equation holds

$$\mathrm{d}\dot{y}_+ = \left.\frac{\partial f_\Pi}{\partial(y,\dot{y})}\right|_{t=t^1} \begin{pmatrix}\mathrm{d}y_-\\ \mathrm{d}\dot{y}_-\end{pmatrix} \tag{2.50}$$

from Eq. (2.41), let us estimate the Jacobian $\frac{\partial f_\Pi}{\partial(y,\dot{y})}$ at the collision by stored experimental data via the least-squares. We approximate $\mathrm{d}y_-, \mathrm{d}\dot{y}_-$ and $\mathrm{d}\dot{y}_+$ in (2.50) by difference between stored data by the $(n-2)$-th experiment and the last data, i.e., data of the $(n-1)$-th experiment. Thus, the following data sets are defined as

$$\begin{aligned}\Delta Y_{-(n-1)} &:= \begin{bmatrix} y^{-\top}_{(1)} - y^{-\top}_{(n-1)},\ \dot{y}^{-\top}_{(1)} - \dot{y}^{-\top}_{(n-1)}\\ \vdots \\ y^{-\top}_{(n-2)} - y^{-\top}_{(n-1)},\ \dot{y}^{-\top}_{(n-2)} - \dot{y}^{-\top}_{(n-1)}\end{bmatrix},\\ \Delta\dot{Y}_{+(n-1)} &:= \begin{bmatrix} \dot{y}^{+\top}_{(1)} - \dot{y}^{+\top}_{(n-1)}\\ \vdots \\ \dot{y}^{+\top}_{(n-2)} - \dot{y}^{+\top}_{(n-1)}\end{bmatrix}.\end{aligned} \tag{2.51}$$

The size of $\Delta Y_{-(n-1)}$ is $(n-2)\times 4$ and that of $\Delta\dot{Y}_{+(n-1)}$ is $(n-2)\times 2$. From Eqs. (2.50) and (2.51), we have

$$\Delta\dot{Y}_{+(n-1)} \approx \Delta Y_{-(n-1)} \left.\frac{\partial f_\Pi}{\partial(y,\dot{y})}^\top\right|_{t=t^1}. \tag{2.52}$$

By solving Eq. (2.52), we can estimate the Jacobian as

$$\left.\frac{\partial f_\Pi}{\partial(y,\dot{y})}^\top\right|_{t=t^1} \approx \Delta Y_{-(n-1)}{}^\dagger \Delta\dot{Y}_{+(n-1)}, \tag{2.53}$$

where $(\cdot)^\dagger$ represents the pseudo inverse matrix of $(\cdot)$. We can also utilize MATLAB's arithmetic operator of the matrix left division to solve Eq. (2.53) easily. Consequently, from Eqs. (2.49) and (2.53) we obtain

$$\left.\begin{pmatrix} \partial_y f_\Pi(y,\dot{y})^* \\ \partial_{\dot{y}} f_\Pi(y,\dot{y})^* \end{pmatrix}\right|_{t=t^1} \approx \Delta Y_{-(n-1)}{}^\dagger \Delta \dot{Y}_{+(n-1)}. \tag{2.54}$$

We let the notations $\partial_y \widetilde{f_\Pi(y_-,\dot{y}_-)^*}_{(n-1)}$ and $\partial_{\dot{y}} \widetilde{f_\Pi(y_-,\dot{y}_-)^*}_{(n-1)}$ denote the estimations given by Eq. (2.54), respectively.

Here let us summarize the proposed learning algorithm.

Step 0 **:** Set appropriate positive definite matrices Λ_y, $\Lambda_{\dot{y}}$ and $\Lambda_{\bar{u}}$ as weight matrices, and an appropriate initial condition x_{t^0}. Execute the laboratory experiment with x_{t^0} and zero control input (or an appropriate initial input). Let $Q_{(0)}$, $y_{(0)}$ and $\dot{y}_{(0)}$ denote the corresponding data obtained by the experiment, respectively. Then, execute preliminary experiments at least 4 times with appropriate initial conditions around x_{t^0} and zero control input (or an appropriate initial input) in order to obtain data sets $\Delta Y_{-(5)}$ and $\Delta \dot{Y}_{+(5)}$ for the first learning control input.

Set $i = 0$. Then, go to Step 1.

Step $3i+1$ **:** Execute the (3i+1)-th laboratory experiment via the following iteration law

$$\begin{cases} Q_{t^0(3i+1)} = (q_{t^1(3i)}^\top, -\dot{q}_{t^1(3i)}^\top)^\top \\ \bar{u}_{(3i+1)} = K_P \mathcal{R}(q_{(3i)}) - K_D \mathcal{R}(\dot{q}_{(3i)}) \end{cases}.$$

Go to Step 3i+2.

Step $3i+2$ **:** Execute the (3i+2)-th laboratory experiment via the following iteration law with a sufficiently small positive constant $\epsilon_{(i)}$

$$\begin{cases} Q_{t^0(3i+2)} = Q_{t^0(3i+1)} \\ \bar{u}_{(3i+2)} = \bar{u}_{(3i+1)} + \epsilon_{(i)} \mathcal{R}(\widetilde{\nabla_y \hat{\Gamma}}_{y(3i)}) \end{cases}.$$

Here $\widetilde{\nabla_y \hat{\Gamma}}_{y(3i)}$ is calculated by Eq. (2.54) with data sets $\Delta Y_{-(5+i)}$ and $\Delta \dot{Y}_{+(5+i)}$ as

$$\begin{aligned} \widetilde{\nabla_y \hat{\Gamma}}_{y(3i)} = & (\mathrm{id} - \mathcal{R}C)\nu_1 \Lambda_y (\mathrm{id} - C\mathcal{R})(y_{(3i)}) \\ & - \partial_y \widetilde{f_\Pi(y_-,\dot{y}_-)^*}_{(5+i)} \mathcal{R} \nu_1 \Lambda_{\dot{y}} (\dot{y}_{(3i)} - f_\Pi(y_{-(3i)}, \dot{y}_{-(3i)}) \mathbf{1}(t)) \\ & - \mathcal{D}_t \big((\mathrm{id} - \partial_{\dot{y}} \widetilde{f_\Pi(y_-,\dot{y}_-)^*}_{(5+i)} \mathcal{R}) \nu_1 \Lambda_{\dot{y}} (\dot{y}_{(3i)} - f_\Pi(y_{-(3i)}, \dot{y}_{-(3i)}) \mathbf{1}(t)) \big). \end{aligned}$$

Go to Step 3i+3.

Step $3i+3$ **:** Execute the (3i+3)-th laboratory experiment via the following iteration law with an appropriate positive definite matrix $K_{(i)}$

$$\begin{cases} Q_{t^0(3i+3)} = Q_{t^0(3i)} \\ \bar{u}_{(3i+3)} = \bar{u}_{(3i)} - K_{(i)}\big(\Lambda_{\bar{u}}\bar{u}_{(3i)} + \dfrac{1}{\epsilon_{(i)}}\mathcal{R}(y_{(3i+2)} - y_{(3i+1)})\big) \end{cases}.$$

Set $i = i+1$. Then, go to Step $3i+1$.

Remark 2.12 As mentioned in Remark 2.10, if the learning procedure is executed around a symmetric trajectory, one can iterate the following procedure after executing Step 0 in the above algorithm

$$\begin{cases} Q_{t^0(2i+1)} = Q_{t^0(2i)} \\ \bar{u}_{(2i+1)} = \bar{u}_{(2i)} + \epsilon_{(i)}\mathcal{R}(\widetilde{\nabla_y\hat{\Gamma}}_{y(2i)}) \end{cases}$$
$$\begin{cases} Q_{t^0(2i+2)} = Q_{t^0(2i)} \\ \bar{u}_{(2i+1)} = \bar{u}_{(2i)} - K_{(i)}\big(\Lambda_{\bar{u}}\bar{u}_{(2i)} + \dfrac{1}{\epsilon_{(i)}}\mathcal{R}(y_{(2i+1)} - y_{(2i)})\big) \end{cases}. \quad (2.55)$$

2.4 Numerical example

We apply the proposed algorithm in the previous section to the compass gait biped depicted in Fig. 2.1 to generate an optimal gait trajectory on the level ground. The physical parameters of the robot in Table 2.1 are chosen as $m_H = 10.0, m_L = 5.0$ [kg] and $a = b = 0.5$ [m]. Gains $K_P = \text{diag}(4,4)$ and $K_D = \text{diag}(2,2)$ are chosen for the PD feedback (2.25). We utilize the following design parameters with respect to weighting functions for the cost function (2.39) as $\Lambda_y = \text{diag}(30,30)$, $\Lambda_{\dot{y}} = \text{diag}(1\times10^{-3}, 1\times10^{-3})$ and $\Lambda_{\bar{u}} = \text{diag}(1\times10^{-6}, 1\times10^{-6})$, that with respect to the filter function ν_1 in (2.40) as $\Delta t = 5\times10^{-3}[s]$ and those with respect to ILC algorithm as $K_{(\cdot)} = \text{diag}(400,400)$ and $\epsilon_{(\cdot)} = 1$. We generate optimal trajectories with some initial conditions which are heuristically chosen so that the robot barely overcomes the potential barrier. Since both two algorithms in the previous section, that is, 3 Step scheme and 2 Step one in Remark 2.12, succeeded in learning, only results by 2 Step scheme are shown.

The case of the initial condition : $(-0.15, 0.15, 0.82, 0.35)$

Firstly, we proceed 35 steps of the learning procedure which means 75 simulations including 5 preliminary experiments with the initial condition:

$$(q^1_{t^0}, q^2_{t^0}, \dot{q}^1_{t^0}, \dot{q}^2_{t^0}) = (-0.15, 0.15, 0.82, 0.35).$$

Figure 2.5 shows the history of the cost function (2.39) along the iteration decreasing monotonically. It implies that the output trajectory converges to an (at least locally) optimal one smoothly. Figure 2.6 represents the animations of the robot before and after learning, respectively and it implies that the robot stops with almost standing posture before learning and a walking motion seems to be generated eventually. Figure 2.7 exhibits the phase portrait of q-$\dot{q}$ and that of q^1 - q^2, respectively. The fact that an almost periodic trajectory is generated follows from that the phase portraits in these figures form almost closed orbits. Figure 2.8 shows the generated learning control input $\bar{u}$ and Fig. 2.9 does the control input u in Eq. (2.25). We observe 200 steps consecutive walking with these inputs. Figure 2.10 shows the time revolution of the ZMP calculated by

$$\mathrm{ZMP} = \frac{-v^1}{\dot{\sigma_p}^2 + (2m_L + m_H)g} \quad \text{, where}$$
$$\dot{\sigma_p}^2 = -(m_L a + m_L l + m_H l)(\ddot{q}^1 \sin q^1 + (\dot{q}^1)^2 \cos q^1) + m_L b(\ddot{q}^2 \sin q^2 + (\dot{q}^2)^2 \cos q^2) \tag{2.56}$$

of the generated gait. For calculation of the ZMP in Eq. (2.56), see Appendix A. The ZMP is shifted forward. Regarding the total leg length of the robot and the range of the ZMP position, the generated gait seems feasible. Finally, Fig. 2.11 shows responses of q and $\dot{q}$ at the last step in the proposed method in solid lines and those before learning in dotted lines. It is expected that this figure shows the validity of the use of the 2 Step scheme.

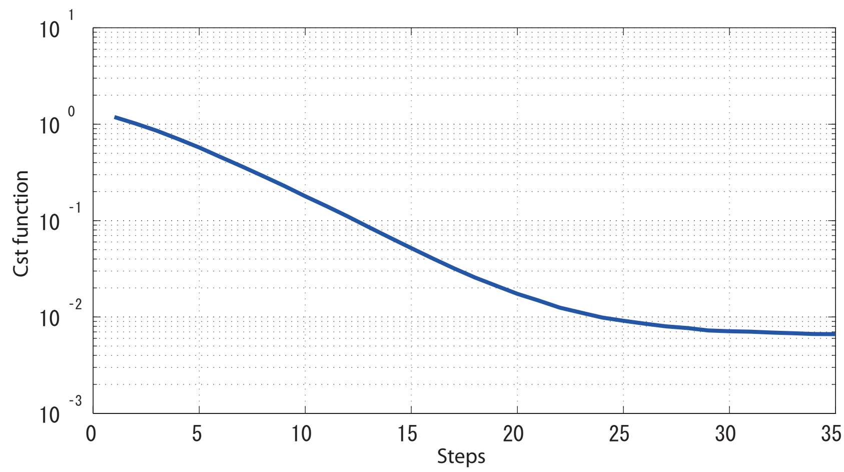

Figure 2.5: Cost function

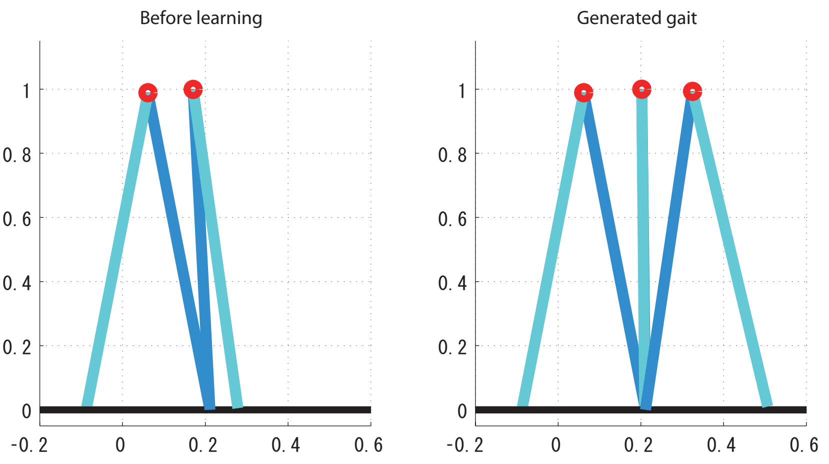

Figure 2.6: Stick diagrams before and after learning

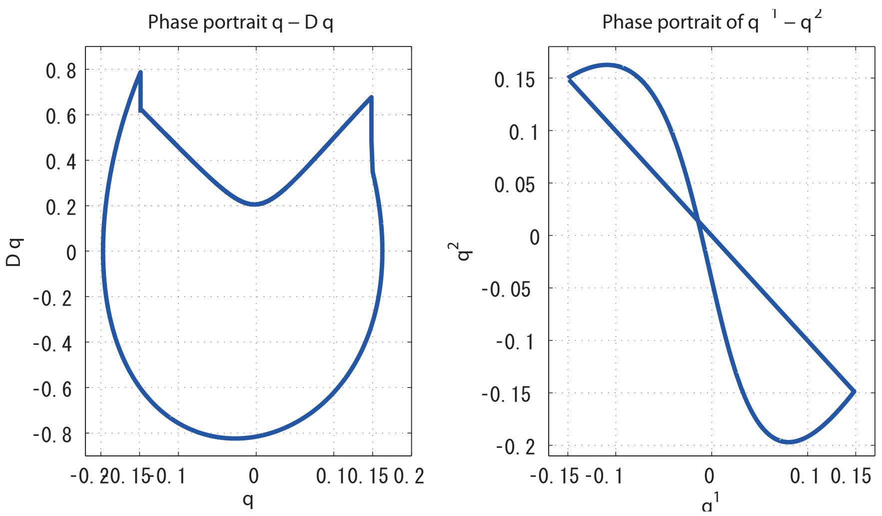

Figure 2.7: Phase portraits

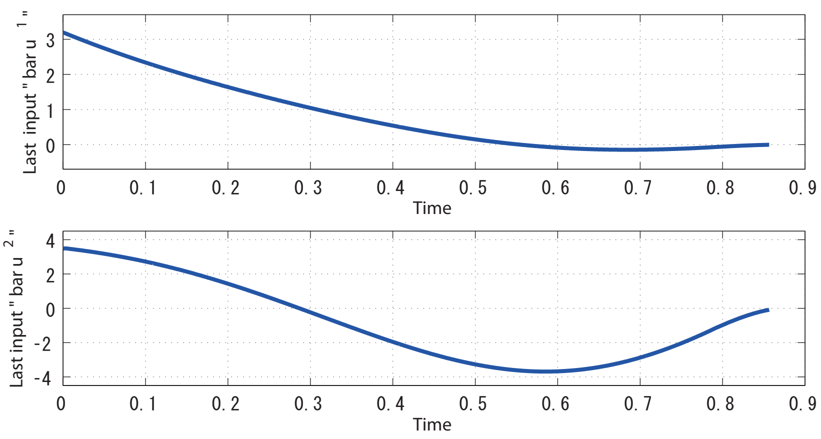

Figure 2.8: Generated learning control inputs $\bar{u}$

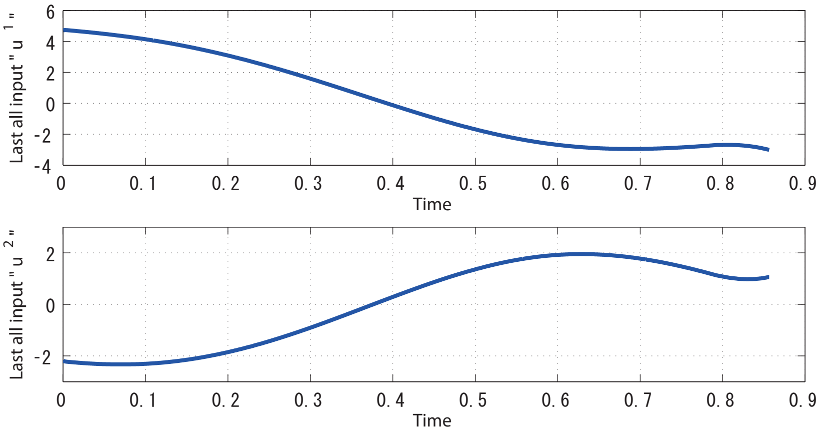

Figure 2.9: Generated all control inputs u

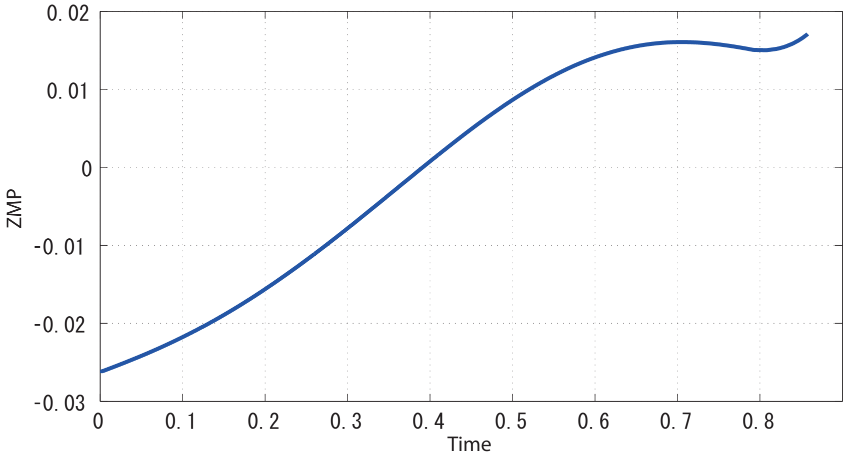

Figure 2.10: ZMP of the generated gait

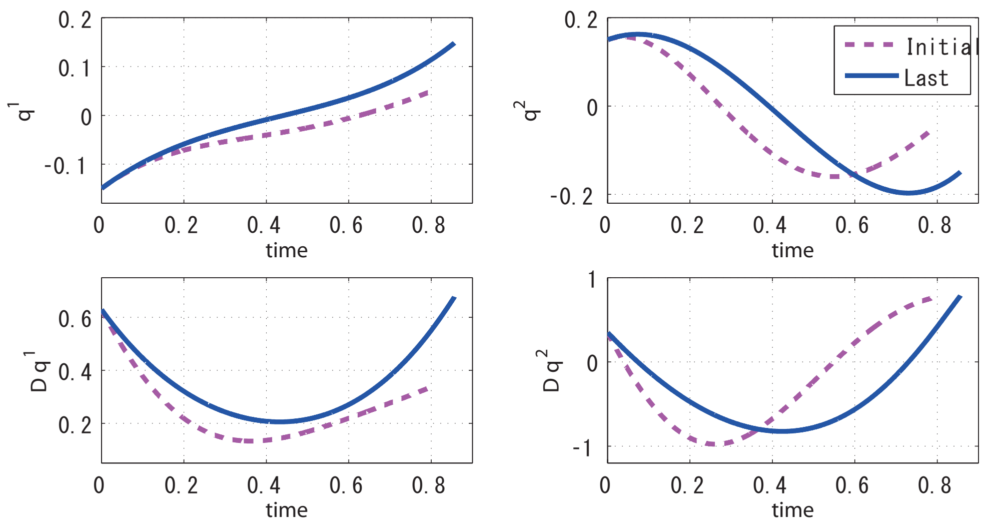

Figure 2.11: Responses of q and $\dot{q}$ before and after learning

The case of the initial condition : $(-0.20, 0.20, 0.83, 0.4)$

Secondly, we proceed 40 steps of the learning procedure which means 85 simulations including 5 preliminary experiments with the initial condition:

$$(q^1_{t^0}, q^2_{t^0}, \dot{q}^1_{t^0}, \dot{q}^2_{t^0}) = (-0.20, 0.20, 0.83, 0.4).$$

Figure 2.12 shows the history of the cost function (2.39) along the iteration decreasing monotonically as Fig. 2.5. Figure 2.13 represents the animations of the robot before and after learning, respectively and it implies that the robot stops with almost standing posture before learning and a walking motion seems to be generated eventually. Figure 2.14 exhibits the phase portrait of q-$\dot{q}$ and that of q^1 - q^2, respectively. It implies that an almost periodic trajectory is also generated with this initial condition. Figure 2.15 shows the generated learning control input $\bar{u}$ and Fig. 2.16 does the control input u in Eq. (2.25). We observe 200 steps consecutive walking with these inputs. Figure 2.17 shows the time revolution of the ZMP in Eq. (2.56) of the generated gait. The ZMP is shifted forward as well as the result in the previous simulation. Regarding the total leg length of the robot and the range of the ZMP position, the generated gait seems feasible. Finally, Fig. 2.18 shows responses of q and $\dot{q}$ at the last step in the proposed method in solid lines and those before learning in dotted lines.

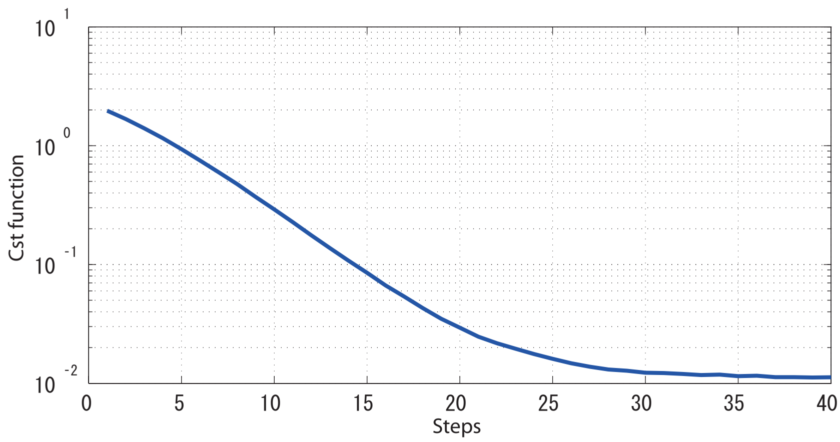

Figure 2.12: Cost function

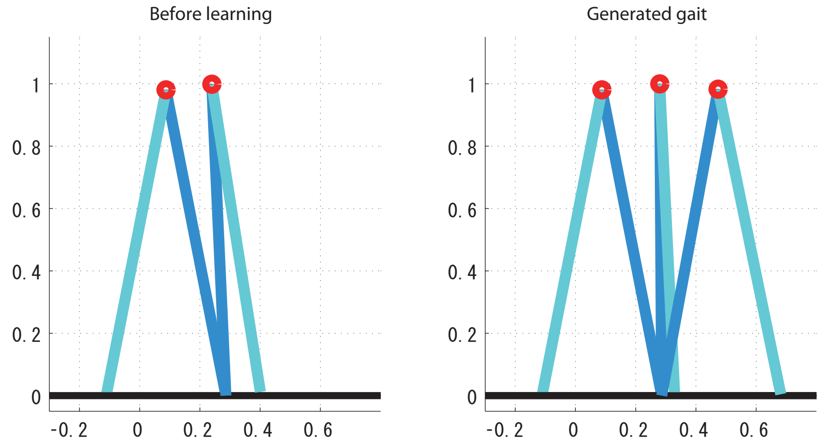

Figure 2.13: Stick diagrams before and after learning

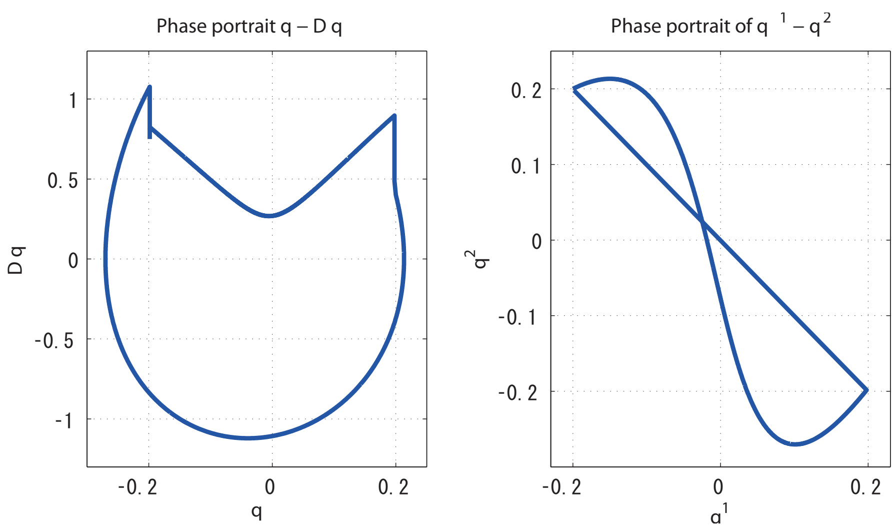

Figure 2.14: Phase portraits

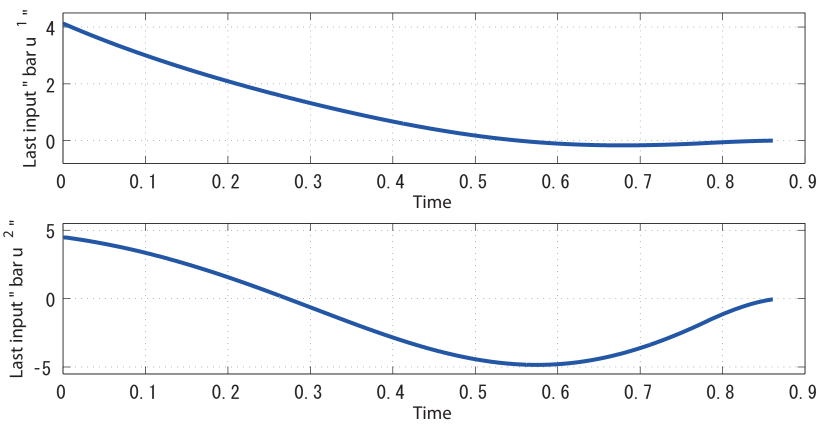

Figure 2.15: Generated learning control inputs $\bar{u}$

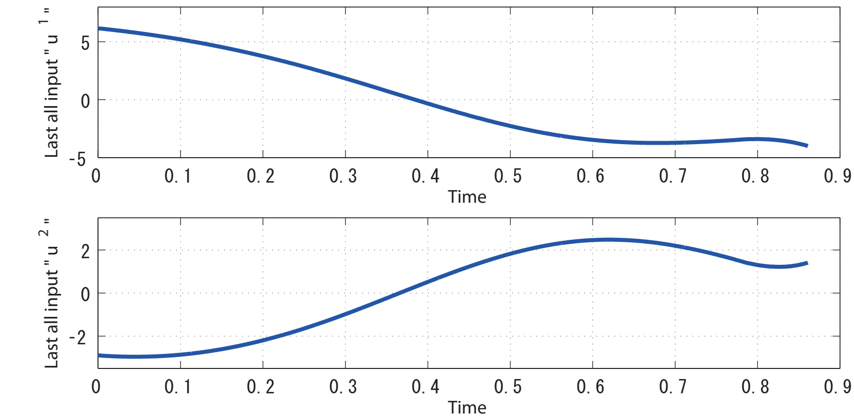

Figure 2.16: Generated all control inputs u

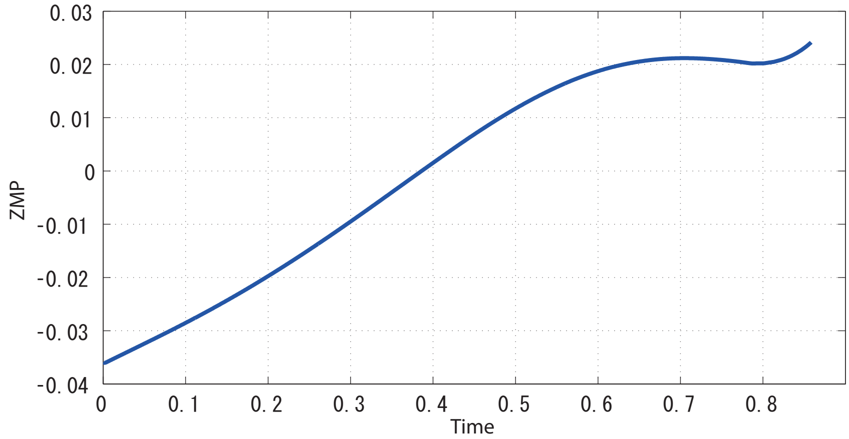

Figure 2.17: ZMP of the generated gait

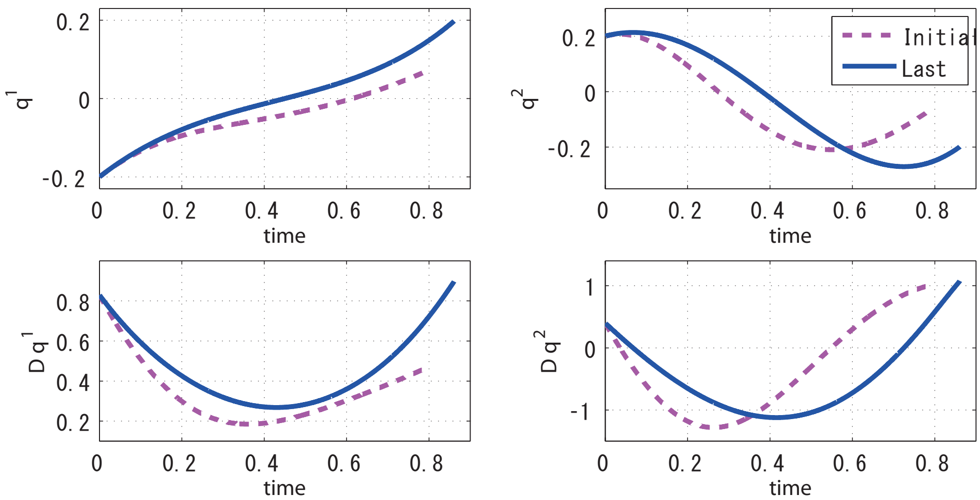

Figure 2.18: Responses of q and $\dot{q}$ before and after learning

The case of the initial condition : $(-0.25, 0.25, 1.05, 0.4)$

Finally, we proceed 60 steps of the learning procedure which means 125 simulations including 5 preliminary experiments with the initial condition:

$$(q^1_{t^0}, q^2_{t^0}, \dot{q}^1_{t^0}, \dot{q}^2_{t^0}) = (-0.25, 0.25, 1.05, 0.4).$$

Figure 2.19 shows the history of the cost function (2.39) along the iteration decreasing monotonically as Figs. 2.5 and 2.12. Figure 2.20 represents the animations of the robot before and after learning, respectively and it implies that the robot stops with almost standing posture before learning and a walking motion seems to be generated eventually. Figure 2.21 exhibits the phase portrait of q-$\dot{q}$ and that of q^1 - q^2, respectively. It implies that an almost periodic trajectory is also generated with this initial condition. Figure 2.22 shows the generated learning control input $\bar{u}$ and Fig. 2.23 does the control input u in Eq. (2.25). We observe 200 steps consecutive walking with these inputs. Figure 2.24 shows the time revolution of the ZMP in Eq. (2.56) of the generated gait. The ZMP is shifted forward as well as the first two simulation results. Although the range of the ZMP position becomes larger than those in Figs. 2.10 and 2.17, the generated gait seems feasible. Finally, Fig. 2.25 shows responses of q and $\dot{q}$ at the last step in the proposed method in solid lines and those before learning in dotted lines.

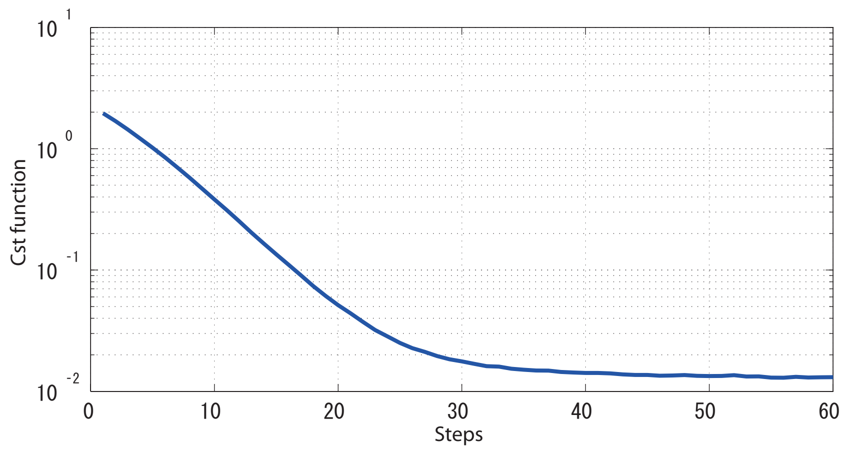

Figure 2.19: Cost function

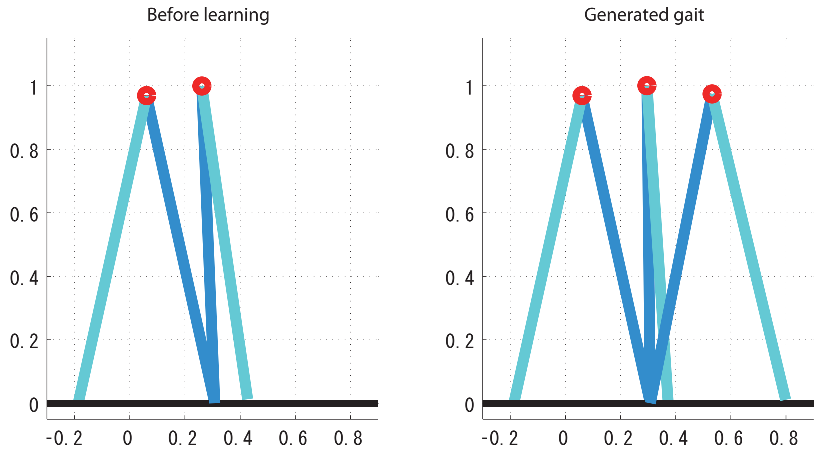

Figure 2.20: Stick diagrams before and after learning

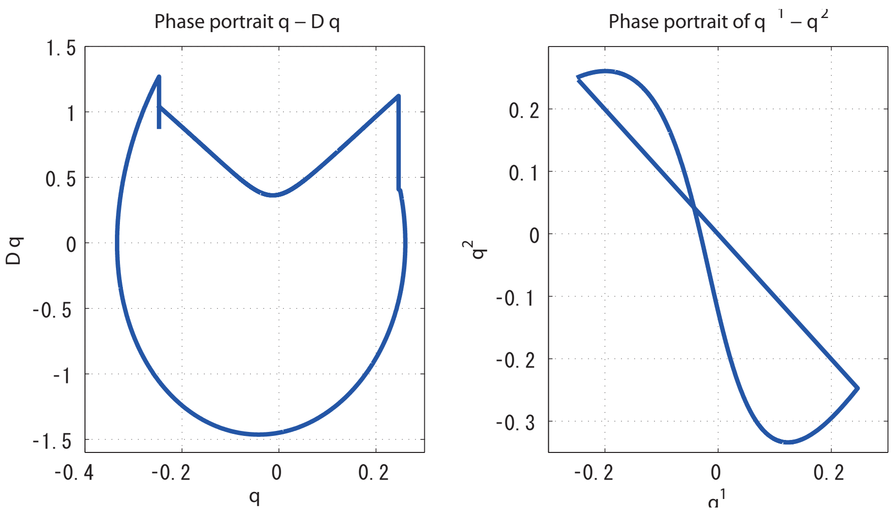

Figure 2.21: Phase portraits

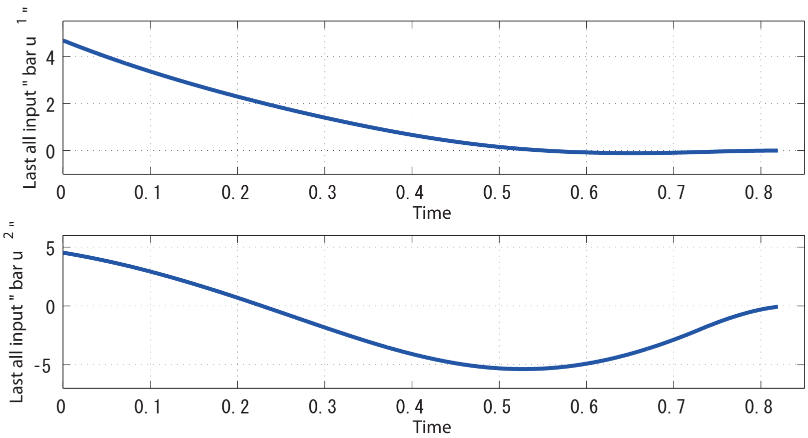

Figure 2.22: Generated learning control inputs $\bar{u}$

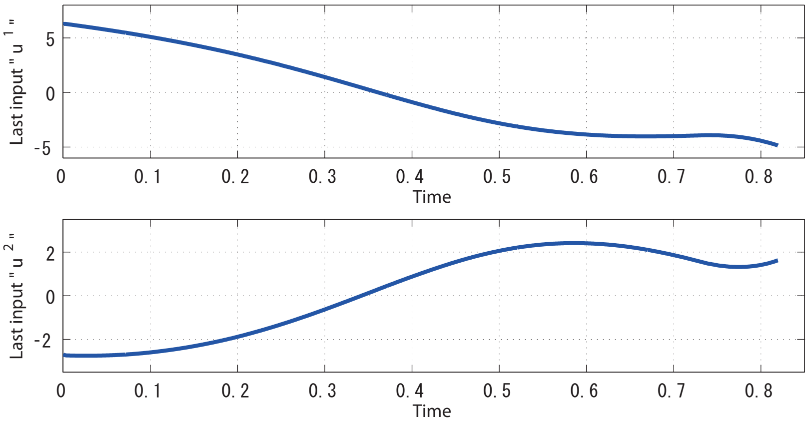

Figure 2.23: Generated all control inputs u

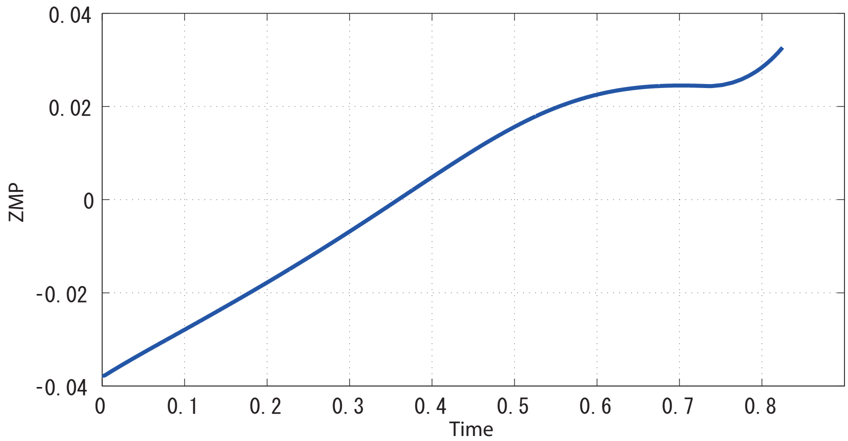

Figure 2.24: ZMP of the generated gait

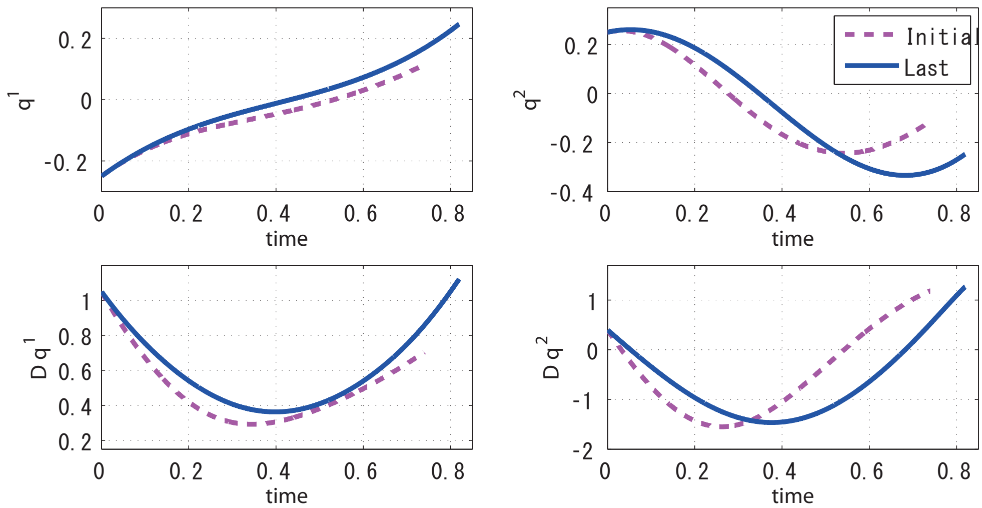

Figure 2.25: Responses of q and $\dot{q}$ before and after learning

In our framework, there are some design parameters, that is, Λ_y, $\Lambda_{\dot{y}}$, $\Lambda_{\bar{u}}$, $K_{(\cdot)}$ and $\epsilon_{(\cdot)}$. First of all, each of them has to be positive definite matrix or positive number. We should choose $\epsilon_{(\cdot)}$'s small enough so that the approximation in Eq. (2.17) holds. The parameters $K_{(\cdot)}$'s are the step parameters in the steepest decent method. Although we set all $K_{(\cdot)}$'s constant in these simulations, generally they are chosen to be large in the beginning of learning, and then they are chosen to be gradually smaller according to the leaning steps. In order to prioritize making the configuration coordinate q periodic over making their velocity $\dot{q}$ periodic, we choose the coefficients of Λ_y larger than the other weighting coefficients. There are two reasons why the coefficients of $\Lambda_{\bar{u}}$ are chosen much smaller than the others. The first learning procedure is executed with zero input because of the lack of a priori information about the initial learning input. Since some control input is necessary to achieve walking on the level ground, the value of the cost function with respect to the learning input necessarily increases at the beginning of learning. If one sets the coefficient big and emphasizes the limitation of the learning input, walking trajectories may not be generated. This is the first reason. The other reason is that the cost with respect to the input is evaluated relatively much bigger than those with respect to the output and its time derivative constraints because of the filter function ν_1. A systematic way to choose these design parameters is our future work.

2.5 Summary

In this chapter, an optimal gait generation framework considering discontinuous state transitions based on iterative learning control of Hamiltonian systems has been proposed. This method can generate optimal feedforward control input and the corresponding periodic trajectory minimizing the L_2 norm of the control input by combining the iterative learning control method and the estimation method of the state transition mapping based on the least-squares. The proposed method does not require the precise knowledge of the plant system nor the discontinuous state transition model which is not accurate for real robots. Applying this technique to the compass gait biped, we generate optimal gait trajectories on the level ground with some initial conditions. Numerical simulations demonstrate the effectiveness of the proposed framework.

Chapter 3

Repetitive control framework using virtual constraint

In the previous chapter, we have proposed an optimal gait generation framework in terms of energy efficiency via iterative learning control (ILC) proposed in [27] which utilizes variational symmetry of Hamiltonian systems. While ILC frameworks, e.g. [1, 27], do not require precise information about the plant system, they require a lot of laboratory experiments under the same initial condition. However, this experimental condition is sometimes strict, because it is difficult to realize the desired initial velocity of the mechanical systems including walking robots.

To solve the problem, in this chapter, we propose a novel optimal gait generation framework using virtual constraints and learning optimal control of Hamiltonian systems. Here, learning optimal control is referred to the combination of ILC [27] and iterative feedback tuning (IFT) [19] based on variational symmetry of Hamiltonian systems. While ILC [1, 12, 27] is to find an optimal feedforward input minimizing a given cost function, IFT [9, 37, 19] is to find optimal parameters of a given feedback controller. Since in the proposed framework, a learning procedure is automatically executed and eventually an optimal periodic walking trajectory is expected to be generated, our framework is classified as repetitive control framework [33, 29, 22] rather than iterative learning control one. Conventional repetitive control is also a kind of a learning method for a trajectory tracking control problem with time periodic reference trajectories without using precise information of the plant. Only the difference between repetitive control and iterative learning control is the type of the reference trajectories: time periodic one (with the infinite length) and one on a finite time interval. However, a repetitive control framework for optimal control problems, as in the iterative leaning control case, was not investigated so far. The authors have proposed a repetitive control framework of Hamiltonian systems based on variational symmetry in [21, 22]. However, since our past method can only deal with reference (or desired) trajectories whose initial states are stationary points and since walking trajectories considered here do not satisfy the condition, the method can not be applied to the optimal gait generation problem. So, the proposed method in this chapter is a kind of modification of [21, 22]. By utilizing virtual constraints and learning optimal control, this method can be applied to trajectories which do not satisfy the condition supposed in [21, 22].

The proposed method is summarized as follows. Firstly, we add a constraint by adding a virtual potential energy to prevent the robot from falling. Secondly, we execute the learning procedure proposed in the previous chapter (see also [75, 78]). The proposed technique restricts the motion of the robot to a symmetric trajectory by the virtual constraint. Due to this additional constraint, we does not need to repeat experiments under the same initial condition. Thirdly, by regarding the potential gain for the constraint as a tuning parameter, we execute iterative feedback tuning to mitigate the strength of the virtual constraint automatically according to the progress of learning control. Consequently, it is expected to generate an optimal gait without constraint eventually. Let us note that the proposed method differs from the existing techniques using virtual constraint, e.g. [32, 39], in that our method automatically optimizes the strength of the constraint. Both ILC [27] and IFT [19] methods utilize variational symmetry of Hamiltonian systems and derivation of iteration laws are similar. However, since both methods influence each other, they can not be used simultaneously. In order to take interference of both methods into account, we introduce an extended system which again has variational symmetry. By considering the extended system instead of the plant system, we can apply ILC and IFT simultaneously.

The remainder of this chapter is organized as follows. Firstly, in section 3.1, the conventional IFT method in [19] is briefly referred to. Secondly, in section 3.2, we discuss learning optimal control method combining ILC and IFT, and then we propose a novel optimal gait generation framework using this method and virtual constraints. Finally, in section 3.4, some numerical simulations demonstrate the effectiveness of the proposed method.

3.1 Iterative feedback tuning (IFT) based on variational symmetry

In [19], an iterative feedback tuning method based on variational symmetry of Hamiltonian systems has been proposed. Here we consider a feedback system of a Hamiltonian system with a generalized canonical transformation [25] mentioned in Section 2.2 so that the feedback system is also described by another Hamiltonian system in the form of (2.1). Therefore the system parameters of the closed loop system H_c, J_c and R_c (for the typical mechanical systems, see Eq. (2.26)) generally depend on the parameters of the feedback controller to be adjusted. For simplicity, in this section, it is supposed that only the Hamiltonian function H_c depends on the tuning parameter $\rho \in \mathbb{R}^s$. The case where J_c and R_c also depend on ρ is considered in [19].

Consider a feedback system in (2.1) with a Hamiltonian $H_c(x, u, \rho)$. In the iterative feedback tuning method proposed in [19], the tuning parameter is considered to be a virtual input for the Hamiltonian system and induce a corresponding output so that the input-output map has variational symmetry mentioned in Subsection 2.1.1. Let us introduce the following 0-order hold operator which maps the parameter $\rho \in \mathbb{R}^s$ to $u_\rho \in L_2^s[t^0, t^1]$ in order to define a virtual input

$$\mathfrak{h} : \mathbb{R}^s \to L_2^s[t^0, t^1] \;:\; u_\rho(t) := (\mathfrak{h}(\rho))(t) \equiv \rho, \;\; \forall t \in [t^0, t^1]. \tag{3.1}$$

For the virtual input u_ρ, let us consider the following input-output map

$$y_\rho = \Sigma_\rho^{x_{t^0}, \bar{u}}(u_\rho) \;:\; \begin{cases} \dot{x} = (J - R) \dfrac{\partial H_c(x, \bar{u}, u_\rho)}{\partial x}^\top, \quad x(t^0) = x_{t^0} \\ y_\rho = -\dfrac{\partial H_c(x, \bar{u}, u_\rho)}{\partial u_\rho}^\top \end{cases}. \tag{3.2}$$

Since this map Σ_ρ is a Hamiltonian system in the form (2.1), Lemma 2.2 and Theorem 2.3 imply that it has variational symmetry with some conditions [19]. Here the following property with respect to $\mathfrak{h}$ defined in (3.1) is exhibited, which will be utilized in the next subsection.

Lemma 3.1 *[19] $\mathfrak{h}^*$ is characterized by the following equation for any $\xi \in L_2^s[t^0, t^1]$*

$$\mathfrak{h}^*(\xi) = \int_{t^0}^{t^1} \xi(t)\,\mathrm{d}t. \tag{3.3}$$

By utilizing the input-output map (3.2) and Eq. (3.3), an iteration algorithm for iterative feedback tuning can be derived in the similar manner as in the case of iterative learning control mentioned in Subsection 2.1.2.

3.2 Learning optimal control combining ILC and IFT

In this section, we combine ILC [27] and IFT [19] algorithms by introducing an extended system which again has variational symmetry. Let us define the extended input u_e by $u_e := (\bar{u}^\top, u_\rho^\top)^\top \in U_e = U \times U_\rho$, the extended output y_e by $y_e := (y^\top, y_\rho^\top)^\top \in Y_e = Y \times Y_\rho$, where $U_\rho, Y_\rho = L_2^s[t^0, t^1]$ and Hamiltonian H_e by $H_e(x, u_e) := H_c(x, \bar{u}, u_\rho)$. Then we have the following extended system

$$y_e = \Sigma_e^{x_{t^0}}(u_e) \ : \ \begin{cases} \dot{x} = (J - R)\,\dfrac{\partial H_e(x, u_e)}{\partial x}^\top, \quad x(t^0) = x_{t^0} \\ y_e = -\dfrac{\partial H_e(x, u_e)}{\partial u_e}^\top \end{cases}. \tag{3.4}$$

Since the extended system (3.4) has the form (2.1), it can be easily proven that this system has variational symmetry with certain conditions. Then we consider a cost function $\hat{\Gamma}_e(u_e, y_e) : U_e \times Y_e \to \mathbb{R}$. The Fréchet derivative of the cost function can be calculated as

$$\begin{aligned} &\delta\hat{\Gamma}_e(u_e, y_e)(\delta u_e, \delta y_e) \\ &\quad = \langle \nabla_{u_e}\hat{\Gamma}_e(u_e, y_e), \delta u_e\rangle_{U_e} + \langle \nabla_{y_e}\hat{\Gamma}_e(u_e, y_e), \delta y_e\rangle_{Y_e} \\ &\quad = \langle \nabla_{u_e}\hat{\Gamma}_e + (\delta\Sigma_e^{x_{t^0}}(u_e))^*(\nabla_{y_e}\hat{\Gamma}_e), \delta u_e\rangle_{U_e}, \end{aligned} \tag{3.5}$$

where $\nabla_{u_e}\hat{\Gamma}_e(u_e, y_e)$ and $\nabla_{y_e}\hat{\Gamma}_e(u_e, y_e)$ represent the partial gradients of the cost function with respect to u_e and y_e, respectively. It follows from the definition of u_e that

$$\delta u_e = \begin{pmatrix} \delta\bar{u} \\ \delta u_\rho \end{pmatrix} = \begin{pmatrix} \delta\bar{u} \\ \delta\mathfrak{h}(\rho)\,\mathrm{d}\rho \end{pmatrix} = \begin{pmatrix} \delta\bar{u} \\ \mathfrak{h}(\mathrm{d}\rho) \end{pmatrix}. \tag{3.6}$$

Here the last equality follows from Definition 2.1 and the linearity of the operator $\mathfrak{h}$, that is,

$$\begin{aligned} \delta\mathfrak{h}(\rho)\,\mathrm{d}\rho &= \mathfrak{h}(\rho + \mathrm{d}\rho) - \mathfrak{h}(\rho) + o(\|\mathrm{d}\rho\|) \\ &= \mathfrak{h}(\mathrm{d}\rho) + o(\|\mathrm{d}\rho\|). \end{aligned}$$

From Eq. (3.6), Eq. (3.5) reduces to

$$
\begin{aligned}
&\delta\hat{\Gamma}_e(u_e, y_e)(\delta u_e, \delta y_e)\\
&= \left\langle \begin{pmatrix} \mathrm{id} & 0 \\ 0 & \mathfrak{h}^* \end{pmatrix} \left(\nabla_{u_e}\hat{\Gamma}_e + (\delta\Sigma_e^{x_{t^0}}(u_e))^*(\nabla_{y_e}\hat{\Gamma}_e)\right), \begin{pmatrix} \delta\bar{u} \\ \mathrm{d}\rho \end{pmatrix} \right\rangle_{U\times\mathbb{R}^s}\\
&= \left\langle \begin{pmatrix} \nabla_{\bar{u}}\hat{\Gamma}_e \\ \mathfrak{h}^*(\nabla_{u_\rho}\hat{\Gamma}_e) \end{pmatrix} + \begin{pmatrix} \mathrm{id} & 0 \\ 0 & \mathfrak{h}^* \end{pmatrix} \mathcal{R}(\delta\Sigma_e^{\psi_{e,t^0}}(w_e))\mathcal{R}(\nabla_{y_e}\hat{\Gamma}_e), \begin{pmatrix} \delta\bar{u} \\ \mathrm{d}\rho \end{pmatrix} \right\rangle_{U\times\mathbb{R}^s}\\
&\approx \left\langle \begin{pmatrix} \nabla_{\bar{u}}\hat{\Gamma}_e \\ \mathfrak{h}^*(\nabla_{u_\rho}\hat{\Gamma}_e) \end{pmatrix} + \begin{pmatrix} \mathcal{R} & 0 \\ 0 & \mathfrak{h}^* \end{pmatrix} \left(\frac{\Sigma_e^{\psi_{e,t^0}}(w_e + \epsilon_e\mathcal{R}(\nabla_{y_e}\hat{\Gamma}_e)) - \Sigma_e^{\psi_{e,t^0}}(w_e)}{\epsilon_e} \right), \begin{pmatrix} \delta\bar{u} \\ \mathrm{d}\rho \end{pmatrix} \right\rangle_{U\times\mathbb{R}^s},
\end{aligned}
\tag{3.7}
$$

where ψ_{e,t^0} and $w_e := (w^\top, \mathfrak{h}(\rho)^\top)^\top$ should be chosen such that the condition (2.8) in Theorem2.3 holds. In the last approximation, the relation $\mathfrak{h}^*\mathcal{R} = \mathfrak{h}^*\mathcal{R}^* = (\mathcal{R}\mathfrak{h})^* = \mathfrak{h}^*$ is utilized (see also Eq. (2.47)). Consequently, the optimal learning control algorithm combining ILC and IFT is given by

$$
\begin{aligned}
&\begin{cases}
x_{t^0(3i+1)} = \psi_{e,t^0(i)}\\
\bar{u}_{(3i+1)} = w_{(i)}\\
\rho_{(3i+1)} = \rho_{(3i)}
\end{cases}\\
&\begin{cases}
x_{t^0(3i+2)} = \psi_{e,t^0(i)}\\
\bar{u}_{(3i+2)} = w_{(i)} + \epsilon_{e(i)}\mathcal{R}(\nabla_y\hat{\Gamma}_{e(3i)})\\
u_{\rho(3i+2)} = \mathfrak{h}(\rho_{(3i)}) + \epsilon_{e(i)}\mathcal{R}(\nabla_{y_\rho}\hat{\Gamma}_{e(3i)})
\end{cases}\\
&\begin{cases}
x_{t^0(3i+3)} = x_{t^0(3i)}\\
\bar{u}_{(3i+3)} = \bar{u}_{(3i)} - K_{(i)}\left(\nabla_{\bar{u}}\hat{\Gamma}_{e(3i)} + \dfrac{1}{\epsilon_{e(i)}}\mathcal{R}(y_{(3i+2)} - y_{(3i+1)})\right)\\
\rho_{(3i+3)} = \rho_{(3i)} - K_{\rho(i)}\left(\displaystyle\int_{t^0}^{t^1} \nabla_{u_\rho}\hat{\Gamma}_{e(3i)} + \dfrac{1}{\epsilon_{e(i)}}\mathcal{R}(y_{\rho(3i+2)} - y_{\rho(3i+1)})\,\mathrm{d}t\right)
\end{cases},
\end{aligned}
\tag{3.8}
$$

provided that the initial control input $\bar{u}_{(0)} \equiv 0$ (or an appropriate initial input), the initial parameter $\rho_{(0)}$ and the initial condition $x_{t^0(0)}$ are appropriately chosen, respectively. Here $\epsilon_{e(\cdot)}$ denotes a sufficiently small positive constant and an appropriate positive definite matrices $K_{(\cdot)}$ and $K_{\rho(\cdot)}$ represent gains, respectively. Here the condition $\psi_{e,t^0(i)}$ and $w_{(i)}$ are chosen such that it satisfies the condition (2.8) in Theorem2.3 with the trajectory governed by the pair $x_{t^0(3i)}$ and $\bar{u}_{(3i)}$ with $\rho_{(3i)}$. A concrete algorithm exhibiting how to select $\psi_{e,t^0(i)}$ and $w_{(i)}$ is given for mechanical systems in the next section.

Remark 3.1 As mentioned in Remarks 2.10 and 2.12, if the learning procedure is executed around a symmetric trajectory, one can utilize the following procedure instead of that in (3.8)

$$\begin{cases} x_{t^0(2i+1)} = x_{t^0(2i)} \\ \bar{u}_{(2i+1)} = \bar{u}_{(2i)} + \epsilon_{e(i)}\mathcal{R}(\nabla_y \hat{\Gamma}_{e(2i)}) \\ u_{\rho(2i+1)} = \mathfrak{h}(\rho_{(2i)}) + \epsilon_{e(i)}\mathcal{R}(\nabla_{y_\rho} \hat{\Gamma}_{e(2i)}) \end{cases}$$
$$\begin{cases} x_{t^0(2i+2)} = x_{t^0(2i)} \\ \bar{u}_{(2i+2)} = \bar{u}_{(2i)} - K_{(i)} \left(\nabla_{\bar{u}} \hat{\Gamma}_{e(2i)} + \dfrac{1}{\epsilon_{e(i)}} \mathcal{R}(y_{(2i+1)} - y_{(2i)}) \right) \\ \rho_{(2i+2)} = \rho_{(2i)} - K_{\rho(i)} \left(\displaystyle\int_{t^0}^{t^1} \nabla_{u_\rho} \hat{\Gamma}_{e(2i)} + \dfrac{1}{\epsilon_{e(i)}} \mathcal{R}(y_{\rho(2i+1)} - y_{\rho(2i)})\, \mathrm{d}t \right) \end{cases} . \tag{3.9}$$

Remark 3.2 Although the proposed algorithm requires time-varying feedback gains during the learning procedure in generating perturbation signals (see $u_{\rho(3i+2)}$ in the iteration procedure (3.8) or $u_{\rho(2i+1)}$ in another procedure (3.9)) in order to approximate output signals of the variational system by utilizing Eq. (3.7), eventually, a generated optimal feedback gain is constant. Unless time-varying feedback gains are available, we substitute a feedforward input with the previous output signal. For example, the following procedure is substituted for the original one in (3.8)

$$\begin{cases} x_{t^0(3i+2)} = \psi_{e,t^0(i)} \\ \bar{u}_{(3i+2)} = w_{(i)} + \epsilon_{e(i)}\mathcal{R}(\nabla_y \hat{\Gamma}_{e(3i)}) + \epsilon_{e(i)}\mathcal{R}(\nabla_{y_\rho} \hat{\Gamma}_{e(3i)}) y_{(3i)} \\ \rho_{(3i+2)} = \rho_{(3i)} \end{cases} .$$

3.3 Optimal gait generation via optimal learning control using virtual constraints

This section proposes a repetitive control framework for gait generation by utilizing optimal learning control proposed in the previous section and virtual constraints. Firstly, we introduce a constraint by adding a virtual potential energy, which plays an important role in our method. Then, we define a cost function and exhibit a proposed algorithm. In this section, we mainly consider the compass gait biped mentioned in Section 2.2 and then proceed to that with a torso in Subsection 3.3.3.

3.3.1 Constraints by virtual potential energies

In the literatures [32, 39], walking control methods using virtual constraints based on the output zeroing control are proposed. In [39], particularly, they can achieve stable symmetric walking gaits using another property of Hamiltonian systems other than those used in this thesis. They set the output function $y = q^1 + q^2$ to zero by the output zeroing control and keep the leg angles bounded by a leg exchange scheme [39]. As a consequence, they guarantee that the robot does not fall and obtain symmetric walking gaits satisfying $q^1 + q^2 = 0$.

On the other hand, we use a similar concept of the virtual constraint to prevent the robot from falling, but do not use the output zeroing control. There are two reasons: one is that the output zeroing control requires the precise knowledge of the plant system and the other is that such constraints consume a lot of control energy. We add a virtual potential energy such as Eq. (3.10) to produce a similar effect to [39]

$$P_c := \frac{k_c}{2}(q^1 + q^2)^2. \tag{3.10}$$

Here, the gain parameter k_c represents the constraint strength. We let k_c sufficiently large at the beginning of the learning steps so that the trajectory of the robot is restricted to a symmetric one, i.e. $q^1 + q^2 = 0$ holds. Due to [39], it is expected that the robot does not fall. The advantages of this method instead of the output zeroing control are as follows. Firstly, it does not require the model parameters of the plant system, since the potential energy (3.10) can be generated by a simple feedback controller

$$u = -K_P q - K_D \dot{q} + \bar{u} - k_c A_c q, \quad A_c := \begin{pmatrix} 1 & 1 \\ 1 & 1 \end{pmatrix}. \tag{3.11}$$

The feedback system is depicted in Fig. 3.1. Secondly, after adding the potential energy, the

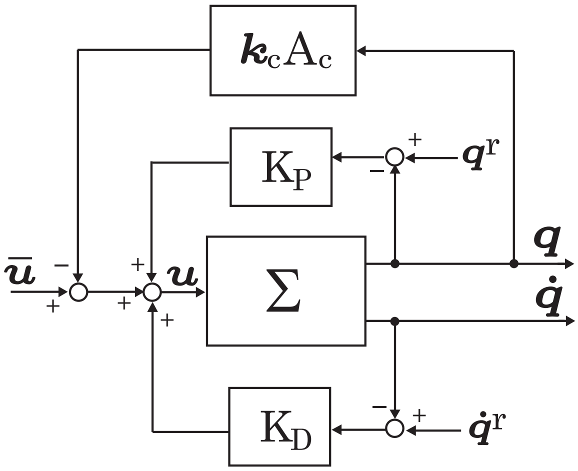

Figure 3.1: Feedback system

plant system preserves the Hamiltonian structure and the constraint parameter k_c is explicitly contained in a new Hamiltonian. The controller (3.11) converts the dynamics of the compass gait biped in (2.21) into another Hamiltonian system of the form (2.19) with a new Hamiltonian $\bar{H}$, a new structure matrix $\bar{J}$ and a new dissipation matrix $\bar{R}$ as

$$\bar{H}(q, p, \bar{u}, k_c) = \frac{1}{2} p^\top M(q)^{-1} p + V(q) + \frac{1}{2} q^\top (K_P + k_c A_c) q - \bar{u}^\top q,$$

$$\bar{J} = \begin{pmatrix} O_{22} & I_2 \\ -I_2 & O_{22} \end{pmatrix}, \quad \bar{R} = \begin{pmatrix} O_{22} & O_{22} \\ O_{22} & K_D \end{pmatrix}. \tag{3.12}$$

By regarding k_c as a tuning parameter, the extended system with the extended input $u_e := (\bar{u}^\top, u_\rho)^\top$ and the extended output $y_e := (y^\top, y_\rho)^\top$, where

$$u_\rho := \mathfrak{h}(k_c), \quad y_\rho := -\frac{1}{2} q^\top A_c q,$$

has the form (3.4). So, we execute optimal learning control procedure combining ILC and IFT proposed in Section 3.2 in order to adjust the constraint strength by IFT, and generate a walking trajectory by ILC. The idea of the proposed framework is summarized as follows.

Step 1 : Add a virtual potential energy to restrict the motion of the robot to a symmetric trajectory. Then, let constraint parameter k_c sufficiently large to expect that the robot does not fall.

Step 2 : By utilizing optimal learning control scheme proposed in Section 3.2, ILC generates an optimal walking gait and simultaneously, IFT mitigates the constraint parameter automatically according to the progress of learning control.

Step 3 : Repeat Step 2 every one step cycle.

As a result, it is expected that an optimal gait is generated without a constraint eventually. The feature of the proposed method is that the robot improves his walk keeping on walking, because the robot does not fall due to Step1. From this aspect, our method is classified as repetitive control framework [33, 29, 22] rather than iterative learning control framework [1, 12, 27]. It also differs from the conventional methods using virtual constraints in that it automatically optimizes the strength of the constraints.

3.3.2 Derivation of the iteration law

Let us consider the following cost function

$$\begin{aligned}\hat{\Gamma}_2(y,\dot{y},\bar{u},y_\rho,u_\rho) := \;& \frac{1}{2}\int_{t^0}^{t^1} (y(\tau)-C\mathcal{R}(y)(\tau))^\top \nu_1(\tau)\Lambda_y(y(\tau)-C\mathcal{R}(y)(\tau))\,\mathrm{d}\tau \\ &+\frac{1}{2}\int_{t^0}^{t^1} F_v(\dot{y}(\tau)-v_{ref})^\top \nu_2(\tau)\Lambda_{\dot{y}}F_v(\dot{y}(\tau)-v_{ref})\,\mathrm{d}\tau + \frac{1}{2}\int_{t^0}^{t^1}\bar{u}(\tau)^\top\Lambda_{\bar{u}}\bar{u}(\tau)\,\mathrm{d}\tau \\ &+\frac{\gamma_{y_\rho}}{2}\int_{t^0}^{t^1} y_\rho^2(\tau)\,\mathrm{d}\tau + \frac{\gamma_{u_\rho}}{2}\int_{t^0}^{t^1} u_\rho^2(\tau)\,\mathrm{d}\tau, \end{aligned} \tag{3.13}$$

where appropriate positive definite matrices $\Lambda_y, \Lambda_{\dot{y}}, \Lambda_{\bar{u}} \in \mathbb{R}^{2\times 2}$ represent weight matrices and appropriate positive constants γ_{y_ρ} and γ_{u_ρ} represent weighting coefficients, respectively. The first term of the cost function (3.13) is also equipped in Eq. (2.39), which is a necessary condition for a periodic trajectory such that $q^1(t^0) \equiv q^2(t^1)$ and $q^2(t^0) \equiv q^1(t^1)$. Figure 3.2 illustrates the condition. Let us note that although another necessary condition with respect to $\dot{q}$ can be utilized as in Eq. (2.39), where initial angular velocities are equivalent to velocities just after touch down. However, it is not equipped here for simplicity of iteration law. In the second term, $v_{ref} \in \mathbb{R}^2$ represents a constant reference angular velocity and $\nu_2(t) \in \mathbb{R}$ denotes a filter function defined

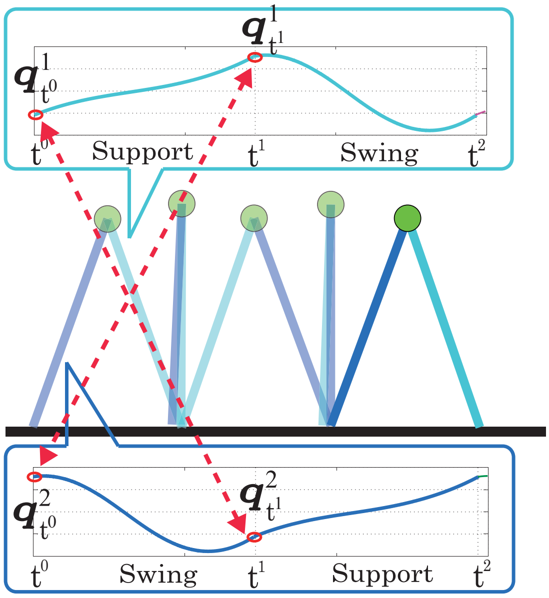

Figure 3.2: Illustration of the restraint condition of the cost function

by

$$\nu_2(t) := \begin{cases} 0 & (t^0 \le t < \frac{t^1-t^0}{2} - \Delta\bar{t}) \\ \frac{1}{2}\left(1-\cos\left(\frac{-\frac{t^1-t^0}{2}+\Delta\bar{t}+t}{\Delta\bar{t}}\pi\right)\right) & (\frac{t^1-t^0}{2} - \Delta\bar{t} \le t < \frac{t^1-t^0}{2}) \\ \frac{1}{2}\left(1-\cos\left(\frac{\frac{t^1-t^0}{2}+\Delta\bar{t}-t}{\Delta\bar{t}}\pi\right)\right) & (\frac{t^1-t^0}{2} \le t < \frac{t^1-t^0}{2} + \Delta\bar{t}) \\ 0 & (\frac{t^1-t^0}{2} + \Delta\bar{t} \le t \le t^1) \end{cases}, \tag{3.14}$$

where a design parameter $\Delta\bar{t}$ denotes a positive constant. Figure 3.3 illustrates $\nu_2(t)$. For any $\zeta \in \mathbb{R}^r$, a penalty function $F_v : \mathbb{R}^r \to \mathbb{R}^r$ is defined as

$$[F_v(\zeta)]^i = \begin{cases} k_{F_v}(\zeta^i)^2 & \text{if } \zeta^i < 0 \\ 0 & \text{otherwise} \end{cases}, \qquad (i = 1, 2, \cdots, r), \tag{3.15}$$

where an appropriate positive constant k_{F_v} represents strength of the penalty. In what follows, the dimension r of the penalty function shall accordingly change with that of the argument (in the case of Eq. (3.13), $r = 2$). The second term encourages the robot to achieve an appropriate constant velocity in the middle of walking. As a consequence, it is aimed at specifying the walking direction (forward or backward) and a rough walking speed, and preventing the robot from stopping during the learning. The third and fourth terms are to minimize the control input and

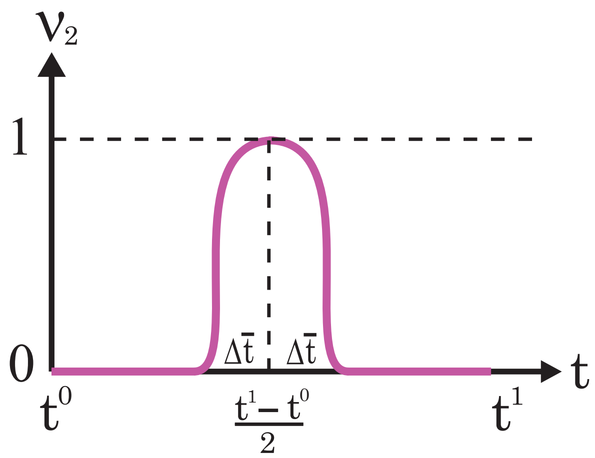

Figure 3.3: Illustration of the filter function $\nu_2(t)$

the feedback input generating virtual potential energy, respectively. The last term is to mitigate the strength of the virtual constraint. In order to utilize variational symmetry of the extended system in (3.12), let us rewrite the cost function (3.13) as

$$\begin{aligned}\hat{\Gamma}_2(y,\dot{y},\bar{u},y_\rho,u_\rho) &\equiv \frac{1}{2}\int_{t^0}^{t^1}(y_e(\tau)-C_e\mathcal{R}(y_e)(\tau))^\top\Lambda_{y_e}(\tau)(y_e(\tau)-C_e\mathcal{R}(y_e)(\tau))\,\mathrm{d}\tau\\ &+\frac{1}{2}\int_{t^0}^{t^1}F_v(\dot{y}_e(\tau)-v_{e,ref})^\top\Lambda_{\dot{y}_e}(\tau)F_v(\dot{y}_e(\tau)-v_{e,ref})\,\mathrm{d}\tau+\frac{1}{2}\int_{t^0}^{t^1}u_e(\tau)^\top\Lambda_{u_e}u_e(\tau)\,\mathrm{d}\tau\\ &=:\hat{\Gamma}_{2e}(y_e,\dot{y}_e,u_e),\end{aligned} \tag{3.16}$$

where

$$C_e := \begin{pmatrix} C & 0\\ 0 & 0\end{pmatrix}\in\mathbb{R}^{3\times 3}\ ,\quad v_{e,ref} := \begin{pmatrix} v_{ref}\\ 0\end{pmatrix}\in\mathbb{R}^3,$$

$$\Lambda_{y_e}(t) := \begin{pmatrix}\nu_1(t)\Lambda_y & 0\\ 0 & \gamma_{y_\rho}\end{pmatrix}\ ,\ \Lambda_{\dot{y}_e}(t) := \begin{pmatrix}\nu_2(t)\Lambda_{\dot{y}} & 0\\ 0 & 0\end{pmatrix}\ ,\ \Lambda_{u_e} := \begin{pmatrix}\Lambda_{\bar{u}} & 0\\ 0 & \gamma_{u_\rho}\end{pmatrix}\in\mathbb{R}^{3\times 3} \tag{3.17}$$

and, in this case, the dimension of F_v is $r=3$.

Since the virtual constraint introduced in Subsection 3.3.1 restricts the motion of the robot to a symmetric trajectory, it is supposed that the learning procedure is executed around a symmetric trajectory. Now let us derive the concrete updating law based on optimal learning control procedure (3.9).

Let us calculate the Fréchet derivative of the cost function (3.16) as follows

$$\begin{aligned}
&\delta\hat{\Gamma}_{2e}(y_e,\dot{y}_e,u_e)(\delta y_e,\delta\dot{y}_e,\delta u_e)\\
&\quad=\langle\Lambda_{y_e}(y_e-C_e\mathcal{R}(y_e),\delta y_e-C_e\mathcal{R}(\delta y_e)\rangle_{Y_e}+\langle\Lambda_{\dot{y}_e}F_v(\dot{y}_e-v_{e,ref}),\delta F_v(\dot{y}_e-v_{e,ref})\mathcal{D}_t(\delta y_e)\rangle_{Y_e}\\
&\qquad+\langle\Lambda_{u_e}u_e,\delta u_e\rangle_{U_e}\\
&\quad=\langle\underbrace{(\mathrm{id}-\mathcal{R}C_e)\Lambda_{y_e}(\mathrm{id}-C_e\mathcal{R})(y_e)-\mathcal{D}_t\left((\delta F_v(\dot{y}_e-v_{e,ref}))^*\Lambda_{\dot{y}_e}F_v(\dot{y}_e-v_{e,ref})\right)}_{=:\,\nabla_{y_e}\hat{\Gamma}_{2e}},\delta y_e\rangle_{Y_e}\\
&\qquad+\langle\underbrace{\Lambda_{u_e}u_e}_{=:\,\nabla_{u_e}\hat{\Gamma}_{2e}},\delta u_e\rangle_{U_e}\\
&\quad=\left\langle\begin{pmatrix}\nabla_y\hat{\Gamma}_{2e}\\ \nabla_{y_\rho}\hat{\Gamma}_{2e}\end{pmatrix},\begin{pmatrix}\delta y\\ \delta y_\rho\end{pmatrix}\right\rangle_{Y_e}+\left\langle\begin{pmatrix}\nabla_{\bar{u}}\hat{\Gamma}_{2e}\\ \nabla_{u_\rho}\hat{\Gamma}_{2e}\end{pmatrix},\begin{pmatrix}\delta\bar{u}\\ \delta u_\rho\end{pmatrix}\right\rangle_{U_e}.
\end{aligned}\tag{3.18}$$

From Eq. (3.15), $(\delta F_v(\dot{y}_e-v_{e,ref}))^*$ can be calculated as

$$[(\delta F_v(\dot{y}_e-v_{e,ref}))^*]^i_j=\begin{cases}0 & (i\neq j)\\ \begin{cases}2k_{F_v}(\dot{y}^i_e-v^i_{e,ref}) & \text{if } \dot{y}^i_e-v^i_{e,ref}<0\\ 0 & \text{otherwise}\end{cases} & (i=j)\end{cases},\quad (i,j=1,2,3).\tag{3.19}$$

Then, The partial gradients $\nabla_y\hat{\Gamma}_{2e}$, $\nabla_{y_\rho}\hat{\Gamma}_{2e}$, $\nabla_{\bar{u}}\hat{\Gamma}_{2e}$ and $\nabla_{u_\rho}\hat{\Gamma}_{2e}$ are calculated from Eq. (3.18) as

$$\begin{aligned}
\begin{pmatrix}\nabla_y\hat{\Gamma}_{2e}\\ \nabla_{y_\rho}\hat{\Gamma}_{2e}\end{pmatrix}&=\begin{pmatrix}\mathrm{id}-\mathcal{R}C & 0\\ 0 & \mathrm{id}\end{pmatrix}\begin{pmatrix}\nu_1\Lambda_y & O_{21}\\ O_{12} & \gamma_{y_\rho}\end{pmatrix}\begin{pmatrix}\mathrm{id}-C\mathcal{R} & 0\\ 0 & \mathrm{id}\end{pmatrix}\begin{pmatrix}y\\ y_\rho\end{pmatrix}\\
&\quad-\mathcal{D}_t\left(\begin{pmatrix}(\delta F_v(\dot{y}-v_{ref}))^* & 0\\ 0 & (\delta F_v(\dot{y}_\rho-0))^*\end{pmatrix}\begin{pmatrix}\nu_2\Lambda_{\dot{y}} & O_{21}\\ O_{12} & 0\end{pmatrix}\begin{pmatrix}F_v(\dot{y}-v_{ref})\\ F_v(\dot{y}_\rho-0)\end{pmatrix}\right)\\
&=\begin{pmatrix}(\mathrm{id}-\mathcal{R}C)\nu_1\Lambda_y(\mathrm{id}-C\mathcal{R})(y)-\mathcal{D}_t((\delta F_v(\dot{y}-v_{ref}))^*\nu_2\Lambda_{\dot{y}}F_v(\dot{y}-v_{ref}))\\ \gamma_{y_\rho}y_\rho\end{pmatrix}
\end{aligned}\tag{3.20}$$

and

$$\begin{pmatrix}\nabla_{\bar{u}}\hat{\Gamma}_{2e}\\ \nabla_{u_\rho}\hat{\Gamma}_{2e}\end{pmatrix}=\begin{pmatrix}\Lambda_{\bar{u}}\bar{u}\\ \gamma_{u_\rho}u_\rho\end{pmatrix}.\tag{3.21}$$

From the iteration law (3.9), Eqs. (3.20) and (3.21), let us summarize the proposed learning procedure.

Step 0 **:** Set appropriate positive definite matrices $\Lambda_y, \Lambda_{\dot{y}}$ and $\Lambda_{\bar{u}}$ as weight matrices, positive constants γ_{y_ρ} and γ_{u_ρ} as weight coefficients and positive constants Δt, $\Delta\bar{t}$ and k_{F_v} as design parameters for the filter functions ν_1 in (2.40) and ν_2 in (3.14) and the penalty function F_v in (3.15). Set the initial control input $\bar{u}_{(0)}$ appropriately (or set $\bar{u}_{(0)} \equiv 0$) and a constant reference angular velocity v_{ref} and let the constraint parameter $k_{c(0)}$ sufficiently large. Let the robot start walking under an appropriate initial condition x_{t^0}.

Set $i = 0$. Then go to Step 1.

Step $2i + 1$ **:** During the (2i+1)-th walking cycle, one utilizes the following controller

$$u = -K_P q - K_D \dot{q} - u_{\rho(2i+1)} A_c q + \bar{u}_{(2i+1)}, \quad A_c := \begin{pmatrix} 1 & 1 \\ 1 & 1 \end{pmatrix}. \tag{3.22}$$

Here the time-varying feedback gain for the virtual constraint $u_{\rho(2i+1)}$ and the feedforward control input $\bar{u}_{(2i+1)}$ are given by

$$\begin{cases} \bar{u}_{(2i+1)} = \bar{u}_{(2i)} + \epsilon_{e(i)} \mathcal{R}(\nabla_y \hat{\Gamma}_{2e(2i)}) \\ u_{\rho(2i+1)} = u_{\rho(2i)} + \epsilon_{e(i)} \mathcal{R}(\nabla_{y_\rho} \hat{\Gamma}_{2e(2i)}) \end{cases},$$

where $\epsilon_{e(i)}$ denotes a sufficiently small positive constant and

$$\nabla_y \hat{\Gamma}_{2e(2i)} = (\mathrm{id} - \mathcal{R}C)\nu_1 \Lambda_y (\mathrm{id} - C\mathcal{R})(y_{(2i)}) - \mathcal{D}_t((\delta F_v(\dot{y}_{(2i)} - v_{ref}))^* \nu_2 \Lambda_{\dot{y}} F_v(\dot{y}_{(2i)} - v_{ref})),$$
$$\nabla_{y_\rho} \hat{\Gamma}_{2e(2i)} = \gamma_{y_\rho} y_{\rho(2i)}.$$

For calculation of $(\delta F_v)^*$, see Eq. (3.19).

Step $2i + 2$ **:** During the (2i+2)-th walking cycle, one utilizes the following controller

$$u = -K_P q - K_D \dot{q} - k_{c(2i+2)} A_c q + \bar{u}_{(2i+2)}. \tag{3.23}$$

Here the feedback gain $k_{c(2i+2)}$ which represents the strength of the virtual constraint and the feedforward control input $\bar{u}_{(2i+1)}$ are given by

$$\begin{cases} \bar{u}_{(2i+2)} = \bar{u}_{(2i)} - K_{(i)} \left(\Lambda_{\bar{u}} \bar{u}_{(2i)} + \dfrac{1}{\epsilon_{e(i)}} \mathcal{R}(y_{(2i+1)} - y_{(2i)}) \right) \\ k_{c(2i+2)} = k_{c(2i)} - K_{\rho(i)} \left(\gamma_{u_\rho} k_{c(2i)} (t^1 - t^0) + \dfrac{1}{\epsilon_{e(i)}} \displaystyle\int_{t^0}^{t^1} \mathcal{R}(y_{\rho(2i+1)} - y_{\rho(2i)})\, \mathrm{d}t \right) \end{cases},$$

where appropriate positive definite matrix $K_{(i)}$ and positive constant $K_{\rho(i)}$ represent learning and tuning gains, respectively.

Set $i = i + 1$. Then, go to Step $2i + 1$.

3.3.3 Extension to the compass gait biped with a torso

In this subsection, let us apply the proposed method to the compass gait biped with a torso depicted in Fig. 3.4. Table 3.1 shows physical parameters and variables. Here we define the

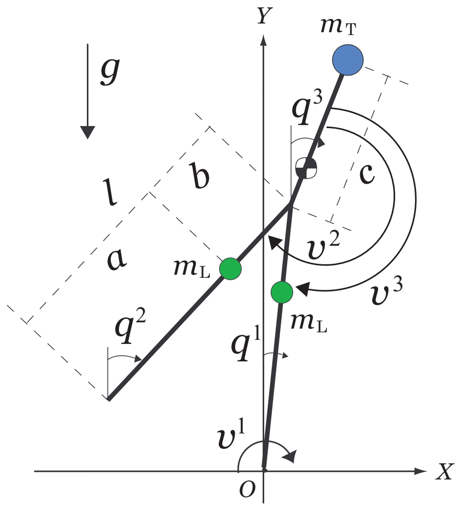

Figure 3.4: The compass gait biped with a torso

Table 3.1: Parameters and variables

Notation	Meaning	Unit
m_T	torso mass	kg
m_L	leg mass	kg
a	length from m_L to the ground	m
b	length from the hip to m_L	m
$l = a + b$	total leg length	m
c	length from the hip to m_T	m
g	gravity acceleration	$\mathrm{m/s^2}$
q^1	stance leg angle w.r.t vertical	rad
q^2	swing leg angle w.r.t vertical	rad
q^3	torso angle w.r.t vertical	rad
v^1	ankle torque	Nm
v^2	torque applied between the torso and the swing leg	Nm
v^3	torque applied between the torso and the stance leg	Nm

input u as

$$u = \begin{pmatrix} u^1 \\ u^2 \\ u^3 \end{pmatrix} := \begin{pmatrix} v^1 - v^3 \\ -v^2 \\ v^2 + v^3 \end{pmatrix} \tag{3.24}$$

in order to simplify the input-output relation in the Hamiltonian form mentioned later as in the definition (2.18). Let us assume the same assumptions as Assumptions 2.3, 2.4, 2.5, 2.6 and 2.7 on this robot. The configuration coordinate is defined as $q := (q^1, q^2, q^3)^\top$ and we utilize similar notations with respect to the state as in Table 2.2.

The dynamics of the robot is described as a typical mechanical system in (2.19) with the friction coefficients $R_D = O_{33}$ and the following inertia matrix and the potential energy

$$M(q) = \begin{pmatrix} m_T l^2 + m_L l^2 + m_L a^2 & -m_L bl\cos(q^1-q^2) & m_T cl\cos(q^1-q^3) \\ -m_L bl\cos(q^1-q^2) & m_L b^2 & 0 \\ m_T cl\cos(q^1-q^3) & 0 & m_T c^2 \end{pmatrix}$$

$$V(q) = m_L\{(a+l)\cos(q^1) - b\cos(q^2)\}g + m_T\{l\cos(q^1) + c\cos(q^3)\}g.$$

The output y corresponding to the input u defined in Eq. (3.24) is given by $y = q$. From Assumptions 2.5 and 2.6, the transition equation is derived as in the case of the compass gait biped (2.24), but the detail is omitted here. See ,e.g., [32].

Let us consider the following cost function, which is a slight modification of that in (3.16)

$$\begin{aligned}\hat{\Gamma}_{3e}(y_e, \dot{y}_e, u_e) =& \frac{1}{2}\int_{t^0}^{t^1} (y_e(\tau) - \tilde{C}_e\mathcal{R}(y_e)(\tau))^\top \Lambda_{y_e}(\tau)(y_e(\tau) - \tilde{C}_e\mathcal{R}(y_e)(\tau))\,\mathrm{d}\tau \\ &+\frac{1}{2}\int_{t^0}^{t^1} F_v(\dot{y}_e(\tau)-\tilde{v}_{e,ref})^\top \Lambda_{\dot{y}_e}(\tau) F_v(\dot{y}_e(\tau)-\tilde{v}_{e,ref})\,\mathrm{d}\tau + \frac{1}{2}\int_{t^0}^{t^1} u_e(\tau)^\top \Lambda_{u_e} u_e(\tau)\,\mathrm{d}\tau,\end{aligned} \tag{3.25}$$

where

$$y_e := \begin{pmatrix} q^1 \\ q^2 \\ q^3 \\ -\dfrac{q^1+q^2}{2} \end{pmatrix}, \quad u_e := \begin{pmatrix} \bar{u}^1 \\ \bar{u}^2 \\ \bar{u}^3 \\ \mathfrak{h}(k_c) \end{pmatrix} \in \mathbb{R}^4,$$

$$\tilde{C}_e := \left(\begin{array}{c|c} \tilde{C} & O_{31} \\ \hline O_{13} & 0 \end{array}\right) = \begin{pmatrix} 0 & 1 & 0 & 0 \\ 1 & 0 & 0 & 0 \\ 0 & 0 & 1 & 0 \\ 0 & 0 & 0 & 0 \end{pmatrix} \in \mathbb{R}^{4\times 4}, \quad \tilde{v}_{e,ref} := \begin{pmatrix} \tilde{v}_{ref} \\ 0 \end{pmatrix} = \begin{pmatrix} \tilde{v}^1_{ref} \\ \tilde{v}^2_{ref} \\ \tilde{v}^3_{ref} \\ 0 \end{pmatrix} \in \mathbb{R}^4, \tag{3.26}$$

$$\Lambda_{y_e}(t) := \begin{pmatrix} \nu_1(t)\Lambda_y & 0 \\ 0 & \gamma_{y_\rho} \end{pmatrix}, \quad \Lambda_{\dot{y}_e}(t) := \begin{pmatrix} \nu_2(t)\Lambda_{\dot{y}} & 0 \\ 0 & 0 \end{pmatrix}, \quad \Lambda_{u_e} := \begin{pmatrix} \Lambda_{\bar{u}} & 0 \\ 0 & \gamma_{u_\rho} \end{pmatrix} \in \mathbb{R}^{4\times 4}.$$

The learning procedure for the compass gait biped with a torso is summarized as follows.

Step 0 **:** Set appropriate positive definite matrices $\Lambda_y, \Lambda_{\dot{y}}$ and $\Lambda_{\bar{u}}$ as weight matrices, positive constants γ_{y_ρ} and γ_{u_ρ} as weight coefficients and positive constants Δt, $\Delta \bar{t}$ and k_{F_v} as design parameters for the filter functions ν_1 in (2.40) and ν_2 in (3.14) and the penalty function F_v in (3.15). Set the initial control input $\bar{u}_{(0)}$ appropriately (or set $\bar{u}_{(0)} \equiv 0$) and set a constant reference angular velocity $\tilde{v}_{e,ref}$ appropriately and let the constraint parameter $k_{c(0)}$ sufficiently large. Let the robot start walking under an appropriate initial condition x_{t^0}.

Set $i = 0$. Then go to Step 1.

Step $2i+1$ **:** During the (2i+1)-th walking cycle, one utilizes the following controller

$$u = -K_P q - K_D \dot{q} - u_{\rho(2i+1)} \tilde{A}_c q + \bar{u}_{(2i+1)}, \quad \tilde{A}_c := \begin{pmatrix} 1 & 1 & 0 \\ 1 & 1 & 0 \\ 0 & 0 & 0 \end{pmatrix}. \tag{3.27}$$

Here the time-varying feedback gain for the virtual constraint $u_{\rho(2i+1)}$ and the feedforward control input $\bar{u}_{(2i+1)}$ are given by

$$\begin{cases} \bar{u}_{(2i+1)} = \bar{u}_{(2i)} + \epsilon_{e(i)} \mathcal{R}(\nabla_y \hat{\Gamma}_{3e(2i)}) \\ u_{\rho(2i+1)} = u_{\rho(2i)} + \epsilon_{e(i)} \mathcal{R}(\nabla_{y_\rho} \hat{\Gamma}_{3e(2i)}) \end{cases},$$

where $\epsilon_{e(i)}$ denotes a sufficiently small positive constant and

$$\nabla_y \hat{\Gamma}_{3e(2i)} = (\mathrm{id} - \mathcal{R}\tilde{C})\nu_1 \Lambda_y (\mathrm{id} - \tilde{C}\mathcal{R})(y_{(2i)}) - \mathcal{D}_t((\delta F_v(\dot{y}_{(2i)} - \tilde{v}_{ref}))^* \nu_2 \Lambda_{\dot{y}} F_v(\dot{y}_{(2i)} - \tilde{v}_{ref})),$$
$$\nabla_{y_\rho} \hat{\Gamma}_{3e(2i)} = \gamma_{y_\rho} y_{\rho(2i)}.$$

For calculation of $(\delta F_v)^*$, see Eq. (3.19).

Step $2i+2$ **:** During the (2i+2)-th walking cycle, one utilizes the following controller

$$u = -K_P q - K_D \dot{q} - k_{c(2i+2)} \tilde{A}_c q + \bar{u}_{(2i+2)}. \tag{3.28}$$

Here the feedback gain $k_{c(2i+2)}$ which represents the strength of the virtual constraint and the feedforward control input $\bar{u}_{(2i+1)}$ are given by

$$\begin{cases} \bar{u}_{(2i+2)} = \bar{u}_{(2i)} - K_{(i)} \left(\Lambda_{\bar{u}} \bar{u}_{(2i)} + \dfrac{1}{\epsilon_{e(i)}} \mathcal{R}(y_{(2i+1)} - y_{(2i)}) \right) \\ k_{c(2i+2)} = k_{c(2i)} - K_{\rho(i)} \left(\gamma_{u_\rho} k_{c(2i)} (t^1 - t^0) + \dfrac{1}{\epsilon_{e(i)}} \displaystyle\int_{t^0}^{t^1} \mathcal{R}(y_{\rho(2i+1)} - y_{\rho(2i)})\, \mathrm{d}t \right) \end{cases},$$

where appropriate positive definite matrix $K_{(i)}$ and positive constant $K_{\rho(i)}$ represent learning and tuning gains, respectively.

Set $i = i+1$. Then, go to Step $2i+1$.

3.4 Numerical examples

We apply the proposed algorithm in the previous section to the compass gait biped with a torso depicted in Fig. 3.4 in order to generate an optimal periodic gait. Here we show the results of three kinds of simulations. The physical parameters of the robot in Table 3.1 are chosen as $m_T = 5.0, m_L = 1.2$ [kg] and $a = b = 0.20, c = 0.12$ [m], which are the same as those of the robot named Skipper II in [39]. For the controller, the following feedback gains are utilized $K_P = \mathrm{diag}(4,4,6)$ and $K_D = \mathrm{diag}(2,2,4)$. In all three simulations, we assign a reference velocity only to $\dot{q}^1$, since $\dot{q}^1$ mainly affects the walking velocity. It is the reason why we do not assign the reference velocity to the center of mass of the robot, that calculation of the center of mass requires the precise knowledge of the robot model, e.g. the inertia matrix.

In the first two simulations, we utilize the following design parameters with respect to weighting functions for the cost function (3.25) as $\Lambda_y = \mathrm{diag}(20, 20, 20)$, $\Lambda_{\dot{y}} = \mathrm{diag}(10, 0, 0)$, $\gamma_{y_\rho} = 1 \times 10^{-2}$, $\Lambda_{\bar{u}} = \mathrm{diag}(1 \times 10^{-4}, 5 \times 10^{-5}, 5 \times 10^{-5})$ and $\gamma_{u_\rho} = 1 \times 10^{-2}$, those with respect to filter functions and penalty function as $\Delta t = 5.0 \times 10^{-3}[s]$, $\Delta \bar{t} = 0.1[s]$ and $k_{F_v} = 0.25$ and those with respect to ILC algorithm as $K_{(\cdot)} = \mathrm{diag}(3, 3, 3)$, $K_{\rho(\cdot)} = 1$ and $\epsilon_{e(\cdot)} = 1$. In each simulation, we proceed 500 steps of the learning procedure, which means the robot continued 1000 steps walking, with the initial constraint parameter: $k_{c(0)} = 30$, with the initial condition:

$$(q^1_{t^0}, q^2_{t^0}, q^3_{t^0}, \dot{q}^1_{t^0}, \dot{q}^2_{t^0}, \dot{q}^3_{t^0}) = (-0.18, 0.20, 0, 1.1, 0.5, 0),$$

and with the initial control input:

$$\begin{aligned} \bar{u}^1_{(0)}(t) &= 0.5 \times \mathbf{1}(t) \\ \bar{u}^2_{(0)}(t) &= -1.5 \times \mathbf{1}(t). \end{aligned} \tag{3.29}$$

In the first simulation, we assign a reference velocity in (3.26) as $\tilde{v}_{ref} = (0.5, 0, 0)^\top$. Figure 3.5 shows the history of the cost function (3.25) along the walking steps. Since the cost function monotonically decreases along the walking steps and then converges to a constant value, this figure implies that at least a local minimum of the cost function has been achieved smoothly. Figure 3.6 shows the history of the virtual potential gain k_c along the walking steps. It implies that the strength of the virtual constraint is adjusted. Although k_c does not converge to zero, it plays a role of a stabilizing feedback controller. Figures 3.7 and 3.8 represent the animations of the robot in the first and the last 5 steps, respectively. These figures show that at the beginning the robot walks awkwardly and then the robot improves his walk as it continues to walk. Figure 3.9 shows $\dot{q}^1$ of the generated gait, its reference $\tilde{v}^1_{ref} = 0.5$ and the filter function $\nu_2(t)$ in (3.14) and Fig. 3.10 shows the time history of the horizontal velocity of the hip joint of the robot. The second term of the cost function (3.25) with appropriately chosen $\tilde{v}_{e,ref}$ encourages the robot to walk forward with appropriate velocity. Figure 3.11 exhibits the phase portrait of q-$\dot{q}$ and Fig. 3.12 shows that of q^1 - q^2, respectively. The fact that a periodic trajectory is generated follows from that the phase portraits in these figures form closed orbits. Figure 3.13 shows the generated learning control input $\bar{u}$ and Fig. 3.14 does the control input u in Eq. (3.28). Finally, Fig. 3.15 exhibits the time history of the ZMP along the walking steps and Fig. 3.16 shows the time revolution of the ZMP of the generated gait. The ZMP of the compass gait biped with a torso is calculated by

$$\begin{aligned} \mathrm{ZMP} &= \frac{-v^1}{\dot{\sigma_p}^2 + (2m_L + m_T)g} \quad \text{, where} \\ \dot{\sigma_p}^2 &= -(m_L a + m_L l + m_T l)(\ddot{q}^1 \sin q^1 + (\dot{q}^1)^2 \cos q^1) + m_L b(\ddot{q}^2 \sin q^2 + (\dot{q}^2)^2 \cos q^2) \\ &\quad + m_T c(\ddot{q}^3 \cos q^3 - (\dot{q}^3)^2 \sin q^3). \end{aligned} \tag{3.30}$$

For calculation of the ZMP in Eq. (3.30), see Appendix A. The ZMP is shifted forward. Regarding the total leg length of the robot and the range of the ZMP position, the proposed framework seems feasible.

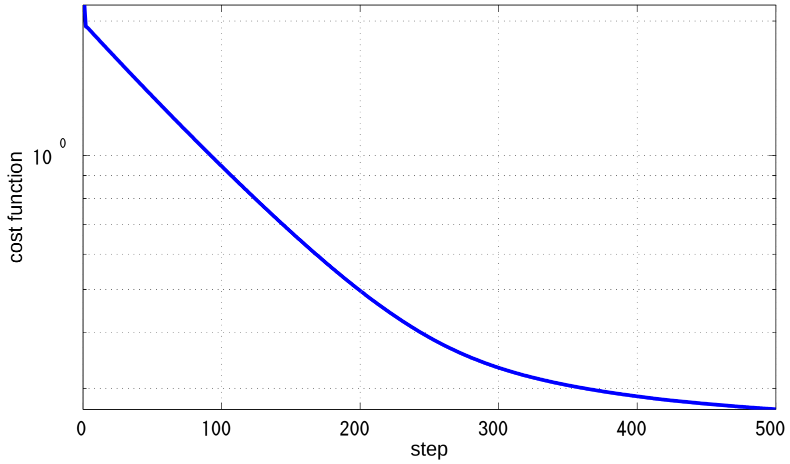

Figure 3.5: Cost function

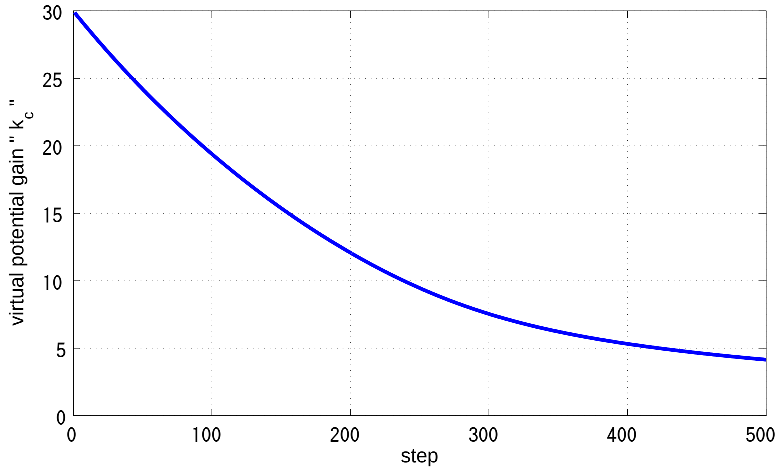

Figure 3.6: Virtual potential gain k_c

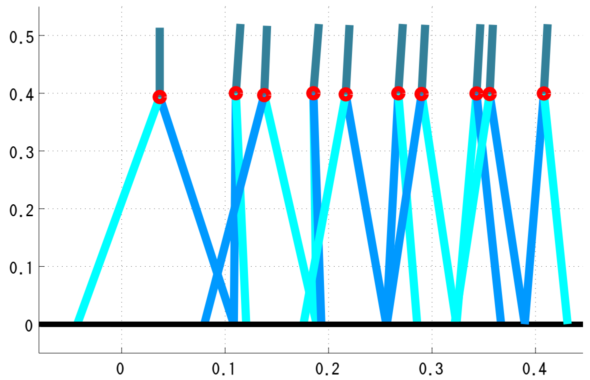

Figure 3.7: Stick diagrams in the first 5 steps

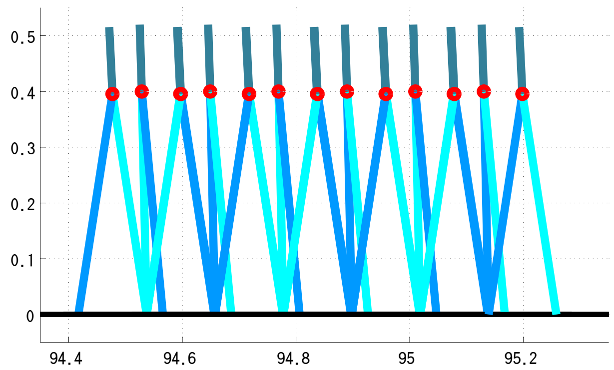

Figure 3.8: Stick diagrams in the last 5 steps

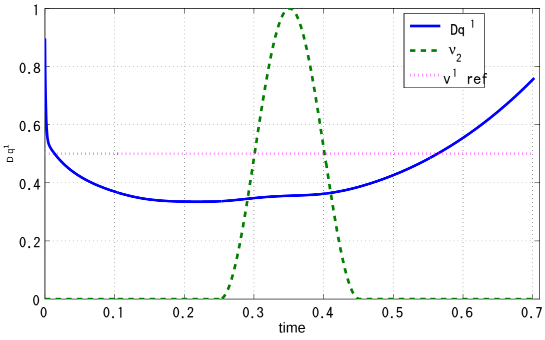

Figure 3.9: $\dot{q}^1$, its reference velocity $\tilde{v}^1_{ref}$ and the filter function ν_2

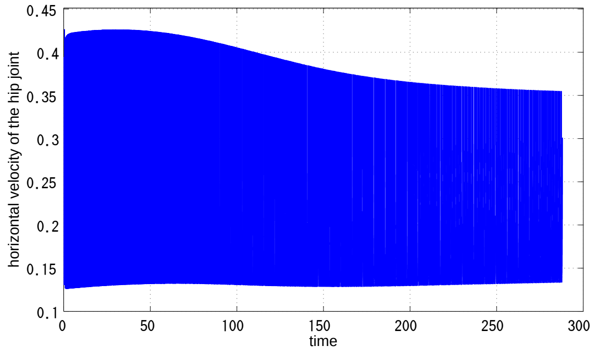

Figure 3.10: Horizontal velocity of the hip joint

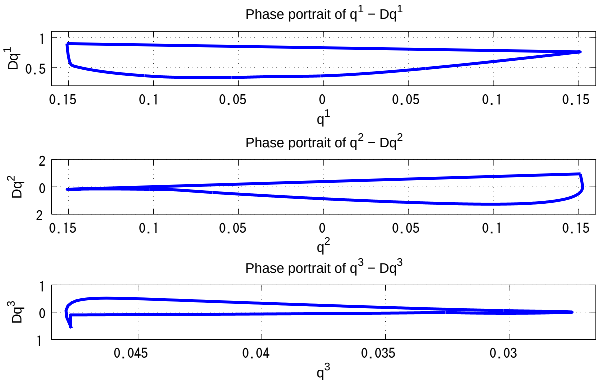

Figure 3.11: Phase portrait of q-$\dot{q}$

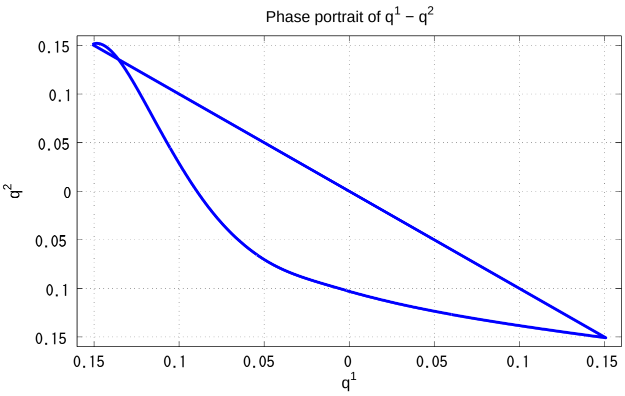

Figure 3.12: Phase portrait of q^1-q^2

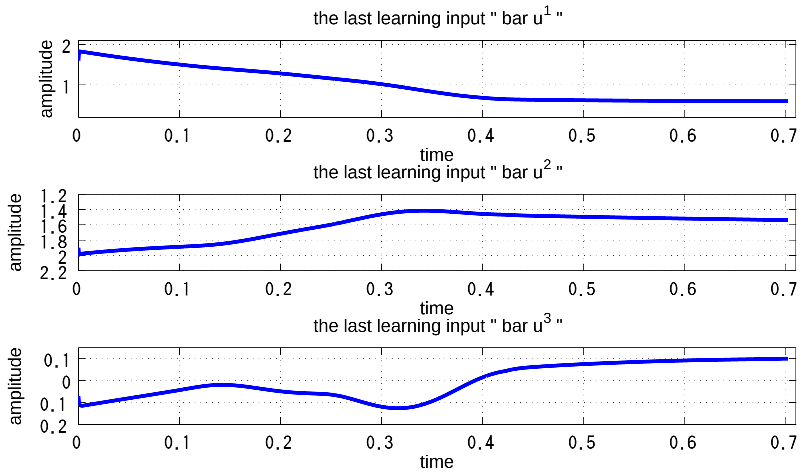

Figure 3.13: Generated learning control inputs $\bar{u}$

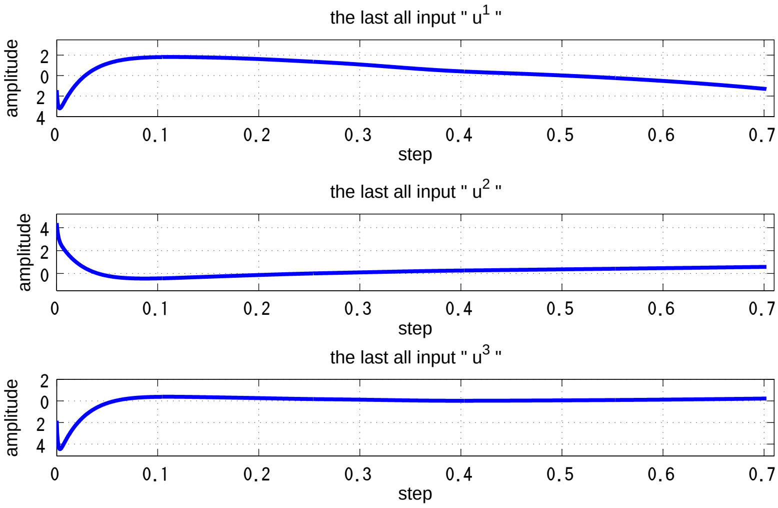

Figure 3.14: Generated all control inputs u

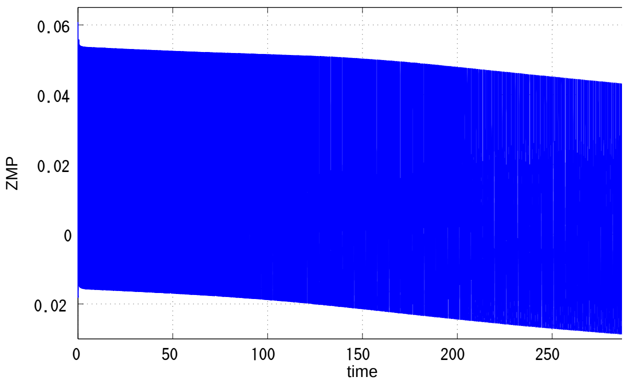

Figure 3.15: ZMP along the all walking steps

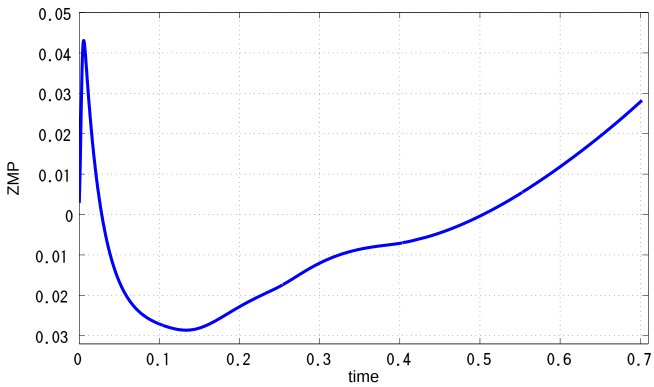

Figure 3.16: ZMP of the generated gait

In the second simulation, we assign a reference velocity in (3.26) as $\tilde{v}_{ref} = (0.8, 0, 0)^\top$. Figure 3.17 shows the history of the cost function (3.25) along the walking steps. Since the cost function monotonically decreases along the walking steps and then converges to a constant value, this figure implies that at least a local minimum of the cost function has been achieved smoothly as in the first simulation results. Figure 3.18 shows the history of the virtual potential gain k_c along the walking steps. It implies that the strength of the virtual constraint is adjusted. Although k_c does not converge to zero, it plays a role of a stabilizing feedback controller. Figures 3.19 and 3.20 represent the animations of the robot in the first and the last 5 steps, respectively. These figures show that at the beginning the robot walks awkwardly and then the robot improves his walk as it continues to walk. Figure 3.21 shows $\dot{q}^1$ of the generated gait, its reference $\tilde{v}^1_{ref} = 0.8$ and the filter function $\nu_2(t)$ and Figure 3.22 shows the time history of the horizontal velocity of the hip joint of the robot. Since the assigned reference velocity here is bigger than that in the first simulation, the velocity of the generated gait is faster than that in the first one. Figure 3.23 exhibits the phase portrait of q-$\dot{q}$ and Fig. 3.24 shows that of q^1 - q^2, respectively. Since the phase portraits in these figures form closed orbits, we can obtain a periodic trajectory as well as the first simulation. Figure 3.25 shows the generated learning control input $\bar{u}$ and Fig. 3.26 does the control input u in Eq. (3.28). Finally, Fig. 3.27 exhibits the time history of the ZMP along the walking steps and Fig. 3.28 shows the time revolution of the ZMP of the generated gait. The ZMP is shifted forward. Regarding the total leg length of the robot and the range of the ZMP position, the proposed framework seems feasible.

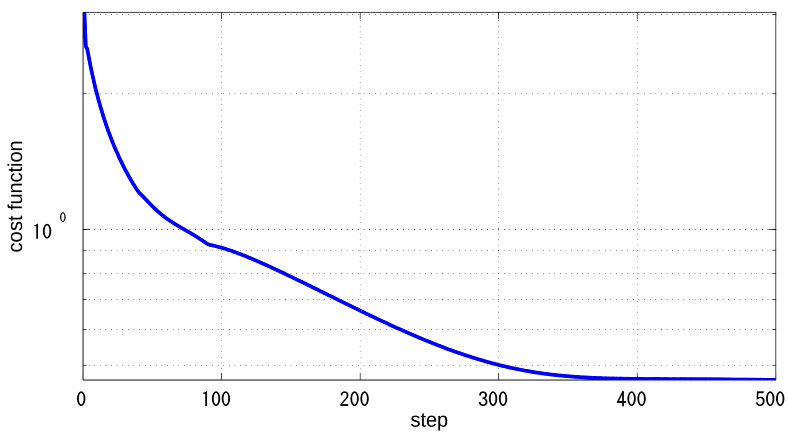

Figure 3.17: Cost function

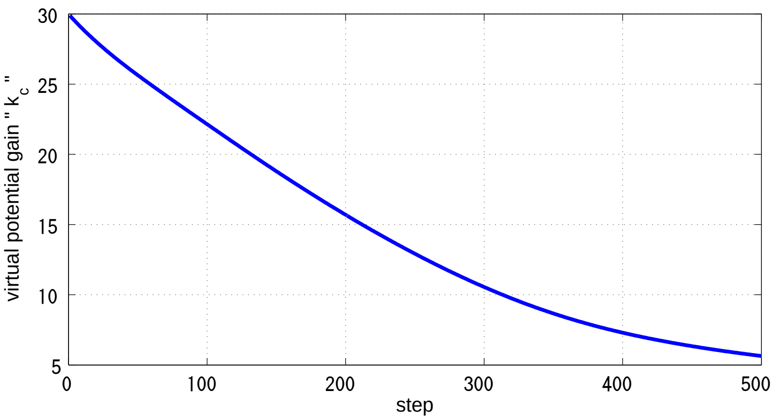

Figure 3.18: Virtual potential gain k_c

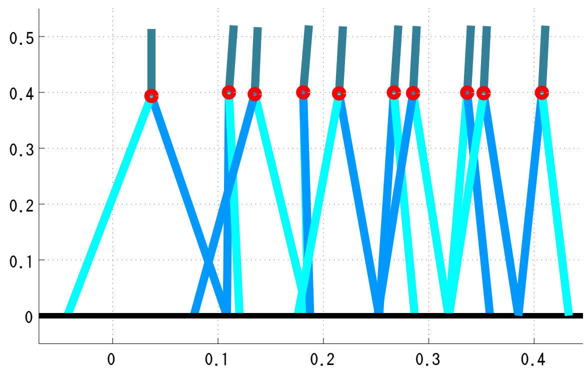

Figure 3.19: Stick diagrams in the first 5 steps

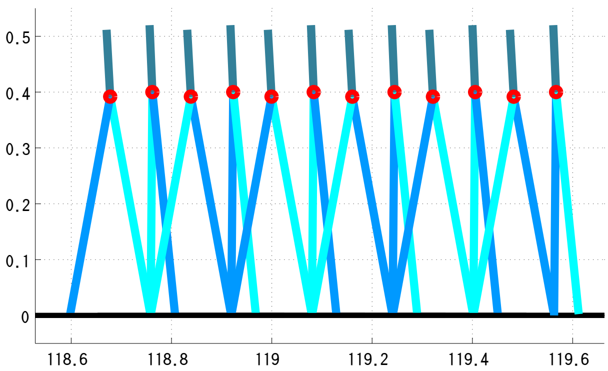

Figure 3.20: Stick diagrams in the last 5 steps

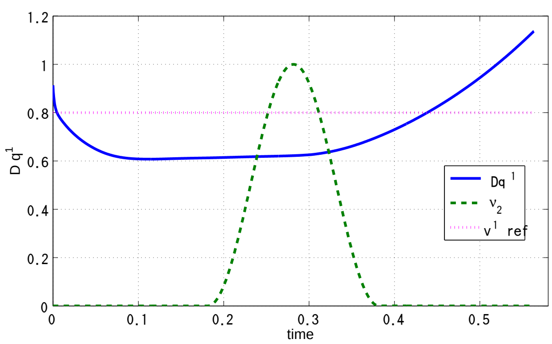

Figure 3.21: $\dot{q}^1$, its reference velocity $\tilde{v}^1_{ref}$ and the filter function ν_2

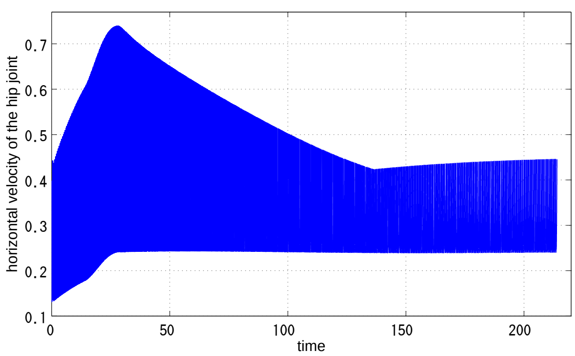

Figure 3.22: Horizontal velocity of the hip joint

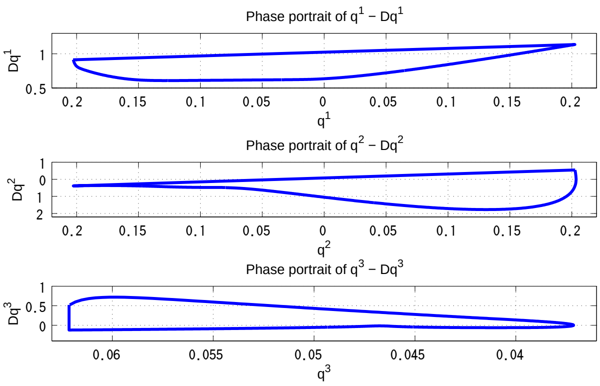

Figure 3.23: Phase portrait of q-$\dot{q}$

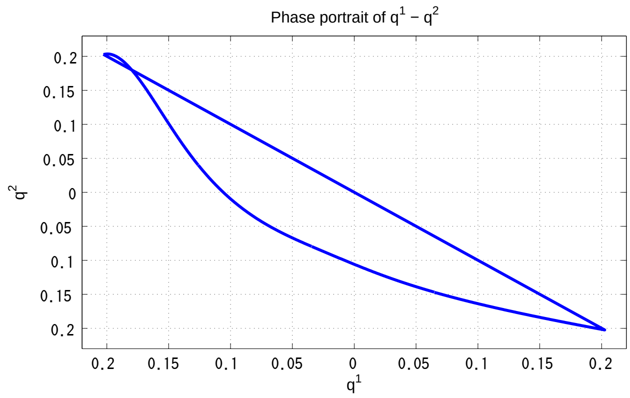

Figure 3.24: Phase portrait of q^1-q^2

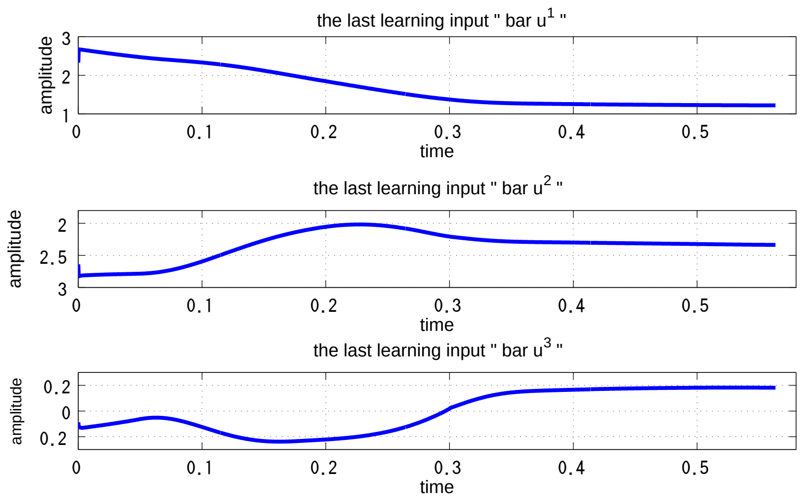

Figure 3.25: Generated learning control inputs $\bar{u}$

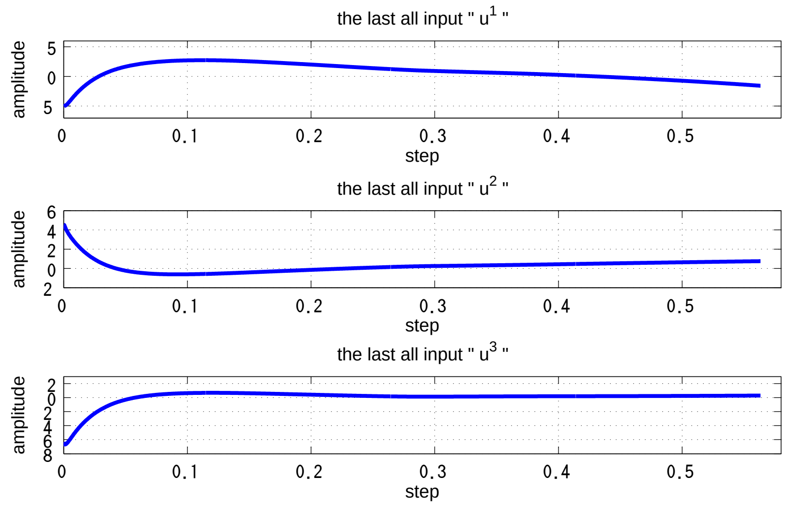

Figure 3.26: Generated all control inputs u

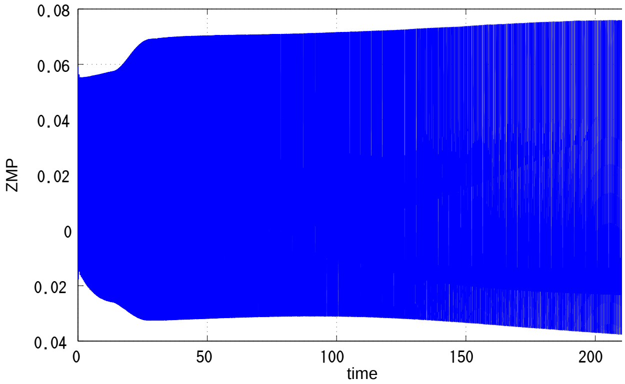

Figure 3.27: ZMP along the all walking steps

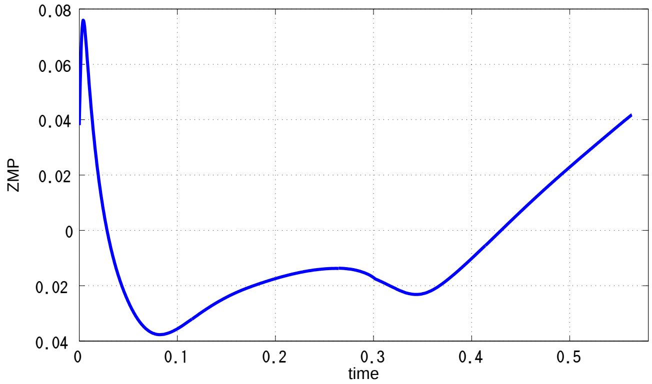

Figure 3.28: ZMP of the generated gait

In the last simulation, we utilize other design parameters with respect to weighting functions for the cost function (3.25) as $\Lambda_y = \mathrm{diag}(10, 10, 10)$, $\Lambda_{\dot{y}} = \mathrm{diag}(5, 0, 0)$, $\gamma_{y_\rho} = 1 \times 10^{-4}$, $\Lambda_{\bar{u}} = \mathrm{diag}(1 \times 10^{-5}, 1 \times 10^{-5}, 1 \times 10^{-5})$ and $\gamma_{u_\rho} = 1 \times 10^{-3}$, those with respect to filter functions and penalty function as $\Delta t = 5.0 \times 10^{-3}[s]$, $\Delta \bar{t} = 0.1[s]$ and $k_{F_v} = 0.25$ and those with respect to ILC algorithm as $K_{(\cdot)} = \mathrm{diag}(2, 2, 2)$, $K_{\rho(\cdot)} = 35$ and $\epsilon_{e(\cdot)} = 1$. We proceed 500 steps of the learning procedure with the initial constraint parameter: $k_{c(0)} = 50$, with the initial condition:

$$(q^1_{t^0}, q^2_{t^0}, q^3_{t^0}, \dot{q}^1_{t^0}, \dot{q}^2_{t^0}, \dot{q}^3_{t^0}) = (-0.23, 0.25, 0, 1.3, 0.6, 0),$$

and with the same initial control input as in Eq. (3.29).

In this simulation, we assign the same reference velocity as the previous simulation, that is, $\tilde{v}_{ref} = (0.8, 0, 0)^\top$. Figure 3.29 shows the history of the cost function (3.25) along the walking steps. Since the cost function monotonically decreases along the walking steps and then converges to a constant value, this figure implies that at least a local minimum of the cost function has been achieved smoothly as in the first two simulation results. Figure 3.30 shows the history of the virtual potential gain k_c along the walking steps. It implies that the strength of the virtual constraint is adjusted. Although k_c does not converge to zero, it plays a role of a stabilizing feedback controller. Figures 3.31 and 3.32 represent the animations of the robot in the first and the last 5 steps, respectively. These figures show that at the beginning the robot walks awkwardly and then the robot improves his walk as it continues to walk. Figure 3.33 shows $\dot{q}^1$ of the generated gait, its reference $\tilde{v}^1_{ref} = 0.8$ and the filter function $\nu_2(t)$ and Fig. 3.34 shows the time history of the horizontal velocity of the hip joint of the robot. Since the assigned reference velocity here is bigger than that in the first simulation, the velocity of the generated gait is faster than that in the first one. Figure 3.35 exhibits the phase portrait of q-$\dot{q}$ and Fig. 3.36 shows that of q^1 - q^2, respectively. Since the phase portraits in these figures form almost closed orbits, we can obtain an almost periodic trajectory. Figure 3.37 shows the generated learning control input $\bar{u}$ and Fig. 3.38 does the control input u in Eq. (3.28). Finally, Fig. 3.39 exhibits the time history of the ZMP along the walking steps and Fig. 3.40 shows the time revolution of the ZMP of the generated gait. The ZMP is shifted forward. Regarding the total leg length of the robot and the range of the ZMP position, the proposed framework seems feasible.

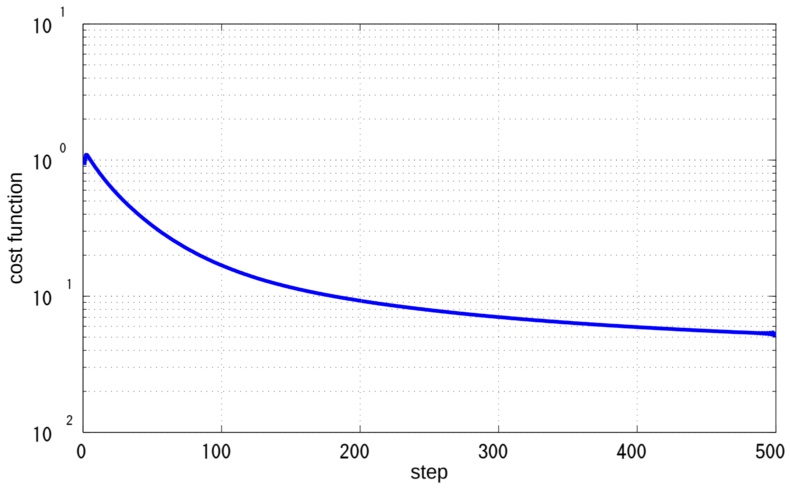

Figure 3.29: Cost function

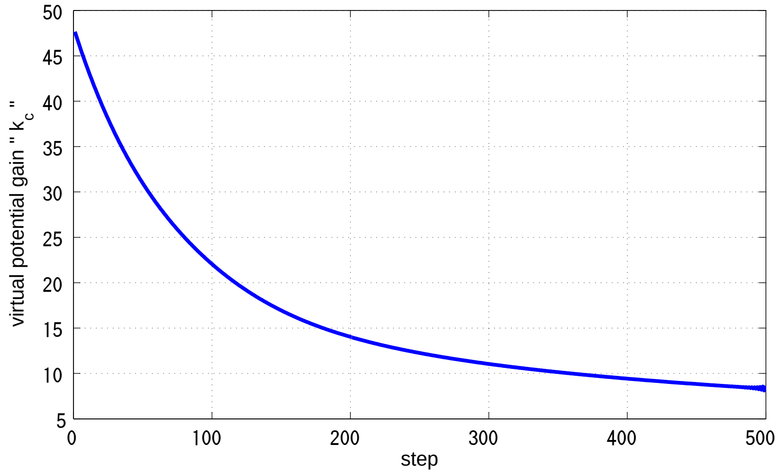

Figure 3.30: Virtual potential gain k_c

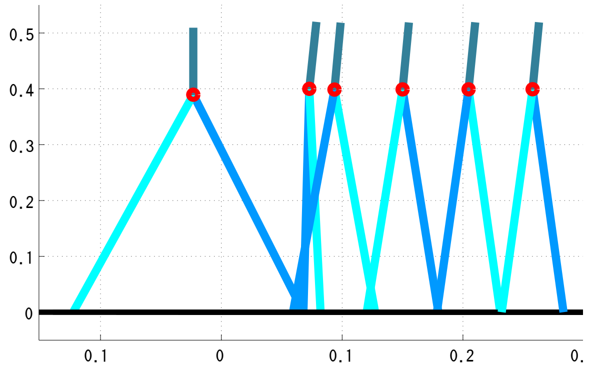

Figure 3.31: Stick diagrams in the first 5 steps

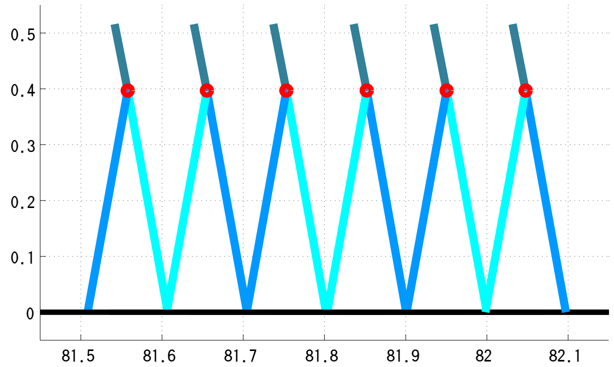

Figure 3.32: Stick diagrams in the last 5 steps

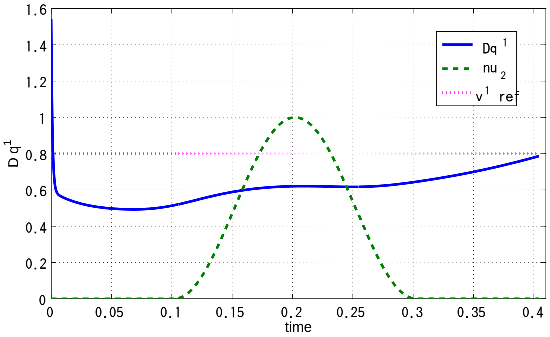

Figure 3.33: $\dot{q}^1$, its reference velocity $\tilde{v}^1_{ref}$ and the filter function ν_2

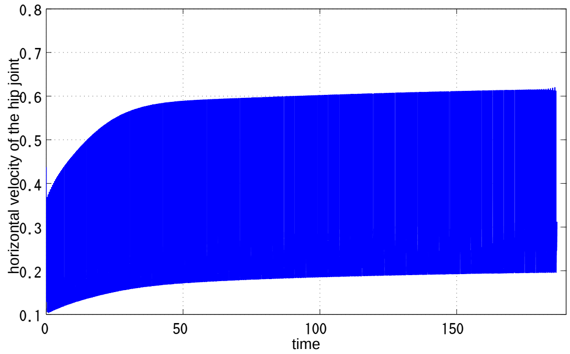

Figure 3.34: Horizontal velocity of the hip joint

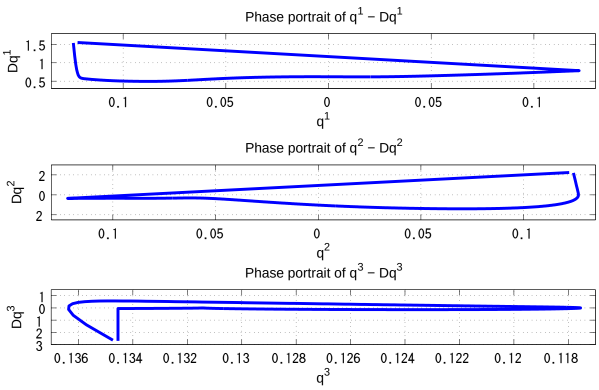

Figure 3.35: Phase portrait of q-$\dot{q}$

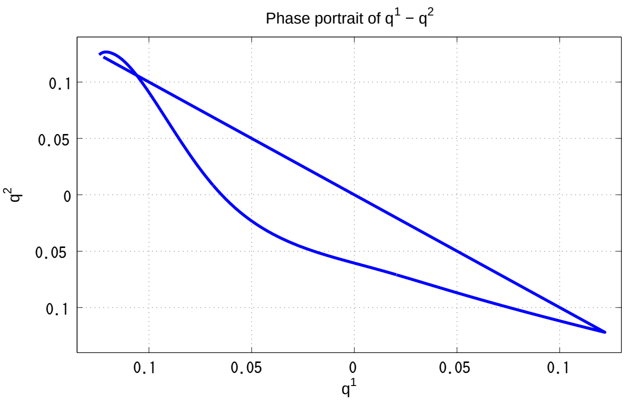

Figure 3.36: Phase portrait of q^1-q^2

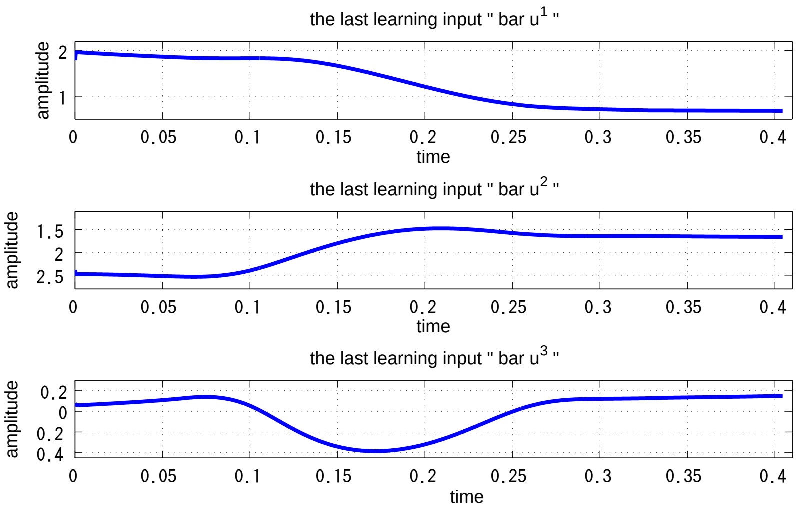

Figure 3.37: Generated learning control inputs $\bar{u}$

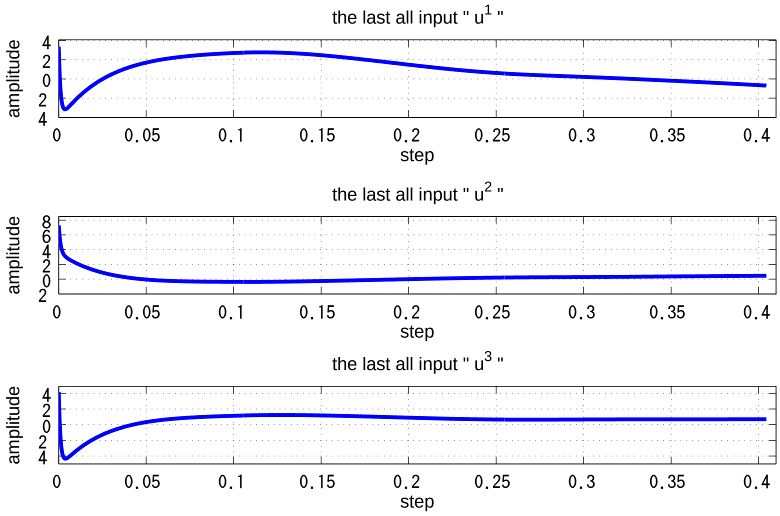

Figure 3.38: Generated all control inputs u

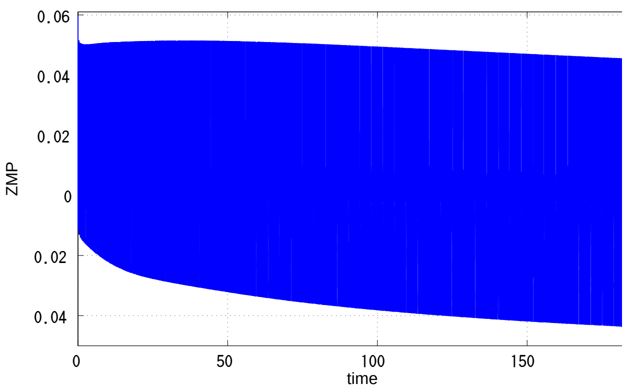

Figure 3.39: ZMP along the all walking steps

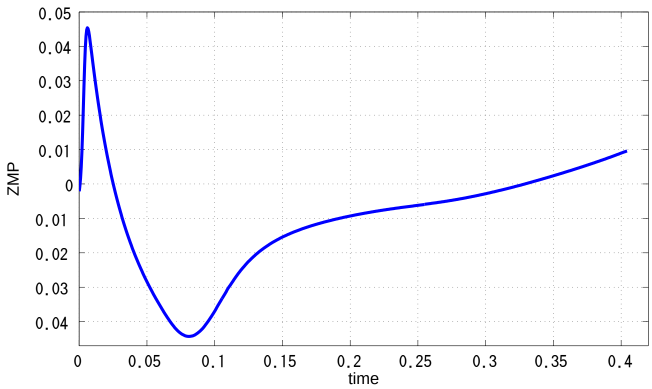

Figure 3.40: ZMP of the generated gait

3.5 Summary

In this chapter, we have proposed a novel optimal gait generation framework using virtual constraints and learning optimal control based on variational symmetry of Hamiltonian systems. Virtual constraints restrict the motion of the robot to a symmetric trajectory and they prevent the robot from falling. The feature of the proposed method is that the robot improves his walk keeping on walking due to constraints, that is, this method does not need to repeat experiments under the same initial condition, which is necessary for conventional ILC frameworks. The proposed technique also differs from the past proposed methods using virtual constraints in that it automatically mitigates the strength of the constraints by IFT according to the progress of learning by ILC. Since ILC and IFT influence each other and they can not be used simultaneously, we introduce an extended system which again has variational symmetry. By considering the extended system instead of the plant system, we can apply ILC and IFT simultaneously. Finally, numerical simulations demonstrate the effectiveness of the proposed framework.

Chapter 4

Passivity based control of stochastic Hamiltonian systems

From this chapter, let us consider not only deterministic systems but also stochastic ones. The aim of this chapter is to introduce stochastic (port-)Hamiltonian systems which are extension of deterministic (port-)Hamiltonian systems [13, 52, 88], and to clarify some of their properties. A port-Hamiltonian system [52, 90, 88] is an input-affine Hamiltonian system. Although deterministic Hamiltonian systems inherently possess some properties such as invariance under a class of transformations and passivity, stochastic Hamiltonian ones do not always possess similar properties.

In Section 4.1, we concentrate on the time-invariant case. Firstly, we show a necessary and sufficient condition to preserve the stochastic Hamiltonian structure of the original system under time-invariant coordinate transformations. Secondly, we derive a condition to maintain stochastic passivity of the system. Thirdly, we introduce stochastic generalized canonical transformations which are extension of generalized canonical transformations proposed in [25]. Stochastic generalized canonical transformations are pairs of coordinate and feedback transformations under which the stochastic port-Hamiltonian structure is preserved. Finally, we propose a stabilization method based on stochastic passivity and stochastic generalized canonical transformations. In the proposed method, we transform a stochastic port-Hamiltonian system to a passive one and then stabilize the system by the output feedback based on stochastic passivity.

In section 4.2, we extend the results on the time-invariant stochastic port-Hamiltonian systems to the time-varying case. Some numerical simulations demonstrate the effectiveness of the proposed method.

4.1 Time-invariant stochastic port-Hamiltonian system (SPHS)

A time-invariant port-Hamiltonian system is described by the following input-affine Hamiltonian system

$$\left\{\begin{array}{rcl} \dot{x} &=& (J(x)-R(x))\,\dfrac{\partial H(x)}{\partial x}^{\top} + g(x)u \\ y &=& g(x)^{\top}\dfrac{\partial H(x)}{\partial x}^{\top} \end{array}\right. . \tag{4.1}$$

As in the case of (2.1), $x(t) \in \mathbb{R}^n, u(t), y(t) \in \mathbb{R}^m$ describe the state, the input and the output, respectively and the structure matrix $J(x) \in \mathbb{R}^{n\times n}$ and the dissipation matrix $R(x) \in \mathbb{R}^{n\times n}$ are skew-symmetric and symmetric positive semi-definite, respectively. $g(x) \in \mathbb{R}^{n\times m}$ represents the control port.

Let us extend the above deterministic system into a stochastic dynamical system which is described by the following stochastic differential equation written in the sense of Itô,

$$\begin{cases} \mathrm{d}x &= (J(x) - R(x)) \dfrac{\partial H(x)}{\partial x}^\top \mathrm{d}t + g(x)u \ \mathrm{d}t + h(x)\,\mathrm{d}w \\ y &= g(x)^\top \dfrac{\partial H(x)}{\partial x}^\top \end{cases} . \tag{4.2}$$

Here $w(t) \in \mathbb{R}^r$ is a standard Wiener process defined on a probability space $(\Omega, \mathcal{F}, \mathcal{P})$, where Ω is a sample space, $\mathcal{F}$ is the sigma algebra of the observable random events and $\mathcal{P}$ is a probability measure on Ω. $h(x) \in \mathbb{R}^{n\times r}$ represents the noise port. We define the system (4.2) as **stochastic port-Hamiltonian system**. In what follows, we suppose that a Hamiltonian $H(x)$ is a sufficiently differentiable function and $h(0) = 0$. Moreover, $g(x)$ and $h(x)$ satisfy reasonable sufficient conditions for the local existence and uniqueness of the solutions. For the details on such conditions, see [40, 46].

In this thesis, according to [48, 34, 51, 16, 57] we introduce the notion of stability in probability as follows.

Definition 4.1 The equilibrium solution $x \equiv 0$ of the system (4.2) is stable in probability if and only if for any $\epsilon > 0$ and $\delta > 0$, there exists $\rho = \rho(\epsilon, \delta) > 0$ such that if the initial condition $x(t^0)$ satisfies $\|x(t^0)\| < \rho(\epsilon, \delta)$, then

$$\mathcal{P}\left\{\sup_{t\geq t_0} \|x(t)\| > \epsilon\right\} < \delta.$$

Definition 4.2 The equilibrium solution $x \equiv 0$ of the system (4.2) is asymptotically stable in probability if and only if it is stable in probability and for any $\epsilon > 0$,

$$\lim_{T\to\infty} \mathcal{P}\left\{\sup_{t\geq T} \|x(t)\| > \epsilon\right\} = 0.$$

The following lemma is obtained in [25] for the port-Hamiltonian system of the form (4.1).

Lemma 4.1 *[25] The deterministic port-Hamiltonian system* (4.1) *is transformed into another one by any time-invariant coordinate transformation.*

This lemma implies that the deterministic port-Hamiltonian structure is preserved under any time-invariant coordinate transformation. However, the stochastic port-Hamiltonian structure does not always preserved under the same class of transformations. Let us prove the following lemma which characterizes the class of time-invariant coordinates which preserve the stochastic port-Hamiltonian structure.

Lemma 4.2 *The stochastic port-Hamiltonian system* (4.2) *is transformed into another stochastic port-Hamiltonian system by a time-invariant coordinate transformation* $\bar{x} = \Phi(x)$ *if and only if there exists a skew-symmetric matrix* $K(x)$ *and a symmetric matrix* $S(x)$ *such that* $R(x) + S(x)$ *is positive semi-definite and they satisfy*

$$\frac{1}{2}\mathrm{tr}\left\{\frac{\partial}{\partial x}\left(\frac{\partial \Phi^i(x)}{\partial x}\right)^{\top} h(x)h(x)^{\top}\right\} = \frac{\partial \Phi^i(x)}{\partial x}(K(x) - S(x))\frac{\partial H(x)}{\partial x}^{\top}, \quad (i = 1, 2, \cdots, n), \tag{4.3}$$

where $\mathrm{tr}\{\cdot\}$ *represents the trace of the argument and* $(\cdot)^i$ *represents the* i*-th row of the argument.*

Proof Firstly, the necessity of Eq. (4.3) is shown. By utilizing the Itô formula in Appendix C.1, the dynamics of the system in the new coordinate $\bar{x}$ is calculated as

$$\begin{aligned} \mathrm{d}\bar{x}^i &= \frac{\partial \Phi^i}{\partial x}\,\mathrm{d}x + \frac{1}{2}\mathrm{tr}\left\{\frac{\partial}{\partial x}\left(\frac{\partial \Phi^i}{\partial x}\right)^{\top} hh^{\top}\right\}\mathrm{d}t \\ &= \left[\frac{\partial \Phi^i}{\partial x}(J - R)\frac{\partial H}{\partial x}^{\top} + \frac{1}{2}\mathrm{tr}\left\{\frac{\partial}{\partial x}\left(\frac{\partial \Phi^i}{\partial x}\right)^{\top} hh^{\top}\right\}\right]\mathrm{d}t + \frac{\partial \Phi^i}{\partial x}gu\,\mathrm{d}t + \frac{\partial \Phi^i}{\partial x}h\,\mathrm{d}w. \end{aligned} \tag{4.4}$$

Suppose that a stochastic port-Hamiltonian system (4.2) is transformed into another one by a time-invariant coordinate $\bar{x} = \Phi(x)$. Then, the following equation holds for all u and w

R.H.S. of Eq. (4.4)

$$\equiv \left[(\bar{J}(\bar{x}) - \bar{R}(\bar{x}))\frac{\partial H(\Phi^{-1}(\bar{x}))^{\top}}{\partial \bar{x}}\right]^i \mathrm{d}t + \left[\bar{g}(\bar{x})u\right]^i \mathrm{d}t + \left[\bar{h}(\bar{x})\,\mathrm{d}w\right]^i. \tag{4.5}$$

This implies that

$$\frac{\partial \Phi}{\partial x}g \equiv \bar{g}, \qquad \frac{\partial \Phi}{\partial x}h \equiv \bar{h}. \tag{4.6}$$

The symbol $[\cdot]^{-1}$ represents the inverse matrix of the argument and if no confusion arises, $\cdot^{-1}$ represents the inverse function of the argument function in what follows. The first term of the right hand side of Eq. (4.5) is calculated as follows:

$$\begin{aligned} &\left[(\bar{J}(\bar{x}) - \bar{R}(\bar{x}))\frac{\partial H(\Phi^{-1}(\bar{x}))^{\top}}{\partial \bar{x}}\right]^i \\ &\quad = \left[\frac{\partial \Phi}{\partial x}\left[\frac{\partial \Phi}{\partial x}\right]^{-1}(\bar{J} - \bar{R})\left[\frac{\partial \Phi}{\partial x}\right]^{-\top}\frac{\partial \Phi}{\partial x}^{\top}\frac{\partial H(\Phi^{-1}(\bar{x}))^{\top}}{\partial \bar{x}}\right]^i \\ &\quad = \frac{\partial \Phi^i}{\partial x}\left[\frac{\partial \Phi}{\partial x}\right]^{-1}(\bar{J} - \bar{R})\left[\frac{\partial \Phi}{\partial x}\right]^{-\top}\frac{\partial H(x)^{\top}}{\partial x}. \end{aligned} \tag{4.7}$$

It follows from Eqs. (4.4), (4.5) and (4.7) that

$$\left[\frac{\partial \Phi^i}{\partial x}(J - R)\frac{\partial H}{\partial x}^{\top} + \frac{1}{2}\mathrm{tr}\left\{\frac{\partial}{\partial x}\left(\frac{\partial \Phi^i}{\partial x}\right)^{\top} hh^{\top}\right\}\right] = \frac{\partial \Phi^i}{\partial x}\left[\frac{\partial \Phi}{\partial x}\right]^{-1}(\bar{J} - \bar{R})\left[\frac{\partial \Phi}{\partial x}\right]^{-\top}\frac{\partial H(x)^{\top}}{\partial x}.$$

Consequently, we have

$$\frac{1}{2}\mathrm{tr}\left\{\frac{\partial}{\partial x}\left(\frac{\partial \Phi^i}{\partial x}\right)^{\top} hh^{\top}\right\} =$$
$$\frac{\partial \Phi^i}{\partial x}\left[\left(\left[\frac{\partial \Phi}{\partial x}\right]^{-1}\bar{J}\left[\frac{\partial \Phi}{\partial x}\right]^{-\top} - J\right) - \left(\left[\frac{\partial \Phi}{\partial x}\right]^{-1}\bar{R}\left[\frac{\partial \Phi}{\partial x}\right]^{-\top} - R\right)\right]\frac{\partial H(x)^{\top}}{\partial x}. \tag{4.8}$$

From Eq. (4.8) we define the matrices $K(x)$ and $S(x)$ as

$$K(x) := \left[\frac{\partial \Phi}{\partial x}\right]^{-1}\bar{J}(\Phi(x))\left[\frac{\partial \Phi}{\partial x}\right]^{-\top} - J(x),$$
$$S(x) := \left[\frac{\partial \Phi}{\partial x}\right]^{-1}\bar{R}(\Phi(x))\left[\frac{\partial \Phi}{\partial x}\right]^{-\top} - R(x).$$

Then, $K(x)$ is skew-symmetric since $J(x)$ and $\bar{J}(\Phi(x))$ are so and, for $R(x)$ is symmetric and $\bar{R}(\Phi(x))$ is symmetric positive semi-definite, $S(x)$ is symmetric and $R(x) + S(x)$ is symmetric positive semi-definite. This proves the necessity of Eq. (4.3).

Secondly, the sufficiency of Eq. (4.3) is shown. The output y can be calculated using Eq. (4.6) in the new coordinate $\bar{x}$ as

$$\begin{aligned} y &= g^{\top}\left[\frac{\partial \Phi}{\partial x}\right]^{\top}\left[\frac{\partial \Phi}{\partial x}\right]^{-\top}\frac{\partial H}{\partial x}^{\top} \\ &= \left(\frac{\partial \Phi}{\partial x}g\right)^{\top}\left(\frac{\partial H}{\partial x}\frac{\partial \Phi^{-1}(\bar{x})}{\partial \bar{x}}\right)^{\top} \\ &= \bar{g}^{\top}\frac{\partial H}{\partial \bar{x}}^{\top}. \end{aligned} \tag{4.9}$$

Therefore, the output y has the same form in the coordinate $\bar{x}$ as in x. Now suppose that Eq. (4.3) holds. Then, by utilizing Eqs. (4.3) and (4.4), the dynamics of the system can be calculated in the new coordinate $\bar{x}$ as

$$\begin{aligned} \mathrm{d}\bar{x}^i &= \left[\frac{\partial \Phi^i}{\partial x}(J-R)\frac{\partial H}{\partial x}^{\top} + \frac{\partial \Phi^i}{\partial x}(K-S)\frac{\partial H}{\partial x}^{\top}\right]\mathrm{d}t + \frac{\partial \Phi^i}{\partial x}gu\,\mathrm{d}t + \frac{\partial \Phi^i}{\partial x}h\,\mathrm{d}w \\ &= \left[\left(\underbrace{\frac{\partial \Phi}{\partial x}(J+K)\frac{\partial \Phi}{\partial x}^{\top}}_{=:\,\bar{J}} - \underbrace{\frac{\partial \Phi}{\partial x}(R+S)\frac{\partial \Phi}{\partial x}^{\top}}_{=:\,\bar{R}}\right)\frac{\partial H(\Phi^{-1}(\bar{x}))}{\partial \bar{x}}^{\top}\right]^i \mathrm{d}t + \underbrace{\frac{\partial \Phi^i}{\partial x}g}_{=:\,\bar{g}^i}u\,\mathrm{d}t + \underbrace{\frac{\partial \Phi^i}{\partial x}h}_{=:\,\bar{h}^i}\mathrm{d}w \\ &= \left[(\bar{J}(\bar{x}) - \bar{R}(\bar{x}))\frac{\partial H(\Phi^{-1}(\bar{x}))}{\partial \bar{x}}^{\top}\right]^i \mathrm{d}t + \left[\bar{g}(\bar{x})u\right]^i \mathrm{d}t + \left[\bar{h}(\bar{x})\,\mathrm{d}w\right]^i. \end{aligned} \tag{4.10}$$

Then, $\bar{J}(\bar{x})$ is skew-symmetric since $J(\Phi^{-1}(\bar{x}))$ and $K(\Phi^{-1}(\bar{x}))$ are so, and $\bar{R}(\bar{x})$ is symmetric positive semi-definite because of the assumption that $R(\Phi^{-1}(\bar{x})) + S(\Phi^{-1}(\bar{x}))$ is so. This proves the sufficiency of Eq. (4.3). ■

Remark 4.3 Consider the deterministic port-Hamiltonian system (4.1) and we apply Lemma 4.2 to the deterministic system. In this case, $h(x) \equiv 0$ holds. Then, Eq. (4.3) is rewritten by

$$\frac{\partial \Phi^i(x)}{\partial x}(K(x) - S(x))\frac{\partial H(x)}{\partial x}^\top = 0, \quad (i = 1, 2, \cdots, n). \tag{4.11}$$

The condition (4.11) holds for any $H(x)$ and $\Phi(x)$ if we select the matrices $K(x) \equiv 0$ and $S(x) \equiv 0$, respectively. This implies that any time-invariant coordinate transformation preserves the deterministic Hamiltonian structure. It shows that Lemma 4.2 implies the existing result for the deterministic port-Hamiltonian system (Lemma 4.1) as a special case.

We now turn to another fundamental property of stochastic port-Hamiltonian systems which is an extension of passivity of deterministic port-Hamiltonian systems. Passivity of deterministic port-Hamiltonian systems is stated by the following lemma.

Lemma 4.3 *[88] Consider the deterministic port-Hamiltonian system* (4.1). *Suppose that a Hamiltonian $H(x)$ is positive semidefinite. Then, the system is passive with the storage function $H(x)$. Furthermore, if $R(x) \equiv 0$, then, the system is lossless with the storage function $H(x)$.*

In the literature [16], the notion of **stochastic passivity** which corresponds to passivity for the deterministic system is introduced for the stochastic system as follows.

Definition 4.4 [16] Consider the following nonlinear stochastic system described by a stochastic differential equation written in the sense of Itô

$$\begin{cases} \mathrm{d}x &= f(x,u)\,\mathrm{d}t + h(x)\,\mathrm{d}w \\ y &= s(x,u) \end{cases}, \tag{4.12}$$

where $f : \mathbb{R}^n \times \mathbb{R}^m \to \mathbb{R}^n$, $h : \mathbb{R}^n \to \mathbb{R}^{n\times r}$ and $s : \mathbb{R}^n \times \mathbb{R}^m \to \mathbb{R}^m$ are sufficiently differentiable functions and $f(0,0) = 0$, $h(0) = 0$ and $s(0,0) = 0$ hold, respectively.

The stochastic system (4.12) is said to be **stochastic passive** if there exists a positive semidefinite function $V : \mathbb{R}^n \to \mathbb{R}$, called the storage function satisfying

$$\mathcal{L}V(x) \leq s(x,u)^\top u. \tag{4.13}$$

Here $\mathcal{L}(\cdot)$ represents the infinitesimal generator [57] of the stochastic process of the system (4.12) defined as

$$\mathcal{L}(\cdot) := \frac{\partial(\cdot)}{\partial x} f + \frac{1}{2}\mathrm{tr}\left\{ \frac{\partial}{\partial x}\left(\frac{\partial(\cdot)}{\partial x}\right)^\top hh^\top \right\}. \tag{4.14}$$

Unlike in the case of the deterministic port-Hamiltonian system, the stochastic port-Hamiltonian system is not always stochastic passive even if a Hamiltonian $H(x)$ is positive semi-definite. The following lemma characterizes stochastic passivity of the stochastic port-Hamiltonian system.

Lemma 4.4 *Consider the stochastic port-Hamiltonian system* (4.2)*. Suppose that a Hamiltonian $H(x)$ is positive semi-definite. Then, the system is stochastic passive if and only if*

$$\frac{1}{2}\mathrm{tr}\left\{\frac{\partial}{\partial x}\left(\frac{\partial H(x)}{\partial x}\right)^{\top} h(x)h(x)^{\top}\right\} \leq \frac{\partial H(x)}{\partial x}R(x)\frac{\partial H(x)}{\partial x}^{\top} \tag{4.15}$$

holds.

Proof Firstly, the necessity of Eq. (4.15) is shown. By utilizing Eq. (4.14), $\mathcal{L}H(x)$ is calculated as

$$\begin{aligned} \mathcal{L}H(x) &= \frac{\partial H}{\partial x}\left((J-R)\frac{\partial H}{\partial x}^{\top} + gu\right) + \frac{1}{2}\mathrm{tr}\left\{\frac{\partial}{\partial x}\left(\frac{\partial H}{\partial x}\right)^{\top} hh^{\top}\right\} \\ &= -\frac{\partial H}{\partial x}R\frac{\partial H}{\partial x}^{\top} + y^{\top}u + \frac{1}{2}\mathrm{tr}\left\{\frac{\partial}{\partial x}\left(\frac{\partial H}{\partial x}\right)^{\top} hh^{\top}\right\}. \end{aligned} \tag{4.16}$$

Since J is skew-symmetric, the following equation holds

$$\frac{\partial H(x)}{\partial x}J(x)\frac{\partial H(x)}{\partial x}^{\top} = 0.$$

Suppose that the system (4.2) is stochastic passive. Then, from Eqs. (4.13), (4.16) we obtain

$$-\frac{\partial H}{\partial x}R\frac{\partial H}{\partial x}^{\top} + y^{\top}u + \frac{1}{2}\mathrm{tr}\left\{\frac{\partial}{\partial x}\left(\frac{\partial H}{\partial x}\right)^{\top} hh^{\top}\right\} \leq y^{\top}u. \tag{4.17}$$

Eq. (4.15) follows from Eq. (4.17).

Secondly, the sufficiency of Eq. (4.15) is shown. Substituting Eq. (4.15) for Eq. (4.16), we obtain

$$\mathcal{L}H(x) \leq y^{\top}u.$$

According to the definition Eq. (4.13), this proves the sufficiency of Eq. (4.15). ■

Due to Lemma 4.4, we obtain the following corollary.

Corollary 4.5 *Consider the stochastic port-Hamiltonian system* (4.2)*. Suppose that a Hamiltonian $H(x)$ is positive semi-definite and $R(x) \equiv 0$. Then, the system is stochastic lossless* [1] *if and only if*

$$\mathrm{tr}\left\{\frac{\partial}{\partial x}\left(\frac{\partial H(x)}{\partial x}\right)^{\top} h(x)h(x)^{\top}\right\} = 0$$

holds. Suppose the system (4.2) *is stochastic lossless and moreover $u \equiv 0$. Then, the Hamiltonian $H(x)$ is a conserved quantity of the stochastic system.*

[1] In this paper, we define the notion of stochastic lossless by Eq. (4.13) replacing "$\leq$" by "$=$" as in the similar manner of the deterministic case.

Remark 4.5 Consider the deterministic port-Hamiltonian system (4.1) and we apply Lemma 4.4 to the system. In this case, $h(x) \equiv 0$ holds. Then, the condition (4.15) always holds. This implies that Lemma 4.4 reduces to Lemma 4.3 for the deterministic port-Hamiltonian system as a special case.

Remark 4.6 Lemma 4.4 can be physically interpreted as follows. While the left hand side of (4.15) indicates energy increase due to noise, evaluated by stochastic calculus, the right hand side represents energy dissipation due to friction. This lemma requires that the influence of friction predominates over that of noise.

4.1.1 Recovery of stochastic passivity via stochastic generalized canonical transformations

The generalized canonical transformations are proposed in [25] to transform both the input and the output of the deterministic port-Hamiltonian system (4.1) into those of another port-Hamiltonian system with another Hamiltonian. They are useful to design feedback controllers for deterministic Hamiltonian systems (see, section 2.2). This section extends such transformations to stochastic versions for the stochastic port-Hamiltonian system (4.2). We clarify the conditions of the transformations by which the transformed system preserves the stochastic Hamiltonian structure and, furthermore, obtains stochastic passivity.

Firstly, we define the **stochastic generalized canonical transformations**. Then, we show the conditions which these transformations should satisfy.

Definition 4.7 A set of transformations

$$\begin{aligned} \bar{x} &= \Phi(x) \\ \bar{H} &= H(x) + U(x) \\ \bar{y} &= y + \alpha(x) \\ \bar{u} &= u + \beta(x) \end{aligned} \tag{4.18}$$

that changes the coordinate x to $\bar{x}$, a Hamiltonian H to $\bar{H}$, the output y to $\bar{y}$ and the input u to $\bar{u}$, is said to be a stochastic generalized canonical transformation for the stochastic port-Hamiltonian system (4.2) if it transforms the system into another one which is also described by (4.2) with another Hamiltonian. Here $\Phi : \mathbb{R}^n \to \mathbb{R}^n$ is an appropriate coordinate transformation, and $U : \mathbb{R}^n \to \mathbb{R}$, $\alpha : \mathbb{R}^n \to \mathbb{R}^m$ and $\beta : \mathbb{R}^n \to \mathbb{R}^m$ are appropriate functions, respectively.

Theorem 4.6 *Consider the stochastic port-Hamiltonian system* (4.2)*. A set of transformations, functions $\Phi(x)$, $U(x)$, $\alpha(x)$ and $\beta(x)$, yields a stochastic generalized canonical transformation defined by* (4.18) *if and only if there exists a skew-symmetric matrix $P(x)$, a symmetric matrix $Q(x)$ such that $R(x)+Q(x)$ is positive semi-definite, and functions $\Phi(x)$, $U(x)$ and $\beta(x)$ satisfy*

$$\frac{1}{2}\mathrm{tr}\left\{\frac{\partial}{\partial x}\left(\frac{\partial \Phi^i}{\partial x}\right)^{\top} hh^{\top}\right\} = \frac{\partial \Phi^i}{\partial x}\left[(J-R)\frac{\partial U}{\partial x}^{\top} + g\beta + (P-Q)\frac{\partial (H+U)}{\partial x}^{\top}\right],$$
$$(i = 1, 2, \cdots, n). \tag{4.19}$$

Further a function $\alpha(x)$ is given by

$$\alpha(x) = g(x)^\top \frac{\partial U(x)}{\partial x}^\top. \tag{4.20}$$

Proof Firstly, the necessity of the theorem is shown. In the same manner as Eq. (4.5), the dynamics of the system in the new coordinate $\bar{x}$ which is transformed by $\bar{x} = \Phi(x)$ is calculated as

$$\mathrm{d}\bar{x}^i = \left[\frac{\partial \Phi^i}{\partial x}(J-R)\frac{\partial H}{\partial x}^\top + \frac{1}{2}\mathrm{tr}\left\{\frac{\partial}{\partial x}\left(\frac{\partial \Phi^i}{\partial x}\right)^\top hh^\top\right\}\right]\mathrm{d}t + \frac{\partial \Phi^i}{\partial x} gu\,\mathrm{d}t + \frac{\partial \Phi^i}{\partial x} h\,\mathrm{d}w. \tag{4.21}$$

Suppose that the stochastic port-Hamiltonian system (4.2) is transformed into another one using a stochastic generalized canonical transformation with Φ, U and β. Then, the following equation holds for all u and w

$$\begin{aligned}
&\text{R.H.S. of Eq. (4.21)}\\
&\equiv \left[(\bar{J}-\bar{R})\frac{\partial \bar{H}(\Phi^{-1}(\bar{x}))}{\partial \bar{x}}^\top\right]^i \mathrm{d}t + \left[\bar{g}\bar{u}\right]^i \mathrm{d}t + \left[\bar{h}\,\mathrm{d}w\right]^i \\
&= \frac{\partial \Phi^i}{\partial x}\left[\frac{\partial \Phi}{\partial x}\right]^{-1}(\bar{J}-\bar{R})\left[\frac{\partial \Phi}{\partial x}\right]^{-\top}\frac{\partial (H(x)+U(x))}{\partial x}^\top \mathrm{d}t + \left[\bar{g}(u+\beta)\right]^i \mathrm{d}t + \left[\bar{h}\,\mathrm{d}w\right]^i.
\end{aligned} \tag{4.22}$$

Here the last equality is implied by

$$\begin{aligned}
\frac{\partial \Phi(x)}{\partial x}^\top \frac{\partial \bar{H}(\Phi^{-1}(\bar{x}))}{\partial \bar{x}}^\top &= \left(\frac{\partial \bar{H}(\Phi^{-1}(\bar{x}))}{\partial \bar{x}}\frac{\partial \bar{x}}{\partial x}\right)^\top \\
&= \frac{\partial \bar{H}(x)}{\partial x}^\top \\
&= \frac{\partial (H(x)+U(x))}{\partial x}^\top.
\end{aligned}$$

Equation (4.22) implies that

$$\frac{\partial \Phi}{\partial x} g \equiv \bar{g}, \qquad \frac{\partial \Phi}{\partial x} h \equiv \bar{h}. \tag{4.23}$$

Using Eqs. (4.21), (4.22) and (4.23), we have

$$\begin{aligned}
&\frac{1}{2}\mathrm{tr}\left\{\frac{\partial}{\partial x}\left(\frac{\partial \Phi^i}{\partial x}\right)^\top hh^\top\right\} = \\
&\qquad \frac{\partial \Phi^i}{\partial x}\left[\left[\frac{\partial \Phi}{\partial x}\right]^{-1}(\bar{J}-\bar{R})\left[\frac{\partial \Phi}{\partial x}\right]^{-\top}\frac{\partial (H+U)}{\partial x}^\top - (J-R)\frac{\partial H}{\partial x}^\top + g\beta\right].
\end{aligned} \tag{4.24}$$

Here we define the matrices $P(x)$ and $Q(x)$ as

$$P(x) := \left[\frac{\partial\Phi}{\partial x}\right]^{-1} \bar{J}(\Phi(x)) \left[\frac{\partial\Phi}{\partial x}\right]^{-\top} - J(x),$$
$$Q(x) := \left[\frac{\partial\Phi}{\partial x}\right]^{-1} \bar{R}(\Phi(x)) \left[\frac{\partial\Phi}{\partial x}\right]^{-\top} - R(x). \tag{4.25}$$

Then, $P(x)$ is skew-symmetric since $J(x)$ and $\bar{J}(\Phi(x))$ are so and, for $R(x)$ is symmetric and $\bar{R}(\Phi(x))$ is symmetric positive semi-definite, $Q(x)$ is symmetric and $R(x) + Q(x)$ is symmetric positive semi-definite. By substituting Eq. (4.25) for Eq. (4.24), Equation (4.19) is obtained immediately.

The change of the output $\alpha(x)$ which yields a stochastic generalized canonical transformation (4.18) can be calculated as

$$\begin{aligned}
\alpha &= \bar{y} - y \\
&= \bar{g}^\top \frac{\partial \bar{H}(\Phi^{-1}(\bar{x}))}{\partial \bar{x}}^\top - g^\top \frac{\partial H(x)}{\partial x}^\top \\
&= g^\top \frac{\partial \Phi(x)}{\partial x}^\top \left[\frac{\partial\Phi(x)}{\partial x}\right]^{-\top} \frac{\partial (H(x)+U(x))}{\partial x}^\top - g^\top \frac{\partial H(x)}{\partial x}^\top \\
&= g^\top \frac{\partial U(x)}{\partial x}^\top .
\end{aligned}$$

This proves the necessity of the theorem.

Secondly, the sufficiency of the theorem is shown. Now suppose that the assumption of the theorem holds. Then, by substituting Eq. (4.19) for (4.21), the dynamics of the system can be calculated in the new coordinate $\bar{x}$ as

$$\begin{aligned}
\mathrm{d}\bar{x}^i &= \left[\frac{\partial\Phi^i}{\partial x}(J-R)\frac{\partial H}{\partial x}^\top + \frac{\partial\Phi^i}{\partial x}\left[(J-R)\frac{\partial U}{\partial x}^\top + g\beta + (P-Q)\frac{\partial(H+U)}{\partial x}^\top\right]\right]\mathrm{d}t \\
&\quad + \frac{\partial\Phi^i}{\partial x} g u \,\mathrm{d}t + \frac{\partial\Phi^i}{\partial x} h \,\mathrm{d}w \\
&= \left[\frac{\partial\Phi}{\partial x}\Big((J+P) - (R+Q)\Big)\frac{\partial\Phi}{\partial x}^\top \frac{\partial(H(\Phi^{-1}(\bar{x})) + U(\Phi^{-1}(\bar{x})))}{\partial\bar{x}}^\top\right]^i \mathrm{d}t \\
&\quad + \frac{\partial\Phi^i}{\partial x} g(u+\beta)\,\mathrm{d}t + \frac{\partial\Phi^i}{\partial x} h\,\mathrm{d}w.
\end{aligned} \tag{4.26}$$

$\bar{J}$, $\bar{R}$, $\bar{g}$ and $\bar{h}$ are given by

$$\bar{J}(\bar{x}) = \frac{\partial\Phi(x)}{\partial x}(J(x)+P(x))\frac{\partial\Phi(x)}{\partial x}^{\top}\Bigg|_{x=\Phi^{-1}(\bar{x})}$$

$$\bar{R}(\bar{x}) = \frac{\partial\Phi(x)}{\partial x}(R(x)+Q(x))\frac{\partial\Phi(x)}{\partial x}^{\top}\Bigg|_{x=\Phi^{-1}(\bar{x})}$$

$$\bar{g}(\bar{x}) = \frac{\partial\Phi(x)}{\partial x}g(x)\Bigg|_{x=\Phi^{-1}(\bar{x})}$$

$$\bar{h}(\bar{x}) = \frac{\partial\Phi(x)}{\partial x}h(x)\Bigg|_{x=\Phi^{-1}(\bar{x})}. \tag{4.27}$$

Then, $\bar{J}(\bar{x})$ is skew-symmetric since $J(\Phi^{-1}(\bar{x}))$ and $P(\Phi^{-1}(\bar{x}))$ are so, and $\bar{R}(\bar{x})$ is symmetric positive semi-definite because of the assumption that $R(\Phi^{-1}(\bar{x})) + Q(\Phi^{-1}(\bar{x}))$ is so. Consequently, the dynamics of the system in the new coordinate $\bar{x}$ is given by

$$\mathrm{d}\bar{x}^i = \left[\left(\bar{J}(\bar{x}) - \bar{R}(\bar{x})\right)\frac{\partial\bar{H}(\Phi^{-1}(\bar{x}))}{\partial\bar{x}}^{\top}\right]^i \mathrm{d}t + \left[\bar{g}(u+\beta)\right]^i \mathrm{d}t + \left[\bar{h}\,\mathrm{d}w\right]^i. \tag{4.28}$$

The output in the new coordinate $\bar{y}$ is obtained by Eq. (4.20) as

$$\begin{aligned} \bar{y} &= y + \alpha(x) \\ &= g^{\top}\frac{\partial H(x)}{\partial x}^{\top} + g^{\top}\frac{\partial U(x)}{\partial x}^{\top} \\ &= g^{\top}\frac{\partial\Phi}{\partial x}^{\top}\left[\frac{\partial\Phi}{\partial x}\right]^{-\top}\frac{\partial(H+U)}{\partial x}^{\top} \\ &= \bar{g}^{\top}\frac{\partial\bar{H}(\Phi^{-1}(\bar{x}))}{\partial\bar{x}}^{\top}. \end{aligned} \tag{4.29}$$

Equations (4.28) and (4.29) imply the sufficiency of the theorem. ■

Remark 4.8 Consider the deterministic port-Hamiltonian system (4.1) and we apply Theorem 4.6 to the system. In this case, $h(x) \equiv 0$ holds. Then, the condition (4.19) in Theorem 4.6 can be rewritten as

$$\frac{\partial\Phi}{\partial x}\left[(J-R)\frac{\partial U}{\partial x}^{\top} + g\beta + (P-Q)\frac{\partial(H+U)}{\partial x}^{\top}\right] = 0.$$

This coincides with the time-invariant version of Theorem 1 (i) in [20] which is a generalized version of a result from [25] incorporating the dissipative element R in (4.1). This implies that in considering the time-invariant case, Theorem 4.6 implies a result for the deterministic port-Hamiltonian system as a special case.

By utilizing Lemma 4.4 and Theorem 4.6, the following theorem states a condition under which a transformed stochastic port-Hamiltonian system by a stochastic generalized canonical transformation becomes stochastic passive with a new Hamiltonian $\bar{H}$ as a storage function and, furthermore, a stabilization method based on stochastic passivity.

Theorem 4.7 *Consider the stochastic port-Hamiltonian system* (4.2) *and transform it by an appropriate stochastic generalized canonical transformation such that* $\bar{H}(\bar{x}) := H(\Phi^{-1}(\bar{x})) + U(\Phi^{-1}(\bar{x})) \geq 0$ *and that* $\bar{H}(\bar{x})$ *is a* $C^d,\ d \geq 1$ *function. Then, the transformed system becomes stochastic passive with new Hamiltonian* $\bar{H}(\bar{x})$ *as a storage function if and only if*

$$\frac{1}{2}\mathrm{tr}\left\{\frac{\partial}{\partial x}\left(\frac{\partial(H+U)}{\partial x}\left[\frac{\partial\Phi}{\partial x}\right]^{-1}\right)^{\top} h(x)h(x)^{\top}\frac{\partial\Phi}{\partial x}^{\top}\right\} \leq \frac{\partial(H+U)}{\partial x}(R+Q)\frac{\partial(H+U)}{\partial x}^{\top} \tag{4.30}$$

holds.

If $\bar{H}(\bar{x})$ *is positive definite, the state* $\bar{x}$ *of the transformed system tends in probability to the largest invariant set whose support is contained in the locus* $\mathcal{L}\bar{H}(\bar{x}) = 0$ *for any* $t \geq 0$, *with the unity feedback* $\bar{u} = -\bar{y}$. *Furthermore, if it holds that* $\bar{\Gamma} \cap \bar{\Pi} = \{0\}$, *then the unity feedback renders the system asymptotically stable in probability. Here, the distribution* $\bar{\Lambda}$, *the sets* $\bar{\Gamma}$ *and* $\bar{\Pi}$ *are defined as*

$$\begin{aligned}
\bar{\Lambda} &= \mathrm{span}\{\mathrm{ad}_{\bar{f}_0}^k \bar{g}_i(\bar{x}) | 0 \leq k \leq n-1, 1 \leq i \leq m\} \\
\bar{\Gamma} &= \{\bar{x} \in \mathbb{R}^n | \mathcal{L}_0^k \bar{H}(\bar{x}) = 0,\ k = 1, 2, \cdots, d\} \\
\bar{\Pi} &= \{\bar{x} \in \mathbb{R}^n | \mathcal{L}_0^k L_\lambda \bar{H}(\bar{x}) = 0, \quad \forall \lambda \in \bar{\Lambda},\ k = 0, 1, \cdots, d-1\},
\end{aligned}$$

where $\bar{f}_0 := (\bar{J}(\bar{x}) - \bar{R}(\bar{x}))\frac{\partial \bar{H}(\bar{x})}{\partial \bar{x}}^{\top}$, *and* $\bar{g}_i$ *represents* i*-th column of* $\bar{g}$. $\mathrm{ad}_{\bar{f}_0}^k \bar{g}_i$ *is defined as*

$$\mathrm{ad}_{\bar{f}_0}^k \bar{g}_i(\bar{x}) = [\bar{f}_0, \mathrm{ad}_{\bar{f}_0}^{k-1} \bar{g}_i](\bar{x}),$$

for any integer $k \geq 1$, *setting* $\mathrm{ad}_{\bar{f}_0}^0 \bar{g}_i = \bar{g}_i$ *with the Lie bracket* $[\cdot, \cdot]$, *see e.g. [41, 45, 67].* $\mathcal{L}_0$ *denotes the operator* (4.14) *in which* f *is replaced by* $\bar{f}_0$ *and* $L_{(\cdot)}$ *represents the Lie derivative along* $(\cdot)$. $\mathcal{L}_0^k L_\lambda \bar{H}$ *can be calculated as*

$$\begin{aligned}
\mathcal{L}_0^k L_\lambda \bar{H}(\bar{x}) &= \mathcal{L}_0^k \frac{\partial \bar{H}}{\partial \bar{x}} \lambda \\
&= \mathcal{L}_0 \mathcal{L}_0^{k-1} \frac{\partial \bar{H}}{\partial \bar{x}} \lambda.
\end{aligned}$$

for any integer $k \geq 1$, *setting* $\mathcal{L}_0^0 L_\lambda \bar{H} = L_\lambda \bar{H}$.

Proof Firstly, the former part of the theorem is shown. Due to Lemma 4.4, the necessary and sufficient condition is that the following inequality holds in the new coordinate transformed by the stochastic generalized canonical transformation

$$\frac{1}{2}\mathrm{tr}\left\{\frac{\partial}{\partial \bar{x}}\left(\frac{\partial \bar{H}(\bar{x})}{\partial \bar{x}}\right)^{\top} \bar{h}(\bar{x})\bar{h}(\bar{x})^{\top}\right\} \leq \frac{\partial \bar{H}(\bar{x})}{\partial \bar{x}} \bar{R}(\bar{x}) \frac{\partial \bar{H}(\bar{x})}{\partial \bar{x}}^{\top}. \tag{4.31}$$

Let us note that the following equation holds

$$\frac{\partial}{\partial \bar{x}}\left(\frac{\partial \bar{H}(\bar{x})}{\partial \bar{x}}\right)^{\top} = \frac{\partial}{\partial x}\left(\frac{\partial \bar{H}(\Phi(x))}{\partial x}\frac{\partial \Phi^{-1}(\bar{x})}{\partial \bar{x}}\right)^{\top}\frac{\partial \Phi^{-1}(\bar{x})}{\partial \bar{x}}$$
$$= \frac{\partial}{\partial x}\left(\frac{\partial \bar{H}(\Phi(x))}{\partial x}\left[\frac{\partial \Phi(x)}{\partial x}\right]^{-1}\right)^{\top}\left[\frac{\partial \Phi(x)}{\partial x}\right]^{-1}. \tag{4.32}$$

By utilizing Eqs. (4.27), (4.31) and (4.32), one can prove Eq. (4.30) holds immediately.

Secondly, the latter part of the theorem is shown. Since the transformed system is stochastic passive, the following inequality holds for the closed loop system with the unity feedback $\bar{u} = -\bar{y}$

$$\mathcal{L}\bar{H}(\bar{x}) \leq -\|\bar{y}\|^2 \leq 0.$$

Then the stochastic version of LaSalle's theorem (Theorem C.1 [49, 16] in Appendix C.2) implies that the state $\bar{x}$ tends in probability to the largest invariant set whose support is contained in the locus $\mathcal{L}\bar{H}(\bar{x}) = 0$ for any $t \geq 0$.

Finally, the rest of the theorem is shown by directly applying Corollary 4.7 in [16]. ■

Example 4.9 Consider a simple mechanical system with random noise (see, Eq. (2.19) for the deterministic case)

$$\begin{cases} \begin{pmatrix} \mathrm{d}q \\ \mathrm{d}p \end{pmatrix} = \begin{pmatrix} 0 & 1 \\ -1 & 0 \end{pmatrix}\begin{pmatrix} \dfrac{\partial H}{\partial q}^{\top} \\ \dfrac{\partial H}{\partial p}^{\top} \end{pmatrix}\mathrm{d}t + \begin{pmatrix} 0 \\ 1 \end{pmatrix} u\,\mathrm{d}t + \begin{pmatrix} 0 \\ ap \end{pmatrix}\mathrm{d}w \\ y = \dfrac{\partial H}{\partial p}^{\top} = \dfrac{p}{M} \end{cases} \tag{4.33}$$

with the Hamiltonian $H = \frac{p^2}{2M}$, where $x := (q,p)^{\top} \in \mathbb{R}^2$ denotes the state, a positive constant M denotes the inertia and $w(t) \in \mathbb{R}$ is a standard Wiener process. Here we suppose that the noise port ap with $a > 0$. Since

$$\frac{1}{2}\mathrm{tr}\left\{\frac{\partial}{\partial x}\left(\frac{\partial H(x)}{\partial x}\right)^{\top} h(x)h(x)^{\top}\right\} = \frac{a^2p^2}{2M}$$
$$\frac{\partial H(x)}{\partial x}R(x)\frac{\partial H(x)}{\partial x}^{\top} = 0,$$

it follows from Lemma 4.4 that this system is not stochastic passive. We assign any positive definite scalar function $U(q)$ so that $\bar{H}$ becomes positive definite. By using Theorem 4.6, we obtain a stochastic generalized canonical transformation as $\bar{q} = q$, $\bar{p} = p$, $\alpha = 0$, $\beta = \frac{\mathrm{d}U(q)}{\mathrm{d}q} - \frac{Q_{22}}{M}p$, where

$$P := 0, \quad Q := \begin{pmatrix} 0 & 0 \\ 0 & Q_{22} \end{pmatrix}.$$

Then by using Theorem 4.7, the condition under which the transformed system becomes stochastic passive is

$$Ma^2 \leq Q_{22}.$$

4.1.2 Numerical example

In this subsection, we consider stabilization of a rolling coin on a horizontal plane [88, 23, 7] depicted in Fig. 4.1 in the presence of noise. Let X-Y denote the orthogonal coordinates of the point of contact of the coin. Let q^1 denote the heading angle of the coin, and (q^2, q^3) the position of the coin in X-Y plane. Furthermore let p^1 be the angular velocity with respect to the heading

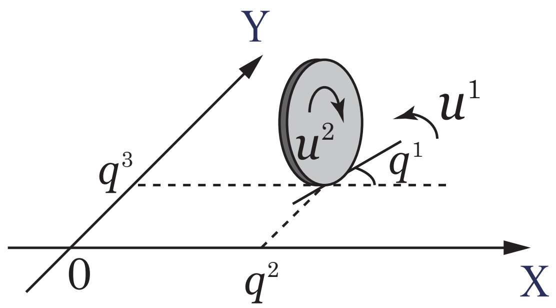

Figure 4.1: A rolling coin

angle, p^2 be the rolling angular velocity of the coin, u^1 and u^2 be the accelerations with respect to p^1 and p^2, respectively. Finally, let all the parameters unity for simplicity, e.g. the radius of the coin and the moments of inertia about the axis perpendicular to the plane of the coin and an axis in the plane, where both axes pass through the coin's center, respectively. Then this system is described by a stochastic port-Hamiltonian system of the form (4.2) with $q = (q^1, q^2, q^3)^\top$, $p = (p^1, p^2)^\top$, $x = (q^\top, p^\top)^\top$, $H(x) = (1/2)p^\top p$ and

$$\begin{aligned}
J(x) &= \begin{pmatrix} 0 & 0 & 0 & 1 & 0 \\ 0 & 0 & 0 & 0 & \cos q^1 \\ 0 & 0 & 0 & 0 & \sin q^1 \\ -1 & 0 & 0 & 0 & 0 \\ 0 & -\cos q^1 & -\sin q^1 & 0 & 0 \end{pmatrix}, \\
R(x) &= O_{55}, \\
g(x) &= \begin{pmatrix} O_{32} \\ I_2 \end{pmatrix}, \\
h(x) &= \begin{pmatrix} O_{32} \\ \mathrm{diag}\{h^1(x), h^2(x)\} \end{pmatrix}, \\
y &= g(x)^\top \frac{\partial H(x)}{\partial x}^\top = p,
\end{aligned} \tag{4.34}$$

where $h^1(x)$ and $h^2(x)$ represent appropriate functions for the noise port. For the details of nonholonomic Hamiltonian systems, see Appendix B.

In [23, 24], a stabilization technique of deterministic nonholonomic Hamiltonian systems (B.1) is proposed, where a system is converted into a canonical form of nonholonomic Hamiltonian systems by a generalized canonical transformation with any potential function U such that it has the form $U((q^1)^2+(q^2)^2,q^3)$ and is smooth positive definite on $(q^1,q^2)\neq 0$ and satisfies

$$(q^1,q^2)\neq 0 \ \Rightarrow\ \frac{\partial U}{\partial q}\neq 0, \tag{4.35}$$

and a special coordinate transformation $\bar{x}=\Phi(x)$. Then stabilization of a specified invariant set

$$\Pi_0 := \left\{x \mid q^1=q^2=0\ ,\ p^1=p^2=0\right\} \tag{4.36}$$

is achieved. The purpose of this subsection is to stabilize the invariant set Π_0 in probability in the presence of noise by utilizing the same coordinate transformation proposed in [24].

Since the Hamiltonian of the system (4.34) is positive semi-definite, let us transform the system into anther stochastic passive system by the stochastic generalized canonical transformation with a potential function $U((q^1)^2+(q^2)^2,q^3)$ and the following coordinate transformation $\bar{x}=\Phi(x)$ proposed in [24]

$$\begin{aligned}
\bar{q} &= \begin{pmatrix}\Phi^1(x)\\ \Phi^2(x)\\ \Phi^3(x)\end{pmatrix} = \begin{pmatrix}\tan q^1\\ q^2\\ 2q^3-q^2\tan q^1\end{pmatrix},\\
\bar{p} &= \begin{pmatrix}\Phi^4(x)\\ \\ \Phi^5(x)\end{pmatrix} = \begin{pmatrix}\dfrac{p^1}{1+\tan^2 q^1}\\ p^2\sqrt{1+\tan^2 q^1}\end{pmatrix}.
\end{aligned} \tag{4.37}$$

In order to obtain the stochastic generalized canonical transformation, let us decide the rest design parameters $\beta(x), P(x)$ and $Q(x)$ by utilizing Theorem4.6. The following choice satisfies Eq. (4.19)

$$\begin{aligned}
P(x) &= O_{55}\\
Q(x) &= \left(\begin{array}{c|cc} O_{33} & \multicolumn{2}{c}{O_{32}}\\ \hline O_{23} & Q_{44}(x) & Q_{45}(x)\\ & Q_{45}(x) & Q_{55}(x)\end{array}\right) =: \left(\begin{array}{c|c} O_{33} & O_{32}\\ \hline O_{23} & \tilde{Q}(x)\end{array}\right)\\
\beta(x) &= \begin{pmatrix}\frac{\partial U}{\partial q^1}+p^1Q_{44}(x)+p^2Q_{45}(x)\\ \frac{\partial U}{\partial q^2}\cos q^1+\frac{\partial U}{\partial q^3}\sin q^1+p^1Q_{45}(x)+p^2Q_{55}(x)\end{pmatrix}\\
\alpha(x) &= g^\top\frac{\partial U}{\partial x}^\top = \begin{pmatrix}0&0&0&1&0\\0&0&0&0&1\end{pmatrix}\begin{pmatrix}\frac{\partial U}{\partial q_1}\\ \frac{\partial U}{\partial q_2}\\ \frac{\partial U}{\partial q_3}\\ 0\\ 0\end{pmatrix} = O_{21},
\end{aligned} \tag{4.38}$$

where free parameters $Q_{44}(x), Q_{45}(x)$ and $Q_{55}(x)$ should be chosen so that $\tilde{Q}(x)$ in Eq. (4.38) becomes symmetric positive semi-definite. Furthermore in order to obtain stochastic passivity, let us derive another condition for $Q_{44}(x), Q_{45}(x)$ and $Q_{55}(x)$ from Theorem 4.7. It follows from the inequality (4.30) that

$$\frac{1}{2}(h^1(x)^2 + h^2(x)^2) \leq (p^1)^2 Q_{44}(x) + 2p^1 p^2 Q_{45}(x) + (p^2)^2 Q_{55}(x). \tag{4.39}$$

If there exist functions $Q_{44}(x), Q_{45}(x)$ and $Q_{55}(x)$ for a noise port $h(x)$ such that they satisfy the condition (4.39), and let $\tilde{Q}(x)$ in Eq. (4.38) become symmetric positive semi-definite, the transformed system obtains stochastic passivity. From another viewpoint, the inequality (4.39) implies the condition for the noise port $h(x)$ under which the system can be stabilized based on its stochastic passivity. Let us note that the condition (4.38) is independent of the choice of a potential function $U((q^1)^2 + (q^2)^2, q^3)$. In what follows, we suppose that there exist functions $Q_{44}(x), Q_{45}(x)$ and $Q_{55}(x)$ such that the equality in the condition (4.39) holds and $\tilde{Q}(x)$ in Eq. (4.38) becomes symmetric positive semi-definite.

The transformed system is given by

$$\bar{J}(\bar{x}) = \begin{pmatrix} 0 & 0 & 0 & 1 & 0 \\ 0 & 0 & 0 & 0 & 1 \\ 0 & 0 & 0 & -\bar{q}^2 & \bar{q}^1 \\ -1 & 0 & \bar{q}^2 & 0 & -\bar{p}^2\bar{q}^1/(1+(\bar{q}^1)^2) \\ 0 & -1 & -\bar{q}^1 & \bar{p}^2\bar{q}^1/(1+(\bar{q}^1)^2) & 0 \end{pmatrix},$$

$$\bar{R}(\bar{x}) = \left.\left(\begin{array}{c|cc} O_{33} & \multicolumn{2}{c}{O_{32}} \\ \hline O_{23} & \cos^4 q^1 Q_{44}(x) & \cos q^1 Q_{45}(x) \\ & \cos q^1 Q_{45}(x) & \dfrac{Q_{55}(x)}{\cos^2 q^1} \end{array}\right)\right|_{x=\Phi^{-1}(\bar{x})},$$

$$\bar{g}(\bar{x}) = \begin{pmatrix} O_{32} \\ \mathrm{diag}\{1/(1+(\bar{q}^1)^2), \sqrt{1+(\bar{q}^1)^2}\} \end{pmatrix}, \tag{4.40}$$

$$\bar{h}(\bar{x}) = \left.\begin{pmatrix} O_{32} \\ \mathrm{diag}\{h^1(x)\cos^2 q^1, h^2(x)/\cos q^1\} \end{pmatrix}\right|_{x=\Phi^{-1}(\bar{x})}.$$

Equation (4.40) implies that the transformed system has the form of (4.2). Since this system obtains stochastic passivity, it can be easily proven by Theorem 4.7 that with the unity feedback $\bar{u} = -\bar{y}$, the state $\bar{x}$ tends in probability to the largest invariant set whose support is contained in the locus $\mathcal{L}\bar{H}(\bar{x}) = 0$. Now let us show that this largest invariant set coincides with our target set Π_0 in (4.36). Since $Q_{44}(x), Q_{45}(x)$ and $Q_{55}(x)$ are chosen to hold the equality in the condition (4.39), the following equation holds

$$\frac{1}{2}\mathrm{tr}\left\{\frac{\partial}{\partial \bar{x}}\left(\frac{\partial \bar{H}(\bar{x})}{\partial \bar{x}}\right)^{\top} \bar{h}(\bar{x})\bar{h}(\bar{x})^{\top}\right\} = \frac{\partial \bar{H}(\bar{x})}{\partial \bar{x}}\bar{R}(\bar{x})\frac{\partial \bar{H}(\bar{x})}{\partial \bar{x}}^{\top}.$$

Then the passivity of the transformed system yields

$$\mathcal{L}\bar{H}(\bar{x}) = \bar{y}^\top \bar{u}. \tag{4.41}$$

Equation (4.41) implies that we should show that the input/output nulling set coincides with Π_0. The following calculation

$$\begin{aligned} 0 &\equiv \bar{y} \\ &= \bar{g}^\top \frac{\partial \bar{H}}{\partial \bar{x}}^\top \\ &= \begin{pmatrix} (1+(\bar{q}^1)^2)\bar{p}^1 \\ \bar{p}^2 \Big/ \sqrt{1+(\bar{q}^1)^2} \end{pmatrix} \end{aligned}$$

requires $\{\bar{x} \mid \bar{p} = 0\}$ for the input/output nulling set. Under the condition $\{\bar{x} \mid \bar{p} = 0\}$, we can calculate

$$\begin{aligned} \mathcal{L}_0 L_{\bar{g}_1} \bar{H}(\bar{x})\Big|_{\bar{p}=0} &= -(1+(\bar{q}^1)^2)\left(\frac{\partial U}{\partial \bar{q}^1} - \bar{q}^2 \frac{\partial U}{\partial \bar{q}^3}\right) \\ \mathcal{L}_0 L_{\bar{g}_2} \bar{H}(\bar{x})\Big|_{\bar{p}=0} &= -\left(\frac{\partial U}{\partial \bar{q}^2} + \bar{q}^1 \frac{\partial U}{\partial \bar{q}^3}\right) \Big/ \sqrt{1+(\bar{q}^1)^2}. \end{aligned}$$

From the conditions:

$$\begin{aligned} \mathcal{L}_0 L_{\bar{g}_1} \bar{H}(\bar{x})\Big|_{\bar{p}=0} &\equiv 0 \\ \mathcal{L}_0 L_{\bar{g}_2} \bar{H}(\bar{x})\Big|_{\bar{p}=0} &\equiv 0, \end{aligned}$$

the input/output nulling set is obtained as

$$\left\{ \bar{x} \;\Big|\; \frac{\partial U}{\partial \bar{q}} \bar{J}_{12}(\bar{q}) = 0,\ \bar{p} = 0 \right\},$$

where

$$\bar{J}_{12}(\bar{q}) := \begin{pmatrix} 1 & 0 \\ 0 & 1 \\ -\bar{q}^2 & \bar{q}^1 \end{pmatrix}.$$

From the condition of the potential function U (see Eq. (4.35)) and the coordinate transformation Φ in (4.37), it can be easily calculated as

$$\begin{aligned} \left\{ \bar{x} \;\Big|\; \frac{\partial U}{\partial \bar{q}} \bar{J}_{12}(\bar{q}) = 0,\ \bar{p} = 0 \right\} &= \left\{ \bar{x} \mid \bar{q}^1 = \bar{q}^2 = 0\ ,\ \bar{p}^1 = \bar{p}^2 = 0 \right\} \\ &= \left\{ x \mid q^1 = q^2 = 0\ ,\ p^1 = p^2 = 0 \right\} \\ &\equiv \Pi_0. \end{aligned} \tag{4.42}$$

From Theorem 4.7 and Eq. (4.42), the controller

$$\begin{aligned} u &= -\beta(x) - (y + \alpha(x)) \\ &= -\begin{pmatrix} \frac{\partial U}{\partial q^1} + p^1(1+Q_{44}(x)) + p^2 Q_{45}(x) \\ \frac{\partial U}{\partial q^2}\cos q^1 + \frac{\partial U}{\partial q^3}\sin q^1 + p^1 Q_{45}(x) + p^2(1+Q_{55}(x)) \end{pmatrix} \end{aligned} \tag{4.43}$$

renders the invariant set Π_0 stable in probability. The purpose of this subsection has been achieved.

Remark 4.10 Due to Brockett's condition [8], deterministic nonholonomic systems can not be asymptotically stabilized around a fixed point under any continuous static feedback controller. In the case of the stochastic system (4.34), it is easily shown that the condition in Theorem 4.7 that $\bar{\Gamma} \cap \bar{\Pi} = \{0\}$ does not hold. Since

$$\mathcal{L}_0 \bar{H}(\bar{x}) = \frac{\partial \bar{H}}{\partial \bar{x}} \bar{f}_0 + \frac{1}{2} \operatorname{tr} \left\{ \frac{\partial}{\partial \bar{x}} \left(\frac{\partial \bar{H}}{\partial \bar{x}} \right)^{\top} \bar{h} \bar{h}^{\top} \right\} = 0,$$

we have $\bar{\Gamma} = \mathbb{R}^5$. From the adobe argument, we have

$$\bar{\Pi} = \left\{ \bar{x} \;\middle|\; \frac{\partial U}{\partial \bar{q}} \bar{J}_{12}(\bar{q}) = 0,\ \bar{p} = 0 \right\}.$$

Therefore $\bar{\Gamma} \cap \bar{\Pi} \neq \{0\}$ is shown. In literatures [23, 26], a discontinuous static feedback controller and a time-varying feedback controller which render the origin of a deterministic nonholonomic port-Hamiltonian system asymptotically stable, are proposed, respectively. In the next section, we propose a time-varying feedback controller which renders the origin of a stochastic nonholonomic port-Hamiltonian system asymptotically stable in probability.

Finally, let us show some simulation results. Here we consider the noise port as

$$h(x) = \begin{pmatrix} 0 & 0 \\ 0 & 0 \\ 0 & 0 \\ k^1 p^1 & 0 \\ 0 & k^2 p^2 \end{pmatrix}$$

and we set a potential function as $U = 1/2 q^{\top} q$, design parameters as $Q_{44} = (k^1)^2/2$, $Q_{45} = 0$ and $Q_{55} = k_2^2/2$ with $k^1 = k^2 = 15$ and the initial condition as

$$(q^1, q^2, q^3, p^1, p^2) = (0.1, 0.4, 0.2, 0, 0).$$

We simulate a standard Wiener process in the same manner as in [57].

Firstly, we consider a scenario where noise does not exist, that is, $h(x) \equiv 0$ and a feedback controller designed by a deterministic method in [23], which corresponds to the controller (4.43) with $Q(x) = 0$ is applied. Figure 4.2 shows the motion of the coin in X-Y plane and Fig. 4.3 shows time responses of q and p. It implies that the controller designed for the deterministic system works well without noise.

However, secondly, we consider a scenario where there exists noise and the same feedback controller as in the previous scenario is applied. Figure 4.4 shows the motion of the coin in X-Y plane and Fig. 4.5 shows time responses of q and p, respectively. They imply that the behavior of the system seems unstable with the controller for the deterministic system in the presence of noise.

Finally, we consider a scenario where there exists the same noise as in the previous scenario and the feedback controller (4.43) designed by the proposed method is applied. Figure 4.6 shows the motion of the coin in X-Y plane and Fig. 4.7 shows time responses of q and p, respectively. They imply that the proposed controller works well even in the presence of noise.

These simulation results demonstrate the effectiveness of the proposed framework.

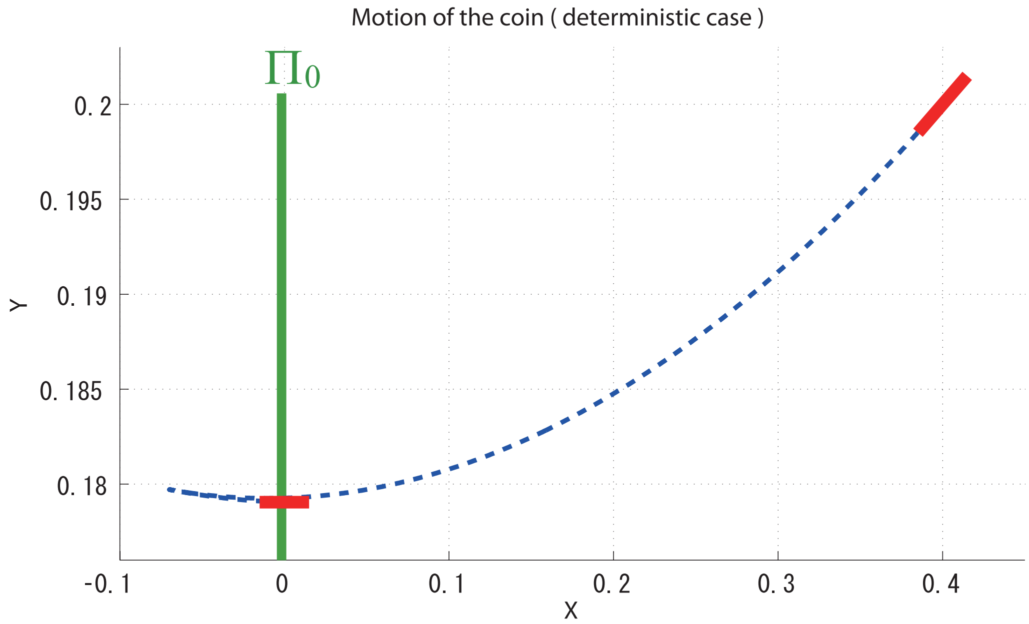

Figure 4.2: Motion of the coin in the deterministic case

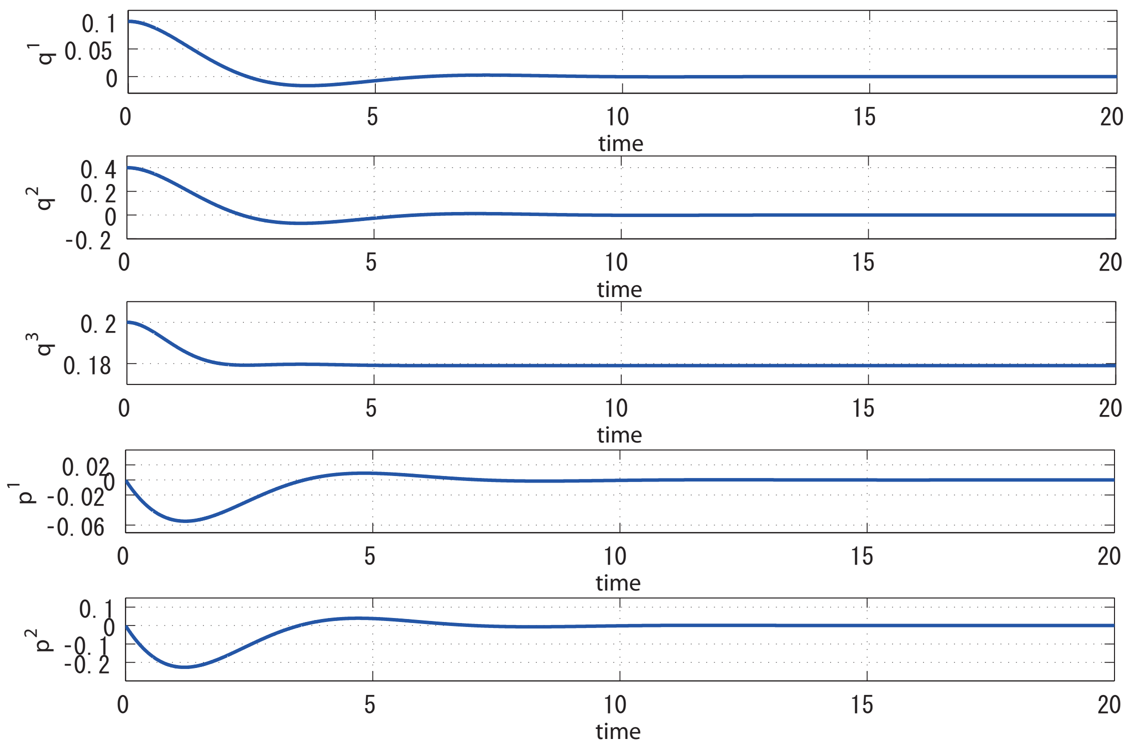

Figure 4.3: Responses of q and p in the deterministic case

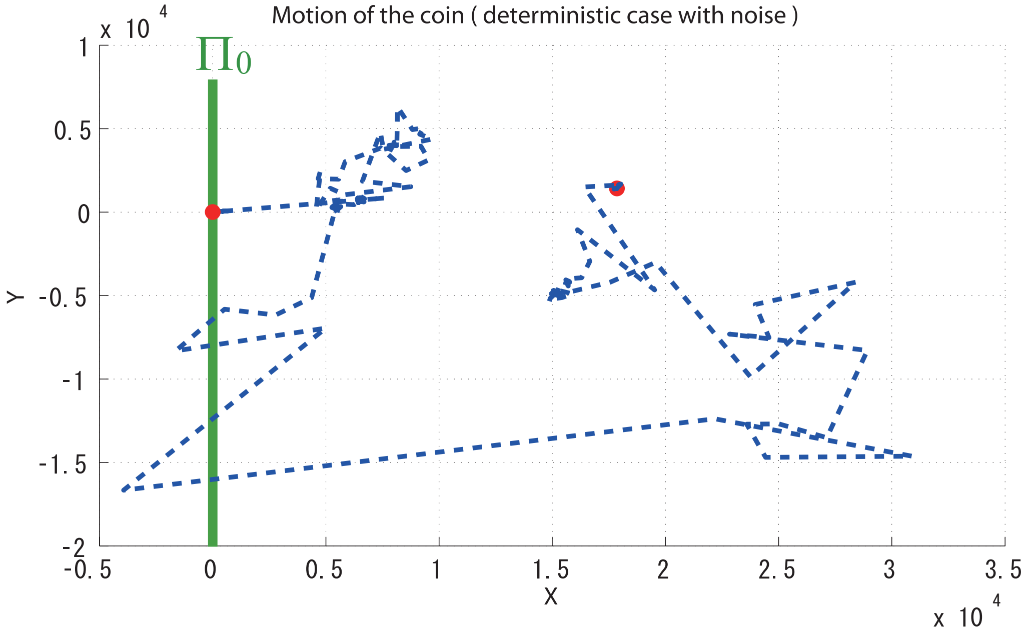

Figure 4.4: Motion of the coin in the deterministic case with noise

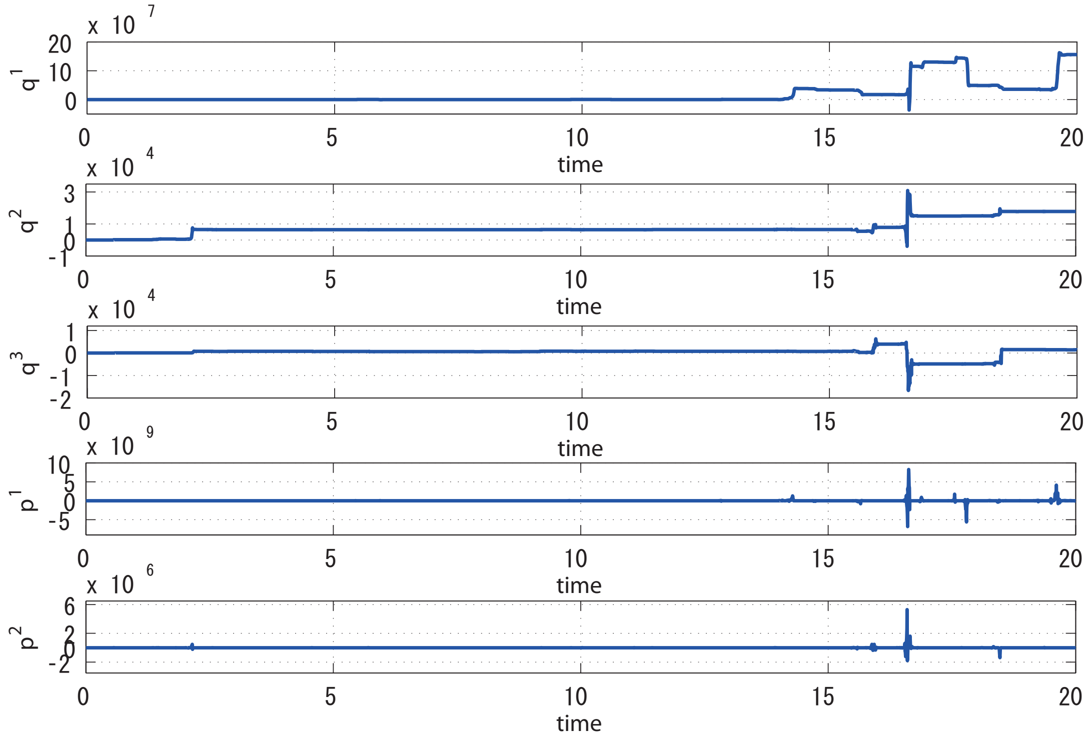

Figure 4.5: Responses of q and p in the deterministic case with noise

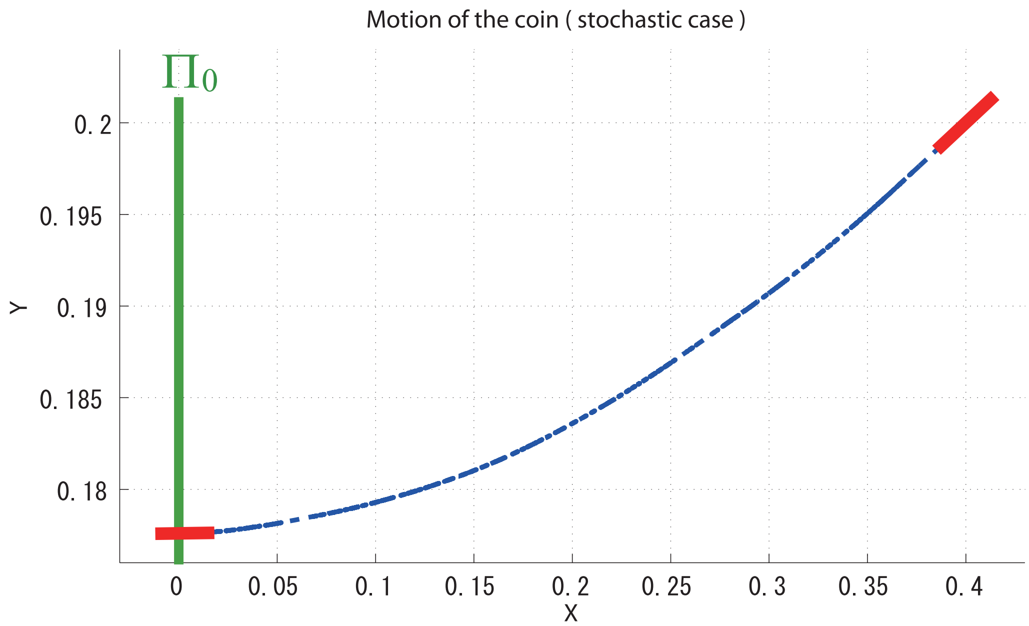

Figure 4.6: Motion of the coin in the stochastic case

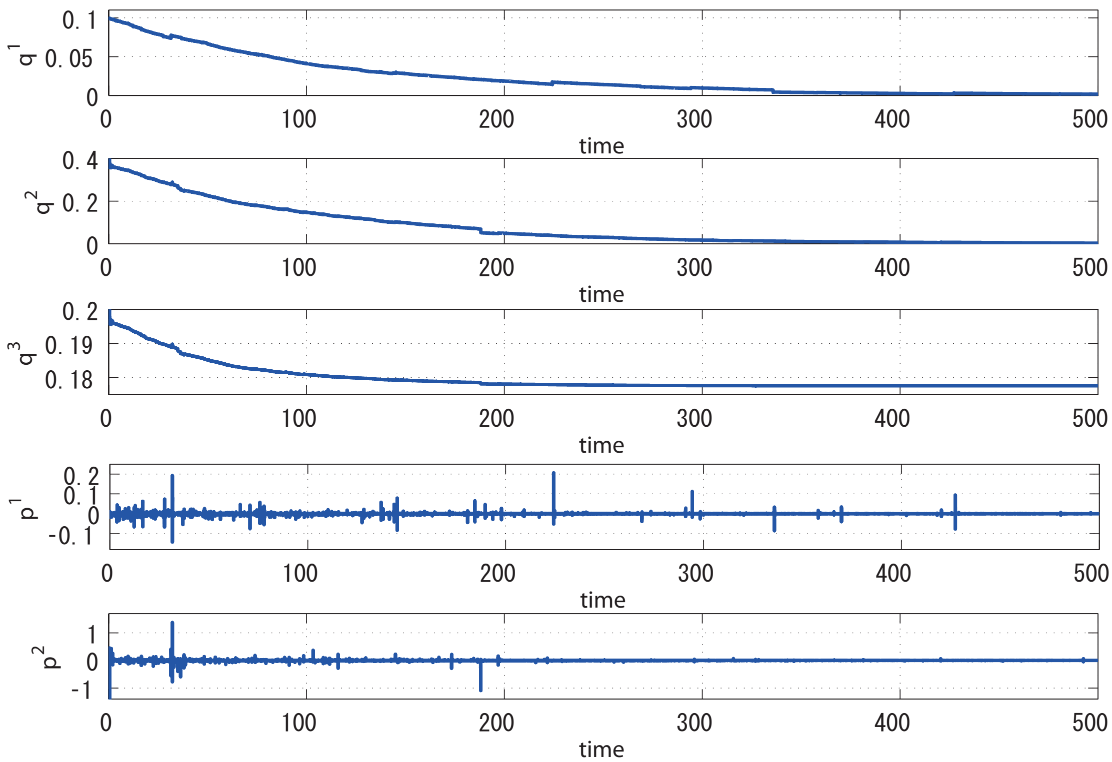

Figure 4.7: Responses of q and p in the stochastic case

4.2 Extension to time-varying stochastic port-Hamiltonian systems

In this section, let us consider a time-varying stochastic port-Hamiltonian system described by

$$\begin{cases} \mathrm{d}x = (J(x,t) - R(x,t)) \dfrac{\partial H(x,t)}{\partial x}^{\top} \mathrm{d}t + g(x,t)u\,\mathrm{d}t + h(x,t)\,\mathrm{d}w \\ y \ = g(x,t)^{\top} \dfrac{\partial H(x,t)}{\partial x}^{\top} \end{cases} \tag{4.44}$$

As in the time-invariant case in (4.2), $x(t) \in \mathbb{R}^n, u(t), y(t) \in \mathbb{R}^m$ describe the state, the input and the output, respectively. The structure matrix $J(x,t) \in \mathbb{R}^{n\times n}$ and the dissipation matrix $R(x,t) \in \mathbb{R}^{n\times n}$ are skew-symmetric and symmetric positive semi-definite for all x and t, respectively. $g(x,t) \in \mathbb{R}^{n\times m}$ represents the control port. Here $w(t) \in \mathbb{R}^r$ is a standard Wiener process defined on a probability space $(\Omega, \mathcal{F}, \mathcal{P})$. $h(x,t) \in \mathbb{R}^{n\times r}$ represents the noise port. We suppose that a Hamiltonian $H(x,t)$ is a sufficiently differentiable function and $h(0,t) = 0$. Moreover, $g(x,t)$ and $h(x,t)$ satisfy reasonable sufficient conditions for the local existence and uniqueness of the solutions.

Since the literature [16] deals with **stochastic passivity** for only time-invariant stochastic systems, let us extend this notion to time-varying systems in a manner analogous to the deterministic time-varying case in [67, 25].

Definition 4.11 A general time-varying stochastic system (C.1) (see Appendix C) is said to be **stochastic passive** if there exists a non-negative function $V(x,t) : \mathbb{R}^n \times \mathbb{R} \to \mathbb{R}$ such that $V(x,t) \geq V(0,t) = 0$ and it satisfies

$$\mathcal{L}V(x,t) \leq s(x,u,t)^{\top} u.$$

Here $\mathcal{L}(\cdot)$ represents the infinitesimal generator, which is a redefinition of that in (4.14) for time-varying functions.

$$\mathcal{L}(\cdot) := \frac{\partial(\cdot)}{\partial t} + \frac{\partial(\cdot)}{\partial x} f + \frac{1}{2}\mathrm{tr}\left\{ \frac{\partial}{\partial x}\left(\frac{\partial(\cdot)}{\partial x}\right)^{\top} hh^{\top} \right\}. \tag{4.45}$$

In what follows we utilize Eq. (4.45) for the infinitesimal generator, since it encompasses Eq. (4.14).

4.2.1 Some theorems on time-varying stochastic port-Hamiltonian systems

In this subsection, we extend some results proven in Section 4.1 to the time-varying case.

Firstly let us show the following lemma which characterizes time-varying coordinate transformations preserving the stochastic Hamiltonian structure of the form (4.44).

Lemma 4.8 *The time-varying stochastic port-Hamiltonian system* (4.44) *is transformed into another time-varying stochastic port-Hamiltonian system by the following time-varying coordinate transformation*

$$\begin{cases} \bar{x} \ = \ \Phi(x,t) \\ \bar{t} \ = \ t \end{cases} \tag{4.46}$$

if and only if there exists a skew-symmetric matrix $K(x,t)$ *and a symmetric matrix* $S(x,t)$ *such that* $R(x,t)+S(x,t)$ *is positive semi-definite and they satisfy*

$$\frac{1}{2}\mathrm{tr}\left\{\frac{\partial}{\partial x}\left(\frac{\partial \Phi^i(x,t)}{\partial x}\right)^{\top} h(x,t)h(x,t)^{\top}\right\}$$
$$=\frac{\partial \Phi^i(x,t)}{\partial x}(K(x,t)-S(x,t))\frac{\partial H(x,t)}{\partial x}^{\top}-\frac{\partial \Phi^i(x,t)}{\partial t},\quad (i=1,2,\cdots,n).$$

Proof It can be easily proven in a similar manner to Lemma 4.2. ■

Secondly, The following lemma characterizes stochastic passivity of time-varying stochastic port-Hamiltonian systems.

Lemma 4.9 *Consider the time-varying stochastic port-Hamiltonian system* (4.44). *Suppose that a Hamiltonian* $H(x,t)$ *is a non-negative function such that* $H(x,t)\geq H(0,t)=0$ *Then, the system is stochastic passive if and only if*

$$\frac{\partial H(x,t)}{\partial t}+\frac{1}{2}\mathrm{tr}\left\{\frac{\partial}{\partial x}\left(\frac{\partial H(x,t)}{\partial x}\right)^{\top} h(x,t)h(x,t)^{\top}\right\}\leq \frac{\partial H(x,t)}{\partial x}R(x,t)\frac{\partial H(x,t)}{\partial x}^{\top} \tag{4.47}$$

holds.

Proof It can be easily proven in a similar manner to Lemma 4.4. ■

Thirdly, we define the stochastic generalized canonical transformations for time-varying stochastic port-Hamiltonian systems. Then, we show the conditions which these transformations should satisfy.

Definition 4.12 A set of transformations

$$\begin{aligned}\bar{x}&=\Phi(x,t)\\ \bar{t}&=t\\ \bar{H}&=H(x,t)+U(x,t)\\ \bar{y}&=y+\alpha(x,t)\\ \bar{u}&=u+\beta(x,t)\end{aligned} \tag{4.48}$$

that changes the coordinate x to $\bar{x}$, a Hamiltonian H to $\bar{H}$, the output y to $\bar{y}$ and the input u to $\bar{u}$ is said to be a stochastic generalized canonical transformation for the stochastic port-Hamiltonian system (4.44) if it transforms the system into another one which is also described by (4.44) with another Hamiltonian. Here $\Phi:\mathbb{R}^n\times\mathbb{R}\to\mathbb{R}^n$ is an appropriate coordinate transformation, and $U:\mathbb{R}^n\times\mathbb{R}\to\mathbb{R}$, $\alpha:\mathbb{R}^n\times\mathbb{R}\to\mathbb{R}^m$ and $\beta:\mathbb{R}^n\times\mathbb{R}\to\mathbb{R}^m$ are appropriate functions, respectively.

Theorem 4.10 *Consider the time-varying stochastic port-Hamiltonian system* (4.44)*. A set of transformations, functions $\Phi(x,t)$, $U(x,t)$, $\alpha(x,t)$ and $\beta(x,t)$, yields a stochastic generalized canonical transformation defined by* (4.48) *if and only if there exists a skew-symmetric matrix $P(x,t)$, a symmetric matrix $Q(x,t)$ such that $R(x,t)+Q(x,t)$ is positive semi-definite, and functions $\Phi(x,t)$, $U(x,t)$ and $\beta(x,t)$ satisfy*

$$\frac{\partial \Phi^i}{\partial t}+\frac{1}{2}\mathrm{tr}\left\{\frac{\partial}{\partial x}\left(\frac{\partial \Phi^i}{\partial x}\right)^{\top} hh^{\top}\right\}=\frac{\partial \Phi^i}{\partial x}\left[(J-R)\frac{\partial U}{\partial x}^{\top}+g\beta+(P-Q)\frac{\partial (H+U)}{\partial x}^{\top}\right],$$
$$(i=1,2,\cdots,n). \qquad (4.49)$$

Further a function $\alpha(x,t)$ is given by

$$\alpha(x,t)=g(x,t)^{\top}\frac{\partial U(x,t)}{\partial x}^{\top}. \qquad (4.50)$$

Proof The proof is completed in a similar manner to that of Theorem 4.6. Firstly, the necessity of the theorem is shown. The dynamics of the system in the new coordinate $\bar{x}$ which is transformed by (4.46) is calculated as

$$\mathrm{d}\bar{x}^i=\left[\frac{\partial \Phi^i}{\partial t}+\frac{\partial \Phi^i}{\partial x}(J-R)\frac{\partial H}{\partial x}^{\top}+\frac{1}{2}\mathrm{tr}\left\{\frac{\partial}{\partial x}\left(\frac{\partial \Phi^i}{\partial x}\right)^{\top} hh^{\top}\right\}\right]\mathrm{d}t+\frac{\partial \Phi^i}{\partial x}gu\,\mathrm{d}t+\frac{\partial \Phi^i}{\partial x}h\,\mathrm{d}w. \qquad (4.51)$$

Suppose that the time-varying stochastic port-Hamiltonian system (4.44) is transformed into another one using a stochastic generalized canonical transformation with Φ, U and β. Then, the following equation holds for all u and w

R.H.S. of Eq. (4.51)

$$\equiv\left[(\bar{J}-\bar{R})\frac{\partial \bar{H}(\Phi^{-1}(\bar{x},\bar{t}),\bar{t})}{\partial \bar{x}}^{\top}\right]^i \mathrm{d}\bar{t}+\left[\bar{g}\bar{u}\right]^i\mathrm{d}\bar{t}+\left[\bar{h}\,\mathrm{d}w\right]^i$$
$$=\frac{\partial \Phi^i}{\partial x}\left[\frac{\partial \Phi}{\partial x}\right]^{-1}(\bar{J}-\bar{R})\left[\frac{\partial \Phi}{\partial x}\right]^{-\top}\frac{\partial (H(x,t)+U(x,t))}{\partial x}^{\top}\mathrm{d}t+\left[\bar{g}(u+\beta)\right]^i\mathrm{d}t+\left[\bar{h}\,\mathrm{d}w\right]^i. \qquad (4.52)$$

Equation (4.52) and that $\bar{t}$ is identical to t due to Eq. (4.46) imply that

$$\frac{\partial \Phi}{\partial x}g\equiv\bar{g}, \qquad \frac{\partial \Phi}{\partial x}h\equiv\bar{h}. \qquad (4.53)$$

Using Eqs. (4.51), (4.52) and (4.53), we have

$$\frac{\partial \Phi^i}{\partial t}+\frac{1}{2}\mathrm{tr}\left\{\frac{\partial}{\partial x}\left(\frac{\partial \Phi^i}{\partial x}\right)^{\top} hh^{\top}\right\}=$$
$$\frac{\partial \Phi^i}{\partial x}\left[\left[\frac{\partial \Phi}{\partial x}\right]^{-1}(\bar{J}-\bar{R})\left[\frac{\partial \Phi}{\partial x}\right]^{-\top}\frac{\partial (H+U)}{\partial x}^{\top}-(J-R)\frac{\partial H}{\partial x}^{\top}+g\beta\right]. \qquad (4.54)$$

Here we define the matrices $P(x,t)$ and $Q(x,t)$ as

$$P(x,t) := \left[\frac{\partial \Phi}{\partial x}\right]^{-1} \bar{J}(\Phi(x,t),t) \left[\frac{\partial \Phi}{\partial x}\right]^{-\top} - J(x,t),$$
$$Q(x,t) := \left[\frac{\partial \Phi}{\partial x}\right]^{-1} \bar{R}(\Phi(x,t),t) \left[\frac{\partial \Phi}{\partial x}\right]^{-\top} - R(x,t). \tag{4.55}$$

Then, $P(x,t)$ is skew-symmetric since $J(x,t)$ and $\bar{J}(\Phi(x,t),t)$ are so and, for $R(x,t)$ is symmetric and $\bar{R}(\Phi(x,t),t)$ is symmetric positive semi-definite, $Q(x,t)$ is symmetric and $R(x,t) + Q(x,t)$ is symmetric positive semi-definite. By substituting Eq. (4.55) for Eq. (4.54), Equation (4.49) is obtained immediately.

The change of the output $\alpha(x,t)$ which yields a stochastic generalized canonical transformation (4.48) can be calculated as

$$\begin{aligned}
\alpha &= \bar{y} - y \\
&= \bar{g}^\top \frac{\partial \bar{H}(\Phi^{-1}(\bar{x},\bar{t}),\bar{t})}{\partial \bar{x}}^\top - g^\top \frac{\partial H(x,t)}{\partial x}^\top \\
&= g^\top \frac{\partial \Phi(x,t)}{\partial x}^\top \left[\frac{\partial \Phi(x,t)}{\partial x}\right]^{-\top} \frac{\partial (H(x,t)+U(x,t))}{\partial x}^\top - g^\top \frac{\partial H(x,t)}{\partial x}^\top \\
&= g^\top \frac{\partial U(x,t)}{\partial x}^\top .
\end{aligned}$$

This proves the necessity of the theorem.

Secondly, the sufficiency of the theorem is shown. Now suppose that the assumption of the theorem holds. Then, by substituting Eq. (4.49) for (4.51), the dynamics of the system can be calculated in the new coordinate as

$$\begin{aligned}
\mathrm{d}\bar{x}^i &= \left[\frac{\partial \Phi^i}{\partial x}(J-R)\frac{\partial H}{\partial x}^\top + \frac{\partial \Phi^i}{\partial x}\left[(J-R)\frac{\partial U}{\partial x}^\top + g\beta + (P-Q)\frac{\partial (H+U)}{\partial x}^\top\right]\right]\mathrm{d}t \\
&\quad + \frac{\partial \Phi^i}{\partial x} g u \,\mathrm{d}t + \frac{\partial \Phi^i}{\partial x} h \,\mathrm{d}w \\
&= \left[\frac{\partial \Phi}{\partial x}\Big((J+P) - (R+Q)\Big)\frac{\partial \Phi}{\partial x}^\top \frac{\partial (H(\Phi^{-1}(\bar{x},\bar{t}),\bar{t}) + U(\Phi^{-1}(\bar{x},\bar{t}),\bar{t}))}{\partial \bar{x}}^\top\right]^i \mathrm{d}\bar{t} \\
&\quad + \frac{\partial \Phi^i}{\partial x} g(u+\beta)\,\mathrm{d}\bar{t} + \frac{\partial \Phi^i}{\partial x} h \,\mathrm{d}w.
\end{aligned} \tag{4.56}$$

$\bar{J}$, $\bar{R}$, $\bar{g}$ and $\bar{h}$ are given by

$$\bar{J}(\bar{x},\bar{t}) = \frac{\partial\Phi(x,t)}{\partial x}(J(x,t)+P(x,t))\frac{\partial\Phi(x,t)}{\partial x}^\top\Bigg|_{\substack{x=\Phi^{-1}(\bar{x},\bar{t})\\ t=\bar{t}}}$$

$$\bar{R}(\bar{x},\bar{t}) = \frac{\partial\Phi(x,t)}{\partial x}(R(x,t)+Q(x,t))\frac{\partial\Phi(x,t)}{\partial x}^\top\Bigg|_{\substack{x=\Phi^{-1}(\bar{x},\bar{t})\\ t=\bar{t}}}$$

$$\bar{g}(\bar{x},\bar{t}) = \frac{\partial\Phi(x,t)}{\partial x}g(x,t)\Bigg|_{\substack{x=\Phi^{-1}(\bar{x},\bar{t})\\ t=\bar{t}}}$$

$$\bar{h}(\bar{x},\bar{t}) = \frac{\partial\Phi(x,t)}{\partial x}h(x,t)\Bigg|_{\substack{x=\Phi^{-1}(\bar{x},\bar{t})\\ t=\bar{t}}} . \tag{4.57}$$

Then, $\bar{J}(\bar{x},\bar{t})$ is skew-symmetric since $J(\Phi^{-1}(\bar{x},\bar{t}),\bar{t})$ and $P(\Phi^{-1}(\bar{x},\bar{t}),\bar{t})$ are so, and $\bar{R}(\bar{x},\bar{t})$ is symmetric positive semi-definite because of the assumption that $R(\Phi^{-1}(\bar{x},\bar{t}),\bar{t})+Q(\Phi^{-1}(\bar{x},\bar{t}),\bar{t})$ is so. Consequently, the dynamics of the system in the new coordinate $\bar{x}$ is given by

$$\mathrm{d}\bar{x}^i = \left[\left(\bar{J}(\bar{x},\bar{t}) - \bar{R}(\bar{x},\bar{t})\right)\frac{\partial\bar{H}(\Phi^{-1}(\bar{x},\bar{t}),\bar{t})}{\partial\bar{x}}^\top\right]^i \mathrm{d}\bar{t} + \left[\bar{g}(u+\beta)\right]^i \mathrm{d}\bar{t} + \left[\bar{h}\,\mathrm{d}w\right]^i. \tag{4.58}$$

The output in the new coordinate $\bar{y}$ is obtained by Eq. (4.50) as

$$\begin{aligned}\bar{y} &= y + \alpha(x,t)\\ &= g^\top\frac{\partial H(x,t)}{\partial x}^\top + g^\top\frac{\partial U(x,t)}{\partial x}^\top\\ &= g^\top\frac{\partial\Phi}{\partial x}^\top\left[\frac{\partial\Phi}{\partial x}\right]^{-\top}\frac{\partial(H+U)}{\partial x}^\top\\ &= \bar{g}^\top\frac{\partial\bar{H}(\Phi^{-1}(\bar{x},\bar{t}),\bar{t})}{\partial\bar{x}}^\top .\end{aligned} \tag{4.59}$$

Equations (4.58) and (4.59) imply the sufficiency of the theorem. ■

Finally, the following theorem states a condition where a transformed stochastic port-Hamiltonian system by a stochastic generalized canonical transformation becomes stochastic passive and, furthermore, the output convergence based on stochastic passivity.

Theorem 4.11 *Consider the time-varying stochastic port-Hamiltonian system* (4.44) *and transform it by an appropriate stochastic generalized canonical transformation such that* $\bar{H}(\bar{x},\bar{t}) :=$

$H(\Phi^{-1}(\bar{x},\bar{t}),\bar{t}) + U(\Phi^{-1}(\bar{x},\bar{t}),\bar{t}) \geq \bar{H}(0,\bar{t}) = 0$. *Then, the transformed system becomes stochastic passive with new Hamiltonian* $\bar{H}(\bar{x},\bar{t})$ *as a storage function if and only if*

$$-\frac{\partial(H+U)}{\partial x}\left[\frac{\partial\Phi}{\partial x}\right]^{-1}\frac{\partial\Phi}{\partial t}+\frac{\partial(H+U)}{\partial t}+\frac{1}{2}\mathrm{tr}\left\{\frac{\partial}{\partial x}\left(\frac{\partial(H+U)}{\partial x}\left[\frac{\partial\Phi}{\partial x}\right]^{-1}\right)^{\top}h(x)h(x)^{\top}\frac{\partial\Phi}{\partial x}^{\top}\right\}$$
$$\leq \frac{\partial(H+U)}{\partial x}(R+Q)\frac{\partial(H+U)}{\partial x}^{\top} \tag{4.60}$$

holds.

Furthermore, suppose that

$$\lim_{\|\bar{x}\|\to\infty}\inf_{0\leq\bar{t}<\infty}\bar{H}(\bar{x},\bar{t})=\infty$$

and if one of the following conditions holds:

(i) for each initial state $\bar{x}_0\in\mathbb{R}^n$ *there is a* $d>2$ *such that*

$$\sup_{0\leq\bar{t}<\infty}E[\|\bar{x}(\bar{t})\|^d]<\infty. \tag{4.61}$$

(ii) $\bar{h}(\bar{x},\bar{t})$ *is bounded.*

(iii) Almost every sample path of

$$\int_0^{\bar{t}}\bar{h}(\bar{x}(\tau),\tau)\,\mathrm{d}w(\tau)$$

is uniformly continuous on $\bar{t}\geq 0$.

Then under the unity feedback $\bar{u}=-\bar{y}$, *for every initial state* $\bar{x}_0\in\mathbb{R}^n$, $\lim_{\bar{t}\to\infty}\bar{H}(\bar{x},\bar{t})$ *exists and is finite almost surely and, moreover,*

$$\lim_{\bar{t}\to\infty}\bar{y}(\bar{t})=0$$

holds almost surely.

Proof Firstly, the former part of the theorem is shown. Due to Lemma 4.9, the necessary and sufficient condition is that the following inequality holds in the new coordinate transformed by the stochastic generalized canonical transformation

$$\frac{\partial\bar{H}(\Phi^{-1}(\bar{x},\bar{t}),\bar{t})}{\partial\bar{t}}+\frac{1}{2}\,\mathrm{tr}\left\{\frac{\partial}{\partial\bar{x}}\left(\frac{\partial\bar{H}(\Phi^{-1}(\bar{x},\bar{t}),\bar{t})}{\partial\bar{x}}\right)^{\top}\bar{h}\bar{h}^{\top}\right\}\leq\frac{\partial\bar{H}}{\partial\bar{x}}\bar{R}\frac{\partial\bar{H}}{\partial\bar{x}}^{\top}. \tag{4.62}$$

The first term in the left hand side of (4.62) is calculated as

$$\frac{\partial\bar{H}(\Phi^{-1}(\bar{x},\bar{t}),\bar{t})}{\partial\bar{t}}=\frac{\partial(H+U)}{\partial x}\frac{\partial\Phi^{-1}(\bar{x},\bar{t})}{\partial\bar{t}}+\frac{\partial(H+U)}{\partial t}. \tag{4.63}$$

Since the Jacobian of the coordinate transformation (4.46) is given by

$$\mathcal{J} = \begin{pmatrix} \dfrac{\partial \Phi(x,t)}{\partial x} & \dfrac{\partial \Phi(x,t)}{\partial t} \\ O_{1n} & 1 \end{pmatrix},$$

the Jacobian of the inverse coordinate transformation which coincides with $\mathcal{J}^{-1}$ is obtained as

$$\begin{aligned} \mathcal{J}^{-1} &= \begin{pmatrix} \left[\dfrac{\partial \Phi(x,t)}{\partial x}\right]^{-1} & -\left[\dfrac{\partial \Phi(x,t)}{\partial x}\right]^{-1} \dfrac{\partial \Phi(x,t)}{\partial t} \\ O_{1n} & 1 \end{pmatrix} \\ &\equiv \begin{pmatrix} \dfrac{\partial \Phi^{-1}(\bar{x},\bar{t})}{\partial \bar{x}} & \dfrac{\partial \Phi^{-1}(\bar{x},\bar{t})}{\partial \bar{t}} \\ O_{1n} & 1 \end{pmatrix}. \end{aligned} \tag{4.64}$$

It follows from Eq. (4.64) that

$$\frac{\partial \Phi^{-1}(\bar{x},\bar{t})}{\partial \bar{t}} = -\left[\frac{\partial \Phi(x,t)}{\partial x}\right]^{-1} \frac{\partial \Phi(x,t)}{\partial t}. \tag{4.65}$$

Let us substitute Eq. (4.65) for Eq. (4.63), and then Eqs. (4.32), (4.57), (4.62) and (4.63) imply that Eq. (4.60) holds immediately.

Secondly, the latter part of the theorem is shown. Since the transformed system is stochastic passive, the following inequality holds for the closed loop system with the unity feedback $\bar{u} = -\bar{y}$

$$\mathcal{L}\bar{H}(\bar{x},\bar{t}) \leq -\|\bar{y}\|^2 \leq 0.$$

Then the rest of the theorem is shown by directly applying Theorem C.2 and Remark C.1 in Appendix C.2. ■

4.2.2 Numerical example

In this subsection, we again consider the rolling coin on a horizontal plane depicted in Fig. 4.1 in the presence of noise as in subsection 4.1.2. In subsection 4.1.2, we designed a continuous static controller which stabilizes an invariant set in probability in the presence of noise. On the other hand, the literature [25] has proposed time-varying asymptotically stabilizing controllers for deterministic nonholonomic Hamiltonian systems. In this method, a special class of time-varying generalized canonical transformations is introduced in which a time-varying potential function $U(x,t)$ is parameterized by an arbitrary periodic function $\alpha(q,t)$ which is the parameter of the change of the output. The purpose of this subsection is to design a time-varying feedback controller which renders the origin asymptotically stable in probability based on the framework in [25].

Firstly, we consider the following form of the new Hamiltonian

$$\begin{aligned}\bar{H} &= H + p^\top \alpha + \frac{1}{2}\alpha^\top \alpha + V(\bar{q}) \\ &= \frac{1}{2}(p+\alpha)^\top (p+\alpha) + V(\bar{q}),\end{aligned}$$

where $\alpha(q,t)$ is any periodic odd function and an appropriate function $V(\bar{q})$ should be chosen so that $\bar{H}$ is non-negative in the new coordinate. Here we utilize the following functions which are the same as those in [25]

$$\alpha(q,t) = \begin{pmatrix} q^3 \sin t \\ 0 \end{pmatrix} \tag{4.66}$$

$$V(\bar{q}) = \frac{1}{2}\bar{q}^\top K \bar{q}, \tag{4.67}$$

where K is defined as $K := \mathrm{diag}\{k^1, k^2, k^3\}$ with appropriate positive numbers k^1, k^2 and k^3. Then let us construct the time-varying stochastic generalized canonical transformation with the following coordinate transformation utilized in [25]

$$\begin{aligned}\bar{q} &= \begin{pmatrix} q^1 - q^3 \cos t \\ q^2 \\ q^3 \end{pmatrix} \\ \bar{p} &= \begin{pmatrix} p^1 + q^3 \sin t \\ p^2 \end{pmatrix}.\end{aligned} \tag{4.68}$$

In order to obtain a time-varying stochastic generalized canonical transformation, let us decide the rest design parameters $\beta(x,t)$, $P(x,t)$ and $Q(x,t)$ by utilizing Theorem4.10. The following choice satisfies Eq. (4.49)

$$\begin{aligned}P(x,t) &= O_{55} \\ Q(x,t) &= \left(\begin{array}{c|cc} O_{33} & \multicolumn{2}{c}{O_{32}} \\ \hline O_{23} & Q_{44}(x,t) & 0 \\ & 0 & Q_{55}(x,t) \end{array}\right)\end{aligned} \tag{4.69}$$

$$\beta(x,t) = \begin{pmatrix} q^3 \cos t + k^1(q^1 - q^3\cos t) + p^2 \sin t \sin q^1 + (p^1 + q^3 \sin t) Q_{44}(x,t) \\ -k^1(q^1 - q^3 \cos t)\sin q^1 \cos t + k^2 q^2 \cos q^1 + k^3 q^3 \sin q^1 + p^2 Q_{55}(x,t) \end{pmatrix}, \tag{4.70}$$

where free parameters $Q_{44}(x,t)$ and $Q_{55}(x,t)$ should be chosen so that $Q(x,t)$ in Eq. (4.69) becomes symmetric positive semi-definite. Furthermore in order to obtain stochastic passivity, let us derive another condition for $Q_{44}(x,t)$ and $Q_{55}(x,t)$ from Theorem 4.11. It follows from the inequality (4.60) that

$$(p^1 + q^3 \sin t)^2 Q_{44}(x,t) + (p^2)^2 Q_{55}(x,t) \geq \frac{h^1(x,t)^2 + h^2(x,t)^2}{2}. \tag{4.71}$$

In what follows, we suppose that there exist functions $Q_{44}(x,t)$ and $Q_{55}(x,t)$ such that the equality in the condition (4.71) holds and $Q(x,t)$ in Eq. (4.69) becomes symmetric positive semi-definite.

The transformed system is given by

$$\begin{aligned}
\bar{J}(\bar{x},\bar{t}) &= \left.\begin{pmatrix} 0 & 0 & 0 & 1 & -\sin q^1 \cos t \\ 0 & 0 & 0 & 0 & \cos q^1 \\ 0 & 0 & 0 & 0 & \sin q^1 \\ -1 & 0 & 0 & 0 & \sin q^1 \sin t \\ \sin q^1 \cos t & -\cos q^1 & -\sin q^1 & -\sin q^1 \sin t & 0 \end{pmatrix}\right|_{\substack{x=\Phi^{-1}(\bar{x},\bar{t}) \\ t=\bar{t}}} \\
\bar{R}(\bar{x},\bar{t}) &= Q(x,t)\Big|_{\substack{x=\Phi^{-1}(\bar{x},\bar{t}) \\ t=\bar{t}}} \\
\bar{g}(\bar{x}) &= \begin{pmatrix} O_{32} \\ I_2 \end{pmatrix} \\
\bar{h}(\bar{x}) &= \left.\begin{pmatrix} O_{32} \\ \mathrm{diag}\{h^1(x,t), h^2(x,t)\} \end{pmatrix}\right|_{\substack{x=\Phi^{-1}(\bar{x},\bar{t}) \\ t=\bar{t}}} \\
\bar{y} &= \bar{p}.
\end{aligned} \tag{4.72}$$

Equation (4.72) implies that the transformed system has the form of (4.44). Since this system obtains stochastic passivity, it can be easily proven by Theorem 4.11 that

$$\lim_{\bar{t}\to\infty} \bar{y} = 0$$

almost surely with the unity feedback $\bar{u} = -\bar{y}$. Generally Theorem 4.11 only guarantees that the convergence of the output. However, in this case, we can show that the unity feedback also renders the origin of the system (4.34) asymptotically stable almost surely. Let $\bar{u} = \bar{y} = \bar{p} \equiv 0$ of the system (4.72). Then it follows from Eq. (4.68) and the condition (4.71) that $h(x,t) \equiv 0$. The literature [25] has proven that the transposed system (4.72) has the zero-state observability with respect to x without noise. These two facts prove the claim. Eventually, we obtain the following time-varying feedback controller which renders the origin asymptotically stable in probability as

$$u = -\beta(x,t) - (y + \alpha(x,t)) \tag{4.73}$$

(see, Eqs.(4.66) and (4.70) for $\alpha(x,t)$ and $\beta(x,t)$).

Finally, let us show some simulation results. Here we consider the noise port as $h^1(x,t) = 0$ and $h^2(x,t) = k^2 p^2$ and we set a matrix K in (4.67) as $K = \mathrm{diag}\{1,1,1\}$, design parameters as $Q_{44} = 0$ and $Q_{55} = k_2^2/2$ with $k^2 = 8$ and the initial condition as

$$(q^1, q^2, q^3, p^1, p^2) = (0, 0, 1.0, 0, 0).$$

We simulate a standard Wiener process in the same manner as in [57].

Firstly, we consider a scenario where noise does not exist, that is, $h(x,t) \equiv 0$ and a feedback controller designed by a deterministic method in [25], which corresponds to the case where

$Q(x,t) = 0$, is applied. Figure 4.8 shows the motion of the coin in X-Y plane and Fig. 4.9 shows time responses of q and p. They imply that the controller designed for the deterministic system works well without noise. Here let us note that the convergence is slow and oscillatory in the case of equipping time-varying feedback controllers [63, 25].

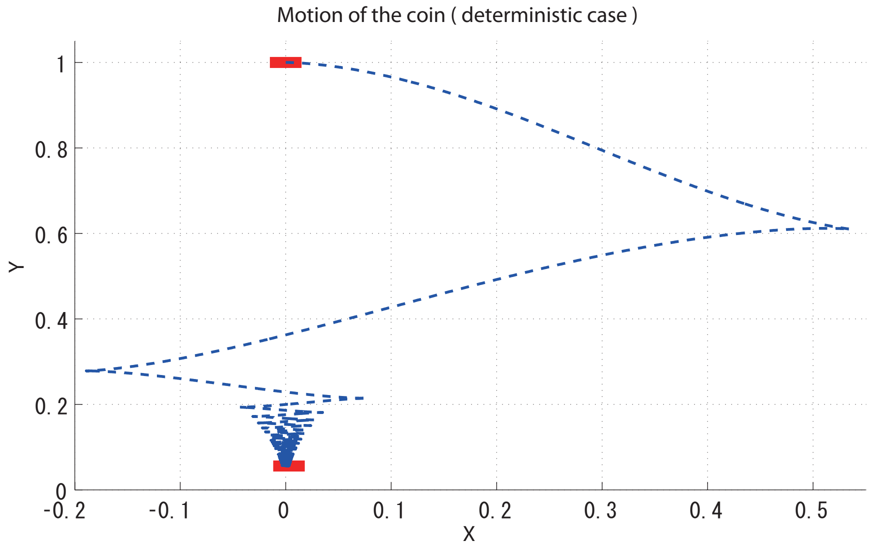

Figure 4.8: Motion of the coin in the deterministic case

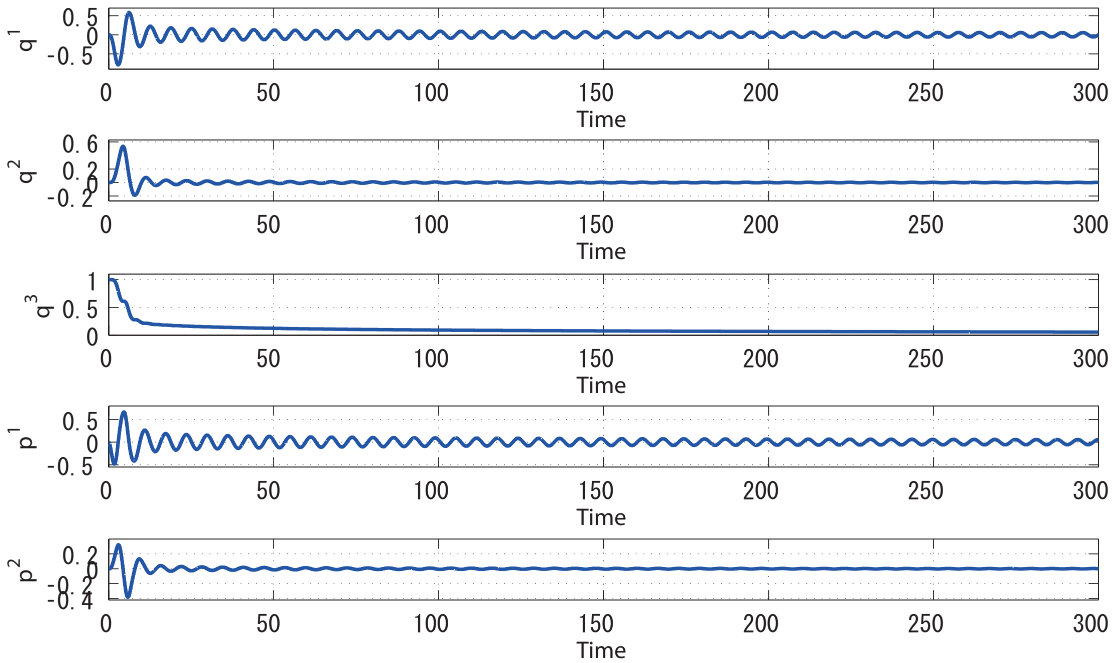

Figure 4.9: Responses of q and p in the deterministic case

However, secondly, we consider a scenario where there exists noise and the same feedback controller as in the previous scenario is applied. Figure 4.10 shows the motion of the coin in

X-Y plane and Fig. 4.11 shows time responses of q and p. They imply that the behavior of the system seems unstable with the controller for the deterministic system in the presence of noise.

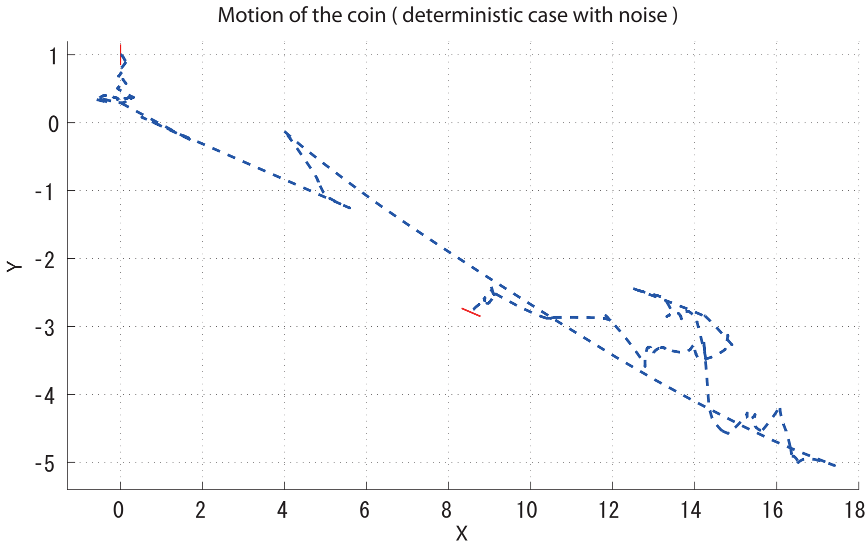

Figure 4.10: Motion of the coin in the deterministic case with noise

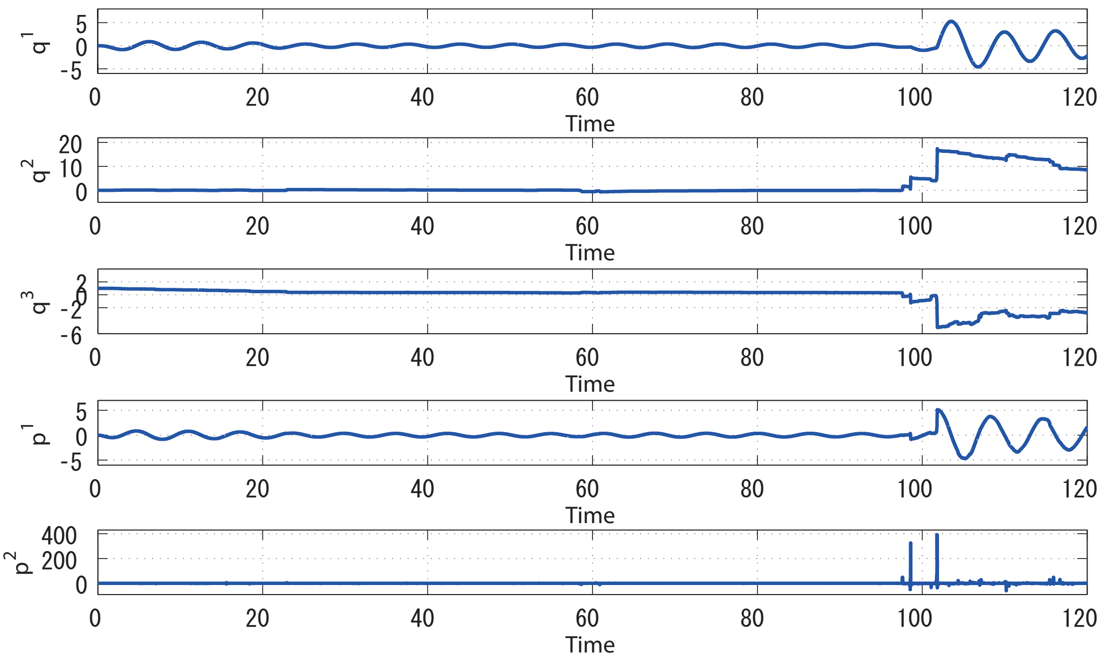

Figure 4.11: Responses of q and p in the deterministic case with noise

Finally, we consider a scenario where there exists the same noise as in the previous scenario and the feedback controller (4.73) designed by the proposed method is applied. Figure 4.12 shows the motion of the coin in X-Y plane and Fig. 4.13 shows time responses of q and p.

They imply that the proposed controller works well even in the presence of noise, although the convergence is slower and more oscillatory than the case without noise.

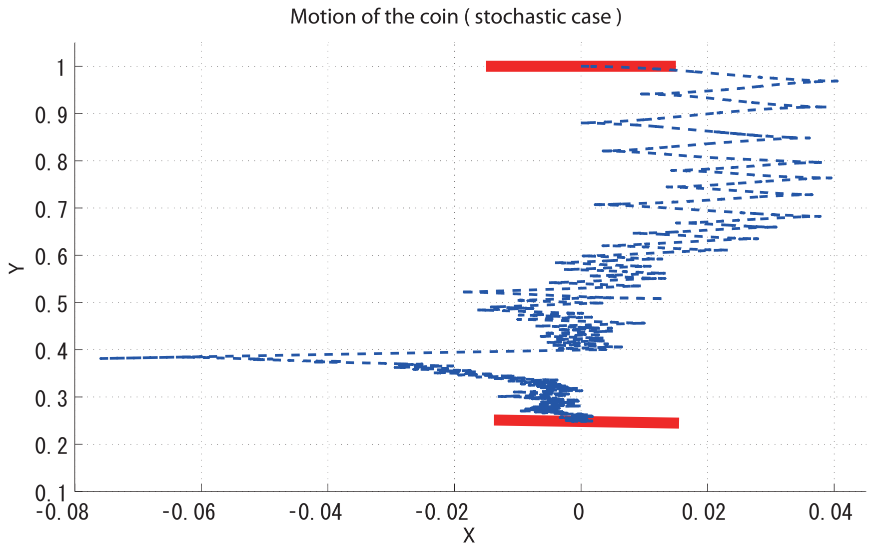

Figure 4.12: Motion of the coin in the stochastic case

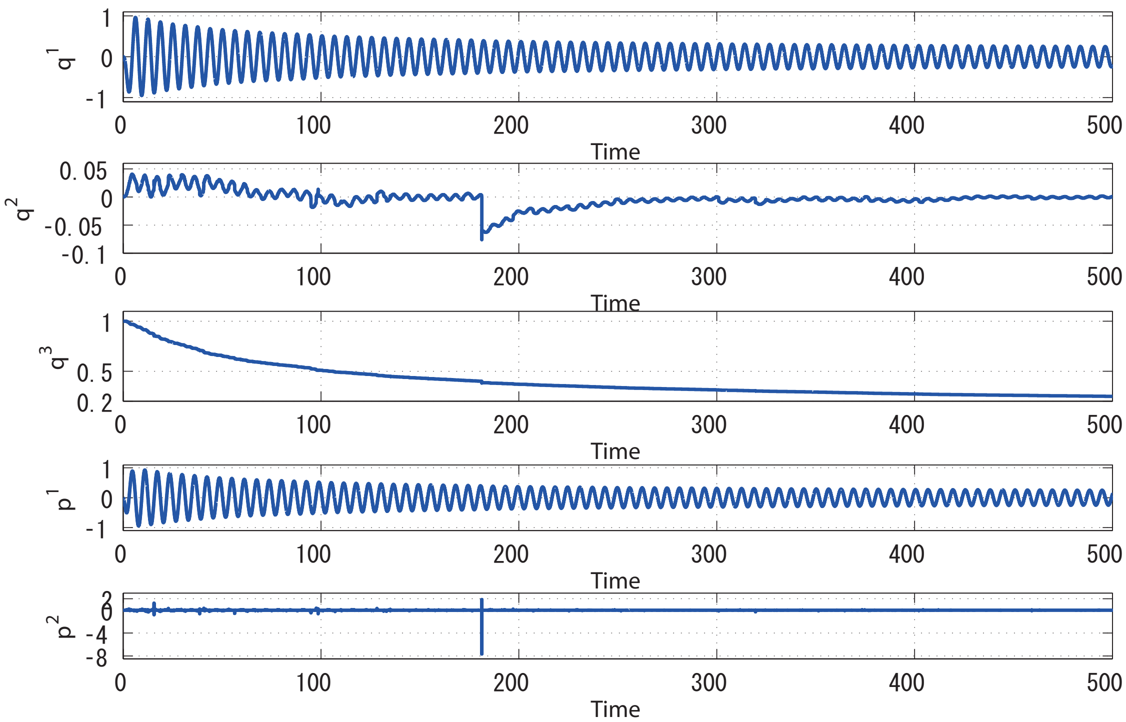

Figure 4.13: Responses of q and p in the stochastic case

These simulation results demonstrate the effectiveness of the proposed framework.

4.3 Summary

This chapter has introduced stochastic port-Hamiltonian systems and has clarified some of their properties. We concentrated on the time-invariant case and then extended some results to the time-varying case. Firstly, we have shown a necessary and sufficient condition to preserve the stochastic Hamiltonian structure of the original system under coordinate transformations. Secondly, we have derived a condition to maintain stochastic passivity of the system. Thirdly, we have introduced stochastic generalized canonical transformations. Fourthly, we have provided a condition that the transformed system by this transformation becomes stochastic passive and have proposed a stabilization method based on passivity and stochastic generalized canonical transformations. Finally, numerical simulations demonstrate the effectiveness of the proposed method.

Chapter 5

Observer based stochastic trajectory tracking control of mechanical systems

The previous chapter has introduced stochastic port-Hamiltonian systems and has proposed a stabilization framework of those systems based on stochastic passivity (see also [68, 70, 69]). Then stochastic trajectory tracking control was considered in the authors' previous work in [70] as an application of time-varying stabilization method. In [70] bounded stability is achieved, where it is guaranteed that the norm of tracking error becomes arbitrarily small in probability. However, this method can only be applied to the mechanical systems with constant inertia matrices in the presence of noise for the following reason. Since the time derivative of an energy-based Lyapunov function, which is used in the passivity-based control, e.g. Hamiltonian function, depends only on a part of the state of the plant, boundedness of the state can not be guaranteed in the presence of noise which does not vanish at the origin. To solve this problem, we tried to find a Lyapunov function whose time derivative is negative definite, but it was difficult to construct it for general mechanical systems with noise. Regarding the difficulty, one of the purposes of this chapter is to propose a new stochastic trajectory tracking control method for general mechanical systems.

Another motivation is that the proposed controllers in the previous chapter (see also [68, 70, 69]) are state feedback ones, so full state information is necessary to implement them. However, in practice, there are a lot of mechanical systems whose position measurements are only available because of the lack of velocity sensors. On output feedback control of deterministic systems, various methods are proposed, e.g. [85, 83, 58, 65]. Observer based control methods are also studied by many researchers in, e.g. [56, 5, 4], where the velocity signal is reconstructed by an observer and is utilized for the state feedback controller instead of the true signal. On the other hand, in stochastic control research area, there are few methods to deal with such problems. A stochastic output feedback stabilization controller based on the backstepping technique is proposed in [14]. However, stochastic trajectory tracking framework by only using position measurements is not considered so far.

This chapter proposes an observer based stochastic trajectory tracking control framework. Here we assume that only position measurements are available. Velocity information is reconstructed by the position information. We consider general mechanical systems in the presence of noise as stochastic systems and derive conditions for stabilizing and tracking controllers based on [81, 61, 5, 4] to achieve each control objective. Controllers and observers proposed in [81, 5, 4] utilize the sliding mode control theory. By taking advantage of those results, we overcome the drawback of our previous result [70] and the proposed method gives conditions for controller and observer gains under which the norm of the set of tracking and estimation errors remains arbitrarily small in probability.

5.1 Mechanical systems in the presence of noise

We consider a mechanical systems in the presence of noise as the following stochastic dynamical system described by a stochastic differential equation written in the sense of Itô

$$\begin{cases} \mathrm{d}q = v\,\mathrm{d}t + W_q(q,v)\,\mathrm{d}w_1 \\ \mathrm{d}v = M(q)^{-1}\{\tau - C(q,v)v - G(q)\}\,\mathrm{d}t + W_v(q,v)\,\mathrm{d}w_2 \end{cases}. \tag{5.1}$$

Here $q(t), v(t) \in \mathbb{R}^n$ describe the configuration coordinate and the generalized velocity, respectively. The symmetric positive definite matrix $M(q) \in \mathbb{R}^{n\times n}$ represents the inertia matrix, $C(q,v)v \in \mathbb{R}^n$ represents the Coriolis and centrifugal torques, $G(q) \in \mathbb{R}^n$ denotes the gravitational torques and $\tau \in \mathbb{R}^n$ represents the control input. $w_1(t) \in \mathbb{R}^{r_1}$ and $w_2(t) \in \mathbb{R}^{r_2}$ are standard Wiener processes defined on a probability space $(\Omega, \mathcal{F}, \mathcal{P})$. $\mathcal{F}_s$ represents the sigma algebra generated by $\{(q(s), v(s)) \mid 0 \le s \le t\}$. $W_q : \mathbb{R}^n \times \mathbb{R}^n \to \mathbb{R}^{n\times r_1}$ and $W_v : \mathbb{R}^n \times \mathbb{R}^n \to \mathbb{R}^{n\times r_2}$ represent noise ports, respectively. We sometimes treat $M(q)$ as the inertia matrix and other times, as the inertia tensor. For example, for $\alpha, \beta \in \mathbb{R}^n$, $M(q)(\alpha,\beta) := [M(q)]_{ij}\alpha^i\beta^j \equiv \alpha^\top M(q)\beta$. Here $[M(q)]_{ij}$, α^i and β^j are the components of the tensor $M(q)$ and the vectors α and β, respectively and we use the Einstein summation convention. Tensor notation is a convenient way to describe derivatives. For example, $\mathcal{D}_q M(q)(\alpha,\beta)(\cdot)$ is a first order tensor and is defined as

$$[\mathcal{D}_q M(q)(\alpha,\beta)]_k = \frac{\partial [M(q)]_{ij}}{\partial q^k}\alpha^i\beta^j.$$

For a second order tensor $A(\cdot,\cdot)$, we define the transposition $A^\top(\cdot,\cdot)$ as $[A^\top]_{ij} = [A]_{ji}$, that is, $A^\top(\alpha,\beta) = [A^\top]_{ij}\alpha^i\beta^j = [A]_{ji}\alpha^i\beta^j$. We define the norm of the matrix B as $\|B\| := \sqrt{\lambda_{\max}(B^\top B)}$, where $\lambda_{\max}(B)$ represents the maximum eigenvalue of the matrix B.

The matrix $C(q,v)$ has the following property [56, 5].

Remark 5.1 By defining $C(q,v)$ using the Christoffel symbols, $\mathcal{D}_t M(q) - 2C(q,v)$ is skew-symmetric. Moreover, for this choice $C(q,v)$ satisfies the following equations for any $\xi, \eta, \zeta \in \mathbb{R}^n, a, b \in \mathbb{R}$

$$C(q,\xi)\eta = C(q,\eta)\xi$$

$$C(q, a\zeta + b\xi)\eta = aC(q,\zeta)\eta + bC(q,\xi)\eta.$$

We assume the following.

Assumption 5.2 W_q and W_v satisfy the local Lipschitz conditions and the linear growth conditions, i.e, for all α, β, there exist positive constants $W_{q,M}$ and $W_{v,M}$ such that

$$\|W_q(\alpha,\beta)\| \le W_{q,M}(1 + \|\alpha\| + \|\beta\|),$$
$$\|W_v(\alpha,\beta)\| \le W_{v,M}(1 + \|\alpha\| + \|\beta\|).$$

Assumption 5.3 The inertia tensor $M(q)$, its first and second order derivatives with respect to q, and the matrix $C(q,\cdot)$ are bounded with respect to q, respectively. For any $q, \xi, \eta \in \mathbb{R}^n$, there exist positive constants $M_m, M_M, \bar{M}_M, \bar{\bar{M}}_M$ and C_M satisfying

$$\begin{aligned} M_m \leq \|M(q)\| \leq M_M \\ \|\mathcal{D}_q M(q)(\xi,\cdot)(\cdot)\| \leq \bar{M}_M \|\xi\| \\ \|\mathcal{D}_q^2 M(q)(\xi,\eta)(\cdot)(\cdot)\| \leq \bar{\bar{M}}_M \|\xi\| \|\eta\| \\ \|C(q,\xi)\| \leq C_M \|\xi\|. \end{aligned}$$

5.2 Observer based trajectory tracking control

In this section, we consider observer based trajectory tracking control of mechanical systems in the presence of noise. In the sequel, q_d represents an at least twice differentiable desired trajectory and $\dot{q}_d, \ddot{q}_d$ are the time derivative and the twice time derivative of q_d, respectively. Position and velocity errors are denoted by $q_e := q - q_d$ and $v_e := v - \dot{q}_d$, respectively. $\hat{q}$ and $\hat{v}$ denote the estimated position and velocity, respectively, and $\tilde{q} := q - \hat{q}$ and $\tilde{v} := v - \hat{v}$ represent the estimation errors. We use the following notation $x_d := (q_d^\top, \dot{q}_d^\top)^\top, x_e := (q_e^\top, v_e^\top)^\top$, $\tilde{x} := (\tilde{q}^\top, \tilde{v}^\top)^\top$ and $x := (x_e^\top, \tilde{x}^\top)^\top$. We assume the following assumption with respect to the desired trajectory.

Assumption 5.4 The desired trajectory q_d is bounded by N_{q_d} and its velocity $\dot{q}_d$ is bounded by $N_{\dot{q}_d}$, i.e.,

$$\begin{aligned} N_{q_d} = \sup_t \|q_d(t)\| \\ N_{\dot{q}_d} = \sup_t \|\dot{q}_d(t)\|. \end{aligned}$$

Let us equip the notion of (Q_0, Q_1, ρ)-stability [48] in order to consider the stochastic bounded stability (refer to Definitions 4.1 and 4.2 for comparison).

Definition 5.5 [48] The systems is (Q_0, Q_1, ρ)-stable if for any initial condition $x(0) \in Q_0$, the probability with respect to the sample path $x(t)$ satisfies

$$\mathcal{P}\{x(t) \in Q_1, \quad \text{for } 0 \leq t < \infty\} \geq \rho.$$

The purpose of the section is to derive conditions for the controller and observer gains under which the tracking and estimation error x remains bounded in probability and the margin of error is assignable. The rest of this section, firstly, we define the controller and observer in Eqs. (5.2) and (5.3), and then we introduce a stochastic Lyapunov function [48] V in Eq. (5.6). Secondly, we calculate the variation of functions along a sample path with the infinitesimal operator $\mathcal{L}(\cdot)$ in (4.45) , since the time variation of the stochastic Lyapunov function plays a key role in investigating stability of stochastic systems as the case of deterministic systems. Then we evaluate a bound of the time variation of V by inequality (5.18). By utilizing the bound, finally, we prove that a stochastic bounded trajectory tracking control can be achieved if proposed conditions for the controller and observer gains hold.

We utilize the same controller and observer as proposed in [81, 61, 5, 4]. Before defining them, we equip the following notations

$$\begin{aligned} s_1 &:= v_e + \Lambda_1 q_e \\ s_2 &:= \tilde{v} + \Lambda_2 \tilde{q}, \\ v_o &:= v - s_2 = \hat{v} - \Lambda_2 \tilde{q}, \end{aligned}$$

where Λ_1 and Λ_2 represent positive diagonal matrices, respectively. The controller and observer proposed in [5, 4] are as follows:

$$\tau = M(q)\ddot{q}_d + C(q, v_o)\dot{q}_d + G(q) - K_d(s_1 - s_2), \tag{5.2}$$

$$\begin{cases} \mathrm{d}\hat{q} \; = \; (z + L_d\tilde{q})\,\mathrm{d}t =: \hat{v}\,\mathrm{d}t \\ \mathrm{d}z \; = \; L_p\tilde{q}\,\mathrm{d}t + M(q)^{-1}\{\tau - C(q, v_o)\dot{q}_d - G(q) + K_d(s_1 - s_2)\}\,\mathrm{d}t, \end{cases} \tag{5.3}$$

where L_d and L_p represent symmetric positive definite matrices, respectively. From Eqs. (5.1) and (5.2), the tracking error dynamics is given by

$$\begin{cases} \mathrm{d}q_e \; = \; v_e\,\mathrm{d}t + W_q(q, p)\,\mathrm{d}w_1 \\ \mathrm{d}v_e \; = \; M(q)^{-1}\{C(q, v_o)\dot{q}_d - C(q, v)v - K_d(s_1 - s_2)\}\,\mathrm{d}t + W_v(q, v)\,\mathrm{d}w_2 \end{cases}. \tag{5.4}$$

From Eqs. (5.1) and (5.3), the estimation error dynamics is also given by

$$\begin{cases} \mathrm{d}\tilde{q} \; = \; \tilde{v}\,\mathrm{d}t + W_q(q, p)\,\mathrm{d}w_1 \\ \mathrm{d}\tilde{v} \; = \; M(q)^{-1}\{C(q, v_o)\dot{q}_d - C(q, v)v - K_d(s_1 - s_2)\}\,\mathrm{d}t - (L_p\tilde{q} + L_d\tilde{v})\,\mathrm{d}t \\ \qquad\quad -L_dW_q(q, v)\,\mathrm{d}w_1 + W_v(q, v)\,\mathrm{d}w_2 \end{cases}. \tag{5.5}$$

We consider the following Lyapunov function proposed in [5, 4] as stochastic Lyapunov function

$$\begin{aligned} V &= \frac{1}{2}v_e^\top M(q)v_e + v_e^\top M(q)\Lambda_1 q_e + \frac{1}{2}q_e^\top 2\Lambda_1 K_d q_e + \frac{1}{2}s_2^\top M(q)s_2 + \frac{1}{2}\tilde{q}^\top 2\Lambda_2 K_d\tilde{q} \\ &= \frac{1}{2}x^\top \underbrace{\begin{bmatrix} 2\Lambda_1 K_d & \Lambda_1 M(q) & 0 & 0 \\ M(q)\Lambda_1 & M(q) & 0 & 0 \\ 0 & 0 & 2\Lambda_2 K_d + \Lambda_2 M(q)\Lambda_2 & \Lambda_2 M(q) \\ 0 & 0 & M(q)\Lambda_2 & M(q) \end{bmatrix}}_{=:\,P(q)} x, \end{aligned} \tag{5.6}$$

where a symmetric positive definite matrix K_d should be chosen so that the Schur complement is satisfied, i.e.,

$$2K_d - M(q)\Lambda_1 > 0. \tag{5.7}$$

In order to evaluate the time variation of the Lyapunov function (5.6) along the sample path x governed by Eqs. (5.4) and (5.5), let us calculate $\mathcal{L}V$ along x. From Eqs. (5.6) and (4.45), $\mathcal{L}V$ is calculated as

$$\begin{aligned}\mathcal{L}V = & s_1^\top\{C(q,v_o)\dot{q}_d - C(q,v)v - K_d(s_1-s_2)\} + v_e^\top M(q)\Lambda_1 v_e + \frac{1}{2}s_1^\top \mathcal{D}_t M(q)s_1 \\ & - \frac{1}{2}q_e^\top \Lambda_1 \mathcal{D}_t M(q)\Lambda_1 q_e + 2q_e^\top \Lambda_1 K_d v_e + s_2^\top\{C(q,v_o)\dot{q}_d - C(q,v)v - K_d(s_1-s_2) \\ & - M(q)(L_p\tilde{q} + L_d\tilde{v})\} + s_2^\top M(q)\Lambda_2\tilde{v} + \frac{1}{2}s_2^\top \mathcal{D}_t M(q)s_2 + 2\tilde{q}^\top\Lambda_2 K_d\tilde{v} + \omega_{x_e} + \omega_{\tilde{x}},\end{aligned} \tag{5.8}$$

where ω_{x_e} and $\omega_{\tilde{x}}$ are defined as follows:

$$\begin{aligned}\omega_{x_e} &:= \frac{1}{2}\,\mathrm{tr}\left\{\mathcal{D}^2_{q_e} V W_q W_q^\top\right\} + \frac{1}{2}\,\mathrm{tr}\left\{\mathcal{D}^2_{v_e} V W_v W_v^\top\right\}, \\ \omega_{\tilde{x}} &:= \frac{1}{2}\,\mathrm{tr}\left\{\mathcal{D}^2_{\tilde{q}} V W_q W_q^\top\right\} + \frac{1}{2}\,\mathrm{tr}\left\{\mathcal{D}^2_{\tilde{v}} V (L_d W_q W_q^\top L_d^\top + W_v W_v^\top)\right\}.\end{aligned} \tag{5.9}$$

For the simplicity of calculation, we utilize the same assumption as in [5, 4].

Assumption 5.6 L_d, L_p, Λ_1 and Λ_2 are constant diagonal matrices and L_d and L_p can be written as

$$\begin{aligned}L_d &= l_d I + \Lambda_2 \\ L_p &= l_d\Lambda_2,\end{aligned}$$

where a positive constant l_d represents an observer gain.

By utilizing Assumption 5.6 and Remark 5.1, we can reduce Eq. (5.8) to

$$\begin{aligned}\mathcal{L}V = & - v_e^\top(K_d - M(q)\Lambda_1)v_e - q_e^\top\Lambda_1 K_d\Lambda_1 q_e - \tilde{v}^\top K_d\tilde{v} - \tilde{q}^\top\Lambda_2 K_d\Lambda_2\tilde{q} \\ & - s_2^\top(l_d M(q) - 2K_d)s_2 - s_1^\top C(q,s_2)\dot{q}_d + v_e^\top C(q,v)\Lambda_1 q_e + s_2^\top C(q,s_2)v_e \\ & - s_2^\top C(q,v)v_e + \omega_{x_e} + \omega_{\tilde{x}}.\end{aligned} \tag{5.10}$$

Here observer gains K_d and l_d should be chosen so that

$$\begin{aligned}K_d - M(q)\Lambda_1 > 0, \\ l_d M(q) - 2K_d > 0.\end{aligned} \tag{5.11}$$

Let us note that the condition (5.7) holds under the condition (5.11). In what follows, for a matrix A, A_m and A_M denote lower and upper bounds of $\|A\|$, respectively. Then with Assumptions 5.3 and 5.4, an upper bound of Eq. (5.10) can be evaluated as

$$\begin{aligned}\mathcal{L}V \le & -\min\left\{K_{d,m} - M_M\Lambda_{1,M}, K_{d,m}\Lambda_{1,m}^2, K_{d,m}\Lambda_{2,m}^2\right\}\|x\|^2 \\ & + C_M N_{\dot{q}_d}\Big(\|s_1\|\|s_2\| + \Lambda_{1,M}\|v_e\|\|q_e\| + \|s_2\|\|v_e\|\Big) \\ & + C_M\Big(\Lambda_{1,M}\|v_e\|^2\|q_e\| + \|s_2\|^2\|v_e\| + \|s_2\|\|v_e\|^2\Big) + \|\omega_{x_e}\| + \|\omega_{\tilde{x}}\|.\end{aligned} \tag{5.12}$$

The arithmetic and geometric mean inequality yields

$$\begin{aligned}\|s_1\|^2 &\le \|v_e\|^2 + 2\Lambda_{1,M}\|v_e\|\|q_e\| + \Lambda_{1,M}^2\|q_e\|^2 \\ &\le 2\|v_e\|^2 + 2\Lambda_{1,M}^2\|q_e\|^2 \\ &\le 2(1+\Lambda_{1,M}^2)\|x\|, \\ \|s_2\|^2 &\le 2(1+\Lambda_{2,M}^2)\|x\|. \end{aligned} \tag{5.13}$$

From inequalities (5.12) and (5.13), we have

$$\begin{aligned}\mathcal{L}V \le\; -\Bigg[&\min\left\{K_{d,m}-M_M\Lambda_{1,M}, K_{d,m}\Lambda_{1,m}^2, K_{d,m}\Lambda_{2,m}^2\right\} \\ &- C_M N_{\dot{q}_d}\left(\Lambda_{1,M}+\sqrt{2(1+\Lambda_{2,M}^2)}\left(\sqrt{2(1+\Lambda_{1,M}^2)}+1\right)\right) \\ &- C_M\left(\Lambda_{1,M}+2(1+\Lambda_{2,M}^2)+\sqrt{2(1+\Lambda_{2,M}^2)}\right)\|x\|\Bigg]\|x\|^2 + \|\omega_{x_e}\| + \|\omega_{\tilde{x}}\|. \end{aligned} \tag{5.14}$$

Then we evaluate $\|\omega_{x_e}\|$ and $\|\omega_{\tilde{x}}\|$ in inequality (5.14). By the following calculation that $\mathcal{D}_{v_e}^2 V = M(q)$, Assumptions 5.2 and 5.4 and Eq. (5.9), we evaluate the second term of ω_{x_e} as

$$\begin{aligned}\operatorname{tr}\left\{\mathcal{D}_{v_e}^2 V W_v W_v^\top\right\} &= \sum_{i=1}^{r_2}\lambda_i\left(W_v^\top M W_v\right) \\ &\le r_2\lambda_{\max}\left(W_v^\top M W_v\right) \\ &\le r_2\sqrt{M_M}W_{v,M}(1+\|q\|+\|v\|) \\ &\le r_2\sqrt{M_M}W_{v,M}(1+\|q_e\|+N_{q_d}+\|v_e\|+N_{\dot{q}_d}). \end{aligned} \tag{5.15}$$

From the following calculation that

$$\begin{aligned}\mathcal{D}_{q_e}^2 V = \frac{1}{2}\mathcal{D}_q^2 M(q)(v_e,v_e)(\cdot)(\cdot) + \mathcal{D}_q M(q)(v_e,\Lambda_1(\cdot))(\cdot) \\ + \mathcal{D}_q^2 M(q)(v_e,\Lambda_1 q_e)(\cdot)(\cdot) + [\mathcal{D}_q M(q)(v_e)]^\top(\cdot)(\Lambda_1(\cdot)) + 2\Lambda_1 K_d\end{aligned}$$

and Assumptions 5.2, 5.3 and 5.4, the first term of ω_{x_e} can be evaluated as

$$\begin{aligned}\operatorname{tr}\left\{\mathcal{D}_{q_e}^2 V W_q W_q^\top\right\} \le & r_1\left(\frac{1}{2}\bar{\bar{M}}_M\|v_e\|^2+2\Lambda_{1,M}\bar{M}_M\|v_e\|+\Lambda_{1,M}\bar{\bar{M}}_M\|q_e\|\|v_e\|+2K_{d,M}\Lambda_{1,M}\right)^{\frac{1}{2}}W_{q,M} \\ &\times(1+\|q_e\|+N_{q_d}+\|v_e\|+N_{\dot{q}_d}). \end{aligned} \tag{5.16}$$

Similarly, we have

$$\begin{aligned}\operatorname{tr}\left\{\mathcal{D}_{\tilde{q}}^2 V W_q W_q^\top\right\} &\le \frac{r_1}{2}\left(\frac{1}{2}\bar{\bar{M}}_M\|s_2\|^2+2\Lambda_{2,M}\bar{M}_M\|s_2\|+\Lambda_{2,M}^2 M_M+2K_{d,M}\Lambda_{2,M}\right)^{\frac{1}{2}} \\ &\quad\times W_{q,M}(1+\|q_e\|+N_{q_d}+\|v_e\|+N_{\dot{q}_d}) \\ \operatorname{tr}\left\{\mathcal{D}_{\tilde{v}}^2 V W_q W_q^\top\right\} &\le \frac{\sqrt{M_M}}{2}\left(r_1 L_{d,M}W_{q,M}+r_2 W_{v,M}\right)(1+\|q_e\|+N_{q_d}+\|v_e\|+N_{\dot{q}_d}). \end{aligned} \tag{5.17}$$

Consequently, from Eq. (5.10) and inequalities (5.15), (5.16) and (5.17), an upper bound of $\mathcal{L}V$ can be evaluated as

$$
\begin{aligned}
\mathcal{L}V \leq & -\Bigg[\min\left\{K_{d,m}-M_M\Lambda_{1,M},\, K_{d,m}\Lambda_{1,m}^2,\, K_{d,m}\Lambda_{2,m}^2\right\} \\
& - C_M N_{\dot{q}_d}\left(\Lambda_{1,M}+\sqrt{2(1+\Lambda_{2,M}^2)}\left(\sqrt{2(1+\Lambda_{1,M}^2)}+1\right)\right) \\
& - C_M\left(\Lambda_{1,M}+2(1+\Lambda_{2,M}^2)+\sqrt{2(1+\Lambda_{2,M}^2)}\right)\|x\|\Bigg]\|x\|^2 \\
& + \left\{\frac{r_1}{2}\left(\frac{1}{2}\bar{\bar{M}}_M\|v_e\|^2+2\Lambda_{1,M}\bar{M}_M\|v_e\|+\Lambda_{1,M}\bar{\bar{M}}_M\|q_e\|\|v_e\|+2K_{d,M}\Lambda_{1,M}\right)^{\frac{1}{2}}W_{q,M}\right. \\
& + \frac{r_2}{2}\sqrt{M_M}W_{v,M}+\frac{r_1}{2}\left(\frac{1}{2}\bar{\bar{M}}_M\|s_2\|^2+2\Lambda_{2,M}\bar{M}_M\|s_2\|+\Lambda_{2,M}^2M_M+2K_{d,M}\Lambda_{2,M}\right)^{\frac{1}{2}}W_{q,M} \\
& \left.+\frac{\sqrt{M_M}}{2}\left(r_1(l_d+\Lambda_{2,M})W_{q,M}+r_2W_{v,M}\right)\right\}(1+\|q_e\|+N_{q_d}+\|v_e\|+N_{\dot{q}_d}). \qquad (5.18)
\end{aligned}
$$

Finally, we provide conditions for the controller and observer gains under which the tracking and estimation error x remains bounded in probability and the margin of error is assignable. Here we give the following lemma.

Lemma 5.1 *Consider the system* (5.1)*, the controller* (5.2)*, the observer* (5.3) *and Assumptions 5.2,5.3, 5.4 and 5.6. For any* $\delta_0,\ \delta_1 \in \mathbb{R},\ 0 < \delta_0 < \delta_1$*, we define the following region*

$$S_{\delta_0\delta_1} := \{x \big|\ \delta_0 \leq \|x\| \leq \delta_1\}.$$

Then a sufficient condition under which $\mathcal{L}V$ *with respect to the Lyapunov function* V *in* (5.6) *along the sample path* x *becomes negative on* $S_{\delta_0\delta_1}$ *is given by*

$$
\begin{aligned}
K_{d,m} > & \max\left\{\frac{D_1(\Lambda_1,\Lambda_2,\delta_1)}{\Lambda_{1,m}^2}+\frac{D_2(K_d,l_d,\Lambda_1,\Lambda_2,\delta_1)}{\Lambda_{1,m}^2\delta_0^2},\frac{D_1(\Lambda_1,\Lambda_2,\delta_1)}{\Lambda_{2,m}^2}+\frac{D_2(K_d,l_d,\Lambda_1,\Lambda_2,\delta_1)}{\Lambda_{2,m}^2\delta_0^2},\right. \\
& \left. D_1(\Lambda_1,\Lambda_2,\delta_1)+\frac{D_2(K_d,l_d,\Lambda_1,\Lambda_2,\delta_1)}{\delta_0^2}+M_M\Lambda_{1,M}\right\}, \\
l_dM_m > & 2K_{d,M}, \qquad (5.19)
\end{aligned}
$$

where $D_1(\Lambda_1,\Lambda_2,\delta_1)$ *and* $D_2(K_d,l_d,\Lambda_1,\Lambda_2,\delta_1)$ *are defined by*

$$
\begin{aligned}
D_1(\Lambda_1,\Lambda_2,\delta_1) &:= C_M N_{\dot{q}_d}\Big(\Lambda_{1,M}+\sqrt{2(1+\Lambda_{2,M}^2)}\,\Big(\sqrt{2(1+\Lambda_{1,M}^2)}+1\Big)\Big)\\
&\quad + C_M\Big(\Lambda_{1,M}+2(1+\Lambda_{2,M}^2)+\sqrt{2(1+\Lambda_{2,M}^2)}\Big)\delta_1,\\
D_2(K_d,l_d,\Lambda_1,\Lambda_2,\delta_1) &:= \Big\{\frac{r_1}{2}\Big(\bar{\bar{M}}_M\delta_1^2\Big(\frac{1}{2}+\Lambda_{1,M}\Big)+2\Lambda_{1,M}\bar{M}_M\delta_1+2K_{d,M}\Lambda_{1,M}\Big)^{\frac{1}{2}}W_{q,M}\\
&\quad+\frac{r_1}{2}\Big(\frac{1}{2}\bar{\bar{M}}_M(1+\Lambda_{2,M})^2\delta_1^2+2\Lambda_{2,M}\bar{M}_M(1+\Lambda_{2,M})\delta_1+\Lambda_{2,M}^2M_M+2K_{d,M}\Lambda_{2,M}\Big)^{\frac{1}{2}}W_{q,M}\\
&\quad+\frac{r_2}{2}\sqrt{M_M}W_{v,M}+\frac{\sqrt{M_M}}{2}\big(r_1(l_d+\Lambda_{2,M})W_{q,M}+r_2W_{v,M}\big)\Big\}(1+N_{q_d}+N_{\dot{q}_d}+2\delta_1). \quad (5.20)
\end{aligned}
$$

Proof Under the condition $l_dM_m > 2K_{d,M}$, on $S_{\delta_0\delta_1}$, inequality (5.18) is reduced to

$$
\begin{aligned}
\mathcal{L}V \le &-\Big[\min\big\{K_{d,m}-M_M\Lambda_{1,M},K_{d,m}\Lambda_{1,m}^2,K_{d,m}\Lambda_{2,m}^2\big\}-D_1(\Lambda_1,\Lambda_2,\delta_1)\Big]\delta_0^2\\
&+D_2(K_d,l_d,\Lambda_1,\Lambda_2,\delta_1), \quad (5.21)
\end{aligned}
$$

where $D_1(\Lambda_1,\Lambda_2,\delta_1)$ and $D_2(K_d,l_d,\Lambda_1,\Lambda_2,\delta_1)$ are given by Eq. (5.20). The rest of the condition in (5.19) is immediately derived from inequality (5.21). ■

We are ready to state the main result.

Theorem 5.2 *Consider the system* (5.1)*, the controller* (5.2)*, the observer* (5.3) *and Assumptions 5.2,5.3, 5.4 and 5.6. For any* $\lambda_1\in\mathbb{R},\ \lambda_1>0$ *and* $\rho\in\mathbb{R},\ 0<\rho<1$*, we assign any* λ_0 *which satisfies* $0<\lambda_0<\lambda_1(1-\rho)$*. Then, under the condition* (5.19) *in Lemma 5.1 with the following* δ_0 *and* δ_1*:*

$$\delta_0=\sqrt{\frac{2\lambda_0}{P_M}},\qquad \delta_1=\sqrt{\frac{2\lambda_1}{P_m}}, \quad (5.22)$$

the system is (Q_0^x,Q_1^x,ρ)*-stable (see Definition 5.5), where* Q_0^x *and* Q_1^x *are defined as*

$$
\begin{aligned}
Q_0^x &:= \{x|\ \lambda_0<V(x)<\lambda_1(1-\rho)\},\\
Q_1^x &:= \{x|\ V(x)<\lambda_1\} \quad (5.23)
\end{aligned}
$$

In Eq. (5.22)*,* P_m *and* P_M *represent lower and upper bounds for* $P(q)$ *in* (5.6)*, i.e,* $P_m\le\|P(q)\|\le P_M,\ \text{for }{}^\forall q$ *holds.*

Under the condition, the following probability inequality also holds

$$\mathcal{P}\left\{\sup_{0\le t<\infty}\|x(t)\|<\sqrt{\frac{2\lambda_1}{P_M}}\right\}\ge\rho.$$

Before proving the theorem, the stopped process [48] is introduced.

Definition 5.7 [48] Define $t \cap s := \min\{t, s\}$. Suppose that τ_S is the first time of exit of the process $x(t)$ from an open set S, i.e., $\tau_S := \inf\{t \geq 0 \mid x(t) \notin S\}$. Then, the stopped process $x(t \cap \tau_S)$ is defined as

$$x(t \cap \tau_S) := \begin{cases} x(t) & t < \tau_S \\ x(\tau_S) & t \geq \tau_S \end{cases}.$$

Here we prove the Theorem 5.2.

Proof Firstly, we derive the condition under which $\mathcal{L}V(x)$ is negative on the region of x satisfying $\lambda_0 < V(x) < \lambda_1$. Since

$$\frac{P_m\|x\|^2}{2} \leq V(x) \leq \frac{P_M\|x\|^2}{2}, \tag{5.24}$$

it is sufficient to consider the condition under which

$$\mathcal{L}V(x) < 0 \quad \text{on} \quad \sqrt{\frac{2\lambda_0}{P_M}} < \|x\| < \sqrt{\frac{2\lambda_1}{P_m}}. \tag{5.25}$$

By utilizing Lemma 5.1, a condition satisfies (5.25) is easily obtained as the condition (5.19) with δ_0 and δ_1 defined in Eq. (5.22). With the condition and the Dynkin's formula [46, 57], for $0 \leq s \leq t$ we have

$$E[V(x(t \cap \tau_{S_{\delta_0\delta_1}}))|\mathcal{F}_s] - V(x(s)) = \int_s^{t\cap\tau_{S_{\delta_0\delta_1}}} E\left[\mathcal{L}V(x(u))|\mathcal{F}_s\right] \mathrm{d}u < 0. \tag{5.26}$$

Since $E[V(x(t\cap\tau_{S_{\delta_0\delta_1}}))|\mathcal{F}_s] < V(x(s))$ holds from the inequality (5.26), $\{V(x(t\cap\tau_S));\ t \geq 0\}$ is a nonnegative supermartingale. By utilizing the supermartingale property [15, 49], we obtain the following probability inequality

$$\begin{aligned} \frac{V(x(0))}{\lambda_1} &\geq \mathcal{P}\left\{\sup_{0\leq t<\infty} V(x(t \cap \tau_{S_{\delta_0\delta_1}})) \geq \lambda_1\right\} \\ &= \mathcal{P}\left\{\sup_{0\leq t<\infty} V(x(t)) \geq \lambda_1\right\}. \end{aligned}$$

Consequently, if the initial condition for $x(0)$ is chosen from Q_0^x in (5.23), we have

$$\mathcal{P}\left\{\sup_{0\leq t<\infty} V(x(t)) < \lambda_1\right\} \geq 1 - \frac{\lambda_1(1-\rho)}{\lambda_1} = \rho. \tag{5.27}$$

Under the condition which Eq.(5.27) holds, the last statement can be easily shown, since

$$\left\{x \middle| \sup_{0\leq t<\infty} \|x(t)\| < \sqrt{\frac{2\lambda_1}{P_M}}\right\} \subset \left\{x \middle| \sup_{0\leq t<\infty} V(x(t)) < \lambda_1\right\}$$

holds from inequality (5.24). This proves the theorem. ∎

Table 5.1: Physical parameters

θ_i	joint angle of the i-th link	[rad]
m_i	mass of the i-th link	[kg]
l_i	length of the i-th link	[m]
l_{gi}	length to the center of gravity	[m]
$\bar{I}_i$	inertia of the i-th link	[kgm^2]
d_i	friction coefficient of the i-th link	[Nms/rad]

5.3 Numerical example

This section exhibits the effectiveness of the proposed method via numerical simulations. Here let us consider a two-link robot manipulator moving on a horizontal plane depicted in Fig. 5.1. As in the figure, the joint angles of the first and the second links are denoted by θ_1 and θ_2, respectively. The physical parameters of this apparatus are summarized in Table 5.1.

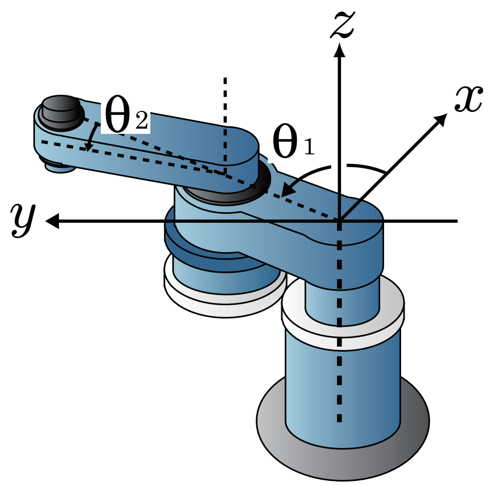

Figure 5.1: 2-link robot manipulator

Then the dynamics of this apparatus is described by Eq. (5.1). Here the configuration coordinate $q := (\theta_1, \theta_2)^\top \in \mathbb{R}^2$ and the inertia matrix $M(q)$ and the Coriolis matrix $C(q, v)$ including some friction effects are given by

$$
\begin{aligned}
M(q) &= \begin{pmatrix} b_1 + b_2 + 2b_3 \cos(q^2) & b_2 + b_3 \cos(q^2) \\ b_2 + b_3 \cos(q^2) & b_2 \end{pmatrix} \\
C(q, v) &= \begin{pmatrix} 2b_3 \sin(q^2) v^2 - d_1 & b_3 \sin(q^2) v^2 \\ -b_3 \sin(q^2) v^1 & -d_2 \end{pmatrix},
\end{aligned}
\tag{5.28}
$$

where

$$\begin{aligned} b_1 &:= \bar{I}_1 + m_1 l_{g2}^2 + m_2 l_1^2 = \frac{4}{3} m_1 l_{g2}^2 + m_2 l_1^2 \\ b_2 &:= \bar{I}_2 + m_2 l_{g2}^2 = \frac{4}{3} m_2 l_{g2}^2 \\ b_3 &:= l_1 m_2 l_{g2}. \end{aligned}$$

Since this apparatus moves on a horizontal plane, we let $G(q) = 0$. The concrete parameters used in the simulations are $b_1 = 2.292$, $b_2 = 0.600$, $b_3 = 0.750$, $d_1 = 0.2415$ and $d_2 = 0.2457$. We define the desired trajectory of q as

$$q_d(t) = \begin{pmatrix} \frac{3}{4\pi} \cos\left(\frac{2\pi}{3} t\right) - \frac{3}{4\pi} \\ \frac{3}{4\pi} \cos\left(\frac{2\pi}{3} t\right) - \frac{3}{4\pi} \end{pmatrix},$$

and the noise ports W_q and W_v as

$$\begin{aligned} W_q(q, v) &= 5 \times 10^{-5} \begin{pmatrix} q^1 + v^1 + 3 \\ q^2 + v^2 + 3 \end{pmatrix} \\ W_v(q, v) &= 0.1 \begin{pmatrix} q^1 + v^1 + 3 \\ q^2 + v^2 + 3 \end{pmatrix}. \end{aligned} \tag{5.29}$$

In this simulation, we utilize the following upper bounds $M_M = 4.83$, $M_m = 3.00$, $\bar{M}_M = 1.82$, $\bar{\bar{M}}_M = 1.0 \times 10^{-3}$, $C_M = 1.89$, $W_{q,M} = 8.90 \times 10^{-5}$, $W_{v,M} = 2.24 \times 10^{-1}$, $N_{q_d} = 0.34$ and $N_{\dot{q}_d} = 0.71$. Here M_M, M_m, $\bar{M}_M$ and $\bar{\bar{M}}_M$ are calculated by a numerical computation at a range of $|q^2| \leq \frac{\pi}{2}$ by 1×10^{-3}. The other bounds are calculated at ranges of $|q^1|$, $|q^2| \leq \frac{\pi}{2}$, $|v^1|$, $|v^2| \leq 5$ by 0.1, respectively.

By utilizing Theorem 5.2, let us decide the controller and observer gains. Firstly, we set $\lambda_1 = 650$ and $\rho = 0.5$ and then we choose $\lambda_0 = 324$ so that $0 < \lambda_0 < \lambda_1(1 - \rho)$ holds. Upper and lower bounds P_M and P_m of stochastic Lyapunov function V in (5.6) are obtained as follows. From the definition (5.6), we have

$$P = T_2^\top T_1^\top \operatorname{diag}\{2K_d\Lambda_1^{-1} - M, M, 2K_d\Lambda_2^{-1}, M\} T_1 T_2, \tag{5.30}$$

where

$$T_1 := \begin{pmatrix} I & 0 & 0 & 0 \\ I & I & 0 & 0 \\ 0 & 0 & I & 0 \\ 0 & 0 & I & I \end{pmatrix}, \quad T_2 := \begin{pmatrix} \Lambda_1 & 0 & 0 & 0 \\ 0 & I & 0 & 0 \\ 0 & 0 & \Lambda_2 & 0 \\ 0 & 0 & 0 & I \end{pmatrix}.$$

It follows from Eq. (5.30) that

$$\begin{aligned} P_M &= \frac{3 + \sqrt{5}}{2} \max\{\Lambda_{1,M}, \Lambda_{2,M}, 1\} \max\{2K_{d,M}\Lambda_{1,m}^{-1} - M_m, M_M, 2K_{d,M}\Lambda_{2,m}^{-1}\}, \\ P_m &= \frac{3 - \sqrt{5}}{2} \min\{\Lambda_{1,m}, \Lambda_{2,m}, 1\} \min\{2K_{d,m}\Lambda_{1,M}^{-1} - M_M, M_m, 2K_{d,m}\Lambda_{2,M}^{-1}\}. \end{aligned} \tag{5.31}$$

Consequently, we decide the controller and observer gains so that the condition in Theorem 5.2 is satisfied with design parameters λ_1, λ_0 and ρ, as

$$K_d = \begin{pmatrix} 1345 & 0 \\ 0 & 1345 \end{pmatrix} \quad , \quad \Lambda_1 = \Lambda_2 = \begin{pmatrix} 1 & 0 \\ 0 & 1 \end{pmatrix} \quad , \quad l_d = 900.$$

Theorem 5.2 guarantees that

$$\mathcal{P}\left\{ \sup_{0 \le t < \infty} \|x(t)\| < \sqrt{\frac{2\lambda_1}{P_M}} \right\} \approx \mathcal{P}\left\{ \sup_{0 \le t < \infty} \|x(t)\| < 0.4296 \right\} \ge 0.5. \quad (5.32)$$

We executed 12 seconds of simulation with the initial condition:

$$(q_e^1(0), q_e^2(0), v_e^1(0), v_e^2(0), \tilde{q}^1(0), \tilde{q}^2(0), \tilde{v}^1(0), \tilde{v}^2(0)) = (4.0 \times 10^{-4}, 1.0 \times 10^{-4}, 0, 0, 0, 0, 0, 0).$$

Figure 5.2 exhibits the time responses of $q = (q^1, q^2)^\top$ in solid lines and their desired trajectories $q_d = (q_d^1, q_d^2)^\top$ in dotted lines, respectively. Figure 5.3 shows the time responses of $v = (v^1, v^2)^\top$ in solid lines and their desired trajectories $\dot{q}_d = (\dot{q}_d^1, \dot{q}_d^2)^\top$ in dotted lines, respectively. Figure 5.4 shows the estimation errors with the observer in (5.3), that is, the time histories of $q^1 - \hat{q}^1, q^2 - \hat{q}^2, v^1 - \hat{v}^1$ and $v^2 - \hat{v}^2$ are exhibited, respectively. Figure 5.5 shows the tracking errors with respect to the desired trajectory, that is, the time histories of $q^1 - q_d^1, q^2 - q_d^2, v^1 - \dot{q}_d^1$ and $v^2 - \dot{q}_d^2$ are exhibited, respectively. Figure 5.6 shows the time history of $\|x(t)\|$. Although the simulation is only executed in a finite time interval $0 \le t \le 12$, Eq. (5.32) is satisfied at least in this interval. Finally, Fig. 5.7 shows other three time histories of sample paths $\|x(t)\|$, which are independent of the sample path in Fig. 5.6. It implies that inequality (5.32) also holds for other sample paths. These simulation results demonstrate the effectiveness of the proposed framework.

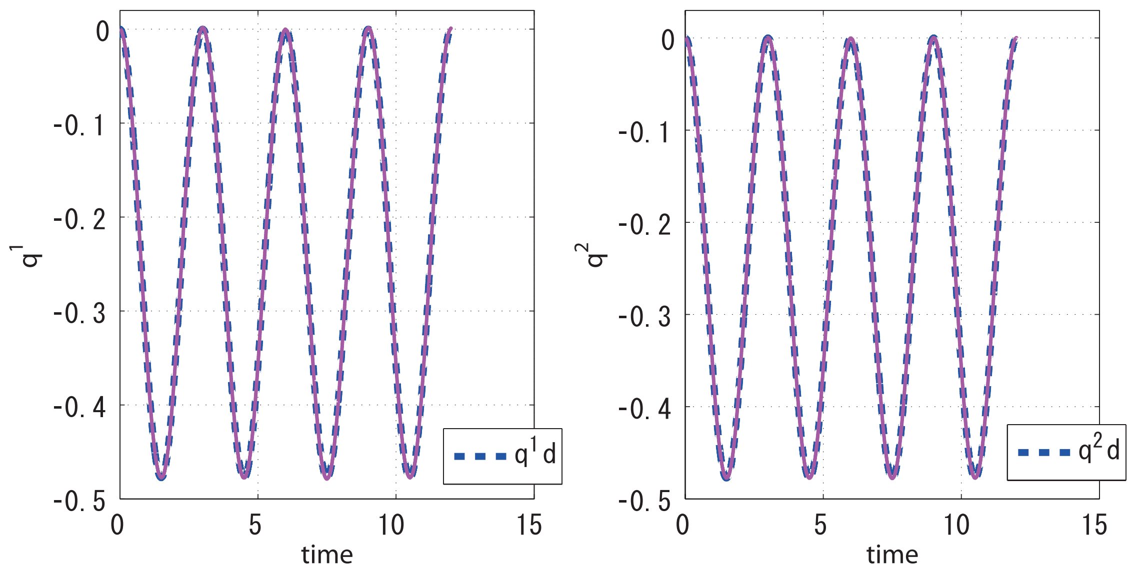

Figure 5.2: Responses of q^1 and q^2

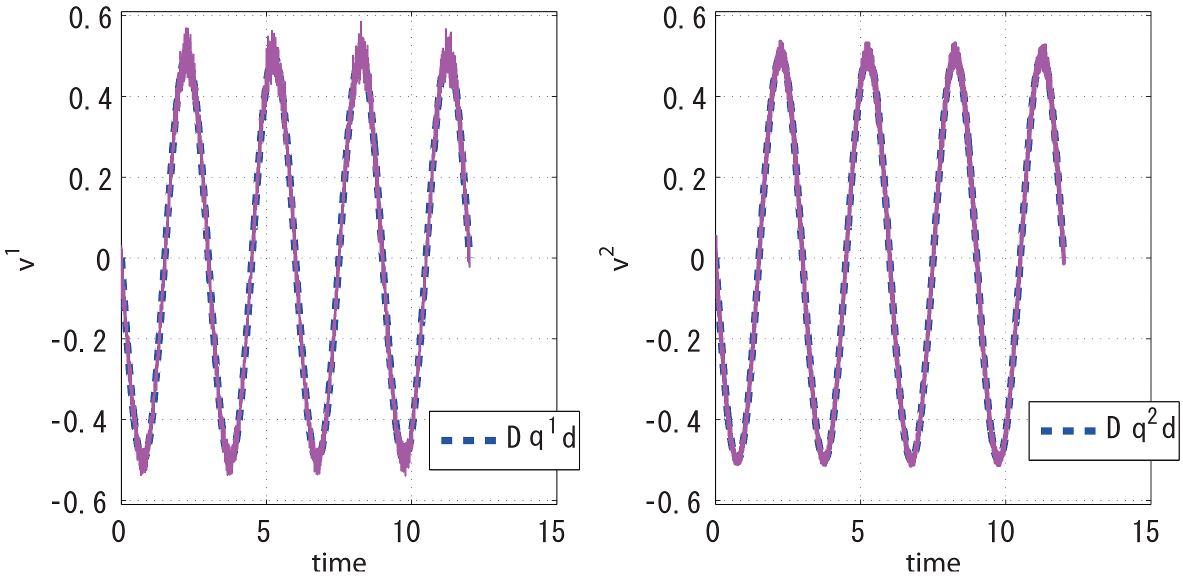

Figure 5.3: Responses of v^1 and v^2

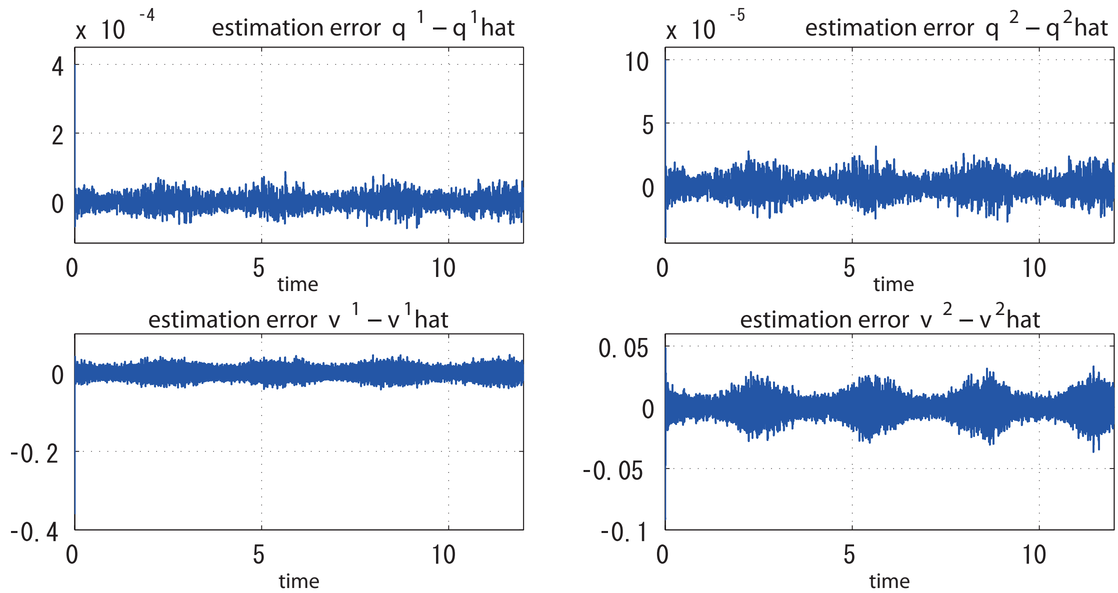

Figure 5.4: Time histories of the estimation errors

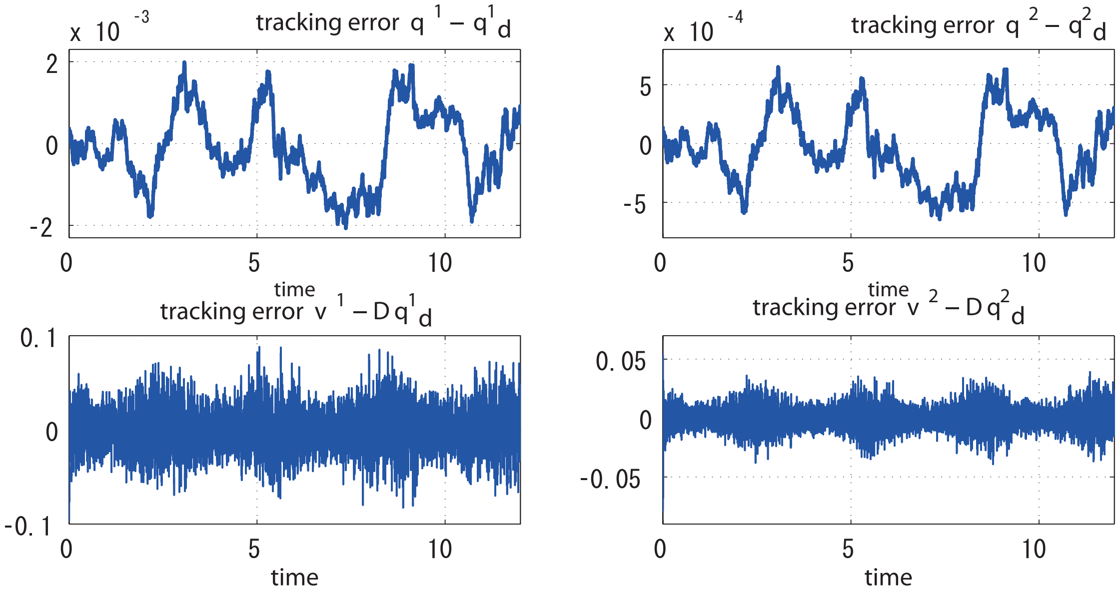

Figure 5.5: Time histories of the tracking errors

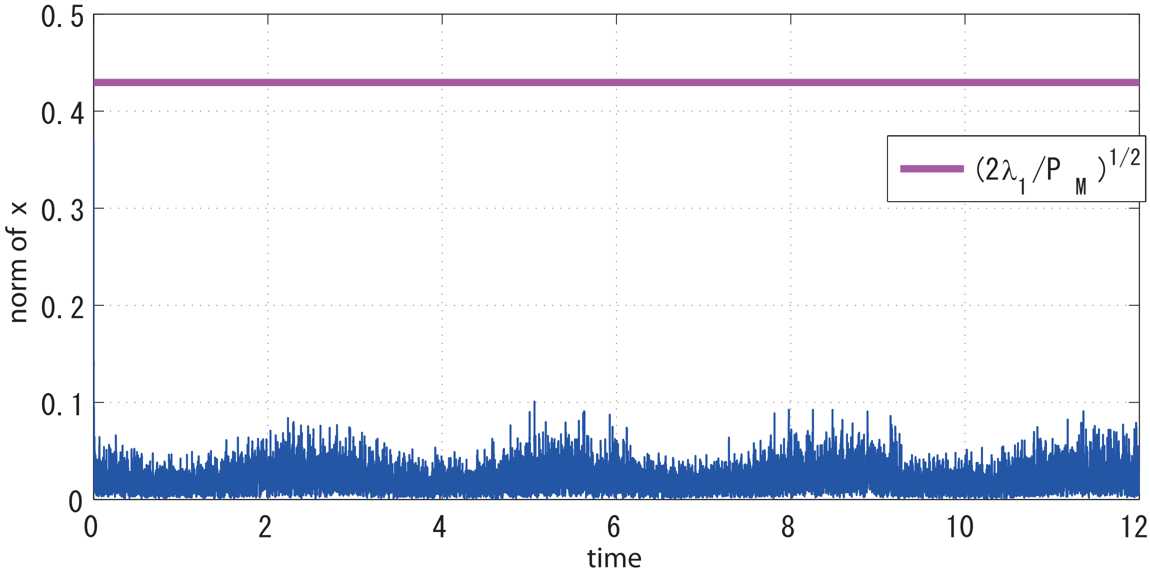

Figure 5.6: Time history of $\|x(t)\|$

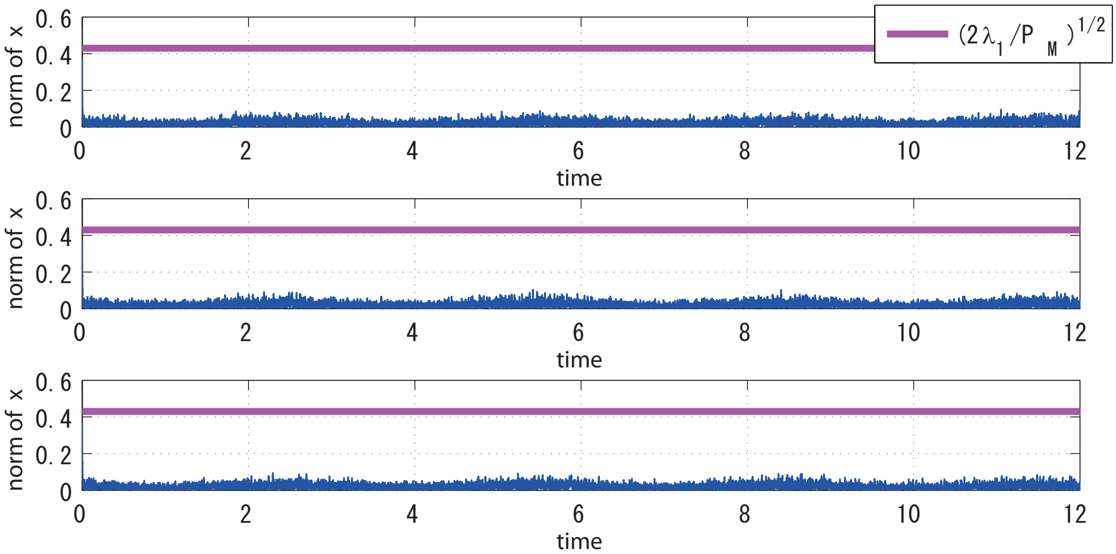

Figure 5.7: Time histories of $\|x(t)\|$ of other 3 sample passes

5.4 Summary

This chapter has introduced an observer based stochastic trajectory tracking control of mechanical systems. We considered mechanical systems in the presence of noise as stochastic systems and the situation that only position measurements were available. We have derived conditions for the controller and observer gains under which the tracking and estimation error remains bounded in probability and the margin of error is assignable. The stochastic bounded stability has been proven by utilizing supermartingale property. Finally, numerical simulations demonstrate the effectiveness of the proposed method.

Chapter 6

Symmetric property of stochastic Hamiltonian systems

This chapter introduces the variational and its adjoint systems of stochastic Hamiltonian systems and reveals some of their properties, particularly an extension of variational symmetry of deterministic Hamiltonian systems (see, Lemma 2.2).

Firstly, in Section 6.1, let us define the variational system of a general nonlinear stochastic system (C.1) in Appendix C in a manner analogous to the deterministic systems [13, 27]. Then its adjoint system is defined based on a system utilized in the stochastic maximum principle [47, 62] in stochastic optimal control, e.g., [6, 62, 95] and references therein. Here let us note that the stochastic adjoint system [6, 95] is a nontrivial extension of the deterministic one [13, 27]. Finally, an input-output relation between both systems is shown.

In Section 6.2, let us concentrate on stochastic Hamiltonian systems. Firstly, we show that a variational system of the stochastic Hamiltonian system is described by another linear one. Secondly, we derive a condition under which an adjoint system coincides with the time-reversal version of the variational one. This property is an extension of variational symmetry of deterministic Hamiltonian systems, which plays an important role in learning optimal control proposed in Chapters 2 and 3.

In the sequel, we utilize the same notation $\partial_{(\cdot)}$ as the partial Fréchet derivative with respect to $(\cdot)$ in order to denote the partial differential with respect to $(\cdot)$. For example, for a smooth function $f(x,t)$, the following holds

$$\begin{aligned}\partial_x f(x,t) &= f(x+\mathrm{d}x,t) - f(x,t) + o(\|\mathrm{d}x\|)\\ &= \frac{\partial f(x,t)}{\partial x}\,\mathrm{d}x.\end{aligned}$$

6.1 Variational and its adjoint systems of nonlinear stochastic systems

Let $(x(t,\epsilon), u(t,\epsilon), y(t,\epsilon)),\ \ t\in[0,t^1]$ denote a family of state-input-output trajectories of the system (C.1) in Appendix C parameterized by ϵ, such that $x(t,0)=x(t), u(t,0)=u(t), y(t,0)=y(t),\ \ t\in[0,t^1]$. We define the variational system of (C.1) as the system in which the following quantities

$$x_v(t) = \frac{\partial x(t,0)}{\partial \epsilon}\ , \quad u_v(t) = \frac{\partial u(t,0)}{\partial \epsilon}\ , \quad y_v(t) = \frac{\partial y(t,0)}{\partial \epsilon}$$

are governed. In order to derive a stochastic differential equation which the variational process x_v satisfies, let us calculate the differentiation of $x(t,\epsilon)$ with respect to the time t. We have that

$$\begin{aligned}
&\partial_t x(t,\epsilon) \\
&= f(x(t,\epsilon), u(t,\epsilon), t)\,\mathrm{d}t + h(x(t,\epsilon), t)\,\mathrm{d}w \\
&= f(x(t,0), u(t,0), t)\,\mathrm{d}t + \left\{ \frac{\partial f(x(t,0), u(t,0), t)}{\partial x} \frac{\partial x(t,0)}{\partial \epsilon} + \frac{\partial f(x(t,0), u(t,0), t)}{\partial u} \frac{\partial u(t,0)}{\partial \epsilon} \right\} \epsilon\,\mathrm{d}t \\
&\quad + \sum_{i=1}^{r} \frac{\partial h_i(x(t,0), t)}{\partial x} \frac{\partial x(t,0)}{\partial \epsilon} \epsilon\,\mathrm{d}w^i + o(|\epsilon|) \\
&= f(x(t), u(t), t)\,\mathrm{d}t + \left\{ \frac{\partial f(x(t), u(t), t)}{\partial x} x_v + \frac{\partial f(x(t), u(t), t)}{\partial u} u_v \right\} \epsilon\,\mathrm{d}t + h(x(t), t)\,\mathrm{d}w \\
&\quad + \sum_{i=1}^{r} \frac{\partial h_i(x(t), t)}{\partial x} x_v \epsilon\,\mathrm{d}w^i + o(|\epsilon|),
\end{aligned} \tag{6.1}$$

where $o(\cdot)$ represents the Landau notation (see Eq. (2.2)). From Eq. (6.1), the following stochastic differential equation is obtained which x_v should satisfy

$$\begin{aligned}
\mathrm{d}x_v &= \lim_{\epsilon \to 0} \frac{\partial_t x(t,\epsilon) - \partial_t x(t,0)}{\epsilon} \\
&= \frac{\partial f(x,u,t)}{\partial x} x_v\,\mathrm{d}t + \frac{\partial f(x,u,t)}{\partial u} u_v\,\mathrm{d}t + \sum_{i=1}^{r} \frac{\partial h_i(x,t)}{\partial x} x_v\,\mathrm{d}w^i.
\end{aligned} \tag{6.2}$$

The following equation can be obtained in a similar manner to Eq. (6.1),

$$y_v = \frac{\partial s(x,u,t)}{\partial x} x_v + \frac{\partial s(x,u,t)}{\partial u} u_v. \tag{6.3}$$

Definition 6.1 Consider the system (C.1) in Appendix C. The variational system of the system (C.1) is defined as

$$\left\{ \begin{array}{rcl}
\mathrm{d}x &=& f(x,u,t)\,\mathrm{d}t + h(x,t)\,\mathrm{d}w\ , \quad x(0) = x_0 \\
\mathrm{d}x_v &=& \frac{\partial f(x,u,t)}{\partial x} x_v\,\mathrm{d}t + \frac{\partial f(x,u,t)}{\partial u} u_v\,\mathrm{d}t + \sum_{i=1}^{r} \frac{\partial h_i(x,t)}{\partial x} x_v\,\mathrm{d}w^i, \\
&& x_v(0) = x_{v,0} \\
y_v &=& \frac{\partial s(x,u,t)}{\partial x} x_v + \frac{\partial s(x,u,t)}{\partial u} u_v
\end{array} \right. . \tag{6.4}$$

In this thesis, we define an adjoint system of the variational system (6.4) based on a system utilized in the stochastic maximum principle in stochastic optimal control [62, 95].

Definition 6.2 Consider the system (C.1) in Appendix C. The variational adjoint system of the system (C.1) is defined as

$$\begin{cases} \mathrm{d}x &= f(x,u,t)\,\mathrm{d}t + h(x,t)\,\mathrm{d}w \ , \quad x(0)=x_0 \\ \mathrm{d}x_a &= -\dfrac{\partial f(x,u,t)}{\partial x}^\top x_a\,\mathrm{d}t - \dfrac{\partial s(x,u,t)}{\partial x}^\top u_a\,\mathrm{d}t - \displaystyle\sum_{i=1}^r \dfrac{\partial h_i(x,t)}{\partial x}^\top z_i\,\mathrm{d}t + \sum_{i=1}^r z_i\,\mathrm{d}w^i, \\ & \quad x_a(t^1) = x_{a,t^1} \\ y_a &= \dfrac{\partial f(x,u,t)}{\partial u}^\top x_a + \dfrac{\partial s(x,u,t)}{\partial u}^\top u_a \end{cases} ,\tag{6.5}$$

where $(x_a(t), z(t)) \in \mathbb{R}^n \times \mathbb{R}^{n\times r}$ is a pair of [1]$\{\mathcal{F}_t\}_{t\geq 0}$-adapted processes.

Let us note that the variational adjoint equation is to be solved backwards, since the terminal condition x_{a,t^1} is given. However, the solution $(x_a(t), z(t))$ is required to be $\{\mathcal{F}_t\}_{t\geq 0}$-adapted. Any pair of processes $(x_a(t), z(t))$ satisfying (6.5) is called an adapted solution. For the detail of the backward stochastic differential equation, see [6, 44, 95].

Here let us prove the following theorem with respect to an input-output relation between the variational and its adjoint systems, which is an extension in the deterministic case.

Theorem 6.1 *Consider the variational system* (6.4) *and its adjoint system* (6.5) *on a time interval* $t \in [0, t^1]$. *Suppose that a pair of processes* (x_a, z) *is an adapted solution of the adjoint system* (6.5) *and that the initial condition of the variational system* $x_{v,0}$ *and the terminal state of the adjoint system* x_{a,t^1} *are the stochastic variables satisfying*

$$x_{v,0} = 0, \quad x_{a,t^1} = 0. \tag{6.6}$$

Then the following relation holds

$$E\left[\int_0^{t^1} y_a(t)^\top u_v(t)\,\mathrm{d}t\right] = E\left[\int_0^{t^1} u_a(t)^\top y_v(t)\,\mathrm{d}t\right]. \tag{6.7}$$

Proof Let us calculate the time variation of $x_a(t)^\top x_v(t)$ with the Itô formula in Appendix C.1 as

$$\mathrm{d}\left(x_a^\top x_v\right) = \mathrm{d}x_a^\top x_v + x_a^\top\,\mathrm{d}x_v + \frac{1}{2}\,\mathrm{tr}\left\{\frac{\partial^2 (x_a^\top x_v)}{\partial (x_v, x_a)^2}\begin{pmatrix}\mathcal{D}_x h_1 x_v, \cdots, \mathcal{D}_x h_d x_v \\ z_1, \cdots, z_r\end{pmatrix}\begin{pmatrix}\mathcal{D}_x h_1 x_v, \cdots, \mathcal{D}_x h_d x_v \\ z_1, \cdots, z_r\end{pmatrix}^\top\right\}\mathrm{d}t, \tag{6.8}$$

where the following notation is utilized

$$\frac{\partial^2 (x_a^\top x_v)}{\partial (x_v, x_a)^2} := \frac{\partial}{\partial (x_v, x_a)}\left(\frac{\partial (x_a^\top x_v)}{\partial (x_v, x_a)}\right)^\top .$$

[1] A process $x(t)$ is called $\{\mathcal{F}_t\}_{t\geq 0}$-adapted if for each $t \geq 0$ the function $x(t)$ is $\mathcal{F}_t$-measurable.

By substituting Eqs. (6.4) and (6.5) for Eq. (6.8), we have

$$
\begin{aligned}
\mathrm{d}(x_a^\top x_v) = & \left(- \left(\frac{\partial f}{\partial x}^\top x_a + \frac{\partial s}{\partial x}^\top u_a + \sum_{i=1}^r \frac{\partial h_i}{\partial x}^\top z_i \right) \mathrm{d}t + \sum_{i=1}^r z_i \, \mathrm{d}w^i \right)^\top x_v \\
& + x_a^\top \left(\frac{\partial f}{\partial x} x_v \, \mathrm{d}t + \frac{\partial f}{\partial u} u_v \, \mathrm{d}t + \sum_{i=1}^r \frac{\partial h_i}{\partial x} x_v \, \mathrm{d}w^i \right) \\
& + \frac{1}{2} \left(\mathrm{tr} \left\{ \sum_{i=1}^r z_i x_v^\top \frac{\partial h_i}{\partial x}^\top \right\} + \mathrm{tr} \left\{ \sum_{i=1}^r \frac{\partial h_i}{\partial x} x_v z_i^\top \right\} \right) \mathrm{d}t \\
= & \left(x_a^\top \frac{\partial f}{\partial u} u_v - u_a^\top \frac{\partial s}{\partial x} x_v \right) \mathrm{d}t - \sum_{i=1}^r z_i^\top \frac{\partial h_i}{\partial x} x_v \, \mathrm{d}t + \sum_{i=1}^r \left(z_i^\top + \frac{\partial h_i}{\partial x} \right) x_v \, \mathrm{d}w^i \\
& + \mathrm{tr} \left\{ \sum_{i=1}^r \frac{\partial h_i}{\partial x} x_v z_i^\top \right\} \mathrm{d}t \\
= & \left(\left(y_a^\top - u_a^\top \frac{\partial s}{\partial u} \right) u_v - u_a^\top \left(y_v - \frac{\partial s}{\partial u} u_v \right) \right) \mathrm{d}t - \sum_{i=1}^r z_i^\top \frac{\partial h_i}{\partial x} x_v \, \mathrm{d}t \\
& + \sum_{i=1}^r \left(z_i^\top + \frac{\partial h_i}{\partial x} \right) x_v \, \mathrm{d}w^i + \mathrm{tr} \left\{ \sum_{i=1}^r z_i^\top \frac{\partial h_i}{\partial x} x_v \right\} \mathrm{d}t \\
= & (y_a^\top u_v - u_a^\top y_v) \, \mathrm{d}t + \sum_{i=1}^r \left(z_i^\top + \frac{\partial h_i}{\partial x} \right) x_v \, \mathrm{d}w^i
\end{aligned}
$$

The integration on $t \in [0, t^1]$ and the expectation yield

$$
\begin{aligned}
& E[x_a(t^1)^\top x_v(t^1)] - E[x_a(0)^\top x_v(0)] \\
& \quad = E\left[\int_0^{t^1} (y_a^\top u_v - u_a^\top y_v) \, \mathrm{d}t \right] + E\left[\int_0^{t^1} \sum_{i=1}^r \left(z_i^\top + \frac{\partial h_i}{\partial x} \right) x_v \, \mathrm{d}w^i \right]. \qquad (6.9)
\end{aligned}
$$

Since solutions $x_v(t)$ and $(x_a(t), z(t))$ are adapted processes and $h(x)$ is a sufficiently differentiable function, the property of the Itô integral, e.g. [40, 46], yields

$$
E\left[\int_0^{t^1} \sum_{i=1}^r \left(z_i^\top + \frac{\partial h_i}{\partial x} \right) x_v \, \mathrm{d}w^i \right] = 0. \qquad (6.10)
$$

Equation (6.7) follows from Eqs. (6.6), (6.9) and (6.10). This proves the theorem. ■

6.2 Variational and its adjoint systems of stochastic Hamiltonian systems

This section investigates some properties of variational systems and their adjoint ones of stochastic Hamiltonian systems. Let us consider the following stochastic Hamiltonian system described as

$$\begin{cases} \mathrm{d}x &= (J(x,t) - R(x,t)) \dfrac{\partial H(x,u,t)}{\partial x}^{\top} \mathrm{d}t + h(x,t)\,\mathrm{d}w \ , \quad x(0) = x_0 \\ y &= -\dfrac{\partial H(x,u,t)}{\partial u}^{\top} \end{cases} . \tag{6.11}$$

As in the case of the stochastic port-Hamiltonian system in (4.44), $x(t) \in \mathbb{R}^n, u(t), y(t) \in \mathbb{R}^m$ describe the state, the input and the output, respectively. The structure matrix $J(x,t) \in \mathbb{R}^{n\times n}$ and the dissipation matrix $R(x,t) \in \mathbb{R}^{n\times n}$ are skew-symmetric and symmetric positive semi-definite for all x and t, respectively. Here $w(t) \in \mathbb{R}^r$ is a standard Wiener process defined on a probability space $(\Omega, \mathcal{F}, \mathcal{P})$. A sufficiently differentiable function $h(x,t) \in \mathbb{R}^{n\times r}$ represents the noise port. We suppose that Hamiltonian $H(x,u,t)$ is a sufficiently differentiable function and $h(0,t) = 0$. Moreover, $h(x,t)$ satisfies reasonable sufficient conditions for the local existence and uniqueness of the solutions.

Firstly, we show a property of the variational system of the stochastic Hamiltonian system (6.11).

Theorem 6.2 *Consider the stochastic Hamiltonian system in* (6.11). *Suppose that J and R are constant matrices. Then the variational system of the system* (6.11) *is described by another linear stochastic Hamiltonian system:*

$$\begin{cases} \mathrm{d}x &= (J(x,t) - R(x,t)) \dfrac{\partial H(x,u,t)}{\partial x}^{\top} \mathrm{d}t + h(x,t)\,\mathrm{d}w \ , \quad x(0) = x_0 \\ \mathrm{d}x_v &= (J - R) \dfrac{\partial H_v(x,u,x_v,u_v t)}{\partial x_v}^{\top} \mathrm{d}t + \displaystyle\sum_{i=1}^{r} \dfrac{\partial h_i(x,t)}{\partial x} x_v \,\mathrm{d}w^i \ , \quad x_v(0) = x_{v,0} \\ y_v &= -\dfrac{\partial H_v(x,u,x_v,u_v,t)}{\partial u_v}^{\top} \end{cases} , \tag{6.12}$$

where a Hamiltonian is given by

$$H_v(x,u,x_v,u_v,t) = \frac{1}{2}\begin{pmatrix} x_v \\ u_v \end{pmatrix}^{\top} \frac{\partial^2 H(x,u,t)}{\partial (x,u)^2} \begin{pmatrix} x_v \\ u_v \end{pmatrix} .$$

Proof This theorem can be proven in a similar manner as Theorem 1 in [27]. According to the definition of the variational system in (6.2), the variational system of the stochastic Hamiltonian system (6.11) is obtained as

$$
\begin{aligned}
\mathrm{d}x_v &= \frac{\partial}{\partial x}\left((J-R)\frac{\partial H}{\partial x}^{\top}\right) x_v\,\mathrm{d}t + \frac{\partial}{\partial u}\left((J-R)\frac{\partial H}{\partial x}^{\top}\right) u_v\,\mathrm{d}t + \sum_{i=1}^{r}\frac{\partial h_i}{\partial x} x_v\,\mathrm{d}w^i \\
&= (J-R,\ O_{nn})\frac{\partial^2 H}{\partial (x,u)^2}\begin{pmatrix} x_v \\ u_v \end{pmatrix}\mathrm{d}t + \sum_{i=1}^{r}\frac{\partial h_i}{\partial x} x_v\,\mathrm{d}w^i \\
&= (J-R,\ O_{nn})\left(\frac{\partial}{\partial (x_v,u_v)}\left\{\frac{1}{2}\begin{pmatrix} x_v \\ u_v \end{pmatrix}^{\top}\frac{\partial^2 H}{\partial (x,u)^2}\begin{pmatrix} x_v \\ u_v \end{pmatrix}\right\}\right)^{\top}\mathrm{d}t + \sum_{i=1}^{r}\frac{\partial h_i}{\partial x} x_v\,\mathrm{d}w^i \\
&= (J-R)\frac{\partial H_v}{\partial x_v}^{\top}\mathrm{d}t + \sum_{i=1}^{r}\frac{\partial h_i}{\partial x} x_v\,\mathrm{d}w^i. \qquad (6.13)
\end{aligned}
$$

Then let us calculate the output y_v from Eq. (6.3) in a similar calculation as Eq. (6.13) as

$$
\begin{aligned}
y_v &= -\frac{\partial}{\partial x}\left(\frac{\partial H}{\partial u}\right)^{\top} x_v + \frac{\partial}{\partial u}\left(\frac{\partial H}{\partial u}\right)^{\top} u_v \\
&= (O_{nn}, -I_n)\frac{\partial^2 H}{\partial (x,u)^2}\begin{pmatrix} x_v \\ u_v \end{pmatrix} \\
&= (O_{nn}, -I_n)\left(\frac{\partial H_v}{\partial (x_v,u_v)}\right)^{\top} \\
&= -\frac{\partial H_v}{\partial u_v}^{\top}. \qquad (6.14)
\end{aligned}
$$

Equations (6.13) and (6.14) prove the theorem. ■

Remark 6.3 Theorem 6.2 reduces to Lemma 2.1 for the deterministic Hamiltonian systems in (2.1) as a special case.

Finally, we derive conditions under which an adjoint system of the stochastic Hamiltonian system (6.11) coincides with the time-reversal version of its variational one. This property is an extension of variational symmetry in Lemma 2.2.

Theorem 6.3 *Consider the stochastic Hamiltonian system in* (6.11). *Suppose that J and R are constant matrices and that $J-R$ is nonsingular. Furthermore, suppose that there exists a nonsingular matrix $T \in \mathbb{R}^{n\times n}$ satisfying*

$$J = -TJT^{-1}, \quad R = TRT^{-1} \qquad (6.15)$$

$$\frac{\partial^2 H(x,u,t)}{\partial (x,u)^2} = \begin{pmatrix} T & O_{nn} \\ O_{nn} & I_n \end{pmatrix}\frac{\partial^2 H(x,u,t)}{\partial (x,u)^2}\begin{pmatrix} T^{-1} & O_{nn} \\ O_{nn} & I_n \end{pmatrix} \qquad (6.16)$$

$$(J-R)T\frac{\partial h_i(x,t)}{\partial x}^{\top}T^{-1}(J-R)^{-1}\frac{\partial h_i(x,t)}{\partial x} = O_{nn}, \qquad (i = 1, 2, \cdots, r). \qquad (6.17)$$

Then there exist the following processes $z_i,\ i=1,2,\cdots,r$ in the adjoint system in (6.5)

$$z_i = -T^{-1}(J-R)^{-1}\frac{\partial h_i(x,t)}{\partial x}(J-R)Tx_a, \qquad (i=1,2,\cdots,r), \tag{6.18}$$

and the dynamics of the adjoint system of the stochastic Hamiltonian system coincides with the time-reversal version of its variational one in (6.12)*.*

Proof This theorem can be proven in a similar manner as Theorem 1 in [27]. According to the definition of the adjoint system in (6.5), the adjoint system of the stochastic Hamiltonian system (6.11) is obtained as

$$\begin{aligned} \mathrm{d}x_a &= -\frac{\partial}{\partial x}\left((J-R)\frac{\partial H}{\partial x}^\top\right)^\top x_a\,\mathrm{d}t + \frac{\partial}{\partial x}\left(\frac{\partial H}{\partial u}^\top\right)^\top u_a\,\mathrm{d}t - \sum_{i=1}^r \frac{\partial h_i}{\partial x}^\top z_i\,\mathrm{d}t + \sum_{i=1}^r z_i\,\mathrm{d}w^i \\ &= (-I_n,\ O_{nn})\left[\begin{pmatrix} J-R & O_{nn} \\ O_{nn} & -I_n\end{pmatrix}\frac{\partial^2 H}{\partial (x,u)^2}\right]^\top \begin{pmatrix} x_a \\ u_a\end{pmatrix}\mathrm{d}t - \sum_{i=1}^r \frac{\partial h_i}{\partial x}^\top z_i\,\mathrm{d}t + \sum_{i=1}^r z_i\,\mathrm{d}w^i. \end{aligned} \tag{6.19}$$

The output y_a can be calculated as

$$\begin{aligned} y_a &= \frac{\partial}{\partial u}\left((J-R)\frac{\partial H}{\partial x}^\top\right)^\top x_a - \frac{\partial}{\partial u}\left(\frac{\partial H}{\partial u}\right)^\top u_a \\ &= (O_{nn},\ I_n)\left[\begin{pmatrix} J-R & O_{nn} \\ O_{nn} & -I_n\end{pmatrix}\frac{\partial^2 H}{\partial (x,u)^2}\right]^\top \begin{pmatrix} x_a \\ u_a\end{pmatrix}. \end{aligned} \tag{6.20}$$

Here let us transform the system (6.19) by a coordinate transformation $\bar{x}_a = -(J-R)Tx_a$. Then the dynamics of the transformed system is calculated by the Itô formula in Appendix C.1 as (see also Eq. (4.4))

$$\begin{aligned} \mathrm{d}\bar{x}_a &= -(J-R)T\left((-I_n, O_{nn})\left[\begin{pmatrix} J-R & O_{nn} \\ O_{nn} & -I_n\end{pmatrix}\frac{\partial^2 H}{\partial (x,u)^2}\right]^\top \begin{pmatrix} x_a \\ u_a\end{pmatrix}\mathrm{d}t - \sum_{i=1}^r \frac{\partial h_i}{\partial x}^\top z_i\,\mathrm{d}t + \sum_{i=1}^r z_i\,\mathrm{d}w^i\right) \\ &\quad + \frac{1}{2}\begin{pmatrix} \mathrm{tr}\left\{\mathcal{D}^2_{x_a}(-(J-R)^1 T x_a) z z^\top\right\} \\ \vdots \\ \mathrm{tr}\left\{\mathcal{D}^2_{x_a}(-(J-R)^n T x_a) z z^\top\right\}\end{pmatrix}\mathrm{d}t \\ &= -(J-R, O_{nn})\begin{pmatrix} -T & O_{nn} \\ O_{nn} & -I_n\end{pmatrix}\frac{\partial^2 H}{\partial (x,u)^2}\begin{pmatrix} -(J+R) & O_{nn} \\ O_{nn} & -I_n\end{pmatrix}\begin{pmatrix} x_a \\ u_a\end{pmatrix}\mathrm{d}t + \sum_{i=1}^r (J-R)T\frac{\partial h_i}{\partial x}^\top z_i\,\mathrm{d}t \\ &\quad - \sum_{i=1}^r (J-R)Tz_i\,\mathrm{d}w^i \end{aligned}$$

$$
\begin{aligned}
&= -(J-R,\ O_{nn})\begin{pmatrix} -T & O_{nn} \\ O_{nn} & -I_n \end{pmatrix}\frac{\partial^2 H}{\partial(x,u)^2}\begin{pmatrix} -T^{-1} & O_{nn} \\ O_{nn} & -I_n \end{pmatrix}\begin{pmatrix} T(J+R) & O_{nn} \\ O_{nn} & I_n \end{pmatrix}\begin{pmatrix} x_a \\ u_a \end{pmatrix}\mathrm{d}t \\
&\quad + \sum_{i=1}^{r}(J-R)T\frac{\partial h_i}{\partial x}^{\top} z_i\,\mathrm{d}t - \sum_{i=1}^{r}(J-R)Tz_i\,\mathrm{d}w^i \\
&= -(J-R,\ O_{nn})\begin{pmatrix} T & O_{nn} \\ O_{nn} & I_n \end{pmatrix}\frac{\partial^2 H}{\partial(x,u)^2}\begin{pmatrix} T^{-1} & O_{nn} \\ O_{nn} & I_n \end{pmatrix}\begin{pmatrix} -(J-R)Tx_a & O_{nn} \\ O_{nn} & u_a \end{pmatrix}\mathrm{d}t \\
&\quad + \sum_{i=1}^{r}(J-R)T\frac{\partial h_i}{\partial x}^{\top} z_i\,\mathrm{d}t - \sum_{i=1}^{r}(J-R)Tz_i\,\mathrm{d}w^i \\
&= -(J-R,\ O_{nn})\begin{pmatrix} T & O_{nn} \\ O_{nn} & I_n \end{pmatrix}\frac{\partial^2 H}{\partial(x,u)^2}\begin{pmatrix} T^{-1} & O_{nn} \\ O_{nn} & I_n \end{pmatrix}\begin{pmatrix} \bar{x}_a \\ u_a \end{pmatrix}\mathrm{d}t \\
&\quad + \sum_{i=1}^{r}(J-R)T\frac{\partial h_i}{\partial x}^{\top} T^{-1}(J-R)^{-1}\frac{\partial h_i}{\partial x}\bar{x}_a\,\mathrm{d}t - \sum_{i=1}^{r}\frac{\partial h_i}{\partial x}\bar{x}_a\,\mathrm{d}w^i.
\end{aligned}
$$

Here the fourth equality follows from

$$
\begin{aligned}
T(J+R) &= (TJT^{-1} + TRT^{-1})T \\
&= -(J-R)T
\end{aligned}
$$

with the condition (6.15) and the last equality follows from Eq. (6.18). The conditions (6.16) and (6.17) and Eq. (6.18) yield

$$
\mathrm{d}\bar{x}_a = -(J-R, O_{nn})\frac{\partial^2 H(x,u,t)}{\partial(x,u)^2}\begin{pmatrix} \bar{x}_a \\ u_a \end{pmatrix}\mathrm{d}t - \sum_{i=1}^{r}\frac{\partial h_i(x,t)}{\partial x}\bar{x}_a\,\mathrm{d}w^i. \tag{6.21}
$$

It follows from Eq. (6.20) with a similar calculation, that

$$
\begin{aligned}
y_a &= -(O_{nn},\ I_n)\ \frac{\partial^2 H(x,u,t)}{\partial(x,u)^2}\begin{pmatrix} \bar{x}_a \\ u_a \end{pmatrix} \\
&= -\frac{\partial H_v(x,u,\bar{x}_a,u_a,t)}{\partial u_a}^{\top}.
\end{aligned} \tag{6.22}
$$

Theorem is immediately proven by comparing Eqs. (6.21) and (6.22) with the dynamics of the variational system in (6.12). ■

Remark 6.4 In Theorem 6.3, conditions (6.15) and (6.16) are the same as those assumed in Lemma 2.2 and the other one (6.17) is required only for the stochastic Hamiltonian system. The nonsingular matrix (2.27) equipped in Lemma2.2 satisfies the conditions (6.15) and (6.16) as in Lemma 2.2. Here let us check how strict the condition (6.17) is by a case study of the following typical mechanical system with noise, which we are mainly interested in for optimal gait generation of walking robots (see Chapters 2 and 3)

$$\begin{cases} \begin{pmatrix} \mathrm{d}q \\ \mathrm{d}p \end{pmatrix} = \begin{pmatrix} O_{mm} & I_m \\ -I_m & -R_D \end{pmatrix} \begin{pmatrix} \dfrac{\partial H(q,p,u,t)}{\partial q}^{\top} \\ \dfrac{\partial H(q,p,u,t)}{\partial p}^{\top} \end{pmatrix} \mathrm{d}t + \begin{pmatrix} O_{mm} \\ I_m \end{pmatrix} u\,\mathrm{d}t + \begin{pmatrix} O_{md} \\ h_p(q,p,t) \end{pmatrix} \mathrm{d}w \\ y = -\dfrac{\partial H(q,p,u,t)}{\partial u}^{\top} = q \end{cases} \tag{6.23}$$

with the state $x := (q^\top, p^\top)^\top \in \mathbb{R}^{2m}$ and the Hamiltonian

$$H(q,p,u,t) = \frac{1}{2} p^\top M(q)^{-1} p + V(q,t) - u^\top q. \tag{6.24}$$

Here a positive definite matrix $M(q) \in \mathbb{R}^{m\times m}$ denotes the inertia matrix. A positive semi-definite matrix $R_D \in \mathbb{R}^{m\times m}$ denotes the friction coefficients and a scalar function $V(q,t) \in \mathbb{R}$ denotes the potential energy of the system. $w(t) \in \mathbb{R}^r$ denotes a standard Wiener process and $h_p(q,p,t) \in \mathbb{R}^{m\times r}$ represents the noise port.

Since we have

$$\frac{\partial h_i(q,p,t)}{\partial x} = \begin{pmatrix} O_{mm} & O_{mm} \\ \frac{\partial h_{p,i}}{\partial q} & \frac{\partial h_{p,i}}{\partial p} \end{pmatrix}$$

$$(J-R)^{-1} = \begin{pmatrix} -R_D & -I_m \\ I_m & O_{mm} \end{pmatrix},$$

the condition (6.17) is reduced to

$$\begin{aligned} &(J-R) T \frac{\partial h_i}{\partial x}^{\top} T^{-1} (J-R)^{-1} \frac{\partial h_i}{\partial x} \\ &= \begin{pmatrix} O_{mm} & I_m \\ -I_m & -R_D \end{pmatrix} \begin{pmatrix} I_m & O_{mm} \\ O_{mm} & -I_m \end{pmatrix} \begin{pmatrix} O_{mm} & \frac{\partial h_{p,i}}{\partial q}^{\top} \\ O_{mm} & \frac{\partial h_{p,i}}{\partial p}^{\top} \end{pmatrix} \begin{pmatrix} I_m & O_{mm} \\ O_{mm} & -I_m \end{pmatrix} \begin{pmatrix} -R_D & -I_m \\ I_m & O_{mm} \end{pmatrix} \begin{pmatrix} O_{mm} & O_{mm} \\ \frac{\partial h_{p,i}}{\partial q} & \frac{\partial h_{p,i}}{\partial p} \end{pmatrix} \\ &= \begin{pmatrix} O_{mm} & I_m \\ -I_m & -R_D \end{pmatrix} \begin{pmatrix} O_{mm} & \frac{\partial h_{p,i}}{\partial q}^{\top} \\ O_{mm} & -\frac{\partial h_{p,i}}{\partial p}^{\top} \end{pmatrix} \begin{pmatrix} -\frac{\partial h_{p,i}}{\partial q} & -\frac{\partial h_{p,i}}{\partial p} \\ O_{mm} & O_{mm} \end{pmatrix} \\ &= O_{2m2m}. \end{aligned} \tag{6.25}$$

Equation (6.25) implies that the condition (6.17) always holds for the typical mechanical system with noise in (6.23) with any noise port $h_p(q,p,t)$.

6.3 Summary

This chapter has introduced the variational and its adjoint systems of stochastic Hamiltonian systems and has revealed some of their properties. Firstly, we have defined the variational and its adjoint systems of general nonlinear stochastic systems and have clarified their input-output relation which is an extension of that in deterministic systems. Secondly, we have shown that a variational system of a stochastic Hamiltonian system is described by another linear one. Finally, we have derived conditions under which the adjoint system coincides with the time-reversal version of the variational one. This property is an extension of variational symmetry of deterministic Hamiltonian systems, which plays an important role in learning optimal control proposed in Chapters 2 and 3.

Chapter 7

Conclusion

The ultimate goal of this thesis is to propose a novel optimal gait generation framework based on physical property and learning control with stochastic control theory. This thesis consists of two parts: control of deterministic Hamiltonian systems and that of stochastic Hamiltonian systems. In the former part, we have proposed an extension of iterative learning control of Hamiltonian systems to deal with the optimal gait generation problem. In the latter part, we have introduced a stochastic Hamiltonian system and have clarified some useful properties of the system.

Chapter 2 has proposed an iterative learning control type optimal gait generation framework based on variational symmetry of Hamiltonian systems. This method allows one to take discontinuous state transitions during learning into account. The proposed framework is expected to generate an optimal periodic gait trajectory which minimizes the L_2 norm of the control input and it does not require the information of the robot model nor the transition mapping. Applying the proposed method to the compass gait biped, we have generated an optimal gait trajectory on the level ground. Numerical simulations have demonstrated the effectiveness of the proposed framework.

Chapter 3 has proposed a repetitive control type optimal gait generation framework by utilizing learning optimal control of Hamiltonian systems and virtual constraints. Virtual constraints restrict the motion of the robot to a symmetric trajectory and prevent the robot from falling. The proposed method updates the control input by ILC and simultaneously mitigates the strength of the virtual constraints by IFT according to the progress of learning. As a result, the robot improves his walk keeping on walking and an optimal periodic walking trajectory without constraints is expected to be generated eventually. Numerical simulations have exhibited the validity of the proposed framework.

Chapter 4 has introduced stochastic port-Hamiltonian systems and has clarified some of their properties. Firstly, we have shown a necessary and sufficient condition to preserve the stochastic Hamiltonian structure of the original system under coordinate transformations. Secondly, a condition to maintain stochastic passivity of the system has been derived. Thirdly, stochastic generalized canonical transformations have been introduced. Fourthly, we have proposed a stabilization method based on passivity and stochastic generalized canonical transformations. Finally, numerical simulations have demonstrated the effectiveness of the proposed method.

Chapter 5 has introduced an observer based stochastic trajectory tracking control of mechanical systems. We have derived conditions for the controller and observer gains under which the set of tracking and estimation errors remains bounded in probability and the margin of error is assignable. The stochastic bounded stability has been proven by utilizing supermartingale property. Numerical simulations have shown the effectiveness of the proposed method.

Chapter 6 has introduced the variational and its adjoint systems of stochastic Hamiltonian systems and has revealed some of their properties. Firstly, we have defined the variational and its adjoint systems of general nonlinear stochastic systems and have clarified their input-output relation which is an extension of that in deterministic systems. Secondly, we have shown that a variational system of a stochastic Hamiltonian system is described by another linear one. Finally, we have derived conditions under which the adjoint system coincides with the time-reversal version of the variational one. This property is an extension of variational symmetry of deterministic Hamiltonian systems, which plays an important role in learning optimal control proposed in Chapters 2 and 3.

This thesis provides a new perspective to the optimal gait generation problem from the stochastic control view point. However there are a lot of open problems in this field. We will continue to complete a novel learning framework based on the above extended properties of stochastic Hamiltonian systems and stochastic stabilization and trajectory tracking methods proposed here. We will also execute laboratory experiments with real walking robots as a future work. The author believes that the results obtained in this thesis provide a useful framework for optimal motion planning problems of mechanical systems and a new application of stochastic control.

Appendix A

ZMP Calculation for the compass gait biped with a torso

Let us calculate the ZMP of the compass gait biped with a torso depicted in Fig. A.1. It is the same model as in Fig. 3.4, but here we equip the Z-axis which completes the right-handed coordinate system X-Y-Z. Let us denote the ZMP position vector as r_{ZMP}, the ground reaction force

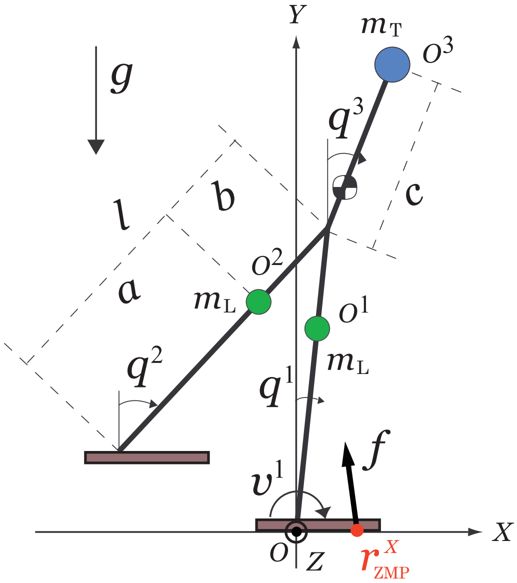

Figure A.1: The compass gait biped and the reaction force acting on its sole

acting on the robot at the ZMP as f, the reaction moment about the origin O as τ, the external torque about the origin as τ_e, the momentum of the robot as σ_p and the gravity acceleration vector as $\boldsymbol{g}$. Then we have the following relations:

$$\tau_e = r_{ZMP} \times f + \tau$$
$$\dot{\sigma_p} = (2m_L + m_T)\boldsymbol{g} + f$$

and they yield

$$\tau_e = r_{ZMP} \times (\dot{\sigma}_p - (2m_L + m_T)\boldsymbol{g}) + \tau. \tag{A.1}$$

Since the planner walking robot is considered, and the horizontal components of the reaction moment at the ZMP are zero, we can write $r_{ZMP} = (r^X_{ZMP}, 0, 0)$, $f = (f^1, f^2, 0)$, $\tau = (0, \tau^2, 0)$ and $\sigma_p = (\sigma^1_p, \sigma^2_p, 0)$. Then we can calculate Eq. (A.1) as

$$\begin{aligned}\begin{pmatrix} 0 \\ 0 \\ -v^1 \end{pmatrix} &= \begin{pmatrix} r^X_{ZMP} \\ 0 \\ 0 \end{pmatrix} \times \begin{pmatrix} \dot{\sigma}^1_p \\ \dot{\sigma}^2_p + (2m_L + m_T)g \\ 0 \end{pmatrix} + \begin{pmatrix} 0 \\ \tau^2 \\ 0 \end{pmatrix} \\ &= \begin{pmatrix} 0 \\ \tau^2 \\ r^X_{ZMP}(\dot{\sigma}^2_p + (2m_L + m_T)g) \end{pmatrix}. \end{aligned} \tag{A.2}$$

Equation (A.2) yields the ZMP position in the x-axis r^X_{ZMP} as

$$r^X_{ZMP} = -\frac{v^1}{\dot{\sigma}^2_p + (2m_L + m_T)g}. \tag{A.3}$$

Let us calculate the momentum of the robot σ_p. From Fig. 3.4, The position vector of each mass is given by

$$\overrightarrow{OO^1} = \begin{pmatrix} a \sin q^1 \\ a \cos q^1 \\ 0 \end{pmatrix}$$

$$\overrightarrow{OO^2} = \begin{pmatrix} l \sin q^1 - b \sin q^2 \\ l \cos q^1 - b \cos q^2 \\ 0 \end{pmatrix}$$

$$\overrightarrow{OO^3} = \begin{pmatrix} l \sin q^1 + c \cos q^3 \\ l \cos q^1 + c \sin q^3 \\ 0 \end{pmatrix}.$$

Then their velocities can be calculated as

$$\dot{\overrightarrow{OO^1}} = \begin{pmatrix} a\dot{q}^1 \cos q^1 \\ -a\dot{q}^1 \sin q^1 \\ 0 \end{pmatrix}$$

$$\dot{\overrightarrow{OO^2}} = \begin{pmatrix} l\dot{q}^1 \cos q^1 - b\dot{q}^2 \cos q^2 \\ -l\dot{q}^1 \sin q^1 + b\dot{q}^2 \sin q^2 \\ 0 \end{pmatrix}$$

$$\dot{\overrightarrow{OO^3}} = \begin{pmatrix} l\dot{q}^1 \cos q^1 - c\dot{q}^3 \sin q^3 \\ -l\dot{q}^1 \sin q^1 + c\dot{q}^3 \cos q^3 \\ 0 \end{pmatrix}.$$

Then we have

$$\sigma_p = m_L\dot{\overrightarrow{OO^1}} + m_L\dot{\overrightarrow{OO^2}} + m_T\dot{\overrightarrow{OO^3}} \tag{A.4}$$

$$= \begin{pmatrix} (m_La + m_Ll + m_Tl)\dot{q}^1\cos q^1 - m_Lb\dot{q}^2\cos q^2 - m_Tc\dot{q}^3\sin q^3 \\ -(m_La + m_Ll + m_Tl)\dot{q}^1\sin q^1 + m_Lb\dot{q}^2\sin q^2 + m_Tc\dot{q}^3\cos q^3 \\ 0 \end{pmatrix} \tag{A.5}$$

It follows from From Eqs. (A.3) and (A.5) that

$$r^X_{ZMP} = \frac{-v^1}{\dot{\sigma_p}^2 + (2m_L + m_T)g} \quad \text{, where}$$

$$\dot{\sigma_p}^2 = -(m_La + m_Ll + m_Tl)(\ddot{q}^1\sin q^1 + (\dot{q}^1)^2\cos q^1) + m_Lb(\ddot{q}^2\sin q^2 + (\dot{q}^2)^2\cos q^2)$$
$$+ m_Tc(\ddot{q}^3\cos q^3 - (\dot{q}^3)^2\sin q^3). \tag{A.6}$$

In the case of the compass gait biped depicted in Fig. 2.1, the ZMP position in the x-axis r^X_{ZMP} can be calculated by Eq. (A.6) with $c = 0$ and $m_T = m_H$ as

$$r^X_{ZMP} = \frac{-v^1}{\dot{\sigma_p}^2 + (2m_L + m_H)g} \quad \text{, where}$$

$$\dot{\sigma_p}^2 = -(m_La + m_Ll + m_Hl)(\ddot{q}^1\sin q^1 + (\dot{q}^1)^2\cos q^1) + m_Lb(\ddot{q}^2\sin q^2 + (\dot{q}^2)^2\cos q^2).$$

Appendix B

Nonholonomic Hamiltonian systems

Here we refer to a mechanical system with nonholonomic constraints, e.g. [89, 26, 7]. Such system can be described by a Hamiltonian system with Lagrangian multipliers

$$\begin{cases} \dot{q} &= \dfrac{\partial H(q,p_0)}{\partial p_0}^\top \\ \dot{p}_0 &= -\dfrac{\partial H(q,p_0)}{\partial u}^\top + A(q)\lambda + B(q)u \\ y &= B(q)^\top \dfrac{\partial H(q,p_0)}{\partial p_0}^\top \\ O_{(m-l)1} &= A(q)^\top \dfrac{\partial H(q,p_0)}{\partial p_0}^\top \end{cases},$$

where $x = (q, p_0) \in \mathbb{R}^{2m}$ denotes the state, the Hamiltonian is defined by $H(q, p_0) := p_0^\top M_0(q)^{-1} p_0$ with an inertia matrix $M_0(q) > 0$, and $A(q)\lambda$ and $B(q)u$ denote the constraint force and the external force, respectively with matrices $A(q) \in \mathbb{R}^{m\times(m-l)}$, $B(q) \in \mathbb{R}^{m\times l}$, $m > l$ and the Lagrangian multiplier $\lambda \in \mathbb{R}^{m-l}$. Appropriate controllability of this system is assumed in what follows.

It was shown in [89] that this Hamiltonian system with constraints can be described by the following port-Hamiltonian system:

$$\begin{cases} \begin{pmatrix} \dot{q} \\ \dot{p} \end{pmatrix} = \begin{pmatrix} O_{mm} & J_{12}(q) \\ -J_{12}(q)^\top & J_{22}(q,p) \end{pmatrix} \begin{pmatrix} \dfrac{\partial H(q,p)}{\partial q}^\top \\ \dfrac{\partial H(q,p)}{\partial p}^\top \end{pmatrix} + \begin{pmatrix} O_{mm} \\ G(q) \end{pmatrix} u \\ y \quad = G(q)^\top \dfrac{\partial H(q,p)}{\partial p}^\top \end{cases} \tag{B.1}$$

with a Hamiltonian

$$H(q,p) = \frac{1}{2} p^\top M(q)^{-1} p,$$

where $p \in \mathbb{R}^l$ and $M(q) \in \mathbb{R}^{l\times l}$.

Appendix C

Some theorems with respect to stochastic control

Let us refer to some theorems which are utilized in this thesis. Here we suppose a general nonlinear stochastic system described by the following stochastic differential equation written in the sense of Itô,

$$\begin{cases} \mathrm{d}x &= f(x,u,t)\,\mathrm{d}t + h(x,t)\,\mathrm{d}w \\ y &= s(x,u,t) \end{cases}, \tag{C.1}$$

where $f : \mathbb{R}^n \times \mathbb{R}^m \times \mathbb{R} \to \mathbb{R}^n, h : \mathbb{R}^n \times \mathbb{R} \to \mathbb{R}^{n\times r}$ and $s : \mathbb{R}^n \times \mathbb{R}^m \times \mathbb{R} \to \mathbb{R}^m$ are sufficiently differentiable functions and they satisfy $f(0,0,t) = 0$, $h(0,t) = 0$ and $s(0,0,t) = 0$, respectively.

C.1 Itô formula

Consider the system (C.1) and a scalar function $V(x,t)$ whose partial derivatives up to order 2 in x and order 1 in t are continuous, respectively. Then the Itô formula [42, 57] states that

$$\mathrm{d}V(x,t) = \left[\frac{\partial V(x,t)}{\partial t} + \frac{\partial V(x,t)}{\partial x} f(x,u,t) + \frac{1}{2}\,\mathrm{tr}\left\{\frac{\partial}{\partial x}\left(\frac{\partial V(x,t)}{\partial x}\right)^{\top} h(x,t)h(x,t)^{\top}\right\}\right]\mathrm{d}t + \frac{\partial V(x,t)}{\partial x} h(x,t)\,\mathrm{d}w.$$

C.2 Stochastic versions of LaSalle's theorem

Let us refer to the stochastic versions of LaSalle's theorem [49, 16, 51]. Firstly, we consider the time-invariant version of the system (C.1) (see the system in (4.12)).

Theorem C.1 *[49, 16] Assume there exists a positive definite function $V(x)$ such that its partial derivative up to order 2 in x is continuous and that $\mathcal{L}V(x) \le 0$ for any $x \in \mathbb{R}^n$. Then the sample path $x(t)$ tends in probability to the largest invariant set whose support is contained in the locus $\mathcal{L}V(x) = 0$ for any $t \ge 0$.*

Then, we consider the time-varying system (C.1).

Theorem C.2 *[51] Assume there exists a positive definite function $V(x,t)$ whose partial derivatives up to order 2 in x and order 1 in t are continuous, respectively, and a function $\gamma \in L_1$ and a continuous function ω such that*

$$\lim_{\|x\|\to\infty} \inf_{0\le t<\infty} V(x,t) = \infty$$

and

$$\mathcal{L}V(x,t) \le \gamma(t) - \omega(x)$$

Moreover, for each initial state $x_0 \in \mathbb{R}^n$ there is a $d > 2$ such that

$$\sup_{0\le t<\infty} E[\|x(t)\|^d] < \infty. \tag{C.2}$$

Then, for every $x_0 \in \mathbb{R}^n$,

$$\lim_{t\to\infty} V(x,t)$$

exists and is finite almost surely and

$$\lim_{t\to\infty} \omega(x) = 0$$

almost surely.

Remark C.1 [51]

The conclusions of Theorem C.2 still hold if the condition (C.2) is replaced by one of the following:

(i) $h(x,t)$ is bounded.

(ii) Almost every sample path of

$$\int_0^t h(x(\tau),\tau)\,\mathrm{d}w(\tau)$$

is uniformly continuous on $t \ge 0$.

Bibliography

[1] S. Arimoto, S. Kawamura, and F. Miyazaki. Bettering operation of robotics. *Journal of Robotic Systems*, 1(2):123–140, 1984.

[2] F. Asano and Z. W. Luo. Energy-efficient and high-speed dynamic biped locomotion based on principle of parametric excitation. *IEEE Trans. Robotics*, 24(6):1289–1301, 2008.

[3] F. Asano, M. Yamakita, N. Kamamichi, and Z. W. Luo. A novel gait generation for biped walking robots based on mechanical energy constraint. *IEEE Trans. Robotics and Automation*, 20(3):565–573, 2004.

[4] H. Berghuis. *Model-based robot control: From theory to practice*. PhD thesis, Univ. Twente, Enschede, The Netherlands, 1993.

[5] H. Berghuis and H. Nijmeijer. A passivity approach to controller-observer design for robots. *IEEE Trans. Robotics and Automation*, 9(6):740–754, 1993.

[6] J. M. Bismut. An introductory approach to duality in optimal stochastic control. *SIAM Review*, 20:62–78, 1978.

[7] A. M. Bloch. *Nonholonomic Mechanics and Control*. Springer-Verlag, New York, 2003.

[8] R. B. Brockett. Asymptotic stability and feedback stabilization. In R. W. Brockett, R. S. Millmann, and H. J. Sussmann, editors, *Differential Geometric Control Theory*, pages 181–191. Birkhäuser, Basel-Boston, 1983.

[9] F. De Bruyne, B. D. O. Anderson, M. Gevers, and N. Linard. Iterative controller optimization for nonlinear systems. In *Proc. 36th IEEE Conf. on Decision and Control*, volume 4, pages 3749–3754, 1997.

[10] R. S. Bucy. Stability and positive supermartingales. *J. Differential Equations*, 1(2):151–155, 1965.

[11] C. I. Byrnes, A. Isidori, and J. C. Willems. Passivity, feedback equivalence, and the global stabilization of minimum phase nonlinear systems. *IEEE Trans. Autom. Contr.*, 36(11):1228–1240, 1991.

[12] Y. Chen and C. Wen. *Iterative Learning Control: Convergence, Robustness and Applications*, volume 248 of *Lecture Notes on Control and Information Science*. Springer-Verlag, 1999.

[13] P. E. Crouch and A. J. van der Schaft. *Variational and Hamiltonian Control Systems*, volume 101 of *Lecture Notes on Control and Information Science*. Springer-Verlag, Berlin, 1987.

[14] H. Deng and M. Krstić. Output-feedback stochastic nonlinear stabilization. *IEEE Trans. Autom. Contr.*, 44(2):328–333, 1999.

[15] E. B. Dynkin. *Markov Processes*. Springer, Berlin, 1965.

[16] P. Florchinger. A passive system approach to feedback stabilization of nonlinear control stochastic systems. *SIAM J. Control Optim.*, 37(6):1848–1864, 1999.

[17] K. Fujimoto, T. Horiuchi, and T. Sugie. Optimal control of Hamiltonian systems with input constraints via iterative learning. In *Proc. 42nd IEEE Conf. on Decision and Control*, pages 4387–4392, 2003.

[18] K. Fujimoto, T. Horiuchi, and T. Sugie. Iterative learning optimal control of hamiltonian systems based on variational symmetry. *Trans. the Institute of Systems Control and Information Engineers*, 21(1):10–17, 2008. (in Japanese).

[19] K. Fujimoto and I. Koyama. Iterative feedback tuning for Hamiltonian systems. In *Proc. 17th IFAC World Congress*, pages 15678–15683, 2008.

[20] K. Fujimoto, K. Sakurama, and T. Sugie. Trajectory tracking control of port-controlled Hamiltonian systems via generalized canonical transformations. *Automatica*, 39(12):2059–2069, 2003.

[21] K. Fujimoto and S. Satoh. On repetitive control of Hamiltonian systems based on variational symmetry. In *Proc. Mathematical Theory of Networks and Systems*, 2006.

[22] K. Fujimoto and S. Satoh. On repetitive control of hamiltonian systems based on variational symmetry. *Trans. the Society of Instrument and Control Engineers*, 43(8):711–713, 2007. (in Japanese).

[23] K. Fujimoto and T. Sugie. Stabilization of a class of Hamiltonian systems with nonholonomic constraints via canonical transformations. In *Proc. European Control Conference*, 1999.

[24] K. Fujimoto and T. Sugie. Stabilization of a class of nonholonomic systems via generalized canonical transformations. *Trans. Society of Instrument and Control Engineers*, 36(9):749–756, 2000. (in Japanese).

[25] K. Fujimoto and T. Sugie. Canonical transformation and stabilization of generalized Hamiltonian systems. *Systems & Control Letters*, 42(3):217–227, 2001.

[26] K. Fujimoto and T. Sugie. Stabilization of Hamiltonian systems with nonholonomic constraints based on time-varying generalized canonical transformations. *Systems & Control Letters*, 44(4):309–319, 2001.

[27] K. Fujimoto and T. Sugie. Iterative learning control of Hamiltonian systems: I/O based optimal control approach. *IEEE Trans. Autom. Contr.*, 48(10):1756–1761, 2003.

[28] G. Gaeta and N. R. Quintero. Lie-point symmetries and stochastic differential equations. *J. Phys. A: Math. Gen.*, 32:8485–8505, 1999.

[29] J. Ghosh and B. Paden. Nonlinear repetitive control. *IEEE Trans. Autom. Contr.*, AC-45(5):949–954, 2000.

[30] A. Goswami, B. Espiau, and A. Keramane. Limit cycles in a passive compass gait biped and passivity-mimicking control laws. *Autonomous Robots*, 4(3):273–286, 1997.

[31] A. Goswami, B. Thuilot, and B. Espiau. Compass-like biped robot part i: Stability and bifurcation of passive gaits. *INRIA Research Report*, (2996), 1996.

[32] J. W. Grizzle, G. Abba, and F. Plestan. Asymptotically stable walking for biped robots: analysis via systems with impulse effects. *IEEE Trans. Autom. Contr.*, 46(1):51–64, 2001.

[33] S. Hara, Y. Yamamoto, T. Omata, and M. Nakano. Repetitive control system: A new type servo system for periodic exogenous signals. *IEEE Trans. Automatic Control*, 33(7):659–668, 1988.

[34] R. Z. Has'minskii. *Stochastic Stability of Differential Equations*. Sijthoff and Noordhoff, Maryland, USA, 1980.

[35] K. Hirai, M. Hirose, Y. Haikawa, and T. Takenaka. The development of honda humanoid robot. In *Proc. IEEE Int. Conf. Robotics and Automation*, pages 1321–1326, 1998.

[36] K. Hitomi, T. Shibata, Y. Nakamura, and S. Ishii. Reinforcement learning for quasi-passive dynamic walking of an unstable biped robot. *Robotics and Autonomous Systems*, 54(12):982–988, 2006.

[37] H. Hjalmarsson. Iterative feedback tuning - an overview. *Int. J. Adaptive Control and Signal Processing*, 16:373–395, 2002.

[38] S. Hyon and T. Emura. Energy-preserving control of passive one-legged running robot. *Advanced Robotics*, 18(4):357–381, 2004.

[39] S. Hyon and T. Emura. Symmetric walking control: Invariance and global stability. In *Proc. IEEE ICRA*, pages 1455–1462, 2005.

[40] N. Ikeda and S. Watanabe. *Stochastic differential equations and diffusion processes*. North-Holland/Kodansha, Amsterdam/Tokyo, second edition, 1989.

[41] A. Isidori. *Nonlinear control systems*. Springer-Verlag, London, third edition, 1995.

[42] K. Itô. On a formula concerning stochastic differentials. *Nagoya Math. J.*, 3:55–65, 1951.

[43] S. Kajita, F. Kanehiro, K. Kaneko, K. Fujiwara, K. Harada, K. Yokoi, and H. Hirukawa. Biped walking pattern generation by using preview control of zero-moment point. In *Proc. IEEE Int. Conf. Robotics and Automation*, pages 1620–1626, 2003.

[44] N. El Karoui and L. Mazliak, editors. *Backward Stochastic Differential Equations*. Longman, 1997.

[45] H. K. Khalil. *Nonlinear Systems*. Macmillan Publishing Company, New York, third edition, 1996.

[46] B. Øksendal. *Stochastic differential equations, An introduction with applications*. Springer-Verlag, Berlin Heidelberg New York, fifth edition, 1998.

[47] H. J. Kushner. On the stochastic maximum principle: Fixed time of control. *J. Math. Anal. Appl.*, 11:78–92, 1965.

[48] H. J. Kushner. *Stochastic Stability and Control*. Academic Press, 1967.

[49] H. J. Kushner. *Stochastic stability*. Stability of Stochastic Dynamical Systems; Lecture Notes in Math. 294. Springer-Verlag, Berlin and New York, 1972.

[50] X. Mao. *Stability of Stochastic Differential Equations with Respect to Semimartingales*. Pitman Res. Notes Math. Ser. 251. Longman Scientific and Technical, 1991.

[51] X. Mao. Stochastic versions of the LaSalle theorem. *J. Differential Equations*, 153:175–195, 1999.

[52] B. Maschke and A. J. van der Schaft. Port-controlled Hamiltonian systems: modelling origins and system theoretic properties. In *Proc. 2nd IFAC Symp. Nonlinear Control Systems*, pages 282–288, 1992.

[53] T. McGeer. Passive dynamic walking. *Int. J. Robotics Research*, 9(2):62–82, 1990.

[54] T. Misawa. Conserved quantities and symmetry for stochastic dynamical systems. *Phys. Lett. A*, 195:185–189, 1994.

[55] T. Misawa. Conserved quantities and symmetries related to stochastic dynamical systems. *Ann. Inst. Statist. Math*, 51(4):779–802, 1999.

[56] S. Nicosia and P. Tomei. Robot control by using only joint position measurements. *IEEE Trans. Autom. Contr.*, 35(9):1058–1061, 1990.

[57] A. Ohsumi. *Introduction to Stochastic Systems*. Asakura Publishing, Tokyo, 2002. (in Japanese).

[58] R. Ortega, A. Loría, R. Kelly, and L. Praly. On passivity-based output feedback global stabilization of euler-lagrange systems. In *Proc. 33rd IEEE Conf. on Decision and Control*, pages 381–386, 1994.

[59] R. Ortega, A. J. van der Schaft, B. Maschke, and G. Escobar. Interconnection and damping assignment passivity-based control of port-controlled Hamiltonian systems. *Automatica*, 38(4):585–596, 2002.

[60] K. Osuka and K. Kirihara. Motion analysis and experiments of passive walking robot quartet II. In *Proc. IEEE Int. Conf. Robotics and Automation*, pages 3052–3056, 2000.

[61] B. Paden and R. Panja. Globally asymptotically stable 'pd+' controller for robot manipulators. *Int. J. Control*, 47(6):1697–1712, 1988.

[62] S. Peng. A general stochastic maximum principle for optimal control problems. *SIAM J. Contr. Optimiz.*, 28(4):966–979, 1990.

[63] J.-B. Pomet. Explicit design of time-varying stabilizing control laws for a class of controllable systems without drift. *Systems & Control Letters*, 18:147–158, 1992.

[64] L. S. Pontryagin, V. G. Boltyanskii, R. V. Gamkrelidze, and E. F. Mishchenko. *The Mathematical Theory of Optimal Processes*. John Wiley and Sons, New York, 1962.

[65] S. Sakai and K. Fujimoto. Dynamic output feedback stabilization of a class of nonholonomic Hamiltonian systems. In *Proc. 16th IFAC World Congress*, pages 1967–1970, 2005.

[66] A. Sano, Y. Ikemata, and H. Fujimoto. Analysis of dynamics of passive walking from storage energy and supply rate. In *Proc. IEEE Int. Conf. Robotics and Automation*, pages 2478–2483, 2003.

[67] S. Sastry. *Nonlinear Systems: Anaysis, Stability and Control*, volume 10 of *Interdisciplinary Applied Mathematics*. Springer-Verlag, New York, 1999.

[68] S. Satoh and K. Fujimoto. On passivity based control of stochastic port-hamiltonian systems. In *Proc. 47th IEEE Conf. on Decision and Control*, pages 4951–4956, 2008.

[69] S. Satoh and K. Fujimoto. Passivity based control of stochastic port-hamiltonian systems. *Trans. the Society of Instrument and Control Engineers*, 44(8):670–677, 2008. (in Japanese).

[70] S. Satoh and K. Fujimoto. Stabilization of time-varying stochastic port-Hamiltonian systems and its application to stochastic trajectory tracking control. In *Proc. 37th SICE Symposium on Control Theory*, pages 393–398, 2008. (in Japanese).

[71] S. Satoh and K. Fujimoto. Observer based stochastic trajectory tracking control of mechanical systems. In *Proc. ICROS-SICE Int. Joint Conf. 2009*, pages 1244–1248, 2009.

[72] S. Satoh and K. Fujimoto. On variational and adjoint processes of stochastic port-hamiltonian systems. In *Proc. 38th SICE Symposium on Control Theory*, pages 407–410, 2009. (in Japanese).

[73] S. Satoh and K. Fujimoto. On observer based stochastic trajectory tracking control of mechanical systems. To appear in *Trans. the Society of Instrument and Control Engineers* (in Japanese), 2010.

[74] S. Satoh, K. Fujimoto, and S. Hyon. Gait generation for a hopping robot via iterative learning control based on variational symmetry. In *Proc. IFAC 3rd Workshop on Lagrangian and Hamiltonian Methods for Nonlinear Control*, pages 125–130, 2006.

[75] S. Satoh, K. Fujimoto, and S. Hyon. Gait generation for passive running via iterative learning control. In *Proc. IEEE/RSJ Int. Conf. Intelligent Robots and Systems*, pages 5907–5912, 2006.

[76] S. Satoh, K. Fujimoto, and S. Hyon. Optimal gait generation for the compass gait biped based on variational symmetry. In *Proc. 35th SICE Symposium on Control Theory*, pages 357–360, 2006. (in Japanese).

[77] S. Satoh, K. Fujimoto, and S. Hyon. Optimal gait generation for a one-legged robot based on variational symmetry of hamiltonian systems. *Trans. the Society of Instrument and Control Engineers*, 43(12):1103–1110, 2007. (in Japanese).

[78] S. Satoh, K. Fujimoto, and S. Hyon. Biped gait generation via iterative learning control including discrete state transitions. In *Proc. 17th IFAC World Congress*, pages 1729–1734, 2008.

[79] S. Satoh, K. Fujimoto, and S. Hyon. A framework for optimal gait generation via learning optimal control using virtual constraint. In *Proc. IEEE/RSJ Int. Conf. Intelligent Robots and Systems*, pages 3426–3432, 2008.

[80] S. Satoh, K. Fujimoto, and S. Hyon. A gait generation framework via learning optimal control considering discontinuous state transitions. Submitted (in Japanese), 2009.

[81] J.J. E. Slotine and W. Li. On the adaptive control of robot manipulators. *Int. J. Robotics Research*, 6(3):49–59, 1987.

[82] M. W. Spong. Passivity-base control of the compass gait biped. In *Proc. of IFAC World Congress*, pages 19–23, 1999.

[83] S. Stramigioli, B. M. J. Maschke, and A. J. van der Schaft. Passive output feedback and port interconnection. In *Proc. 4th IFAC Symp. Nonlinear Control Systems*, pages 613–618, 1998.

[84] A. Takanishi, M. Ishida, Y. Yamazaki, and I. Kato. The realization of dynamic walking by the biped walking robot WL-10RD. In *Proc. Int. Conf. Advanced Robotics*, pages 459–466, 1985.

[85] M. Takegaki and S. Arimoto. A new feedback method for dynamic control of manipulators. *Trans. ASME, J. Dyn. Syst., Meas., Control*, 103:119–125, 1981.

[86] R. Tedrake, T. W. Zhang, and H. S. Seung. Stochastic policy gradient reinforcement learning on a simple 3D biped. In *Proc. IEEE/RSJ Int. Conf. Intelligent Robots and Systems*, pages 2849–2854, 2004.

[87] C. Thompson and M. Raibert. Passive dynamic running. In V. Hayward and O. khatib, editors, *Experimental Robotics I*, volume 139 of *Lecture Notes in Control and Information Science*, pages 74–83. Springer-Verlag, Berlin, 1989.

[88] A. J. van der Schaft. *L_2-gain and Passivity Techniques in Nonlinear Control*, volume 218. Lecture Notes on Control and Information Science, Berlin, 1996.

[89] A. J. van der Schaft and B. M. J. Maschke. On the Hamiltonian formulation of nonholonomic mechanical systems. *Reports on Mathematical Physics*, pages 225–233, 1994.

[90] A. J. van der Schaft and B. M. J. Maschke. Mathematical modeling of constrained Hamiltonian systems. In *Proc. 3rd IFAC Symp. Nonlinear Control Systems*, 1995.

[91] M. Vukobratović and J. Stepanenko. On the stability of anthropomorphic systems. *Mathematical Biosciences*, 15:1–37, 1972.

[92] J. C. Willems. Dissipative dynamical systems -part I: General theory. *Arch. Rational Mechanics and Analysis*, 45:321–351, 1972.

[93] J. C. Willems. Dissipative dynamical systems -part II: Linear systems with quadratic supply rates. *Arch. Rational Mechanics and Analysis*, 45:351–393, 1972.

[94] M. Yamakita and K. Furuta. Iterative generation of virtual reference for a manipulator. *Robotica*, 9:71–80, 1991.

[95] J. Yong and X. Y. Zhou. *Stochastic Controls: Hamiltonian Systems and HJB Equations*. Springer-Verlag, New York, 1999.

Published papers

Most of this research have been either published as journal or conference papers. A list is given below.

Chapter 2

[78] S. Satoh, K. Fujimoto, and S. Hyon. Biped gait generation via iterative learning control including discrete state transitions. In *Proc. 17th IFAC World Congress*, pages 1729-1734, 2008.

Related researches have been also published in [74, 75, 77] and another related result has been submitted for publication [80].

Chapter 3

[21] K. Fujimoto and S. Satoh. On repetitive control of Hamiltonian systems based on variational symmetry. In *Proc. Mathematical Theory of Networks and Systems*, 2006.

[22] K. Fujimoto and S. Satoh. On repetitive control of Hamiltonian systems based on variational symmetry. In *Trans. the Society of Instrument and Control Engineers*, 43(8):711-713, 2007. (in Japanese).

[79] S. Satoh and K. Fujimoto and S. Hyon. A framework for optimal gait generation via learning optimal control using virtual constraint. In *Proc. IEEE/RSJ Int. Conf. Intelligent Robots and Systems*, pages 3426-3432, 2008.

Chapter 4

[68] S. Satoh and K. Fujimoto. On passivity based control of stochastic port-Hamiltonian systems. In *Proc. 47th IEEE Conf. on Decision and Control*, Pages 4951-4956, 2008.

[69] S. Satoh and K. Fujimoto. Passivity based control of stochastic port-Hamiltonian systems. *Trans. the Society of Instrument and Control Engineers*, 44(8):670-677, 2008. (in Japanese).

Related research has been presented in [70].

Chapter 5

[71] S. Satoh and K. Fujimoto. Observer based stochastic trajectory tracking control of mechanical systems. In *Proc. ICROS-SICE Int. Joint Conf. 2009*, pages 1244-1248, 2009.

[73] S. Satoh and K. Fujimoto. On observer based stochastic trajectory tracking control of mechanical systems. To appear in *Trans. the Society of Instrument and Control Engineers* (in Japanese), 2010.

Chapter 6

Related research has been presented in [72].